Pedogenesis, Permafrost, and Ecosystem Functioning: Feedbacks and Interactions along Climate Gradients across the Tibetan Plateau

Dissertation

der Mathematisch-Naturwissenschaftlichen Fakultät

der Eberhard Karls Universität Tübingen

zur Erlangung des Grades eines

Doktors der Naturwissenschaften

(Dr. rer. nat.)

vorgelegt von

Dipl.-Geogr. Frank Baumann

aus Rothenburg ob der Tauber

Tübingen

2013

Tag der mündlichen Qualifikation:	30.06.2014
Dekan:	Prof. Dr. Wolfgang Rosenstiel
1. Berichterstatter:	Prof. Dr. Thomas Scholten
2. Berichterstatter:	Prof. Dr. Volker Hochschild
3. Berichterstatter:	Prof. Dr. Heinrich Thiemeyer

Contents

Abbreviations

AGB	Aboveground biomass
BGB	Belowground biomass
CM	Cambisols
CO_2	Carbon dioxide
EAST	Eastern transect
FPOM	Free particulate organic matter
GL	Groundwater influenced soils
HUA	Site Huashixia
IS	Initially formed soils
LIC	Lithogenic inorganic carbon
MAE	Mean annual evaporation
MAP	Mean annual precipitation
MAST	Mean annual soil temperature
MAT	Mean annual air temperature
MLR	Multiple linear regression
MOM	Mineral associated organic matter
OPOM	Occluded particulate organic matter
PF	Permafrost-affected soils
Pg	Petagram ($1Pg = 10^{15}$ g)
PIC	Pedogenic inorganic carbon
PO	Pedogenic oxides
POM	Particulate organic matter
POR	Pedogenic oxides ratios
Rs	Soil Respiration
SEM	Structural equation
SG	Soil group
SIC	Soil inorganic carbon

SM	Soil moisture
SOC	Soil organic carbon
SOM	Soil organic matter
SOM	Soil organic matter
ST	Soil temperature
TN	Total nitrogen
TOTAL	Complete sampling set
VT	Vegetation type
WEST	Western transect
WI	Weathering indices
WUD	Site Wudaoliang

1 Introduction

The Tibetan Plateau is the highest, largest and youngest plateau on the globe. It covers an area of more than 2.4 million km² with an average altitude exceeding 4,000 m ASL (Zheng et al., 2000). As a consequence of extreme environmental conditions due to strong and rapid tectonic uplift, highly adapted and sensitive ecosystems have evolved. Thus, the Tibetan Plateau is considered as a key area for the earth's environmental evolution on regional and global scales, proving to be particularly sensitive to global climate warming (Jin et al., 2007; Liu and Chen, 2000; Liu and Zhang, 1998; Qiu, 2008) and land use changes (Yang et al., 2009b). Due to the specific present-day climate conditions and climate evolution since the last ice age, two thirds of the Tibetan Plateau's total surface are affected by permafrost (Cheng, 2005; Zhao et al., 2000). It represents the largest high-altitude and low-latitude permafrost region on earth, characterised by strong diurnal patterns, high insolation per surface area due to the comparably steep angle of solar radiation, and respective pronounced geothermal gradients (Wang and French, 1994, 1995). Correspondingly, relatively high permafrost temperatures just below the freezing point are evident. This warm permafrost is more sensitive than cold permafrost of high latitudes (Wang and French, 1995).

Compared to high-latitude regions, permafrost degradation processes on the Tibetan Plateau were found to be even more intense (Wang et al., 2000; Yang et al., 2010a; Yang et al., 2004a) and proposed to be enhanced under future environmental change scenarios (Böhner and Lehmkuhl, 2005; Nan et al., 2005). Rapid rises in mean annual air temperatures have been observed over the past decades (Wu et al., 2005; Yang et al., 2004a). Many studies report degradation features, such as increasing permafrost temperatures and active layer thickness as well as soil moisture changes (Cheng and Wu, 2007; Jin et al., 2000; Kang et al., 2010; Wu et al., 2010b; Yang et al., 2010a; Yi et al., 2011). Accordingly, soil hydrology and related soil moisture-temperature regimes are altered (Wang et al., 2008a; Yang et al., 2011; Zhang et al., 2003), leading to essentially changed preconditions for soil development (Chapin III et al., 2000; Vitousek, 1997). The latter include decomposition of organic matter (Stokstad, 2004; Wang et al., 2009), nutrient supply (Anderson et al., 2006; Dharmakeerthi et al., 2005; Hook and Burke, 2000) as well as weathering processes. Hence, soils are the crucial connecting link for ecosystem functioning, having influence on vegetation, hydrology and consequently in turn also on geomorphological processes, such as land surface stability (Sugden, 2004). Alterations of climate parameters in comparable high-latitude arctic permafrost ecosystems show severe changes in general environmental conditions, soil properties, water dynamics and the carbon cycle (Davidson and Janssens, 2006; Grosse et al., 2011; Johnson et al., 2011; Jorgenson et al., 2001; Post et al., 2009; Schuur et al., 2008; Schuur et al., 2009; Zimov et al., 2006).

This thesis focuses on the alpine grasslands bio-ecosystems of the Tibetan Plateau. On a global scale, grassland ecosystems contain at least 10% of the terrestrial ecosystem's carbon and react most sensitive to climate change (Hall et al., 2000; IPCC, 2007; Jobbagy and Jackson, 2000; Schimel et al., 1990; Scurlock and Hall, 1998). More than 62% of the Tibetan Plateau is covered by alpine meadow (30%) and steppe (32%) grassland vegetation, corresponding to an area of 1.6×10^8 ha and 40% of the Chinese grassland area (Hou, 1982; Wu, 1980). About 33.52 Pg C is stored in organic compounds down to a depth of 70 cm, whereof 23.24 Pg can be allocated to the alpine meadow and steppe ecosystems (Wang et al., 2002), thus retaining 23.44% of the Chinese, and 2.5% of the global soil organic carbon storage, respectively (Wang et al., 2002; Wang and Zhou, 2001). Importantly, soils on the Tibetan Plateau account for the highest C stocks of all Chinese soils (Wang and Zhou, 2001). Especially alpine meadow ecosystems are crucial for C storage, currently acting as a carbon sink (Kato et al., 2004), making up 38.2% of total soil carbon in Chinese grassland soils (Ni, 2002). Given the above-described pronounced sensitivity of the region to climate change and prevalent permafrost degradation, periglacial grassland environments of the Tibetan Plateau most likely play an important role for the present and future global C and N cycle, having been identified as one of the most sensitive areas of soil organic matter loss in the last 20 years (Xie et al., 2007). In this context, nutrient availability is crucial for the evolution of potential vegetation, especially under changing climate conditions. For detailed future predictions, it is essential to evaluate beside carbon dynamics also nitrogen mineralisation processes and the related variables, which are rarely available for grassland ecosystems (Rustad et al., 2001).

Wetlands on the Tibetan Plateau occur particularly under permafrost influence in specific relief positions, because evaporation exceeds more than three times precipitation (Wang and French, 1994; Wang et al., 2006). On a worldwide scale, these wetlands contain related to their size by far the highest carbon stocks and relatively quick turnover rates of organic matter for the turf-like upper layers of only some tens of years can be expected (Hirota et al., 2006). The presence and spatial distribution of permafrost (Nan et al., 2005), implies complex land-surface hydrological processes due to seasonal and diurnal variations of soil moisture and soil temperature regimes. Rising air temperatures lead to a greater active layer thickness, thus modifying the strongly interrelated preconditions. These processes will be amplified, if warming is accompanied by drier conditions (Yang et al., 2004a). Wang et al. (2006) reports pronounced land cover and biogeochemical changes, coupled with transformations of alpine meadow and swamp into steppe-like meadows, alpine steppes or even desertified land. Overall, substantial losses of soil organic carbon and nitrogen of degraded grassland ecosystems have been observed on the Tibetan Plateau over the past 20-40 years (Dai et al., 2011; Wang et al., 2001; Wang et al., 2008a; Wang et al., 2007; Yang et al., 2009b). These considerable modifications of the C and N cycles

(Cheng and Wu, 2007; Lin et al., 2011) emphasise the need for a better understanding of interactions between the main influencing parameters.

Land use changes amplify the described degradation processes. Beside construction measures, such as road building, settlement or mining, livestock grazing is the most important factor of direct human impact in the region (Cheng, 2005; Pei et al., 2006; Wu and Tiessen, 2002; Zhang et al., 2006). Particularly overgrazing stimulates the negative feedback loops of climate warming and permafrost degradation (Zhou et al., 2005). This is mainly due to livestock trampling, nutrient and soil organic carbon loss as well as triggered soil erosion presses (Wu et al., 2010a; Zhang et al., 2006; Zhou et al., 2005). High vegetation cover implies higher soil moisture contents, thus reducing the impact of heat cycling on permafrost by changed thermal conductivity, heat capacity and latent heat (Shur and Jorgenson, 2007; Wang et al., 2010). Consequently, the direct influence of climate change can be buffered for a certain time frame, if vegetation cover remains intact. Moreover, Zhao et al. (2004) showed that climate warming is most distinct in the northeastern Tibetan Plateau, implying warming of air, surface temperatures as well as duration and depth of thawing. Hence, the study area will be particularly affected by modifications of the ecosystem combined with a comparably high population density.

Triggered by these widespread permafrost degradation processes, shifts in sedimentary and geomorphological systems are common, implying broad varieties and alterations of weathering intensities. Soil development is closely associated with specific weathering intensities under distinct environmental conditions. Related shifts in the ecosystems can occur quickly, notably if strong proximal sediment input from degraded areas buries intact, well-developed soil profiles including vegetation cover. In other cases, gradually drying up of profiles could lead to lower vegetation cover and finally activated sediment outblow accompanied by deposition in certain relief positions. These processes are mainly linked to an increasing active layer thickness (Yang et al., 2011). Related desertification processes have been reported in various studies (e.g. Wang et al., 2011; Xue et al., 2009; Yan et al., 2009). Precise measurements of the sediment's weathering intensities and soil development processes have not been provided, albeit these could be important tools to quantify stability of soil formation processes of different sub-ecosystems over time.

The described processes are not only relevant on local and regional scales, but also in a global context. Higher decomposition rates of soil organic matter and fundamental modifications of the carbon cycle can be expected with a shift to warmer and drier climate (Zimov et al., 2006). Additionally, desertification and changing sedimentary processes may alter soil organic carbon contents (Qi et al., 2001) as well as weathering and soil forming processes. Besides release of greenhouse gases, changes in water balance as well as vegetation coverage and composition have to be considered. Degradation of alpine meadows is associated with changes of soil water contents,

thus having the potential to hydrological alterations on a regional scale (Wang et al., 2008a). Given the prominent role in the Asian monsoon system, surface-heat-fluxes are crucial for understanding its future development (IPCC, 2007). Moreover, some of the world's largest rivers, such as Yangtze and Yellow River originate on the Tibetan Plateau. Environmental changes in the headwater's regions will have consequences for most of the Asian continent, both in terms of water supply and impacts on riverine sediment flux (Lu et al., 2010).

The described preconditions and processes in the unique and changing ecosystems on the Tibetan Plateau provide an ideal spot to investigate research questions related to ecosystem functioning and soil development under the scope of global climate change.

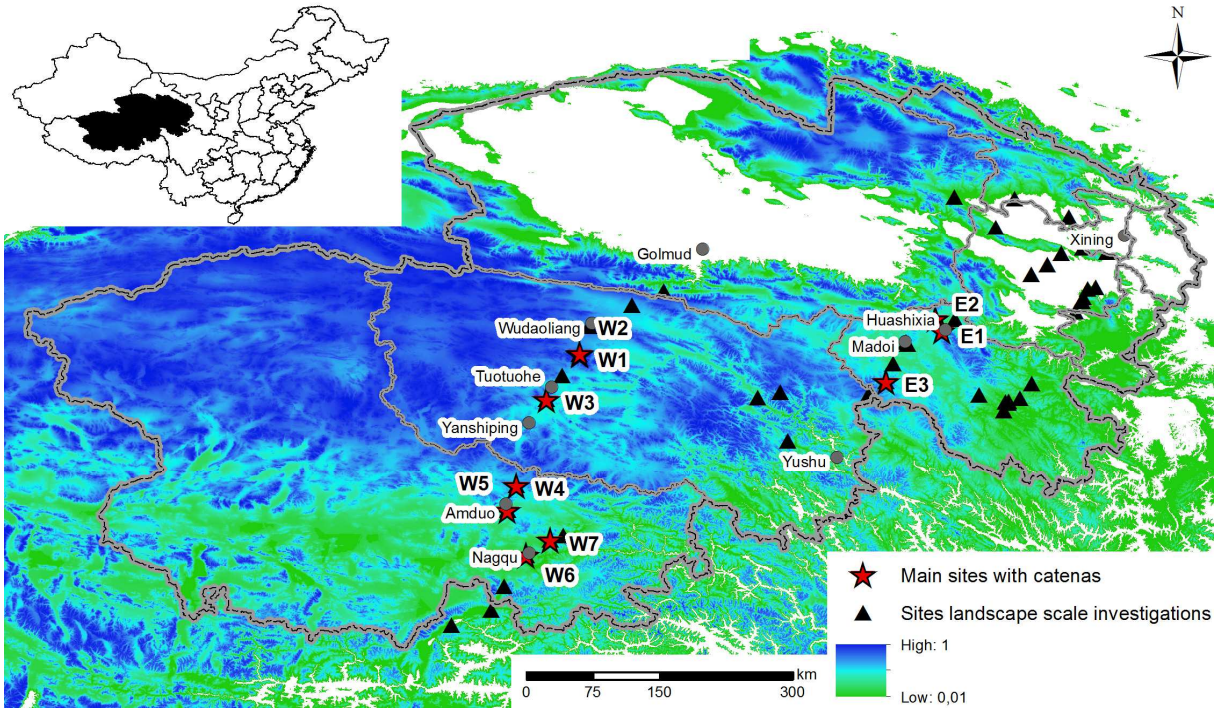

Fig. 1.1 Research sites on the Tibetan Plateau. PFI (permafrost index) indicates the permafrost distribution.

2 Study area and state of the art

2.1 Project environment, field campaigns, and research area

Field expeditions were launched and planned in close cooperation with Peking University, Beijing. The research group of Professor Jin-Sheng He conducted profound plant physiological, respiration and diversity experiments. Specifically, above and belowground biomass, species composition and density, plant chemical parameters and ratios, as well as soil respiration were measured. Thus, site selection constitutes always a compromise of both soil scientific and ecological viewpoints, as all experiments and sampling were performed simultaneously at the same sites to achieve comparable and coherent results. Field data was gathered during three expeditions to the central-eastern Tibetan Plateau in the summers of 2006, 2007 and 2009. Basically, all sites are located along a north-south stretching transect of about 1,200 km length and 200 km width, situated between 90.80 and 101.48°E latitude and 30.31 to 37.69°N longitude, comprising an eastern section between Xining and Yushu and a western part between Golmud and Lhasa with elevations ranging between 2,925 and 5,105 m ASL. In order to study differences between the two monsoonal systems and their influence on pedogenesis and soil weathering, comparable sites were selected and split into an eastern (EAST) and western (WEST) transect, which both are north-south oriented (Fig. 1). Sites on EAST extend along 98.5°E and range from 34.3 to 35.3°N in the region between the settlements of Huashixia and Yushu. WEST stretches along 92.2°E and ranges from 31.4 to 34.7°N between Wudaoliang and Nagqu.

The Tibetan Plateau acts as an anomalous mid-tropospheric heat source, thus being a major component of the Asian monsoonal system. The east-west stretching mountain ranges act as prominent barriers for the relatively moist tropical Indian Monsoon coming from the south (Domrös and Peng, 1988). Kunlun Shan builds up the northern fringe, merging eastwards into the NW-SE ranging Bayan Har Shan. Tanggula Shan (approximately 33°N) is splitting the Tibetan Plateau roughly in half, forming likewise the southern border of continuous permafrost, which is restricted southwards to higher mountainous areas above 4,600-4,700 m ASL (Hövermann and Lehmkuhl, 1994). The Transhimalaja is the most important barrier separating the cold and arid highlands from the comparably warm and moist southern Tibet with the Lhasa valley. At the eastern edge of the plateau, there is no such remarkable mountain range acting as a significant barrier. Instead, deep valleys of major rivers (e.g. Huanghe or Yangtze) are distinctive elements in the landscape. The subtropical East Asian Monsoon transports warmer airmasses with high water vapour content from the eastern lowlands to the Tibetan Plateau through the meridional flow furrows (Weischet and Endlicher, 2000). The intensity of the East Asian Monsoon decreases westwards (Harris, 2006), implying higher temperatures and precipitation in the south and east. During the cold and dry winters, extra-tropical westerlies occur together with the prevailing Mongolian-Siberian high pressure system (Domrös and Peng, 1988). Due to the described large-

scale climatic patterns, precipitation decreases generally from SE to NW. Nevertheless, this may vary considerably due to local mountain ranges, differences in altitude, and extreme relief positions. Mean annual air temperature (MAT) varies between -5.8 and 2.6°C across all sites. For the transects, MAT ranges from -3.5 to -5.7°C (EAST) and -0.2 to -5.6°C (WEST). Mean annual precipitation (MAP) varies between 218 and 604 mm yr^{-1}; transects range from 458 to 521 mm yr^{-1} (EAST) and 285 to 510 mm yr^{-1} (WEST). Overall, more than 80% of the annual precipitation is occurring during summer months from July until September. Mean annual evaporation (MAE) ranges on average from 1,400 to 1,800 mm yr^{-1} for the whole Tibetan Plateau (Wang and French, 1994). For the headwaters of Yangtze River MAE of 1,478 mm yr^{-1} was reported by Hu et al. (2009), 1,264 mm yr^{-1} was measured in the headwaters of the Yellow River around Maduo (Zhang et al., 2010), and 1,770 mm yr^{-1} in the area around Amduo (Feng and Zhu, 2009). Gao et al. (2006) provide evaporation values ranging from 1,500 to 2,300 mm yr^{-1} for Nagqu County rising from SE to NW. Other studies report similar data (Wang et al., 2001; Yao et al., 2000) and give more detailed information about annual patterns as well as influencing parameters (Zhang et al., 2003). Despite variations of the provided values, it is essential to note that MAE largely exceeds MAP for the whole research area.

Permafrost characteristics are closely linked to the mean annual soil temperature (MAST) gradient (Ping et al., 2004; Wang and French, 1994). Accordingly, the active layer thickness increases from north to south and overall with lower altitude, averaging around 1-2 m in continuous permafrost (Cheng and Wu, 2007; Wang et al., 2000). Moreover, Zhao et al. (2000) reports a negative relationship between biomass and active layer thickness in alpine meadow ecosystems. Patches of dense vegetation show isolating effects, hence protecting underlying permafrost leading to shallower active layer depths (Wang et al., 2010; Wang et al., 2009; Zhao et al., 2000). Generally, diurnal temperature fluctuations are extremely high compared to the high latitudes and can reach Δ25-40 °C, thus leading to frequent daily freeze-thaw cycles (Ping et al., 2004). In the central-western part between Tanggula and Kunlun Shan, continuous ice-poor permafrost (Jin et al., 2000) is widespread (Fig. 1), associated with weakened influence of both monsoonal systems. Nevertheless, permafrost degradation led to the formation of numerous small depressions, where surface water accumulates or thermokarst lakes are formed (Niu et al., 2011). In the eastern part, under the influence of the East Asian Monsoon, discontinuous and unstable permafrost is evident. Under certain circumstances taliks have developed (Jin et al., 2000), where soils freeze to a depth of 2-3 m, while the upper limit of the permafrost lies in 4-7 m depth, leading to a vertical disconnection of the permafrost.

Soils are mostly affected by geomorphological, cryogenic (solifluction), and erosive processes, frequently interrupted by fresh, mainly aeolian sedimentation, thus leading to a great variety of substrates for soil formation. Accordingly, soils are mostly young showing frequently polygenet-

ic formation and partly strong degradation features. Especially in the eastern part, this instability is enhanced by intense precipitation during the summer months. This may lead to fluvial erosion and alluvial accumulation, partly also by laminar sheet floods along gentle slopes. Aeolian erosion and re-deposition is forced in such areas during winter by the dry winter monsoon and sparse vegetation (Dietze et al., 2012; Xue et al., 2009). Consequently, buried relict and mostly humic horizons can be observed. Overall, soil development is strongly influenced by water availability, which is in turn related to relief position and permafrost. On steep upper slopes and terraces, weakly developed soils, such as Leptosols, Leptic Cambisols, Haplic Regosols, and Mollic Cryosols are prevalent, whereas Gleysols and Gleyic Fluvisols commonly occur in morphological depressions and next to lakes or rivers (Kaiser, 2004; Kaiser et al., 2007). At sites where permafrost is evident and under more stable conditions, Gelic Gleysols, Gelic Cambisols, Cambic Cryosols and Permagelic/Gelic Histosols are developed. In regions influenced by discontinuous and sporadic permafrost, or generally speaking under warmer and moister conditions, also well-developed Cambisols are evident (IUSS Working Group WRB, 2006). In cold alpine meadows, felty topsoils commonly occur (Kaiser, 2004; Kaiser et al., 2008). The basis for soil formation are in most cases aeolian loess-like sediments being mainly of local origin (Feng et al., 2011) or parent rock reworked by periglacial processes mixed with aeolian derived material (Schlütz and Lehmkuhl, 2009). The composition of the aeolian sediments can be related to the corresponding altitude: typical loess sediments occur up to 3,600 m ASL, whereas in higher regions sandy loess is more dominant (Fang et al., 2003). This is caused by stronger blowout processes, mainly due to sparse vegetation, lower lake levels and higher wind velocities that transport the silty components into the higher atmosphere (Klinge and Lehmkuhl, 2005). Moreover, Pleistocene sand dunes occur frequently around lakes and rivers also in higher regions, often accompanied by lacustrine sediments of palaeo-lakes or fluvial sediments. These sediments can be again sources for blowout of aeolian material (Lehmkuhl, 1997).

Our research sites concentrate on the extensive grassland area largely excluding high mountainous regions. The vegetation represents alpine grasslands, including two main ecosystem types: alpine meadow and alpine steppe (Wang, 1988; Zhang et al., 1988). The most widespread vegetation type is the alpine *Kobresia* meadow ecosystem (Zhou et al., 2005; Zhou, 2001). It occurs at elevations between 3,200 and 5,200 m ASL (Kato et al., 2004). In alpine meadows, mostly perennial tussock grasses, such as *Kobresia pygmaea* and *K. tibetica* occur. Alpine steppes are dominated by short and dense tussock grasses, with *Stipa purpurea* or *Stip subsessiliflora* being dominant. In wetlands *Kobresia littledalei*, *Carex lanceolata*, and *Carex muliensis* are widespread (Chang, 1981). Human influence on the natural ecosystems is high throughout the research area. Most commonly, severe grazing with yak and sheep as well as the accompanying temporary set-

tlements by nomads represent the major land use (cf. chapter 1). Nevertheless, sites were selected with subject to minimal grazing and other anthropogenic disturbances.

2.2 Carbon and nitrogen contents and its control parameters

Soils comprise the largest carbon pool in terrestrial ecosystems, containing more than 1,500 Pg C (e.g. Amundson, 2001; Eswaran et al., 1993; Raich and Schlesinger, 1992). Comparably small modifications within this system have considerable impact on the atmospheric CO_2 concentration, implying positive feedbacks on global warming (e.g. Davidson and Janssens, 2006; Melillo et al., 2002; Post et al., 2009; Schlesinger and Andrews, 2000). Thus, soils play an important role in the global C cycle. Within this system, topsoils show the most rapid responses to environmental changes (Liao et al., 2009; Song et al., 2005), being particularly important for investigating soil ecosystem processes and functioning ((Franzluebbers and Stuedemann, 2010). Hence we focus on the top 20 cm for C and N related investigations. For the transformation of organic matter, generally three steps can be distinguished: decomposition, humification and mineralisation. The latter implies the complete breakdown by microorganisms to CO_2 and water as well as the release of contained plant nutrients. Contrarily, humification produces humic substances, which are resistant against mineralisation processes, thus having a low conversion rate in soils (Scheffer et al., 2002). Humic substances are important for diverse soil chemical and physical processes (Stevenson and Cole, 1999).

SOC contents of grassland soils exceed all other well-aerated soils with estimated 10% of the worldwide carbon; some authors even calculate 30% (140-450 Pg) (Hall et al., 2000). This is due to the overall higher soil organic matter (SOM) production in grasslands compared to forest ecosystems. Moreover, nitrification is generally inhibited in grassland soils, whereby N remains in lower phases of mobility as NH_4^+ or NH_3^+. This may lead as a positive feedback to further accumulation of SOM due to hampered microbial activity (Parton et al., 1988). Humus accumulation mainly occurs in the root area, which has a higher density than in other ecosystems (ca. 90% of the phytomass is allocated belowground) (Hall et al., 2000; Stevenson and Cole, 1999). This is particularly evident for the alpine meadow ecosystems, frequently developing felty topsoils with extremely high belowground biomass (Kaiser et al., 2008). Accordingly, poor aeration under grassland vegetation is common, leading to sequestration of organic matter (Stevenson and Cole, 1999). In the periglacial environments of the Tibetan Plateau, physical weathering is predominant, mainly leading to sandy and silty substrates with low clay contents. Consequently, important soil functions usually associated with clay fractions, such as nutrient supply and water storage, have to be performed by the humic matter. Accordingly, various site parameters are directly dependent and influenced by SOC/SOM contents.

In the course of the above-mentioned mineralisation processes, available C is respired as CO_2 back to the atmosphere. Soil respiration (Rs) is considered as the major pathway of C in terrestrial ecosystems playing a central role in the global carbon cycle (Schlesinger, 1997; Schlesinger and Andrews, 2000). If primary production is higher than Rs, SOM is accumulated and vice versa (Wütherich et al., 2000). It is essential to understand supplementary to SOC contents and stocks, the relationships of Rs to environmental parameters and climate change. Low temperatures and oxygen deficit, e.g. by water saturation, lead to inhibited decomposition and hence to lower Rs rates. Another important parameter is the quality and decomposability of the available organic matter (Shaver et al., 2006). Many studies investigated the interdependencies between Rs and control variables, such as temperature (ST), soil moisture (SM), soil texture, and other climatic or soil parameters (e.g. Chen et al., 2010; Wan et al., 2007). Within-site temporal patterns and corresponding relationships to control variables can be easily obtained by semi-automated high-frequency measurements of all participating parameters (e.g. Savage et al., 2008; Xu et al., 2005). However, the present study attempts to broaden the site and plot scale viewpoint to landscape scale approaches (Fig. 2.1) in order to predict and describe responses of the C cycle to global climate change. Respectively, Rs needs to be set into context to control variables among broad ecosystem types on landscape scale (Craine et al., 2002; Hibbard et al., 2005; Raich and Schlesinger, 1992).

Besides SOC, soil inorganic carbon (SIC) should be considered for evaluating soil C pools and their interdependencies. SIC includes lithogenic inorganic carbon (LIC) and pedogenic inorganic carbon (PIC). Whereas LIC originates from parent rocks or sediments, PIC is formed by dissolution and weathering of carbonatic parent substrates and the related precipitations in soils. To interrelate approximated SOC and SIC stocks for a depth of 1 m, SOC is estimated between 1,500 and 1,600 Pg (e.g. Batjes, 1996; Lal, 2004; Monger and Gallegos, 2000), where SIC is calculated among 695 and 1,738 Pg (e.g. Batjes, 1996; Eswaran et al., 1995). SIC pools exchange C through various physical and chemical reactions. The main pathways are C sequestration by carbonate formation and CO_2 release by acidification and leaching (Lal, 2008; Lal and Kimble, 2000; Ouyang et al., 2008). Thus, many of the alterations associated with global climate change are likely to have not only significant influence on SOC, but also on SIC stocks. Whilst SOC dynamics and controls have been well-investigated on global scales, comparably few studies address SIC (Eswaran et al., 2000; Mi et al., 2008). For China, total SIC stocks in the top 1 m are estimated between 53.3 Pg and 77.9 Pg (Li et al., 2007; Mi et al., 2008; Wu et al., 2009). SIC stocks of the Tibetan grasslands were estimated by Yang et al. (2010b) to 15.2 Pg, with temperature and precipitation have been identified as the most significant parameters correlating with SIC density.

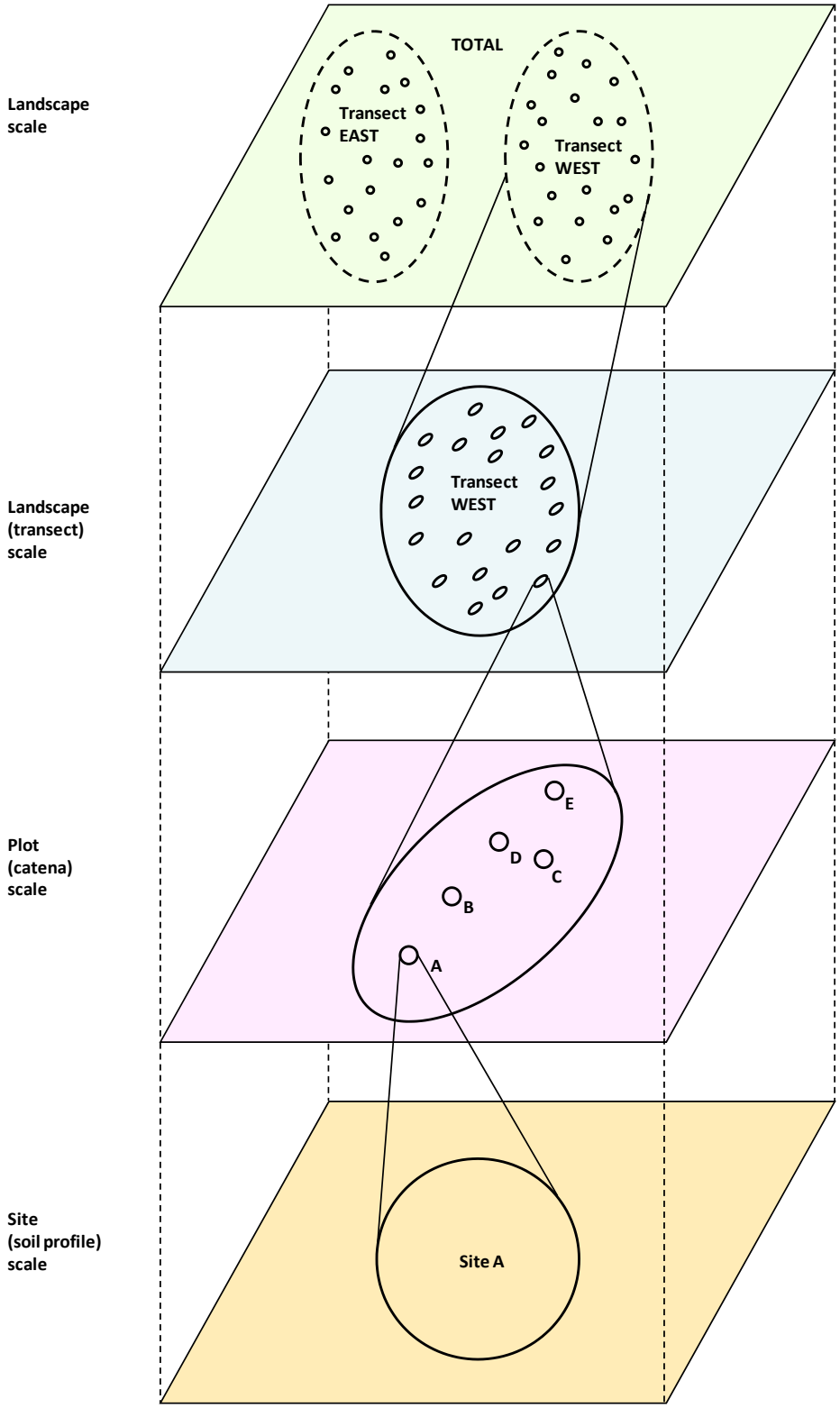

Fig. 2.1 Scheme of the different investigation scales.

A general summary of the nitrogen cycle is given for instance by Stevenson and Cole (1999). Essentially, the total nitrogen (TN) stock is made plant available by mineralisation processes as ammonium-N (NH_4^+-N) and nitrate-N (NO_3^--N). Plants take up N primarily in the form of very mobile NO_3^--N. On a global scale, N plant availability limits plant growth more than water, energy or other nutrients, being strongly chemically bound to SOM (95-95%) (Stahr et al., 1994). Thus, available N pools are directly linked to SOC contents (Stevenson and Cole, 1999). Semi-natural ecosystems like the alpine grasslands on the Tibetan Plateau are generally limited in plant available nutrients. Hence, the productivity of alpine grasslands is determined by the available N pool, the amount of N input as well as by N fixation (Gerzabek et al., 2004; Körner, 2003), modified by water availability to plants over the year (Gründling and Scholten, 2006). Ammonification and nitrification are linked to processes, which are strongly dependent on soil temperature and soil water contents (e.g. Agehara and Warncke, 2005). Nitrate-N contents are commonly very low in soils near water saturation (e.g. Iwatsubo et al., 1989), as aerobic nitrification is inhibited and denitrification increases when soil water content increases. Furthermore, nitrification is a strongly temperature-dependent process (Chapin III et al., 2002; Robinson, 2002), with low temperatures supporting low NO_3^--N contents. Contrarily, NH_4^+-N is a fundamental parameter when investigating N mineralisation and microbial activity under such conditions (Rodrigo et al., 1997), since ammonification works well even near water saturation (Chapin III et al., 2002). Moreover, nitrate-N is more likely to be leached or denitrified (Haider, 1996) from wet or water-saturated soils than ammonium-N (Schlesinger, 1997). The high microbial demands for these nutrients may also limit plant N availability in arctic and other permafrost-influenced ecosystems (Nadelhoffer et al., 1991). At average soil temperatures below 6°C, nitrification works only strongly restricted, hence leading to relative accumulation of ammonium-N (Makarov et al., 2003; Stevenson and Cole, 1999; Zeller et al., 2000). The majority of the ammonium-N is again immobilised by microorganisms and transferred in organic N compounds remaining relatively stable. Only with the dieback of the microorganisms, these compounds are again available for mineralisation (Stahr et al., 1994). The described conditions are evident at permafrost and groundwater influenced sites in the research area, thus overall low proportions of plant available N can be expected in the research area. Contrarily to SOC and TN, only few reliable correlations for mineralised N and soil texture have been reported. Raghubanshi (1992) shows relations between soil texture and bio-geochemical parameters. It is argued that soil texture influences parameters, which are important for N mineralisation, such as aeration, physical distribution of organic matter, and protection by clay-humus-complexes (Anderson et al., 2006; Dodd et al., 2000; Jarvis, 1996). This includes also nitrate-N leaching, as shown by Dodd et al. (2000) for loamy-sandy substrates in a semi-arid steppe. Others do not see direct significant relationships and refer to covariances between the dependent variables (Percival et al., 2000) or assume that diverse feedback mechanisms compensate each other and result in constant settings (Burke et

al., 1997): for example, sandy substrates lead to enhanced mineralisation and consequently at the same time to declining SOC contents, which are in turn relevant for mineralisation of N into plant available forms. However, Schimel et al. (1994) generally assume that in cold regions soil texture has a higher influence than in temperate or warm climate zones. Soil acidity can also inhibit microbial activity and hence mineralisation rates, with nitrification reaching its maximum between pH 5.5 and 8 (Scheffer et al., 2002). Grassland ecosystems exhibit distinct characteristics for both C and N cycles (for detailed description see paragraph about SOC). There exists a general relationship between rooting depth, density of grass coverage and N concentration (Stevenson and Cole, 1999). Fisk and Schmidt (1995) investigated patterns of N mineralisation related to relief positions in both *Kobresia* and *Carex* communities of alpine tundra ecosystems. Their results show significant correlations between N mineralisation and soil water contents for the dryer and warmer *Kobresia* community, whereas *Carex* additionally correlate with soil temperature. While for *Kobresia* meadows the dry conditions reduce biological processes in soils, the wet or partly water-saturated colder soils at *Carex* sites are responsible for the low microbial activity. Accordingly, no nitrification processes could be observed at *Carex* sites, which led the authors to the assumption that soil water has the main impact on nitrification rates (Fisk and Schmidt, 1995). Makarov et al. (2003) confirms the much lower nitrification rates at *Carex* sites compared to *Kobresia* meadows. C availability is essential for decomposition processes both as source material and energy supplier for the involved microorganisms, thus being an essential parameter for N availability (Dharmakeerthi et al., 2005). Makarov et al. (2003) found an even higher influence of organic matter quality in terms of decomposability than e.g. of temperatures. In this context, contents of slightly soluble reactive C were found to be particularly important (Janssen, 1996; Mary et al., 1996; Satti et al., 2003; Shaver et al., 2006).

As described in the general introduction (chapter 1), SOM in soils of the Tibetan Plateau reacts particularly sensitive to environmental changes. This has been approved by several studies using different scientific approaches. Zhang et al. (2007a) applied successfully global carbon models to describe clear responses to climate change, whereas Wang et al. (2007) used remote sensing data and Wang et al. (2008b) SOC fractionation studies to find comparable results. Contrarily, Yang et al. (2009b) found SOC stocks to remain relatively stable for the timeframe from 1980 to 2004. According to their outcomes, this can be ascribed to increased carbon input due to enhanced grassland productivity. The differing results lead to the assumption that response of SOC to changing climate parameters vary spatially to a high extend and on a small scale. This may be caused by numerous environmental factors showing high variations across the landscape at different spatial scales: permafrost distribution, soil texture, and related water logging (Hobbie et al., 2000; Schuur et al., 2008; Yang et al., 2010c). Moreover, freezing commonly affects C and N cycling positively, with stimulating effects particularly on ammonium-N contents (Nielsen et al.,

2001). Accordingly, frequent freeze-thaw cycles lead to dying of microbial biomass followed by an impulse triggered by the energy available for the survived microorganisms. These processes are accompanied by physical processes, as the destruction of soil structure and aggregates have similar effects (Nielsen et al., 2001). Comparable processes can be observed for drying and wetting cycles (Stevenson and Cole, 1999). For grassland ecosystems in Inner Mongolia, northern China, small-scale spatial variability was evident depending on the degree of degradation (Wiesmeier et al., 2009). Generally, also land use changes have to be considered when evaluating SOC patterns (cf. Wu et al., 2003 and chapter 1).

Relationships of C and N contents with control variables have been investigated at varying profoundness for respective climate zones. Whereas several studies exist for temperate zones at local and regional scales (e.g. Callesen et al., 2003; Jobbagy and Jackson, 2000; Post et al., 1982), comparatively little research has been done in high-cold alpine and polar regions (e.g. Bockheim et al., 2003; Ohtsuka et al., 2008; Wang et al., 2002; Zhang et al., 2007b).

Generally, soil temperature is considered as a key factor of many terrestrial biochemical processes, such as soil respiration, decomposition of organic matter, N mineralisation, denitrification, plant productivity, and nutrient uptake by plants. Thus, most research has focused rather on temperature than considering moisture conditions (Callesen et al., 2003; Davidson and Janssens, 2006; Kirschbaum, 2006; Lindroth et al., 1998; Raich and Potter, 1995; Rustad et al., 2001; Saito et al., 2009; Shaver et al., 2006; Shaw and Harte, 2001). Accordingly, soils have been modelled mostly by thermodynamic principles and parameters (Craine et al., 1999), with C and N stocks supposed to decrease with increasing temperature due to intensified decomposition processes. Hence, temperature sensitivity of decomposition is assumed to be greater than that of net primary productivity (Kirschbaum, 1995; Shaver et al., 1992). Low growing-season temperature is regarded as the main limiting factor for plant physiological processes in high-altitude grassland ecosystems (e.g. He et al., 2006; Zhang et al., 1988). Kato et al. (2006) found no significant correlation of seasonal averages of CO_2 exchange to moisture conditions by performing a spatially small-scale study at Haibei Alpine Meadow Research station on the eastern Tibetan Plateau. Accordingly, they argued that warmer conditions would have positive effects on plant growth in alpine meadows, tundra or wet meadow ecosystems. However, most of the research area on the Tibetan Plateau is moisture-limited with evaporation largely exceeding precipitation (cf. subchapter 2.1), thus SM has to be considered as another important parameter (Reichstein et al., 2003).

Many studies have shown, that ST and SM have a distinct impact on soil C and N cycling (Hook and Burke, 2000; Shaver et al., 2006). However, most research, particularly with respect to alpine steppes and meadows, has been solely carried out at local scales. Moreover, incubation or artificial soil heating methods have been frequently applied, without taking parameters on land-

scape scale into account. This may cause difficulties in terms of data interpretation, since spatially extensive studies are necessary for vast and variable research areas, with sites spreading across the geo-ecological diverse landscape (Dharmakeerthi et al., 2005; Hook and Burke, 2000). For example, Fisk et al. (1998) found topographically related SM patterns as the fundamental control of N cycling and production of biomass in alpine tundra ecosystems. Soil forming factors, such as substrate composition and topography were considered only in few studies conducted in steppe ecosystems (Anderson et al., 2006; Dharmakeerthi et al., 2005; Dodd et al., 2000; Hook and Burke, 2000). Many studies found evidence for strong correlations between varying soil texture and SOC (e.g. Giardina et al., 2001; Parton et al., 1994; Schimel et al., 1994), often reporting positive relationships between clay and SOC or TN. Hook and Burke (2000) also found significant correlations with soil texture, where rapidly decreasing C and N contents with increasing sand contents could be observed. Soil texture influences SM dynamics and accordingly the accumulation of SOM, and is thus often regarded as one of the main limiting factors for biochemical processes in grassland ecosystems (Giardina et al., 2001).

Permafrost reduces water infiltration, often leading to water saturation in topsoils. In certain relief positions, such as troughs, depressions, and valleys, this causes ponding surface water during the summer months. If permafrost degrades (cf. chapter 1), active layer thickness would increase leading to drainage processes in the topsoils. As a consequence, higher aeration can be expected associated with enhanced soil respiration rates, triggered by the improvement of oxygen supply to microbial decomposition processes (Wagner et al., 2009). Thus, there is close linkage to the water table observable (Moore and Knowles, 1989). Furthermore, parameters controlling photosynthesis and whole plant C gain, such as SM and nutrient availability, are found to be strongly related to SOC contents in soils (Craine et al., 1999). Accordingly, a number of studies show that changes in moisture and drainage conditions have substantial impact on C and N cycling of soils in certain ecosystems (Hook and Burke, 2000; Janssens et al., 2001; Johnson et al., 1996; Kato et al., 2004; Robinson, 2002; Rodrigo et al., 1997; Shaver et al., 2006). Higher SM may lead together with improved SOC quality to enhanced plant productivity and substrate availability in ecosystems. Hence, higher C and N contents can be observed in soils (Reichstein and Beer, 2008; Reichstein et al., 2003; Schimel et al., 1994), frequently overshadowing the direct effect of temperature as shown also in a broad-scale study about European forest ecosystems (Janssens et al., 2001). If high SM is combined additionally with low soil temperatures, the described processes are amplified by accumulation of SOM (Wang et al., 2006) giving again positive feedback due to the isolating effect of dense vegetation and weakly decomposed SOM (cf. section about SOC). The latter explains the high C contents, even though overall C uptake of the investigated grasslands is much lower than of grasslands at lower altitudes.

2.3 Pedogenesis and weathering processes

Soil development is closely associated with specific weathering intensities under distinct environmental conditions (Brady and Weil, 2008; Jenny, 1994). During chemical weathering processes of bedrocks and sediments, iron and other elements are released. Depending on numerous soil parameters, such as SM, ST, and redox conditions, distinct pedogenic oxides are formed under a certain timeframe (Kämpf et al., 2011), which consist of amorphous and crystalline Fe-, Mn-, Al- and Si-oxides. These pedogenic oxides are characterised by specific degrees of crystallisation, which can be quantified by particular extraction methods. Thus, it is possible to determine intensity, duration, quality, and direction of related pedogenic processes (McKeague, 1967; Mehra and Jackson, 1960; Schlichting and Blume, 1962; Schwertmann, 1964). For the present research, only pedogenic Fe-oxides (PO) fractions are assessed:

- Fet: total iron content (Fe_2O_3)
- Fed: pedogenic (free), well-crystallised iron oxides, hydroxides and oxyhydroxides
- Feo: poorly-crystallised, active and amorphous oxides, hydroxides and oxyhydroxides
- Fep: metalorganic compounds and organically bound Fe (Bascomb, 1968; McKeague, 1967)

By setting the single fractions into relation to each other, statements relating to weathering intensities and conditions as well as to pedogenesis can be made (cf. Tab. 2.1). These pedogenic oxide ratios (POR) have been successfully applied to describe and relatively date geomorphological units (e.g. Aniku and Singer, 1990; Arduino et al., 1984; Mirabella and Carnicelli, 1992; Torrent et al., 1980) as well as soil weathering chronosequences and palaeosols (e.g. Buero and Schwertmann, 1987; Dahms et al., 2012; Diaz and Torrent J., 1989; Mahaney and Fahey, 1980; McFadden and Hendricks, 1985; Rezapour et al., 2010; Sauer et al., 2010; Torrent et al., 2007). However, only few soil surveys systematically investigated PO in periglacial environments with respect to current soil forming processes (Melke, 2007).

Weathering indices (WI) are more difficult to apply, as they have been originally developed for sedimentary geology (e.g. Cullers, 2000; McLennan, 1993; Yang et al., 2004b). Nevertheless, many studies in soil science and geomorphology adopted these geochemical tools for analysing and describing geomorphological units, loess layers, and palaeosols (e.g. Bäumler, 2001; Bäumler and Zech, 2000; Buggle et al., 2011; Buggle et al., 2008; Gallet et al., 1998; Kühn et al., 2013; Wagner, 2005). The WI used for the presented research are listed, described, and referenced in Tab. 2.2. Essentially, it has to be distinguished between three groups of WI based on their main assumptions and characteristics: (1) PI; (2) KN Index B; (3) CIA, CIW, PIA; (4) Ca-free indices FENG and CPA (CIW') (Tab. 2.2). It is important to note, that calculation and correction of CaO implies major differences between the groups. Whereas (1) and (2) do not make any correction

Table 2.1 Overview of pedogenic oxides, pedogenic oxide ratios, and pedogenic oxide differences applied in this thesis.

Pedogenic oxides (PO) / Pedogenic oxide ratio (POR)		**Usage**	**Calculation basis**	**Problematic issues**
Degree of iron release (Blume and Schwertmann, 1969; Mirabella and Carnicelli, 1992)	Fed/Fet *Ratio higher, with increasing weathering intensity / longer soil development*	Measure of iron release from weathering of primary Fe-bearing minerals	Proportion of Fed is higher, the longer and more intensely weathering processes are persisting	
Degree of weathering (Alexander, 1985; Arduino et al., 1984)	(Fed-Feo)/Fet *Ratio higher, with increasing weathering intensity / longer soil development*	Measure for weathering intensities in chronosequences	Proportion of Fed is higher and Feo lower, the longer and more intensely weathering processes are persisting	
Degree of activity (Schwertmann, 1964)	Feo/Fed *Ratio higher, with low weathering status but high current weathering intensities / poorly-developed soils*	Measure of current weathering intensities or soil forming processes	High proportion of Feo (amorphous oxides) show strong recent weathering of primary silicates in still poorly-developed soils; high Fed refers to well crystallised oxides in more developed soils (both in terms of timeframe and intensity)	No relation to Fet; therefore, homogenous material is an essential precondition for application of this ratio
Overall iron (Torrent and Cabedo, 1986)	Fet-Fed *Difference higher, with higher proportion of silicate-bound iron*	Measure of silicate-bound iron in relation to complete iron	Lower proportion of Fed implies higher amount of silicate-bound iron	
Well-crystallised iron oxides	Fed-Feo *Difference higher, with higher proportion of well-crystallised iron*	Measure the relationship between well-crystallised iron oxides and amorphous iron oxides	Lower proportion of Feo implies higher amount of well-crystallised iron oxides	No relation to Fet; therefore, homogenous material is an essential preconditions for this ratio; used for advanced discussion of (Fed-Feo)/Fet
Organically bound iron oxides (Bascomb, 1968; McKeague, 1967)	Fep	Measure of metalorganic compounds and organically bound Fe		No relation to Fet

Table 2.2 Overview of weathering indices applied in this thesis.

Weathering Index (WI)			**Calculation basis**	**Problematic issues**
PI (Parker, 1970); (Bäumler, 2001)	Parker Index *Decreases with increasing weathering intensity*	$(Na_a/0.35 + Mg_a/0.9 + K_a/0.25 + Ca_a/0.7) \times 100$	Leaching and loss of alkali and alkaline earth cations	No immobile reference phase is considered; no calculation of silicate Ca by correction for carbonate content (CaO*)
KN Index A (Kronberg and Nesbitt, 1981)	Kronberg & Nesbitt Index A *Index against 0: chemical weathering prevailing* *Index against 1: physical weathering prevailing*	$(SiO_2 + CaO + K_2O + Na_2O) / (Al_2O_2 + SiO_2 + CaO + K_2O + Na_2O)$	Relative enrichment of Al and Si oxide phases and inversely leaching of Na, K and Ca	No calculation of silicate Ca by correction for carbonate content (CaO*)
KN Index B (Kronberg and Nesbitt, 1981)	Kronberg & Nesbitt Index B *Decreases with increasing weathering intensity*	$(CaO + K_2O + Na_2O) / (Al_2O_3 + CaO + K_2O + Na_2O)$	Degree of feldspar breakdown	
FENG (Feng, 1997)	Feng Index *Increases with increasing weathering intensity*	$(Al_2O_3 + Fe_2O_3) / (Na_2O + K_2O + MgO + P_2O_5)$	Factors out Ca to avoid biases by carbonate content	Fe as an indicator is problematic to use under redoximorphic conditions
CIA (Nesbitt and Young, 1982)	Chemical index of alteration *Increases with increasing weathering intensity*	$[Al_2O_3 / (Al_2O_3 + Na_2O + CaO^* + K_2O)] \times 100$	Quantitative measure of feldspar breakdown; assumption that feldspar is most abundant and reactive mineral; Al as non-mobile component related to unstable alkali and alkaline metals; can be plotted in A-CN-K diagrams (McLennan, 1993; Nesbitt and Young, 1984; Nesbitt et al., 1996)	Plagioclase is more sensitive to weathering than K-feldspar, thus removal of K is lower (Nesbitt and Young, 1984; Nesbitt et al., 1996); further, K shows no consistency during weathering processes, which is predominantly caused by possible absorption of K by clay minerals and stronger bond by sorptive complexes (Buggle et al., 2011; Harnois, 1988)
CIW (Harnois, 1988)	Chemical index of weathering *Increases with increasing weathering intensity*	$[Al_2O_3 / (Al_2O_3 + Na_2O + CaO^*)] \times 100$	Cf. CIA; K-free equivalent of CIA	No consideration of Al associated with K-feldspar, hence CIW could be mistakenly high for K-feldspar-rich rocks, whether they are chemically altered or not (Fedo et al., 1995)
PIA (Fedo et al., 1995)	Pagioclase index of alteration *Increases with increasing weathering intensity*	$[(Al_2O_3 - K_2O)/(Al_2O_3 + CaO^* + Na_2O - K_2O)] \times 100$	Cf. CIA; only investigates plagioclase weathering	Cannot be used if considerable contents of K-feldspar are evident
CPA (CIW') (Buggle et al., 2011); (Cullers, 2000)	Chemical proxy of alteration *Increases with increasing weathering intensity*	$[Al2O_3/(Al_2O_3+Na_2O)] \times 100$	Cf. CIA; only Al and Na based; also avoids Ca	Reacts very sensitive, if Na is increased in some horizons (e.g. by salinity of topsoils)

for CaO, (3) use CaO* which is corrected by the carbonate content to obtain silicate CaO only. To avoid this problem, (4) calculate without CaO, which implies in turn difficulties caused by focusing on only few or one single mobile element. Weathering intensities have been investigated in arctic permafrost and glaciated regions (e.g. Bäumler, 2001; Melke, 2007; Wagner, 2005), whereas only little research has been performed in dry permafrost areas like the Tibetan Plateau. Due to frigid and arid climate conditions, low chemical weathering intensities can be expected (Brady and Weil, 2008; Fedo et al., 1995; McLennan, 1993).

2.4 General objectives

This thesis aims to investigate, how the highly adapted alpine grassland ecosystems of the central-eastern Tibetan Plateau respond to modified environmental parameters. These alterations are mainly triggered by global climate warming and land use changes (chapter 1). Since these modifications are most likely to affect C and N cycling (subchapter 2.2), it is important to identify and quantify related main influencing parameters. Moreover, these cycles strongly govern vegetation composition and communities, which in turn again influence C and N stocks as well as other environmental conditions, such as permafrost distribution and related land-surface stability. Accordingly, the following specific objectives and hypothesis can be stated:

(1) Approaches at different spatial scales are essential to analyse the relevance of control variables due to immense small- and large scale variability of the ecosystem's parameters (Fig. 2.1). Consequently, this large scale survey uses sampling sites along distinct climate gradients, including continuous, discontinuous, and sporadic permafrost as well as seasonal frozen ground at different altitudes and geomorphological positions. Out of this great variety, subsampling sets can be clustered (e.g. single transects and catenas) to describe specific influences of the monsoon systems, climate gradients, and permafrost patterns. By observing changes of C and N along these natural environmental gradients, key controlling factors can be identified and assessed, supported by the high number of samples, the great length of the transects, and the highly variable preconditions for soil formation.

(2) Permafrost state and distribution significantly affects soil hydrology in water-limited periglacial ecosystems. Accordingly, it can be assumed, that SM has a substantial influence on C and N cycling besides commonly considered temperature variables. Notably, comparing plot and landscape scale is essential to analyse the relevance of water availability and temperature regimes at different levels.

(3) High altitude semi-natural alpine grassland ecosystems are generally nutrient-limited. Therefore, it is fundamental to gain closer insights into parameters affecting N mineralisation, specifically under differing environmental conditions.

(4) Pedodiversity across changing and diverse landscapes is assumed to be a crucial parameter to describe C and N dynamics more precisely; hence the influence of pedogenesis and geomorphological conditions on C and N stocks supplementary to the general control parameters climate, temperature, moisture, vegetation, topography, and hydrology is investigated and analysed.

(5) SM content is interrelated to distinct precipitation-temperature ratios and thus in many parts of the research area to specific permafrost distribution patterns, caused by varying influences of monsoon systems between the eastern and western transect as well as along each transect. Hence, C and N stocks as well as the main influencing parameters will be analysed for continuous and discontinuous permafrost in order to identify potential differences.

(6) Land-surface stability is closely related to permafrost distribution and degradation, which may cause aeolian sedimentation processes. Accordingly, soil formation and thus C and N contents are closely connected to these processes. Therefore, another major goal of this study is to develop geochemical tools to distinguish stable from unstable morphological conditions and to characterise specific states of permafrost. It is hypothesised, that intensity of weathering and pedogenesis can be described by weathering indices, pedogenic oxides fractions and pedogenic oxides ratios. These indicators are in turn all supposed to be essentially related to independent moisture parameters showing clear differences along climate transects and specifically between continuous and discontinuous permafrost. By consideration of other independent climate and soil parameters, WI and POR can be evaluated with regard to their validity in comparable ecosystems.

(7) As a synopsis of the outlined objectives, two major goals are evident: firstly, to investigate C and N cycles with particular consideration of the main influencing parameters on different spatial scales (manuscripts 1-5) and secondly, to reveal reliable tools to quantify and describe intensities of weathering and soil formation (manuscript 6). The latter is particularly important to differentiate preconditions for weathering and land-surface stability with respect to changes of ecosystem parameters and related geochemical cycles. All investigated parameters are very closely linked to numerous strong feedback loops that have to be accounted for when interpreting the gained data. By merging the different approaches, better predictions of spatial uncertainties of C and N stocks in relation to landscape patterns should be feasible.

3 Overview of the manuscripts

3.1 Soil carbon and nitrogen dynamics

3.1.1 Control parameters for soil nitrogen and carbon contents

(Manuscript 1, Global Change Biology 15, 3001-3017)

The investigations presented in this manuscript were solely carried out on landscape scale (cf. Fig. 2.1). Accordingly, all sites were included into statistical calculations across different climatic, hydrological and geomorphological regions. Sites containing continuous, discontinuous and sporadic permafrost as well as areas without or heavily degraded permafrost were studied and treated statistically as one single dataset. The main objective was to figure out how C and N contents respond to independent climatic and pedological variables on landscape scale. In this way, impact of global climate change on the periglacial environment of the Tibetan Plateau and its implications on C and N cycles, and hence on nutrient supply for plants, could be assessed appropriately.

As independent parameters, MAT, MAP, MAST, SM, pH, $CaCO_3$ content, and soil texture were selected to describe the dependent variables SOC, TN as well as mineralised plant available nitrogen, i.e. ammonium-N (NH_4^+-N) and nitrate-N (NO_3^--N). Importantly, besides the listed control parameters, the general influence of pedogenesis is evaluated.

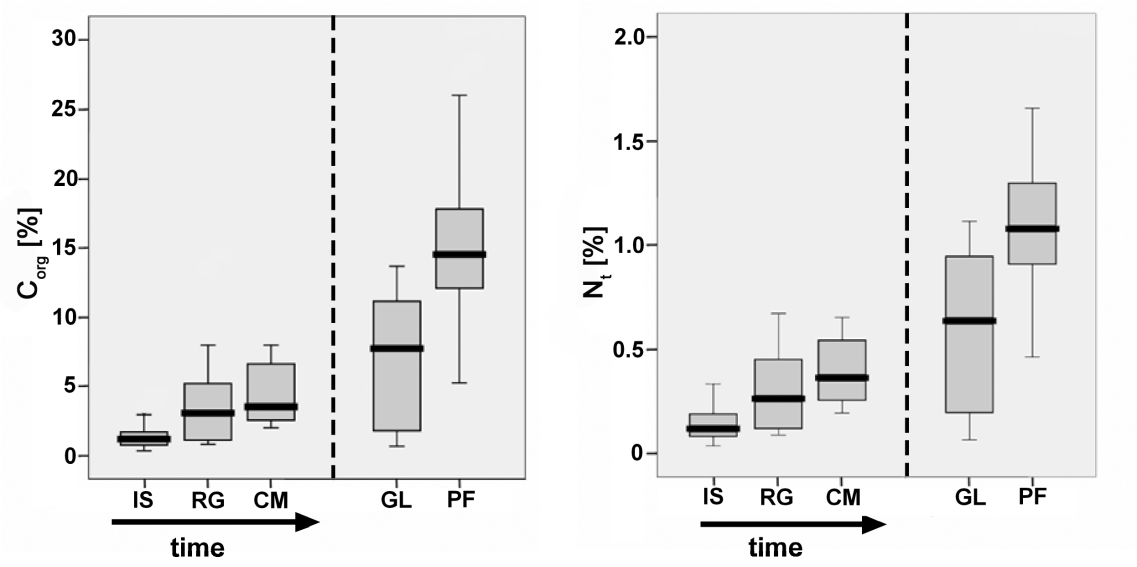

Fig. 3.1 SOC (=C_{org}) and TN (=N_t) stocks related to the degree of soil development. IS, initially formed soils; RG, Regosols; CM, Cambisols; GL, groundwater influenced; PF, permafrost influenced. The boxplots show median, 25% and 75% quartiles with the error bar indicating 5-95% range of the observation.

All examined soil profiles were grouped into five distinct soil groups, representing most of the observed soils. These soil groups can be ordered by their degree and duration of soil development (Fig. 3.1); from initial soil formation to long-term stable pedogenesis under the influence of

permafrost. It could be clearly shown that differences in C and N contents between sites can be related to the presence of permafrost and specific relief positions. There is a clear trend to higher C and N stocks of topsoils with advanced soil development observable, showing high variations on small spatial scales particularly in discontinuous permafrost regions. Consequently, the landscape is very inhomogeneous, reflecting a patchwork of geochemically diverse microecosystems, yielding variations in plant communities, diversity and productivity. These patterns are directly related to soil hydrological regimes, based on different soil drainage classes. Soil texture has a high influence on C and N contents. Whereas sand and silt are strongly correlated, clay has only a weak impact. This is due to the fact, that the research area is dominated by sandy and silty substrates, which exhibit an extremely low negative correlation among each other ($r = -0.95$, $p < 0.01$). Thus, distinct processes control the genesis of sand and silt: recent aeolian sedimentation contributes rather fine proximal generated sands, whereas mature soils are preferably developed on silty material originated from older, mainly glacial loess-like sediments (cf. subchapter 2.1).

Mineralised plant available N can be found almost exclusively as NH_4^+-N. The highest contents occur at water saturated sites, frequently underlain by permafrost, which is in accordance with the current state of research (e.g. Rodrigo et al., 1997; cf. subchapter 2.2). It is most relevant, that the permafrost main soil group (PF) shows by far the highest portions of NH_4^+-N, thus differing clearly from soils solely influenced by groundwater. This supports the assumption that specific organic matter and moisture characteristics are responsible for the high ammonium-N availability (Nadelhoffer et al., 1991). Nitrate-N contents are overall very low, as confirmed by studies performed in comparable ecosystems (e.g. Iwatsubo et al., 1989; cf. subchapter 2.2). However, although low NO_3^--N contents, significant relationships with temperature were detected which can be explained by the strong temperature dependency of nitrification processes (Chapin III et al., 2002; Robinson, 2002).

Moisture parameters were found to have the strongest effect on C and N contents. The general linear model suggests SM as the most important variable, explaining 64% of SOC and 60% of TN variation (Fig. 3.2). Additionally, $CaCO_3$ and sand are included in the models. For the overall interpretation of the results it is essential to analyse, why climate parameters were not considered, since strong relationships between SM and MAP can be commonly expected. However, for the sites on the Tibetan Plateau their correlation is only moderate ($r = 0.45$, $p < 0.01$), thus leading to the conclusion that for SM other environmental controls must be involved. Hence, permafrost has to be considered as the even more relevant variable influencing SM contents. Contrarily, MAT and MAST are highly correlated ($r = 0.91$, $p < 0.01$). This implies rather direct tracing of air into soil temperatures. The shown specific relationships provide strong evidence, that permafrost and relief position are the major determinants for SM in high-altitude periglacial ecosys-

tems. $CaCO_3$ contents mainly control soil acidity, which is an important parameter to assess the state of pedogenesis (Brady and Weil, 2008; Scheffer et al., 2002). This supports the above-mentioned idea of strong interrelationships between C and N contents and pedogenesis.

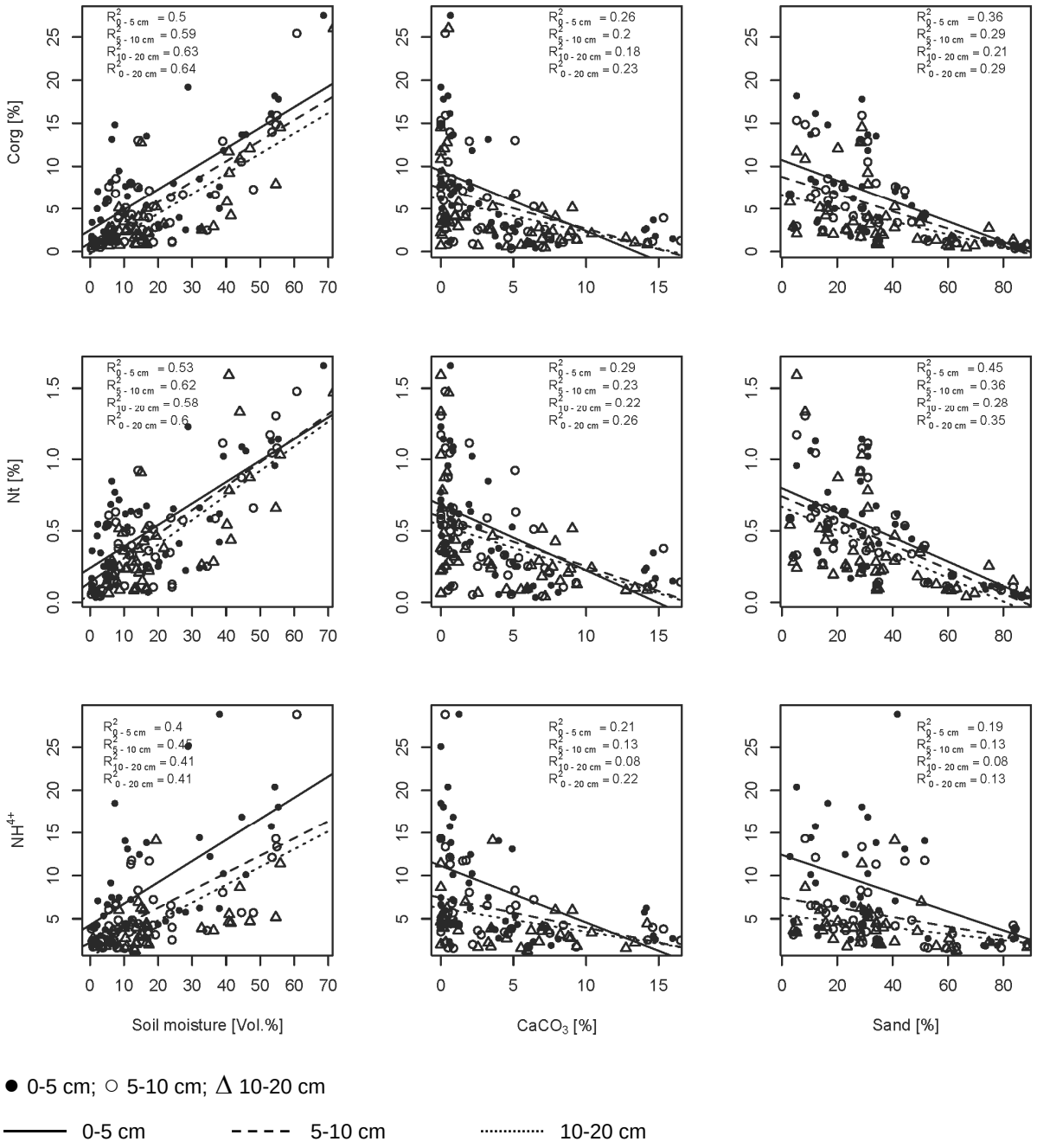

Fig. 3.2 Relationships between dependent and independent variables with the highest impact on the regression model, split into the three depth increments.

In contrast to many other, mainly spatially small-scale studies (e.g. Craine et al., 1999; Kato et al., 2006; cf. subchapter 2.2), the present manuscript indicates that especially nutrient supply is crucial for limiting plant growth even under higher temperatures. This is due to the outlined strong link between hydrological conditions and permafrost, and thus between SM, C, N, and in particular mineralised plant available N. Because rising air temperatures would trigger further

permafrost decay, accompanied by lower SM contents and hence nutrient supply, the effect would be indirectly even inverse. Close linkages between water table, soil drainage and carbon contents or soil respiration have been reported from similar ecosystems (e.g. Johnson et al., 1996; Moore and Knowles, 1989; Robinson, 2002; Shaver et al., 2006). It has been postulated to interpret the opposing findings regarding the influence of moisture and temperature under the aspect, that other factors (SM in the case of the presented study) rather override temperature effects, than negating the fundamental relationship of temperature to C and N cycling (Reichstein and Beer, 2008). Another reason for the weak relations with temperature could be the generally observed temperature-insensitivity of decomposition processes at low temperatures between 3 and 9°C in studies carried out in northern Alaska (Nadelhoffer et al., 1991; MAT of the research area ranges between -5.8 and 2.6°C). Moreover, temperature may be more relevant in ecosystems, where SM or other factors are not limiting or altering the relationships between temperature and soil processes (Craine et al., 1999; Reichstein et al., 2003).

Essentially, results presented in this manuscript clearly show that other factors than temperature predominantly control C and N dynamics on landscape and continental scales (Janssens et al., 2001). Soil temperature is in turn more likely to account for seasonal and diurnal variations at site scale level (Kato et al., 2006; cf. Fig. 2.1).

Another important outcome refers to present and future permafrost degradation features and consequences. Degraded sites exhibit low C and N contents basically caused by two processes: (1) higher mineralisation rates under warmer and dryer conditions, and (2) deposition of proximal airborne sediments. These findings fit well into the general discussion of carbon release under the scope of global climate change (cf. chapter 1). Given the particularly high importance of mineralised N in these generally nutrient-limited alpine grassland ecosystems, the results of this study underline the close connection between plants' available nutrients and degradation processes. The observed rapid decrease of plant available N (i.e. ammonium-N) may limit plant growth supplementary to the direct impact of environmental parameters.

The findings highlighted in manuscript 1 clearly show the need to perform investigations regarding ecosystem responses to changing environmental conditions on different scales. Only the observations on a landscape scale revealed the detangled indirect feedback-mechanisms of altering permafrost environments and the inverse influence of rising temperatures.

3.1.2 Control parameters for soil respiration

(Manuscript 2, PLoS ONE 7 (4), e34968)

The research focus is similar to manuscript 1, as soil respiration (Rs) is the major pathway for C of terrestrial ecosystems, playing a central role in global carbon cycles. Furthermore, the same

sites were used as for manuscript 1 and sampled simultaneously. Thus, Rs patterns and related evaluation of control parameters were also performed on landscape scale across different biomes. Particularly in soil respiration research, this approach is very innovative as only few studies have addressed such large-scale patterns with data compilations (e.g. Bond-Lamberty and Thomson, 2010; Hibbard et al., 2005; Raich and Schlesinger, 1992) and within grassland biomes (e.g. Craine et al., 2002; Raich and Tufekcioglu, 2000). Main objectives were to test whether (1) belowground biomass (BGB) is most closely related to spatial variations in Rs due to high root biomass density, and (2) soil temperature significantly influences spatial pattern of Rs due to metabolic limitation caused by low temperatures in cold, high altitude ecosystems. Similarly to arctic tundra, Tibetan alpine grasslands are characterised by large BGB proportions of total biomass (manuscript 3), high soil SOC densities, specific hydrological and SM patterns (manuscript 1), as well as by the influence of permafrost. Altogether, these features imply a high sensitivity to global climate change (cf. chapter 1).

Table 3.1 Variables included in the regression tree analysis and their importance value.

Variable	*n*	Mean	SD	Range	Importance in regression tree
Soil organic carbon (SOC, %)	42	5.25	4.79	0.339-19.4	1.0000
Aboveground biomass (AGB, g m^{-2})	42	119	100	29.9-530	0.8997
Belowground biomass (BGB, g m^{-2})	42	1816	1957	202-9393	0.8889
Vegetation type (VT)	42	-	-		0.4577
Soil moisture (SM, v/v, %)	42	38.3	50.2	0.44-220	0.4383
Growing season temperature (GST, ^{o}C)	42	6.67	2.25	2.77-11.93	0.1719
Mean annual soil temperature (MAST, ^{o}C)	42	17.0	5.53	–1.12-8.14	0.1621
Growing season precipitation (GSP, mm yr^{-1})	42	306	61.5	170-414	0.0000
Soil temperature (ST, ^{o}C)	42	17.0	5.53	6.30-31.55	0.0000
Soil C/N ratio (C/N, g g^{-1})	39	12.1	2.85	7.97-20.1	0.0000
Soil bulk density (SBD, g cm^{-3})	38	0.94	0.32	0.31-1.65	0.0000
pH	38	7.3	0.52	6.0-8.1	0.0000
Sand content (%)	37	42.3	18.4	20.0-80.0	0.0000
Clay content (%)	37	7.60	6.59	3.0-24	0.0000
Available nitrogen (mmol l^{-1})	37	0.080	0.046	0.026-0.218	0.0000

The 15 examined independent variables are shown in Tab. 3.1. Five of these parameters were selected based on regression analyses: SOC, aboveground biomass (AGB), BGB, vegetation type, and SM. Because these parameters are intercorrelated, structural equation models (SEM) were used to assess the causal relationships among them. The final SEM explained 82.1% of Rs variation (Fig. 3.3). Thereby, increasing BGB and SM were strongly associated with increases of Rs. Accordingly, Rs could be well predicted from these two parameters ($R^2 = 0.82$, $p < 0.001$). The high influence of SM is in accordance with the results reported in manuscript 1 concerning C and N contents, whereas Mahecha et al. (2010) reports evidence for general comparable temperature sensitivities of Rs on a worldwide scale. For the conducted field measurements, no strong effects of ST on Rs could be detected. Hence, Rs does not increase with increasing ST in alpine grassland. Due to covariance between BGB and SM, the contribution of SM in the general linear

models seems small (2% improvement of explanation), but is respectively already partly included in the BGB portion. Importantly, direct and indirect effects of variables could be distinguished: only BGB and SM had direct effects on Rs on landscape scale, whereas the other factors indirectly affected RS through BGB or SM.

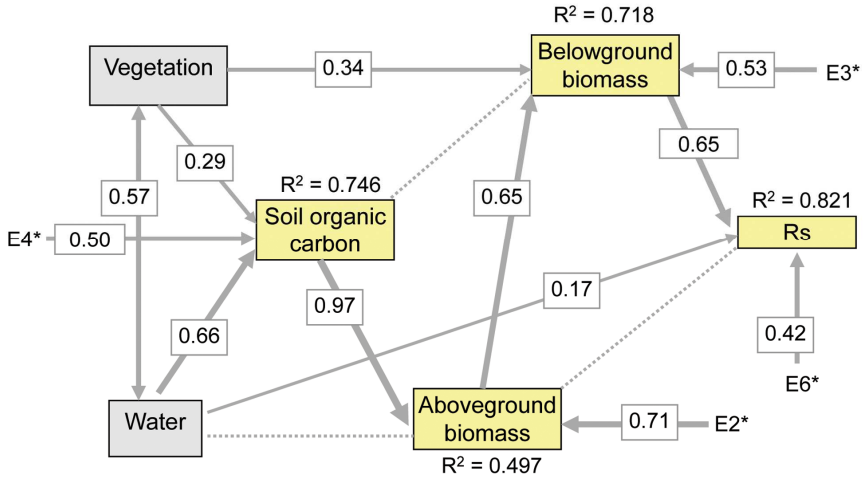

Fig. 3.3 Final structural equation model for soil respiration. Non-significant paths are shown in dashed lines. The thickness of the solid arrows reflects the magnitude of the standardised SEM coefficients. Standardised coefficients are listed on each significant path.

Overall, observed Rs of alpine meadows was 2.5 times higher than of alpine steppes, which is primarily due to differences in biomass and productivity as well as in soil physical properties influencing soil water availability. Averaged across all sites, AGB and BGB, as well as SM were much higher for alpine meadow than for alpine steppe, which significantly increased Rs rates.

The results suggest that a shift from alpine meadow to steppe due to changes of soil hydrological properties as a consequence of permafrost degradation as discussed in manuscript 1, would lead to severe alterations of Rs.

3.1.3 Carbon and nitrogen storage patterns

(Manuscript 3, Environ. Res. Lett. 7, 035401)

This manuscript is well in line with the research approaches of the two previous manuscripts, although concentrating exclusively on the very north-eastern margin of the Tibetan Plateau, north of Qinghai Lake and the Qaidam Basin. The Shule River basin is characterised by low MAT (ca. -5°C) and MAP (ca. 100-300 mm yr^{-1}) (Chen et al., 2011) associated with high evaporation rates (ca. 1,200 mm yr^{-1}) (Xie et al., 2010). This region is located north of the main plateau and hence outside of the main investigation area of the other presented manuscripts. Nevertheless, precisely because of the modified environmental settings and the clearly defined area of a river catchment, a validation of gained insights becomes feasible. The main objective was to test the

spatial distributions of SOC and TN as well as their relationships to soil properties (SM and texture), vegetation (species composition and biomass), and climatic conditions. Soil and vegetation parameters were sampled from 14 plots comprising 42 soil pits, whereas climate data was gained from three climatic stations (Fig. 3.4).

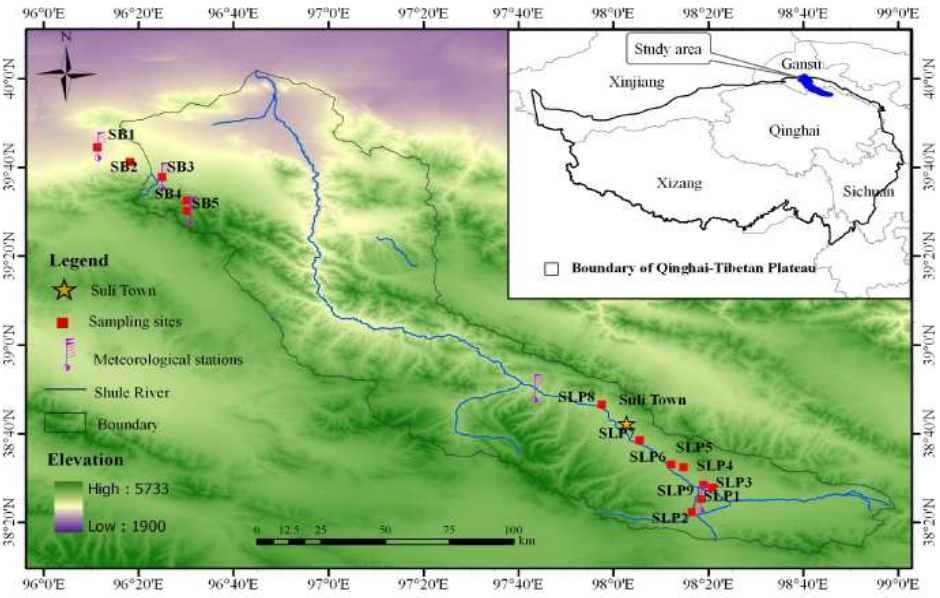

Fig. 3.4 Location of sampling sites in the Shule River Basin at the north-eastern margin of the Tibetan Plateau.

Approximately 96.08 Tg C and 11.61 Tg N are stored in the first meter of soils in the predefined upstream regions of the Shule River basin. The average SOC density is higher (7.72 kg m^{-2}) than Yang et al. (2008) reported for the whole Tibetan Plateau. AGB and BGB show large differences among vegetation types (cf. manuscript 2). SOC density values range from 4.39 kg m^{-2} under desert vegetation to the highest observed SOC density in alpine swamp meadows (19.84 kg m^{-2}). Results reported by other studies from the central Tibetan Plateau revealed higher values for both alpine swamps (49.88 kg m^{-2}; Wang et al., 2002) and meadows (9.05 kg m^{-2}; Yang et al., 2008 vs. 8.70 kg m^{-2} in the present study). Although vegetation types were identical, soil types and climate conditions were very different (i.e. more unstable phases and lower MAP), playing a critical role in determining spatial SOC density distributions (cf. manuscript 4). Moreover, the distinct spatial heterogeneity reported in manuscript1, makes it very difficult to calculate densities and stocks over large spatial scales.

Referred to 1 m, the first 20 cm contain 43% of SOC and 39% of TN, which can be closely related to BGB data. Due to shallow root allocation in alpine ecosystems (cf. Jobbagy and Jackson, 2000; Yang et al., 2009a, manuscript 2), only little SOC can be sequestered in deeper soil layers, hence SOC and TN concentrate in topsoils. Generally, SOC density decreases exponentially with increasing soil depth. However, soils under desert-type vegetation exhibit differing patterns, with the highest values occurring for the pooled 20-40 cm interval. One could argue with the small

amount of AGB input and differing rooting systems with similar BGB inputs than in the 0-20 cm layer. Another explanation could be the presumed higher decomposition levels related to higher temperatures and lower moisture contents. Furthermore, it seems very likely that the frequently observed, mostly aeolian sediment input buries humic horizons and former topsoils leading to syngenetic soil forming conditions and respective dilution of SOC. The related processes are a major outcome of manuscript 1 and closely linked to permafrost degradation processes (cf. manuscript 1 and chapter 1).

Highly significant relationships between SOC density and both AGB and BGB are evident, with BGB being the dominant factor in the topsoils (cf. Hui and Jackson, 2006; manuscript 2). This is confirmed by the high BGB:AGB ratio, which means high portions of BGB in relation to AGB as a result of long-term adaption to extreme environments, observable on a world-wide scale (Mokany et al., 2006). According to Yang et al. (2009a), more than 90% of BGB is concentrated in the top 30 cm of alpine grassland soils. Nevertheless, about 27% of SOC is allocated lower than 40 cm in Shule River basin. This means, that the majority of BGB is distributed much closer to the surface than SOC, which can be attributed to decreasing SOC turnover with depth and migration of SOC as a result of leaching. This allocated SOC material often consists of more persistent and stable soil C pools than close to the surface (cf. manuscript 4; Guggenberger and Kaiser, 2003; Rumpel and Kögel-Knabner, 2011). Significant correlations between SOC density and SM ($r = 0.71$, $p < 0.01$) can be observed on landscape scale (cf. manuscript 1). This is confirmed by the GLM, where beside SM, clay and AGB are included as stable predictors. SM alone accounts for 54% of the variation and was the most significant variable. Similar relationships can be stated for TN. Naturally, the three explanatory variables are intercorrelated, thus only directions of influence can be obtained from the GLM. SM is highly dependent on soil texture, permafrost distribution, and relief position; even more than on the direct climate parameters (cf. manuscript 1). Another example is the interrelation between SM and BGB.

The findings fit well to the results and general discussion of the two previous manuscripts, particularly with respect to frozen soils, their degradation patterns and consequences on ecosystem functioning. It has to be mentioned however, that compared to the central-eastern Tibetan Plateau, permafrost degradation does not play such a prominent role, particularly in terms of sedimentation processes. Large deserts are located around this rather isolated mountain region at the very north-eastern fringe of the Tibetan Plateau. They provide huge sources of aeolian dust and sediments for the above-mentioned sedimentation processes. Moreover, climate conditions are very different with diminishing effects of the monsoonal systems compared to the main investigation area of the other manuscripts. For detailed comparisons of the relevant processes and the differences between the two sub-ecosystems, further detailed research is needed.

3.1.4 Carbon pools and stocks

(Manuscript 4, PLoS ONE 8 (2), e57024)

The previous manuscripts clearly highlight the sensitivity of SOC stored in soils of the Tibetan Plateau to climate and environmental change (manuscript 1 and 3). Consequently, further investigations of SOC stocks and composition are essential to predict future decomposition and potential CO_2 release rates (manuscript 2). For this purpose, two main sites were selected and compared, representing the eastern (EAST) and western transect (WEST) (Fig. 1.1). Site Huashixia (HUA) for EAST is influenced by discontinuous permafrost, whereas Wudaoliang (WUD) on transect WEST features continuous permafrost conditions. At each site, catenas representing the main relief units were established. This approach implies a combination of two different spatial scales: investigations presented in manuscripts 1 and 2 were conducted solely on landscape scale, whereas the present study is based on plot (catena) scales to compare the two transects EAST and WEST on landscape (transect) scale (cf. Fig. 2.1).

To account for these questions, interactions of SOC stocks and corresponding proportions of light and heavy SOC fractions with other soil parameters were examined. Three fractions were isolated using density separation combined with ultrasonic dispersion:

- Free particulate organic matter (FPOM); light fraction (<1.6 g cm^{-3})
- Occluded particulate organic matter (OPOM); light fraction (<1.6 g cm^{-3})
- Mineral associated organic matter (MOM); heavy fraction (>1.6 g cm^{-3})

Overall, site HUA shows much higher SOC contents than WUD, decreasing with soil depth at both sites and in all soil profiles. Moreover, the variation along the catena is more pronounced at HUA. Concerning SOC stocks, corresponding patterns can be observed (mean for 0-30 cm: HUA 10.4 kg m^{-2}; WUD 3.4 kg m^{-2}). Highest stocks are evident in water saturated profiles at HUA (19.3 kg m^{-3}) and lowest at dry sites with low vegetation density at WUD (2.7 kg m^{-3}) (for comparative values see manuscript 3). Partly higher soil moisture at HUA, at some sites even combined with water logging conditions, hampers related microbial decomposition processes (Wagner et al., 2009), leading in combination with a denser vegetation cover to accumulation of SOM (cf. subchapter 2.2; Wang et al., 2006). In the upper 10 cm, 53% of SOC is stored in WUD, whereas only 39% in HUA. This can be partly explained by the long-term adaption processes of grassland species under the more extreme environmental conditions at WUD (i.e. high BGM proportion of total biomass) and the lower tendency to leaching processes in dryer areas (for further discussion see manuscript 3). It also indicates stable conditions, as low dilution effects in topsoils by sediment input (cf. manuscript 6) and slower decomposition rates of SOC under colder temperatures are evident. The results of SOC stocks are generally comparable to other studies conducted on the Tibetan Plateau.

Referring to SOM fractions, contents were determined as follows: OPOM (320 g kg^{-1}) > FPOM (252 g kg^{-1}) > MOM (29 g kg^{-1}). Whereas SOC contents of FPOM decrease with depth, slightly increasing values for OPOM fractions can be observed. This is explicable by the increasing SOC content of the fractions with increasing depth. The depth function of MOM follows the bulk soil contents. About 18% of the total contents in HUA and 14% in WUD are contributed by FPOM, OPOM accounts for 8% at both sites, and MOM is responsible for 74 and 78 %, respectively (Fig. 3.5). Due to the above-discussed processes concerning lower litter production at WUD, lower fraction masses and SOC contents lead to lower proportions of POM on overall SOC stocks. As for bulk soil, largest FPOM and OPOM shares are present in water saturated profiles at HUA due to inhibited further decomposition of SOM.

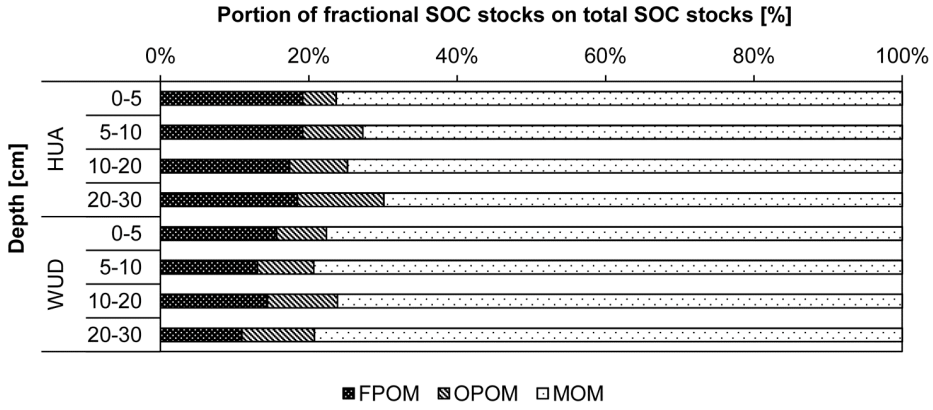

Fig. 3.5 Portion of fractional soil organic carbon (SOC) stocks on total soil organic carbon stocks in particular depth at Huashixia (HUA, top) and Wudaoliang (WUD, bottom).

Correlation with selected soil parameters brought interesting results; also for the interpretation of issues discussed in the other manuscripts. SM and SOC stocks show strong correlations with active layer thickness for HUA in discontinuous permafrost. By contrast, WUD only indicates a moderate correlation for SM vs. active layer thickness. It can be deduced from these results, that continuous permafrost (WUD) implicates more stable conditions with less variation among the investigated environmental parameters (cf. manuscript 6), which can be confirmed by the much lower variation of SOC stocks as well as SM contents. The explicitly lower SOC stocks in WUD can be attributed to drier soil conditions and a shorter vegetation period (cf. general climatic patterns, subchapter 2.1). HUA contains higher portions of easily decomposable POM fractions (especially at water saturated sites), which are particularly important for evaluating potential carbon release due to their short turnover rates and related enhanced vulnerability. The low mass portion of POM related to SOC mass balance must not detract from their large contribution to SOC stocks due to their high SOC contents.

3.1.5 Organic and inorganic carbon

(Manuscript 5, Biogeosciences 9, 2287-2299)

This manuscript broadens the context in both spatial scales and soil carbon patterns. It compares the sites on the Tibetan Plateau (cf. manuscripts 1, 3 and 4) with sites of a NE-SW stretching transect across the Inner Mongolian grasslands and additionally investigates soil inorganic carbon (SIC) besides SOC (Fig. 3.6). Despite SIC is an important component of the global carbon cycle, far less attention has been drawn on SIC than on SOC (Eswaran et al., 2000; Mi et al., 2008; subchapter 2.2). The main objective was to identify key controlling factors of SIC and SOC contents by comparing the two geographically different ecosystems. Moreover, potential responses and feedback mechanisms to changes of the environmental parameters were evaluated.

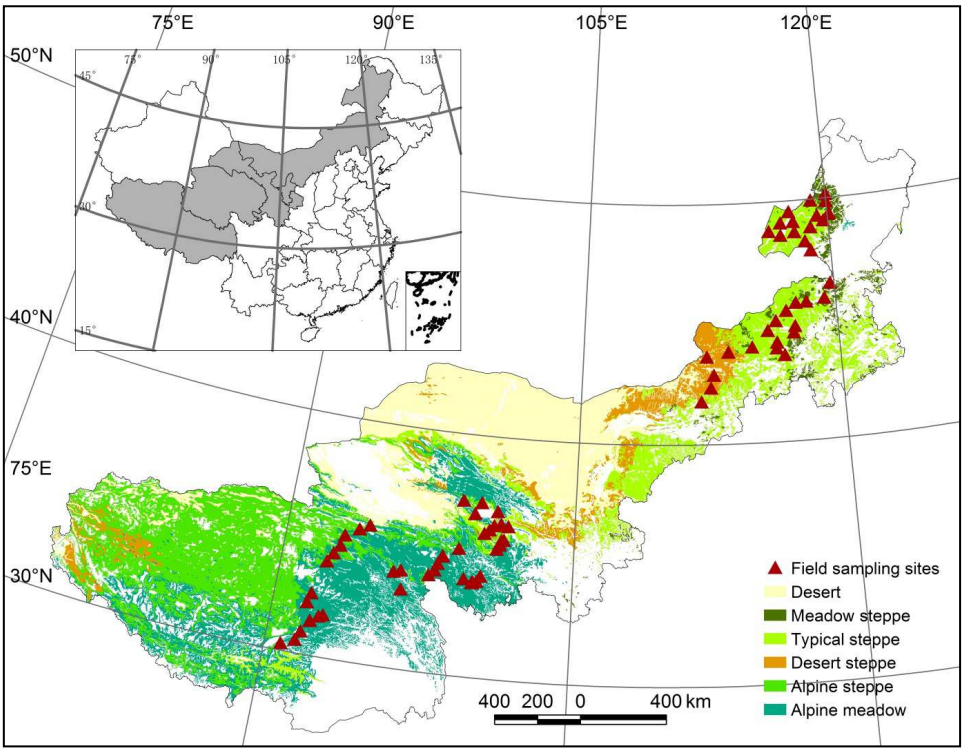

Fig. 3.6 Vegetation map and study sites on the Tibetan Plateau and in Inner Mongolia (1 : 1,000,000) (Chinese Academy of Sciences, 2001).

Across all sites, SOC exceeds approximately nine times the contents of SIC. Significantly higher concentrations for both SIC and SOC are evident for Tibetan grasslands compared to the sites in Inner Mongolia, at site level as well as for depth increments. Since there are no significant differences of soil pH between Tibetan and Inner Mongolian grasslands evident, two other explanations are likely. Firstly, soils on the Tibetan Plateau are younger, thus parent material and substrates trace their characteristics to related soils more strongly (cf. manuscripts 1 and 6) leading to higher lithogenic inorganic carbon (LIC) contents. In addition to it, carbonate migration is lower. Secondly, the much higher elevation of the Tibetan Plateau has a conceivable influence due to lower CO_2 partial pressure (Körner, 2003), which is even enhanced by the lower soil res-

piration. The lower CO_2 partial pressure moves the equilibrium towards more precipitation of carbonates, benefitting the formation of pedogenic inorganic carbon (PIC). Oppositely, differences of SOC can be mainly attributed to climate parameters. Effects of low temperatures and high moisture conditions are discussed in detail as major outcomes in manuscripts 1, 2, 3 and 4.

Distinct parameter sets best explain patterns of SIC and SOC. Climate, soil physical and chemical properties (including pH, MAT, MAP, potential evapotranspiration and SM) best describe SIC, biotic and climatic factors (including vegetation type, AGB, potential evapotranspiration and growing season precipitation) are predominant for SOC.

One major outcome is that pH is the most important factor for describing SIC, explaining 42% of the variation. Acidification accordingly decreases the formation of SIC (Lal and Kimble, 2000; Suarez, 2000). Other influencing factors, which contribute to the overall explanation, are different below and above a threshold of pH 7. Below pH 7, these are moisture variables (i.e. MAP and SM), which is caused by related leaching processes. These become more important, since with higher acidity SIC tends to be in form of dissolved bicarbonate. Contrarily, above pH 7, thermal factors show stronger negative influence due to positive effects on biological activity and Rs, implying increasing soil CO_2 partial pressure, hence inhibiting the formation of carbonates in topsoils.

Linear regression models were used to predict SIC under the scope of soil acidification scenarios. The results imply that given the acidification rate for Chinese grassland soils in the future is comparable to acidification trends that has been measured in cropland soils adjacent to the investigated grassland during the past two decades, SIC will decrease by 30% and 53% in the Inner Mongolian and Tibetan grasslands, respectively. Nevertheless, the negative relationship between soil pH and SOC leads to the assumption that decomposition of SOC would be in turn slowed down (corresponding relationships have been detected and described also in manuscripts 1 and 6). Hence, no significant impact by soil acidification on total soil carbon stocks can be expected, notably also because of the small average proportions of SIC.

3.2 Plot and landscape scale interrelations of weathering processes and pedogenesis

(Manuscript 6, Geoderma, submitted in September 2013)

Manuscript 1 has clearly identified pedogenesis as an important predictor for C and N contents of soils in the periglacial environment of the Tibetan Plateau. Pedogenesis is in turn closely associated with weathering intensities under specific environmental conditions. Therefore, reliable tools are needed to account for varying weathering patterns across permafrost influenced ecosystems. Different geochemically induced weathering indices (WI) and pedogenic oxide ratios (POR) were used (detailed descriptions and discussion in subchapter 2.3) to describe and to

quantify weathering and soil formation processes along climatic gradients, mainly affected by varying influences of the Asian and Indian Monsoon. These climate settings cause particular SM conditions, in turn closely related to permafrost state, substrate, and topography (cf. manuscript 1). Nine sites with in total 30 soil profiles were investigated along the eastern (EAST) and western (WEST) transect. To evaluate relationships of WI and PO with independent climate and soil variables, correlation analyses and regression models were calculated for each group of subsamples and thus on each spatial scale (Fig. 2.1). According to the actual knowledge, the research presented in this manuscript is the first attempt of a comprehensive application of different WI and POR to substrates of currently permafrost-affected soils. In the following, for the different WI and POR abbreviations are used; explanations can be found in Tab. 2.1 and 2.2).

This paper combines the spatial scales applied in manuscripts 1, 2, and 5 (landscape scale) with that of manuscript 4 (plot scale). For this purpose, subsamples were generated. The TOTAL sampling set (landscape scale), was split into two transects EAST and WEST (landscape (transect) scale) and main sites with catenas along each transect (plot (catena) scale), including two main representative sites Wudaoliang (WUD) and Huashixia (HUA) (cf. manuscript 4). These are essential to get a better understanding of small-scale pedogenic processes. The two sites were chosen in respect of similar geomorphological preconditions, such as relief, hydrology, and exposure. Single support sites provide valuable data to analyse trends along transects and to interpolate between the main sites (site (soil profile) scale). Thus, both the variation within sites and along transects is represented in the analyses. An overview of the applied spatial scales is given in Fig. 2.1. Moreover, TOTAL was bulked into four distinct soil groups based on field soil descriptions and laboratory analyses (comparable to manuscript 1): initially formed soils (IS), Cambisols (CM), groundwater influenced soils (GL), and permafrost affected soils (PF).

CIA, CIW and PIA show largely identical results with no differences in indicating weathering tendencies. This is confirmed by correlation analyses among them ($r = 0.99$, $p < 0.01$). It can therefore be concluded that the influence of K is negligible for the investigation area, which is mainly due to the stronger weathering resistance of K-phases (cf. subchapter 2.3, Tab. 2.2), especially in the cold and dry climate of the research area. Additionally, feldspars are predominantly represented by plagioclases (cf. A-CN-K diagrams, Fig. 3.7). Ca-free index CPA exhibits problems with increased salinity in topsoils, particularly at sites with strong ascending water flow under negative water balance. This leads to an underestimation of weathering intensities due to higher Na contents, since CPA considerers Al and Na as the only elements. Even though there are profiles where CPA and other WI show better correspondence to related soil analyses, CIA plots the most comprehensible results, if $CaCO_3$ had been analysed in the laboratory allowing concise calculation of CaO* (Tab. 2.2). Generally, WI trace climate trends along both transects very differentiated (higher MAT and MAP from N to S and W to E).

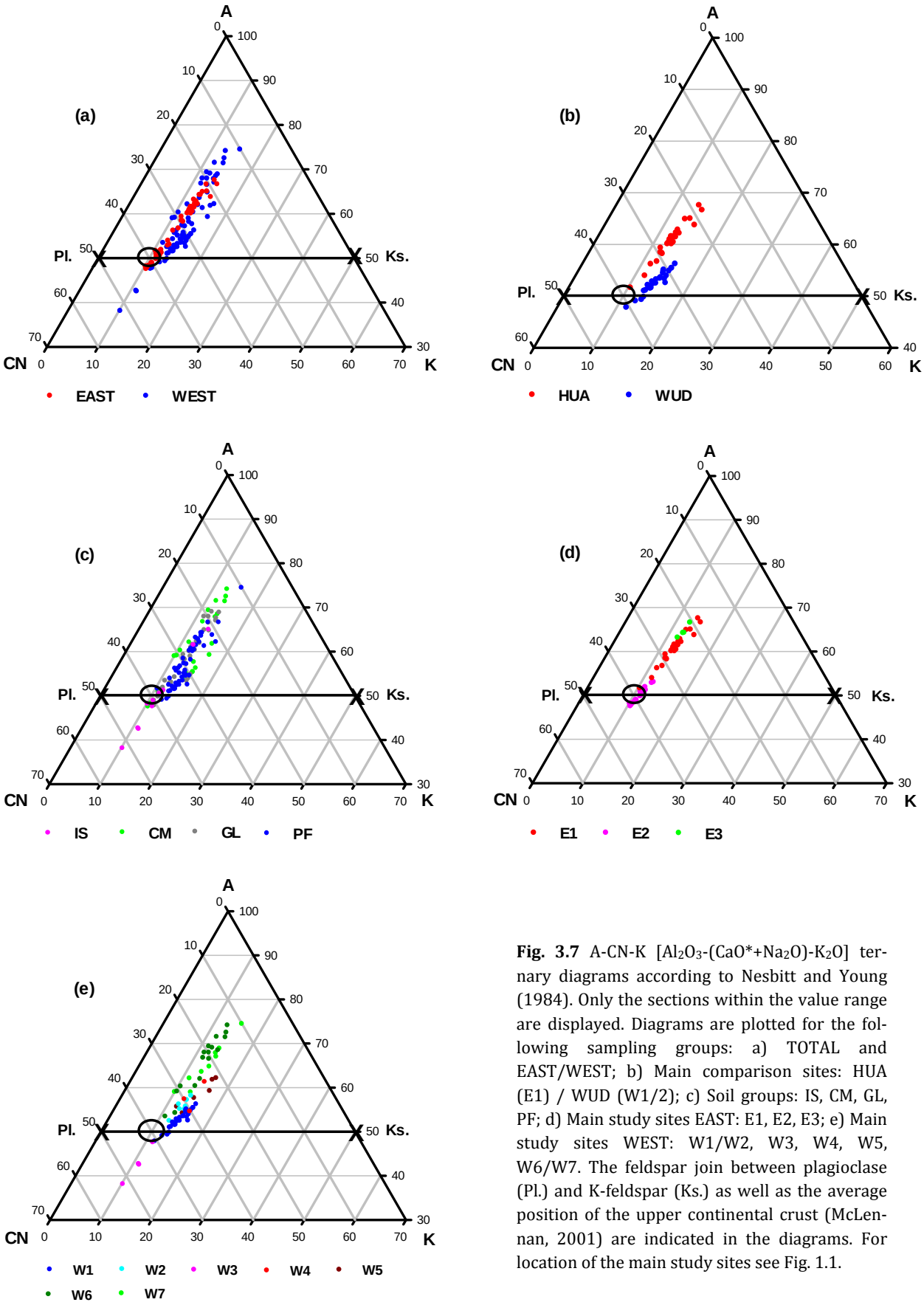

Fig. 3.7 A-CN-K [Al_2O_3-(CaO*+Na_2O)-K_2O] ternary diagrams according to Nesbitt and Young (1984). Only the sections within the value range are displayed. Diagrams are plotted for the following sampling groups: a) TOTAL and EAST/WEST; b) Main comparison sites: HUA (E1) / WUD (W1/2); c) Soil groups: IS, CM, GL, PF; d) Main study sites EAST: E1, E2, E3; e) Main study sites WEST: W1/W2, W3, W4, W5, W6/W7. The feldspar join between plagioclase (Pl.) and K-feldspar (Ks.) as well as the average position of the upper continental crust (McLennan, 2001) are indicated in the diagrams. For location of the main study sites see Fig. 1.1.

Similarly, permafrost distribution is reflected by the oscillations of WI, which are generally high in the zone of discontinuous permafrost of EAST, whereas sites influenced by continuous permafrost show only very small changes in weathering intensities due to stable temperature-moisture (Zhang et al., 2003) as well as sedimentary regimes (manuscript 1). This is true for both variations with soil depth and between sites (manuscript 4). For many profiles, especially in discontinuous permafrost, lower weathering intensities can be observed in topsoils compared to subsoil horizons. Beside the disconnection of frequently turf-like topsoils from the mineral soil body, this also reflects a recent input of aeolian sediments (cf. manuscripts 1 and 3). Related permafrost-degradation processes and phases of instability in the past are responsible for multi-layered soil profiles that occur frequently on the Tibetan Plateau. Weathering trends with soil depth and layering of soil profiles can be accordingly identified and described by WI, being in most cases in good correspondence to layering indicated by other soil parameters.

Ternary diagrams are displayed in Fig. 3.7 for all sampling groups. The plots provide valuable information about weathering intensities as well as with respect to the homogeneity of source materials. For TOTAL, almost 25% of the samples plot below or only slightly above the feldspar join, indicating essentially no weathering processes. Half of all samples are not or only slightly weathered, whereas the second quartile and the maximum value show sites with comparably intense weathering conditions. The comparison between the main representative sites HUA and WUD (Fig. 3.7b) reveals very distinct patterns, both in terms of weathering intensities and source material, hence reflecting typical discontinuous and continuous permafrost conditions, respectively. Besides mean weathering intensities at WUD, also the variance is much smaller than in HUA (comparable patterns for SOC in manuscript 4). This is also evident for the homogeneity of parent material (more stability in sedimentary systems). Climatic trends and permafrost patterns along both transects are displayed in Fig. 3.7d and Fig. 3.7e. EAST (Fig. 3.7d) shows an overall increasing weathering trend coincident to the large-scale climate gradient (increasing MAT and MAP). Sites are basically likewise ordered by their geographical location for WEST (Fig. 3.7e), however showing much higher scattering, since WEST is longer, covering more different climate, geomorphological and geological preconditions.

Multiple linear regression analyses (MLR) were performed for POR and all sampling groups (Tab. 3.2). For TOTAL, (Fed-Feo)/Fet ratio proved to be most useful to estimate relative pedogenic age and to analyse weathering differentiation (Arduino et al., 1984; Wagner, 2005), with 64% of explained variance by the MLR. Moisture parameters and soil acidity have the overall strongest negative influence (i.e. lower weathering intensities associated with higher SM and soil acidity). Since the high impact of soil acidity is related to the buffer of silicate weathering and iron release (Brady and Weil, 2008; Schwertmann, 1964), it has the most significant influence on Fed/Fet. For soil texture, silt and clay are mostly included into the models, with higher clay con-

tents indicating higher weathering intensities and vice versa relations for silt. For Feo/Fed, as an expression of recent soil weathering activity, moisture variables are even more dominant showing inverse effects, related to immature and particularly redoxi-morphic soils with high contents of oxalate-extractable oxides (Schwertmann, 1964). It is pivotal for further interpretations that contrarily to other PO-fractions, Fep shows no significant correlations with Fet contents, hence allowing an evaluation of this PO fraction without being related to Fet. Importantly, 63% of the variation of Fep can be mainly explained by soil acidity and SM, which in turn are closely linked to SOC. It could be demonstrated that pyrophosphate extracts mainly organically bound pedogenic iron, indicated by the high correlation with SOC ($r = 0.89$, $p < 0.01$). Furthermore, Fep is highly positively correlated with SM, but not with temperature parameters. SM was also found to be the most important variable influencing SOC contents (manuscript 1) as well as soil respiration (only parameter after BGB that shows direct effects, manuscript 2) on landscape scale. The line of argument can be completed with the strong negative correlation of Fep with soil acidity. Acid soil conditions correspond to hampered turnover of organic matter (cf. manuscripts 1 and 5) and the formation of fulvic as well as humic acids. Indirectly, this also suggests stable soil forming processes with little carbonatic aeolian sediment input. The connection between Fep and less developed or weathered soils, mainly influenced by permafrost or groundwater, can also be confirmed by the negative correlation with (Fed-Feo)/Fet and the positive relation to Feo/Fed.

Referring to the transects, soil acidity is dominant for EAST with a higher explained variance of the MLR due to a higher small-scale variability of independent variables as a consequence of more unstable discontinuous permafrost conditions (cf. manuscript 4), whereas SM is the most important parameter for WEST. However, WEST is climatically and geologically more diverse (climate parameters are included for WEST). This emphasises the importance to discuss small vs. large scale variability.

The main representative sites HUA and WUD also highlight this issue. For (Fed-Feo)/Fet, WUD shows the highest observed explained variance (85%) of all sampling groups and corresponding dependent variables. SM has the highest influence equally followed by clay content and soil acidity. Contrarily, even though mean and variance of SM are much higher, moisture parameters are not included in HUA. Instead, soil acidity and texture account for the main variation. Accordingly, shifts of substrates due to higher instability and more complex sedimentation processes are immanent for discontinuous permafrost areas (cf. results of WI). Other parameters, such as relief position and slope or geomorphologic activities like sedimentation by wind and water are more important, overprinting the direct effects of SM on weathering and pedogenesis. This idea is supported by the results for Fed/Fet: HUA has the lower p-value and higher R^2, whereas WUD plots above the significance level. Hence, the degree of iron release varies more in HUA.

Table 3.2 Summary of the multiple linear regression model (MLR). The level of significance is marked (*** $p < 0.001$; ** $p < 0.01$; * $p < 0.05$; others $p > 0.05$). Directions of influence indicated by [+] for positive and [-] for negative effects of the variable on the MLR.

	POR	Variables – Ranked by significance	RSquared	RSquared adj.	Significance
TOTAL	Fed/Fet	MAP*** [-], pH*** [-], SM** [-], Silt* [-], Clay [+], MAT [-]	0.55	0.51	***
	(Fed-Feo)/Fet	MAP*** [-], SM*** [-], pH*** [-], MAT [-], Silt [-], Clay [+]	0.64	0.62	***
	Feo/Fed	SM*** [+], MAP*** [+], pH* [+], Silt [+], MAT [+], Clay [-]	0.49	0.45	***
	Fep	pH*** [-], SM*** [+], Sand* [+], Clay [+], MAP [+], MAT [+]	0.63	0.60	***
	Fet-Fed	MAP*** [+], pH*** [+], Sand*** [-], MAT [+], Clay [+], SM [-]	0.50	0.46	***
	Fed-Feo	SM*** [-], MAP*** [-], Clay* [+], pH* [-], Silt [+], MAT [+]	0.59	0.55	***
EAST	Fed/Fet	pH*** [-], SM [-], Clay [-], Sand [+]	0.41	0.32	**
	(Fed-Feo)/Fet	pH** [-], SM** [-], Clay [-], Silt [+]	0.44	0.36	**
	Feo/Fed	SM* [+], MAT [+], Silt [+], Clay [+]	0.35	0.26	*
	Fep	pH*** [-], SM [+], Clay [-], Silt [+]	0.75	0.71	***
	Fed-Feo	pH** [-], SM** [-], Clay [-], Silt [-]	0.42	0.33	**
WEST	Fed/Fet	MAT*** [-], $CaCO_3$* [-], Clay* [+], SM* [-], pH [+], Sand [+], MAP [+]	0.42	0.33	***
	(Fed-Feo)/Fet	SM*** [-], MAT*** [-], pH [+], Clay [+], Sand [-], $CaCO_3$ [-], MAP [+]	0.65	0.59	***
	Feo/Fed	SM*** [+], Sand** [+], MAT** [+], $CaCO_3$ [-], pH [-], Clay [+], MAP [+]	0.70	0.65	***
	Fep	SM*** [+], Clay* [+], pH [-], Sand [+], MAP [+], MAT [-], $CaCO_3$[-]	0.67	0.62	***
	Fet-Fed	Sand*** [-], MAT*** [+], SM*** [-], pH [+], $CaCO_3$ [-], MAP [-], Clay [-]	0.85	0.83	***
	Fed-Feo	SM*** [-], Sand*** [-], pH [+], $CaCO_3$ [-], MAT [-], Clay [+], MAP [-]	0.61	0.54	***
HUA	Fed/Fet	$CaCO_3$** [-], SM** [-], Clay [+], pH [-]	0.76	0.67	**
	(Fed-Feo)/Fet	$CaCO_3$** [-], Silt* [-], Clay [+], pH [-]	0.52	0.40	*
	Fep	SM [+], pH [-], Clay [-], $CaCO_3$ [-]	0.58	0.42	*
	Fet-Fed	Clay*** [+], Silt* [-], pH [+], $CaCO_3$ [+]	0.80	0.75	***
	Fed-Feo	$CaCO_3$** [-], Silt* [-], Clay [+], pH [+]	0.55	0.44	**
WUD	Fed/Fet	SM [-], pH [+], $CaCO_3$ [-]	0.42	0.28	
	(Fed-Feo)/Fet	SM** [-], Clay** [+], $CaCO_3$ [-]	0.90	0.85	***
	Feo/Fed	Clay* [-], SM [+], $CaCO_3$ [+]	0.72	0.59	*
	Fep	Clay* [-], $CaCO_3$ [+], SM [+]	0.64	0.48	

Table 3.2 continued

	POR	Variables – Ranked by significance	RSquared	RSquared adj.	Significance
WUD	Fet-Fed	Clay*** [+], $CaCO_3$ [+]	0.87	0.86	***
	Fed-Feo	Clay*** [+], SM* [-], $CaCO_3$ [-]	0.92	0.89	***
CM	Fed/Fet	pH* [-], MAP [-], Sand [+], SM [-]	0.55	0.43	*
	(Fed-Feo)/Fet	pH [-], MAP [+], Sand [+], SM [-]	0.46	0.31	
	Fet-Fed	Sand*** [-], pH [+], MAP [+], SM [-]	0.86	0.82	***
	Fed-Feo	Sand** [-], SM [-], MAP [-], pH [-]	0.69	0.61	**
GL	Fed/Fet	MAP*** [-], pH* [-], MAT [+], Sand [-], SM [-]	0.70	0.62	***
	(Fed-Feo)/Fet	MAP*** [-], SM** [-], MAT [+], pH [-], Sand [-]	0.72	0.65	***
	Feo/Fed	MAP** [+], SM* [+], Sand [-], MAT [-], pH [-]	0.60	0.50	**
	Fed-Feo	MAT [-], MAP [+], Silt [+], pH [+], SM [+], Clay [+]	0.67	0.59	***
PF	Fed/Fet	pH** [-], MAP** [-], MAT* [-], Clay [+], Sand [+], SM [+]	0.52	0.38	*
	(Fed-Feo)/Fet	MAP** [-], MAT* [-], pH [-], Clay [+], SM [-], Sand [-]	0.59	0.46	**
	Feo/Fed	MAP [+], SM [+], Sand [+], MAT [+], Clay [+], pH [+]	0.59	0.46	**
	Fep	$CaCO_3$*** [-], SM [+], Clay [+], Sand [-], MAT [+]	0.72	0.65	***
	Fet-Fed	pH*** [+], MAP*** [+], Sand [-], Clay [+], MAT [+], SM [+]	0.66	0.56	***
	Fed-Feo	MAP* [-], MAT [-], Clay [+], Sand [-], pH [-], SM [-]	0.55	0.41	**

In relation to soil groups, there is a clear difference evident between GL and PF subsamples, specifically describable by PO: whereas SM is a highly significant variable for GL, PF shows general climatic parameters having the highest influence in the MLR. This can be related to the distinct soil-geographical patterns of these soil groups: permafrost is required as a principal precondition for PF (climate-zonal soil formation), against what GL soils are linked to a greater degree to relief positions and are consequently occurring across different climate regions of the Tibetan Plateau (azonal soil formation). Accordingly, parameters directly and locally influencing soil formation (e.g. SM) are more significant. The included parameters for CM well explain main soil forming processes in cambisols. Furthermore, it is an essential outcome, that Fep contents significantly distinguish GL and PF soil groups (two-tailed t-test with $p < 0.05$), even though both typically reveal considerably high SM and TOC contents (manuscript 1). Correspondingly, only PF calculate a high significant MLR for Fep. Specific redoxi-morphic and soil formation processes with related organic matter structures under the influence of permafrost (cf. manuscripts 1 and 4) are assumed to differentiate GL and PF soil groups. It is important to note that PF also accounts for the highest ammonium-N contents (manuscript 1), which may be related to these processes. However, further research is needed to assess potential connections.

WI, PO fractions, and POR were successfully used to describe patterns of weathering and pedogenesis for climatic gradients along the two transects EAST and WEST. PO and POR reflect soil formation on small spatial scales depending on relief position and substrate genesis in addition to mainly climatically induced long-term weathering processes describable by WI. This can be underlined by the clear differentiation of several soil groups by PO (two-tailed t-tests with $p < 0.05$); whereas for WI only under involvement of the extreme soil group IS significant results were obtained.

4 Summary

This thesis was conducted within the scope of a graduation fellowship from the state of Baden-Württemberg, Germany (Grant No.: VI 4.2-7631.2/Baumann) in cooperation with the Department of Ecology, Peking University, Beijing. Scientists specialised in both ecology and soil science investigated the same sites, thus allowing an interdisciplinary approach to evaluate soil properties, C and N cycles as well as geomorphological processes in close connection to ecosystem interrelations on the Tibetan Plateau. The research sites are located along a 1,200 km long north-south transect at altitudes between 2,925 and 5,105 m ASL. Two thirds of the Tibetan Plateau is influenced by permafrost. Due to the high sensitivity to global climate warming and land use changes, permafrost degradation processes are widespread, increasing the heterogeneity of soil formation, soil hydrology, and related soil chemical processes (i.e. C and N cycling). In order to account for the resulting extremely diverse ecosystem, investigations at different spatial scales related to large-scale climate patterns were performed. The scales comprise the total main transect, the split transect into an eastern and western section, diverse catenas along distinct geomorphological relief units, and finally the single site soil profiles.

The first part of this work examines C and N contents as well as portions of plant available mineralised nitrogen in relation to their main influencing parameters. For investigations on landscape scale, soil moisture was found to have the strongest effect on C and N cycling, followed by $CaCO_3$-content and soil texture. Altogether, the general linear model explains 64% and 60% of the variation of soil organic carbon (SOC) and total nitrogen (NT) contents, respectively. Thereby, two aspects are important: (1) temperature variables have no significant influence and (2) indicators for soil development (i.e. $CaCO_3$ and soil texture) are included besides commonly considered ecological (i.e. moisture, temperature and biomass) parameters. It could be shown that in the highly diverse permafrost-affected ecosystem of the Tibetan Plateau, other factors than precipitation mainly control soil moisture contents and distribution, with permafrost and relief position being the most dominant parameters. Since pedogenic parameters turned out to be important predictors, the degree of soil development can be regarded as an additional control quantity, indicating higher C and N contents of topsoils with longer duration of undisturbed and stable soil development. Mineralised plant available N can be almost exclusively found as ammonium-N, which is closely related to higher soil moisture contents and frigid climate conditions, showing by far the highest contents in the permafrost main soil group. As nitrification is strongly temperature dependent, nitrate-N contents are correspondingly very low. The results provide clear evidence that limitation in plant available nutrients as a negative feedback to lower soil moisture is crucial for plant growth in nutrient-limited alpine grassland ecosystems, even though higher temperatures occur with respect to climate warming. Importantly, these strong feedback mechanisms between altering permafrost conditions (degradation and higher active

layer thickness) and hence reverse influence of rising temperatures (further decay of permafrost and related dryer conditions) could be only detected by conducting this study on landscape scale. These dependencies are based on the overall limitation of moisture, because evaporation exceeds precipitation by far at all investigated sites. Degraded permafrost profiles show low C and N contents combined with distinct depth patterns, mainly caused by higher mineralisation rates and deposition of proximal airborne sediments. This is can be exemplarily shown for the Shule River basin located at the very north-eastern margin of the Tibetan Plateau, where soils under desert-type vegetation have their highest SOC density in soil depths between 20 and 40 cm, but not in the top 20 cm as evident for all other vegetation types. The main reason for these patterns are most likely such syngenetic soil forming processes. Results of soil respiration measurements basically confirm the findings observed for C and N contents. Belowground biomass and soil moisture explain 82% of the variation, whereas no direct effects of temperature could be described. Respiration values of alpine meadows were 2.5 times higher than of alpine steppes, which is a consequence of higher biomass and productivity in alpine meadows.

Besides the relations to control variables, SOC was further analysed with regard to its stocks and composition. The comparison of two main investigation sites for discontinuous and continuous permafrost, respectively, clearly shows higher SOC stocks for discontinuous (10.4 kg m^{-2}) than for continuous permafrost (3.4 kg m^{-2}). Highest values occur at water-saturated profiles (19.3 kg m^{-2}), causing positive feedbacks to even higher SOC accumulation, if in turn denser vegetation isolates the soil. At the same time, these soils contain substantial higher portions of easily decomposable particulate organic matter fractions, which are especially vulnerable to climate change owing to shorter turnover rates. The colder and dryer climate in continuous permafrost areas leads to a lower productivity and an allocation of belowground biomass mainly in the top 10 cm. This can be approved by studies conducted in the Shule River basin, also characterised by low mean annual temperature and precipitation, showing average SOC stocks of 7.7 kg m^{-2}. Moreover, different vegetation types can be distinguished very clearly, ranging from 4.4 kg m^{-2} under desert vegetation to 19.8 kg m^{-2} under partly water-saturated alpine swamp meadow (cf. above-mentioned corresponding respiration rates related to vegetation type patterns).

Moreover, it could be shown that soil inorganic carbon (SIC) and SOC are influenced by different parameter sets. Whereas soil physical and chemical properties are most appropriate to describe SIC, biotic and climatic factors are more important for SOC. Soil pH was found to predict 42% of SIC variation, leading to lower contents with decreasing pH. However, the overall effect of the released carbon under scenarios of potential soil acidification is assumed to be compensated, since SOC reacts vice versa to increased soil acidity.

Since pedological processes proved to have significant influence on C and N contents, it is important to specifically qualify related weathering and sedimentation processes depending on the

state of permafrost as well as land surface stability. To address this issue, weathering indices and pedogenic Fe-oxides were applied to particular sampling groups, distinctly influenced by the Indian and Asian Monsoon systems. The chemical index of alteration (CIA) represents the most useful weathering index, best describing large scale climate trends, varieties of substrates, and specific permafrost patterns. For pedogenic Fe-oxides, (Fed-Feo)/Fet ratio best illustrates small-scale shifts of pedogenesis. This can be confirmed by the differentiability of the main soil groups, which cannot be obtained by CIA. Essentially, groundwater and permafrost influenced soils can be clearly distinguished by distinct parameter sets best explaining each soil group: climate parameters for the permafrost soil group (climate-zonal soil formation), and site-specific variables for groundwater-influenced soils (azonal soil formation). Moreover, the two soil groups can be significantly differentiated by Fep, even though both show high soil moisture and SOC contents. Therefore it can be assumed, that particular redoxi-morphic and soil formation processes with corresponding soil organic matter structures evolve under the influence of permafrost. Altogether, the application at various spatial scales give strong evidence that weathering indices and pedogenic Fe-oxides are useful tools to depict states of permafrost distribution and its degradation features.

Summarising, the described geochemical patchwork (manuscripts 1-5) can be disentangled by applying weathering indices and pedogenic oxides ratios, depending on the scale and process. Together with the evaluation of the prevailing main influencing parameters, they proved to be crucial for assessing C and N cycles and ecosystem functioning on the Tibetan Plateau.

5 Zusammenfassung

Die vorliegende Arbeit wurde im Rahmen eines Stipendiums der Landesgraduiertenförderung Baden-Württemberg (Förderungs-Nr.: VI 4.2-7631.2/Baumann) in Zusammenarbeit mit der Fakultät für Ökologie der Peking University erstellt. Somit waren interdisziplinäre Untersuchungen von Bodeneigenschaften, C- und N-Kreislauf, geomorphologischen Prozessen sowie die direkte Analyse der Wechselbeziehungen dieser Parameter zum Gesamtökosystem des Tibetischen Hochplateaus möglich. Die Forschungsstandorte liegen entlang eines 1200 km langen nord-süd verlaufenden Transekts in Höhen zwischen 2925 und 5105 m ü. NN. Ungefähr zwei Drittel des Tibetischen Hochplateaus sind durch Permafrost beeinflusst und entsprechend besonders empfindlich im Hinblick auf Klimawandel und Landnutzungswechsel. Folglich sind häufig großräumige Degradationsprozesse zu beobachten. Dies führt zu einer steigenden Heterogenität der Bodenbildung, Bodenhydrologie und nachgeordneten bodenchemischen Prozessen, deren wichtigster Bestandteil der C- und N-Kreislauf ist. Um dem resultierenden, extrem diversen Ökosystem in seiner gesamten Breite gerecht zu werden, wurden Analysen auf verschiedenen räumlichen Maßstabsebenen entlang von Klimagradienten durchgeführt. Die Maßstabsebenen umfassen den gesamten Haupttransekt, einen östlichen und westlichen Teiltransekt, diverse Catenen entlang bestimmter geomorphologischer Reliefeinheiten und die Einzelstandorte.

Zunächst wurden C- und N-Gehalte sowie die Anteile pflanzenverfügbaren Stickstoffs in Verbindung mit deren Haupteinflussparametern untersucht. Auf Landschaftsebene hat Bodenfeuchte den größten Einfluss auf die C- und N-Gehalte, gefolgt von $CaCO_3$ und der Korngrößenverteilung. Insgesamt erklärt das lineare Regressionsmodell 64% der Variation von organischen Bodenkohlenstoffgehalten (SOC) und 60% in Bezug auf den Gesamtstickstoff (TN). Dabei ist zweierlei maßgeblich: (1) Temperaturvariablen haben keinen signifikanten Einfluss, während (2) Indikatoren der Bodengenese, wie $CaCO_3$-Gehalt und Korngrößenverteilung neben herkömmlichen ökologischen Variablen, wie beispielsweise Feuchtigkeitsparameter oder Biomasse, in das Regressionsmodell aufgenommen werden. Entsprechend wird in den hoch komplexen, periglazial geprägten Ökosystemen des Tibetischen Hochplateaus die Bodenfeuchteverteilung nicht direkt durch den Niederschlag, sondern vielmehr durch die auf indirektem Wege agierenden Parameter Reliefposition und Permafrost kontrolliert. Da sich bodenkundliche Einflussgrößen als wichtige Prädiktoren herausgestellt haben, kann der Grad der Bodenentwicklung allgemein als eine zusätzliche Stellgröße betrachtet werden: Je länger eine ungestörte und stabile Pedogenese vorliegt, desto höhere C- und N-Gehalte sind zu beobachten. Dies betrifft auch den mineralisierten pflanzenverfügbaren Stickstoff, der fast ausschließlich als Ammonium-N vorliegt, was wiederum eng an erhöhte Bodenfeuchte und kühle Klimaverhältnisse geknüpft ist. Dabei treten die mit Abstand höchsten Werte in der Hauptbodengruppe „Permafrost“ auf. Entsprechend weist Nitrat-N sehr geringe Gehalte auf, da Nitrifikationsprozesse stark temperaturabhängig sind. Die Ergeb-

nisse liefern einen klaren Nachweis dafür, dass eine Limitierung pflanzenverfügbarer Nährstoffe als negative Rückkopplung aufgrund geringerer Bodenfeuchtewerte trotz potenziell steigender Temperaturen im Hinblick auf die globale Erwärmung hervorgerufen werden kann. Die ausgeprägten Rückkopplungsmechanismen zwischen Veränderungen des Permafrosts (Degradationsprozesse und größere Mächtigkeit des Active Layers) und infolgedessen eines umgekehrten Einflusses steigender Temperatur (weiterer Rückgang von Permafrost und damit verbundene trockenere Bedingungen) konnten ausschließlich aufgrund des gewählten Maßstabs auf Landschaftsebene ermittelt werden. Diese Abhängigkeiten basieren auf der negativen Feuchtigkeitsbilanz des Untersuchungsgebietes, da die Evaporation bei weitem die Niederschlagswerte übersteigt. Die niedrigen C- und N-Gehalte sowie die spezifische Tiefenverteilung an degradierten Standorten sind hauptsächlich auf höhere Mineralisationsraten und die Ablagerung von proximal generierten äolischen Sedimenten zurückzuführen. Dies kann exemplarisch für das Einzugsgebiet des Shule River am nordöstlichen Rand des Tibetischen Hochplateaus aufgezeigt werden, wo Böden unter Wüstenvegetation nicht wie alle anderen Vegetationstypen die höchsten SOC-Gehalte in den ersten 20 cm, sondern vielmehr in Bodentiefen zwischen 20 und 40 cm aufweisen. Hauptgrund hierfür sind ebendiese synsedimentären Bodenbildungen. Ergebnisse von Bodenrespirationsmessungen bestätigen grundsätzlich die für C und N-Gehalte gemachten Beobachtungen. Unterirdische Biomasse und Bodenfeuchte erklären 82% der Gesamtvariation, wobei kein direkter Einfluss von Temperatur nachgewiesen werden konnte. Die Bodenrespiration alpiner Matten übersteigt aufgrund der höheren Biomasse und Produktivität die von alpiner Steppenvegetation um das 2,5-fache.

Neben den Beziehungen mit Kontrollvariablen wurde SOC zusätzlich im Hinblick auf Vorräte und Zusammensetzung untersucht. Der Vergleich zwischen den Hauptuntersuchungsstandorten erbrachte deutlich höhere SOC-Vorräte für diskontinuierlichen Permafrost (10.4 kg m^{-2}), während im kontinuierlichen Permafrost lediglich durchschnittlich 3.4 kg m^{-2} ermittelt wurden. Höchste Vorräte finden sich in wassergesättigten Profilen (19.3 kg m^{-2}), da die Isolationswirkung der dichteren Vegetation einen positiven Rückkopplungsmechanismus auslösen und zu einer weiteren Akkumulation von SOC führen kann. Gleichzeitig enthalten diese Böden im Bereich des diskontinuierlichen Permafrosts höhere Anteile an vergleichsweise leicht abbaubaren Fraktionen partikulärer organischer Substanz, die entsprechend anfällig auf Klimaveränderungen reagiert. Die kühleren und trockeneren Verhältnisse im Bereich des kontinuierlichen Permafrosts führen hingegen zu einer geringeren Produktivität und einer schwerpunktmäßigen Verteilung der unterirdischen Biomasse in den obersten 10 cm. Dies kann zusätzlich durch Untersuchungen im ebenfalls durch niedrige Jahresdurchschnittstemperaturen und Niederschlägen geprägten Einzugsgebiet des Shule River nachgewiesen werden. Hier finden sich durchschnittliche SOC-Vorräte von 7.7 kg m^{-2}, die je nach Vegetationseinheit zwischen 4.4 kg m^{-2} unter Wüstenvegeta-

tion und 19.8 kg m^{-2} unter wassergesättigten alpinen Sumpfmatten variieren (vgl. oben beschriebene Respirationswerte in Bezug auf verschiedene Vegetationsmuster).

Ferner konnte gezeigt werden, dass anorganischer Kohlenstoff (SIC) und SOC durch unterschiedliche Parametersets beeinflusst werden: Bodenphysikalische und bodenchemische Eigenschaften beschreiben SIC am besten, während biotische und klimatische Faktoren für SOC relevanter sind. Ein niedrigerer pH-Wert führt demnach zu geringeren SIC-Gehalten und erklärt 42% der Variation. Jedoch kann im Hinblick auf potentielle Bodenversauerung die Kohlenstofffreisetzung aufgrund der umgekehrten Reaktion von SOC kompensiert werden.

Da ein signifikanter Einfluss bodenbildender Prozesse auf C- und N-Gehalte nachgewiesen werden konnte, ist es notwendig damit verbundene Verwitterungs- und Sedimentationsprozesse in Bezug auf Permafrostverteilung und Oberflächenstabilität zu analysieren. Hierfür wurden Verwitterungsindizes und pedogene Fe-Oxide auf verschiedenen Maßstabsebenen und Untergruppen in Bezug auf spezifische klimatische Verhältnisse angewendet. Der „chemical index of alteration“ (CIA) eignet sich dabei am besten um großräumige Klimatrends, Substratunterschiede und spezifische Permafrostverteilungsmuster zu beschreiben. Dagegen zeigen Quotienten pedogener Fe-Oxide kleinräumige bodengenetische Wechsel an, wofür sich vorzugsweise (Fed-Feo)/Fet bewährt hat. Dies kann durch die klare Differenzierbarkeit von Hauptbodengruppen, die durch den CIA nicht möglich ist, untermauert werden. Dabei ist wesentlich, dass Böden, die durch Grundwasser und Permafrost beeinflusst sind, klar zu unterscheiden sind. Klimaparameter haben innerhalb der Hauptbodengruppe „Permafrost“ das größte Gewicht (klimazonale Bodenbildung), während standortspezifische Variablen den Haupteinfluss innerhalb von Grundwasser geprägten Böden aufweisen (azonale Bodenbildung). Zusätzlich können diese Bodengruppen statistisch signifikant durch Fep unterschieden werden, obwohl sie ähnlichen SOC-Gehalten und Bodenfeuchteverhältnissen unterliegen. Folglich entsteht in Permafrost beeinflussten Böden aufgrund bestimmter redoximorpher und bodenbildender Prozesse organische Substanz mit spezifischen Strukturen und Eigenschaften. Insgesamt erweisen sich Verwitterungsindices und pedogene Fe-Oxide als vielversprechende Werkzeuge um diverse Stadien des Permafrosts, dessen räumliche Verteilung und Fragen der Oberflächenstabilität zu analysieren.

Die hohe kleinräumige, geochemische Variabilität (Manuskripte 1-5) kann durch den Einsatz von Verwitterungsindices und pedogenen Oxiden (Manuskript 6) je nach Maßstabsebene und zu beurteilenden Prozessen entflochten werden. Zusammen mit den dargestellten Haupteinflussparametern auf C- und N-Kreisläufe ist eine umfassende Beurteilung der Ökosystemfunktionen des Tibetischen Hochplateaus möglich.

6 References

Agehara, S., Warncke, D.D., 2005. Soil Moisture and Temperature Effects on Nitrogen Release from Organic Nitrogen Sources. Soil Science Society of America Journal 69 (6), 1844.

Alexander, E.B., 1985. Estimating relative ages from iron-oxide/total-iron ratios of soils in the Western Po Valley, Italy - a discussion. Geoderma 35, 257–259.

Amundson, R., 2001. The carbon budget in soils. Annual Review of Earth and Planetary Sciences 29, 535–562.

Anderson, T.M., Dong, Y.A., McNaughton, S.J., 2006. Nutrient acquisition and physiological responses of dominant Serengeti grasses to variation in soil texture and grazing. J Ecology 94 (6), 1164–1175.

Aniku, J.R., Singer, M.J., 1990. Pedogenic iron oxide trends in a marine terrace chronosequence. Soil Science Society of America Journal 54, 147–152.

Arduino, E., Barberis E., Carraro F., Forno M.G., 1984. Estimating relative ages from iron-oxide/total-iron ratios of soils in the western Po Valley, Italy. Geoderma 33, 39–52.

Bascomb, C., 1968. Distribution of pyrophosphate-extractable iron and organic carbon in soils of various groups. Eur J Soil Science 19 (2), 251–268.

Batjes, N., 1996. Total carbon and nitrogen in the soils of the world. Eur J Soil Science 47 (2), 151–163.

Bäumler, R., 2001. Pedogenic studies in aeolian deposits in the high mountain area of eastern Nepal. Quaternary International 76/77, 93–102.

Bäumler, R., Zech, W., 2000. Quaternary paleosols, tephra deposits and landscape history in South Kamchatka, Russia. Catena 41, 199–215.

Blume, H.P., Schwertmann, U., 1969. Genetic evaluation of profile distribution of aluminium, iron, and manganese oxides. Soil Science Society of America Proceedings 33, 438–444.

Bockheim, J.G., Hinkel, K.M., Nelson, F.E., 2003. Predicting Carbon Storage in Tundra Soils of Arctic Alaska. Soil Science Society of America Journal 67, 948–950.

Böhner, J., Lehmkuhl, F., 2005. Environmental change modelling for Central and High Asia: Pleistocene, present and future scenarios. Boreas 34 (2), 220–231.

Bond-Lamberty, B., Thomson, A., 2010. A global database of soil respiration data. Biogeosciences 7 (6), 1915–1926.

Brady, N.C., Weil, R.R., 2008. The nature and properties of soils, 14th ed. Pearson Prentice Hall, Upper Saddle River, N.J, xiv, 965.

Buero, V., Schwertmann, U., 1987. Occurance and transformations of iron and manganese in a colluvial Terra Rossa toposequence of Northern Italy. Catena 14, 519–531.

Buggle, B., Glaser, B., Hambach, U., Gerasimenko, N., Marković, S., 2011. An evaluation of geochemical weathering indices in loess–paleosol studies. Quaternary International 240 (1-2), 12–21.

Buggle, B., Glaser, B., Zöller, L., Hambach, U., Marković, S., Glaser, I., Gerasimenko, N., 2008. Geochemical characterization and origin of Southeastern and Eastern European loesses (Serbia, Romania, Ukraine). Quaternary Science Reviews 27 (9-10), 1058–1075.

Burke, I., Lauenroth, W., Parton, W., 1997. Regional and temporal variation in net primary production and nitrogen mineralization in grasslands. Ecology 78 (6), 1330–1340.

Callesen, I., Liski, J., Raulund-Rasmussen, K., Olsson, M.T., Tau-Strand, L., Vesterdal, L., Westman, C.J., 2003. Soil carbon stores in Nordic well-drained forest soils-relationships with climate and texture class. Global Change Biol 9 (3), 358–370.

Chang, D.H.S., 1981. The vegetation zonation of the Tibetan Plateau. Mountain Research and Development 1, 29–48.

Chapin III, F.S., Matson, P.A., Mooney, H., 2002. Principles of terrestrial ecosystem ecology. Springer, New York.

Chapin III, F.S., Zavaleta, E.S., Eviner, V.T., Naylor, R.L., Vitousek, P.M., Reynolds, H.L., Hooper, D.U., Lavorel, S., Sala, O.E., Hobbie, S.E., Mack, M.C., Díaz, S., 2000. Consequences of changing biodiversity. Nature 405 (6783), 234–242.

Cheng, G., 2005. Permafrost studies in the Qinghai–Tibet Plateau for road construction. Journal of Cold Regions Engineering 19 (1), 19–29.

Cheng, G., Wu, T., 2007. Responses of permafrost to climate change and their environmental significance, Qinghai-Tibet Plateau. J. Geophys. Res. 112 (F2).

Chen, Q., Wang, Q., Han, X., Wan, S., Li, L., 2010. Temporal and spatial variability and controls of soil respiration in a temperate steppe in northern China. Global Biogeochem. Cycles 24 (2), n/a.

Chen, S.Y., Liu, W.J., Ye, B.S., Yang, G.J., Yi, S.H., Wang, F.G., Qin, X., Ren, J.W., Qin, D.H., 2011. Species diversity of the vegetation in relation to biomass and environmental factors in the upper area of the Shule River. Acta Prataculturae Sinica 20, 70–83.

Chinese Academy of Sciences, 2001. Vegetation Atlas of China, Science Press, Beijing.

Craine, J.M., Tilman, D., Wedin, D., Reich, P., Tjoelker, M., Knops, J., 2002. Functional traits, productivity and effects on nitrogen cycling of 33 grassland species. Funct Ecology 16 (5), 563–574.

Craine, J.M., Wedin, D.A., Chapin III, F.S., 1999. Predominance of ecophysiological controls on soil CO2 flux in a Minnesota grassland. Plant and Soil 207, 77–86.

Cullers, R.L., 2000. The geochemistry of shales, siltstones and sandstones of Pennsylvanian–Permian age, Colorado, USA: implications for provenance and metamorphic studies. Lithos 51, 181–203.

Dahms, D., Favilli, F., Krebs, R., Egli, M., 2012. Soil weathering and accumulation rates of oxalate-extractable phases derived from alpine chronosequences of up to 1Ma in age. Geomorphology 151-152, 99–113.

Dai, F., Su, Z., Liu, S., Liu, G., 2011. Temporal variation of soil organic matter content and potential determinants in Tibet, China. Catena 85 (3), 288–294.

Davidson, E.A., Janssens, I.A., 2006. Temperature sensitivity of soil carbon decomposition and feedbacks to climate change. Nature 440 (7081), 165–173.

Dharmakeerthi, R.S., Kay, B.D., Beauchamp, E.G., 2005. Factors Contributing to Changes in Plant Available Nitrogen across a Variable Landscape. Soil Science Society of America Journal 69 (2), 453–462.

Diaz, M., Torrent J., 1989. Mineralogy of iron oxides in two soil chronosequences of central Spain. Catena 16, 291–299.

Dietze, E., Hartmann, K., Diekmann, B., IJmker, J., Lehmkuhl, F., Opitz, S., Stauch, G., Wünnemann, B., Borchers, A., 2012. An end-member algorithm for deciphering modern detrital processes from lake sediments of Lake Donggi Cona, NE Tibetan Plateau, China. Sedimentary Geology 243-244, 169–180.

Dodd, M., Lauenroth, W., Burke, I., 2000. Nitrogen Availability through a Coarse-Textured Soil Profile in the Shortgrass Steppe. Soil Science Society of America Journal 64 (1), 391–398.

Domrös, M., Peng, G., 1988. The Climate of China. Springer, Berlin, Heidelberg, NewYork.

Eswaran, H., Reich, P.F., Kimble, J.M., Beinroth, F.H., Padmanabhan, E., Moncharoen, P., 2000. Global carbon stocks, in: Lal, R., Kimble, J., Eswaran, H., Stewart, B.A. (Eds.), Global climate change and pedogenic carbonates. CRC Press, Boca Raton, pp. 15–25.

Eswaran, H., van Den Berg, E., Reich, P., 1993. Organic Carbon in Soils of the World. Soil Science Society of America Journal 57 (1), 192.

Eswaran, H., van Den Berg, E., Reich, P., Kimble, J., 1995. Global soil carbon resources, in: Lal, R., Kimble, J., Levine, E., Stewart, B.A. (Eds.), Soils and Global Change. CRC/Lewis Publishers, Boca Raton, pp. 27–43.

Fang, X., Lü, L., Mason, J.A., Yang, S., An, Z., Li, J., Zhilong, G., 2003. Pedogenic response to millennial summer monsoon enhancements on the Tibetan Plateau. Quaternary International 106-107, 79–88.

Fedo, C.M., Nesbitt, W.H., Young, G.M., 1995. Unraveling the effects of potassium metasomatism in sedimentary rocks and paleosols, with implications for paleoweathering conditions and provenance. Geol 23 (10), 921.

Feng, J.-L., Hu, Z.-G., Ju, J.-T., Zhu, L.-P., 2011. Variations in trace element (including rare earth element) concentrations with grain sizes in loess and their implications for tracing the provenance of eolian deposits. Quaternary International 236 (1-2), 116–126.

Feng, J.-L., Zhu, L.-P., 2009. Origin of terra rossa on Amdo North Mountain on the Tibetan Plateau, China: Evidence from quartz. Soil Science and Plant Nutrition 55 (3), 407–420.

Feng, Z.-D., 1997. Geochemical characteristics of a loess-soil sequence in central Kansas. Soil Science Society of America Journal 61, 534–541.

Fisk, M.C., Schmidt, S.K., 1995. Nitrogen mineralization and microbial biomass nitrogen dynamics in three alpine tundra communities. Soil Science Society of America Journal 59 (4), 1036–1043.

Fisk, M.C., Schmidt, S.K., Seastedt, T.R., 1998. Topographic patterns of above- and belowground production and nitrogen cycling in alpine tundra. Ecology 79, 2253–2266.

Franzluebbers, A.J., Stuedemann, J.A., 2010. Surface Soil Changes during Twelve Years of Pasture Management in the Southern Piedmont USA. Soil Science Society of America Journal 74 (6), 2131.

Gallet, S., Jahn, B., van Vliet Lanoe, B., Dia, A., Rossello, E., 1998. Loess geochemistry and its implications for particle origin and composition of the upper continental crust. Earth and Planetary Science Letters 156, 157–172.

Gao, Q., Li, Y., Wan, Y., Lin, E., Xiong, W., Jiangcun, W., Wang, B., Li, W., 2006. Grassland degradation in Northern Tibet based on remote sensing data. J GEOGR SCI 16 (2), 165–173.

Gerzabek, M.H., Haberhauer, G., Stemmer, M., Klepsch, S., Haunold, E., 2004. Long-term behaviour of 15N in an alpine grassland ecosystem. Biogeochemistry 70, 59–69.

Giardina, C.P., Ryan, M.G., Hubbard, R.M., Binkley, D., 2001. Tree Species and Soil Textural Controls on Carbon and Nitrogen Mineralization Rates. Soil Science Society of America Journal 65 (4), 1272.

Grosse, G., Romanovsky, V., Jorgenson, T., Anthony, K.W., Brown, J., Overduin, P.P., 2011. Vulnerability and feedbacks of permafrost to climate change. Eos Trans. AGU 92 (9), 73.

Gründling, R., Scholten, T., 2006. The role of pedodiversity and the impact of historical land use for ecosystem functioning (biodiversity) in grassland ecosystems, in: Martinez-Casasnovas, J.A., Pla Sentis, I., Martin, M.C.R., Solanes, J.C.B. (Eds.), Proceedings of the International ESSC Congress on 'Soil and Water Conservation under Changing Land Use' in Lleida, Spain, Palermo, pp. 191–194.

Guggenberger, G., Kaiser, K., 2003. Dissolved organic matter in soil: challenging the paradigm of sorptive preservation. Geoderma 113 (3-4), 293–310.

Haider, K., 1996. Biochemie des Bodens: 48 Tabellen. Enke, Stuttgart, x, 174 S.

Hall, D.O., Scurlock, J.M.O., Ojima, D.S., Parton, W., 2000. Grasslands and the global carbon cycle: modeling the effects of climate change, in: Wigley, T.M.L., Schimel, D.S. (Eds.), The carbon cycle. Cambridge University Press, Cambridge, pp. 102–115.

Harnois, L., 1988. The CIW index: a new chemical index of weathering. Sedimentary Geology 55, 319–322.

Harris, N., 2006. The elevation history of the Tibetan Plateau and its implications for the Asian monsoon. Palaeogeography, Palaeoclimatology, Palaeoecology 241 (1), 4–15.

He, J.-S., Wang, Z., Wang, X., Schmid, B., Zuo, W., Zhou, M., Zheng, C., Wang, M., Fang, J., 2006. A test of the generality of leaf trait relationships on the Tibetan Plateau. New Phytol 170 (4), 835–848.

Hibbard, K.A., Law, B.E., Reichstein, M., Sulzman, J., 2005. An analysis of soil respiration across northern hemisphere temperate ecosystems. Biogeochemistry 73 (1), 29–70.

Hirota, M., Tang, Y., Hu, Q., Hirata, S., Kato, T., Mo, W., Cao, G., Mariko, S., 2006. Carbon Dioxide Dynamics and Controls in a Deep-water Wetland on the Qinghai-Tibetan Plateau. Ecosystems 9 (4), 673–688.

Hobbie, S.E., Schimel, J.P., Trumbore, S.E., Randerson, J.R., 2000. Controls over carbon storage and turnover in high-latitude soils. Global Change Biology 6 (S1), 196–210.

Hook, P.B., Burke, I.C., 2000. Biogeochemistry in a shortgrass landscape: control by topography, soil texture, and microclimate. Ecology 81, 2686–2703.

Hou, X.Y., 1982. Vegetation map of the People's Republic of China (1:4M). Chinese Map Publisher, Beijing.

Hövermann, J., Lehmkuhl, F., 1994. Vorzeitliche und rezente geomorphologische Höhenstufen in Ost- und Zentraltibet. Göttinger Geographische Abhandlungen 95, 15–69.

Hu, H., Wang, G., Liu, G., Li, T., Ren, D., Wang, Y., Cheng, H., Wang, J., 2009. Influences of alpine ecosystem degradation on soil temperature in the freezing-thawing process on Qinghai–Tibet Plateau. Environ Geol 57 (6), 1391–1397.

Hui, D., Jackson, R.B., 2006. Geographical and interannual variability in biomass partitioning in grassland ecosystems: a synthesis of field data. New Phytol 169 (1), 85–93.

IPCC, 2007. Climate Change 2007: The physical science basis. Contribution of working group I to the fourth assessment report of the intergovernmental panel on climate change. Cambridge University Press, Cambridge.

IUSS Working Group WRB, 2006. World reference base for soil resources. World Soil Resources Reports (103).

Iwatsubo, G., Zheng, X., Shidei, T., 1989. An ecological study of soils in the highlands of western Tibet II. Vertical change from 3900 m to 5450 m in elevation. Ecological Research 4, 233–241.

Janssen, B.H., 1996. Nitrogen mineralization in relation to C:N ratio and decomposability of organic materials. Plant Soil 181 (1), 39–45.

Janssens, I.A., Lankreijer, H., Matteucci, G., Kowalski, A.S., Buchmann, N., Epron, D., Pilegaard, K., Kutsch, W., Longdoz, B., Grunwald, T., Montagnani, L., Dore, S., Rebmann, C., Moors, E.J., Grelle, A., Rannik, U., Morgenstern, K., Oltchev, S., Clement, R., Gudmundsson, J., Minerbi, S., Berbigier, P., Ibrom, A., Moncrieff, J., Aubinet, M., Bernhofer, C., Jensen, N.O., Vesala, T., Granier, A., Schulze, E.-D., Lindroth, A., Dolman, A.J., Jarvis, P.G., Ceulemans, R., Valentini, R., 2001. Productivity overshadows temperature in determining soil and ecosystem respiration across European forests. Global Change Biol 7 (3), 269–278.

Jarvis, S.C., 1996. Future trends in nitrogen research. Plant Soil 181 (1), 47–56.

Jenny, H., 1994. Factors of soil formation: A system of quantitative pedology. Dover, New York, xviii, 281.

Jin, H.J., Chang, X.L., Wang, S.L., 2007. Evolution of permafrost on the Qinghai-Xizang (Tibet) Plateau since the end of the late Pleistocene. J. Geophys. Res. 112 (F2).

Jin, H., Li, S., Cheng, G., Shaoling, W., Li, X., 2000. Permafrost and climatic change in China. Global and Planetary Change 26, 387–404.

Jobbagy, E.G., Jackson, R.B., 2000. The vertical distribution of soil organic carbon and its relation to climate and vegetation. Ecological Applications 10, 423–436.

Johnson, K.D., Harden, J., McGuire, A.D., Bliss, N.B., Bockheim, J.G., Clark, M., Nettleton-Hollingsworth, T., Jorgenson, M.T., Kane, E.S., Mack, M., O'Donnell, J., Ping, C.-L., Schuur, E.A., Turetsky, M.R., Valentine, D.W., 2011. Soil carbon distribution in Alaska in relation to soil-forming factors. Geoderma 167-168, 71–84.

Johnson, L.C., Shaver, G.R., Giblin, A.E., Nadelhoffer, K.J., Rastetter, E.R., Laundre, J.A., Murray, G.L., 1996. Effects of drainage and temperature on carbon balance of tussock tundra micros-osms. Oecologia 108, 737–748.

Jorgenson, M.T., Racine, C.H., Walters, J.C., Osterkamp, T.E., 2001. Permafrost degradation and ecological changes associated with a warming climate in central Alaska. Climatic Change 48 (4), 551–579.

Kaiser, K., 2004. Pedogeomorphological transect studies in Tibet: implications for landscape history and present-day dynamics. Prace Geograficzne 200, 147–165.

Kaiser, K., Miehe, G., Barthelmes, A., Ehrmann, O., Scharf, A., Schult, M., Schlütz, F., Adamczyk, S., Frenzel, B., 2008. Turf-bearing topsoils on the central Tibetan Plateau, China: Pedology, botany, geochronology. Catena 73 (3), 300–311.

Kaiser, K., Schoch, W.H., Miehe, G., 2007. Holocene paleosols and colluvial sediments in Northeast Tibet (Qinghai Province, China): Properties, dating and paleoenvironmental implications. Catena 69 (2), 91–102.

Kämpf, N., Scheinost, A.C., Schulze, D.G., 2011. Oxide Minerals, in: Huang, P., Li Y., Sumner M.E (Eds.), Handbook of Soil Science, Properties and Processes. Part III: Soil Mineralogy. CRC Press, pp. 125–168.

Kang, S., Xu, Y., You, Q., Flügel, W.-A., Pepin, N., Yao, T., 2010. Review of climate and cryospheric change in the Tibetan Plateau. Environ. Res. Lett. 5 (1), 15101.

Kato, T., Tang, Y., Gu, S., Cui, X., Hirota, M., Du, M., Li, Y., Zhao, X., Oikawa, T., 2004. Carbon dioxide exchange between the atmosphere and an alpine meadow ecosystem on the Qinghai–Tibetan Plateau, China. Agricultural and Forest Meteorology 124 (1-2), 121–134.

Kato, T., Tang, Y., Gu, S., Hirota, M., Du, M., Li, Y., Zhao, X., 2006. Temperature and biomass influ-ences on interannual changes in CO2 exchange in an alpine meadow on the Qinghai-Tibetan Plateau. Global Change Biol 12 (7), 1285–1298.

Kirschbaum, M.U.F., 1995. The temperature dependence of soil organic matter decomposition, and the effect of global warming on soil organic C storage. Soil Biology and Biochemistry 27, 753–760.

Kirschbaum, M.U.F., 2006. The temperature dependence of organic-matter decomposition—still a topic of debate. Soil Biology and Biochemistry 38 (9), 2510–2518.

Klinge, M., Lehmkuhl, F., 2005. Untersuchungen zur holozänen Bodenentwicklung und Geomorphodynamik in Tibet, in: Eidam, U. (Ed.), Hochgebirge und ihr Umland. Berliner geographische Arbeiten 100. Geograph. Inst. der Humboldt-Univ., Berlin, pp. 81–91.

Körner, C.H., 2003. Alpine plant life: functional plant ecology of high mountain ecosystems. Springer, Berlin.

Kronberg, B., Nesbitt, H.W., 1981. Quantification of weathering, soil geochemistry and soil fertility. Eur J Soil Science 32, 453–459.

Kühn, P., Techmer, A., Weidenfeller, M., 2013. Lower to middle Weichselian pedogenesis and palaeoclimate in Central Europe using combined micromorphology and geochemistry: the loess-paleosol sequence of Alsheim (Mainz Basin, Germany). Quaternary Science Reviews 75, 43–58.

Lal, R., 2004. Agricultural activities and the global carbon cycle. Nutrient Cycling in Agroecosystems 70, 103–116.

Lal, R., 2008. Carbon sequestration. Philosophical Transactions of the Royal Society B: Biological Sciences 363 (1492), 815–830.

Lal, R., Kimble, J., 2000. Pedogenic carbonates and the global carbon cycle, in: Lal, R., Kimble, J., Eswaran, H., Stewart, B.A. (Eds.), Global climate change and pedogenic carbonates. CRC Press, Boca Raton, pp. 1–14.

Lehmkuhl, F., 1997. The spatial distribution of loess and loess-like sediments in the mountain areas of Central and High Asia. Zeitschrift für Geomorphologie 111, 97–116.

Liao, Q., Zhang, X., Li, Z., Pan, G., Smith, P., Yang, J., Wu, X., 2009. Increase in soil organic carbon stock over the last two decades in China's Jiangsu Province. Global Change Biology 15 (4), 861–875.

Lindroth, A., Grelle, A., Moren, A.-S., 1998. Long-term measurements of boreal forest carbon balance reveal large temperature sensitivity. Global Change Biol 4 (4), 443–450.

Lin, X., Zhang, Z., Wang, S., Hu, Y., Xu, G., Luo, C., Chang, X., Duan, J., Lin, Q., Xu, B., Wang, Y., Zhao, X., Xie, Z., 2011. Response of ecosystem respiration to warming and grazing during the

growing seasons in the alpine meadow on the Tibetan plateau. Agricultural and Forest Meteorology 151 (7), 792–802.

Liu, X., Chen, B., 2000. Climatic warming in the Tibetan Plateau during recent decades. International Journal of Climatology 20, 1729–1742.

Liu, X., Zhang, M., 1998. Contemporary climatic change over the Qinghai-Xizang Plateau and its response to the green-house effect. Chinese Geographical Science 8, 289–298.

Li, Z., Han, F., Su, Y., Zhang, T., Sun, B., Monts, D., Plodinec, M., 2007. Assessment of soil organic and carbonate carbon storage in China. Geoderma 138 (1-2), 119–126.

Lu, X., Zhang, S., Xu, J., 2010. Climate change and sediment flux from the Roof of the World. Earth Surf. Process. Landforms, n/a.

Mahaney, W., Fahey, B., 1980. Morphology, composition and age of a buried paleosol, Front Range, Colorado, U.S.A. Geoderma 23, 209–218.

Mahecha, M.D., Reichstein, M., Carvalhais, N., Lasslop, G., Lange, H., Seneviratne, S.I., Vargas, R., Ammann, C., Arain, M.A., Cescatti, A., Janssens, I.A., Migliavacca, M., Montagnani, L., Richardson, A.D., 2010. Global convergence in the temperature sensitivity of respiration at ecosystem level. Science 329 (5993), 838–840.

Makarov, M., Glaser, B., Zech, W., Malysheva, T., Bulatnikova, I., Volkov, A., 2003. Nitrogen dynamics in alpine ecosystems of the northern Caucasus. Plant and Soil 256 (2), 389–402.

Mary, B., Recous, S., Darwis, D., Robin, D., 1996. Interactions between decomposition of plant residues and nitrogen cycling in soil. Plant Soil 181 (1), 71–82.

McFadden, L.D., Hendricks, D.M., 1985. Changes in the Content and Composition of Pedogenic Iron Oxyhydroxides in a Chronosequence of Soils in Southern California. Quaternary Research 23, 189–204.

McKeague, J.A., 1967. An evaluation of 0.1 M pyrophosohate and pyrophasphate-dithionite in comparison with oxalate as extractants of the accumulation products in podzols and some other soils. Can. J. Soil Sci. 47, 95–99.

McLennan, S.M., 1993. Weathering and Global Denudation. The Journal of Geology 101 (2), 295–303.

Mehra, O., Jackson, M., 1960. Iron oxide removal from soils and clays by a dithionite-citrate buffered with sodium bicarbonats. Clays Clay Mineral. 7, 317–327.

Melillo, J.M., Steudler, P.A., Aber, J.D., Newkirk, K., Lux, H., Bowles, F.P., Catricala, C., Magill, A., Ahrens, T., Morrisseau, S., 2002. Soil Warming and Carbon-Cycle Feedbacks to the Climate System. Science 298 (5601), 2173–2176.

Melke, J., 2007. Weathering Processes in the Soils of Tundra of Western Spitsbergen. Polish Journal of Soil Science 40 (2), 217–226.

Mi, N., Wang, S., Liu, J., Yu, G., Zhang, W., Jobbágy, E., 2008. Soil inorganic carbon storage pattern in China. Global Change Biology 14 (10), 2380–2387.

Mirabella, A., Carnicelli, S., 1992. Iron oxide mineralogy in red and brown soils developed on calcareous rocks in central Italy. Geoderma 55, 95–109.

Mokany, K., Raison, R.J., Prokushkin, A.S., 2006. Critical analysis of root: Shoot ratios in terrestrial biomes. Global Change Biol 12 (1), 84–96.

Monger, H.C., Gallegos, R.A., 2000. Biotic and abiotic processes and rates of pedogenic carbonate accumulation, in: Lal, R., Kimble, J., Eswaran, H., Stewart, B.A. (Eds.), Global climate change and pedogenic carbonates. CRC Press, Boca Raton.

Moore, T.R., Knowles, R., 1989. The influence of water table levels on methane and carbon dioxide emissions from peatland soils. Can. J. Soil. Sci. 69 (1), 33–38.

Nadelhoffer, K.J., Giblin, A.E., Shaver, G.R., Laundre, J.A., 1991. Effects of temperature and substrate quality on element mineralization in six arctic soils. Ecology 72, 242–253.

Nan, Z., Li, S., Cheng, G., 2005. Prediction of permafrost distribution on the Qinghai-Tibet Plateau in the next 50 and 100 years. Science in China Series D: Earth Sciences 48 (6), 797–804.

Nesbitt, H.W., Young, G.M., 1982. Early Proterozoic climates and plate motions inferred from major element chemistry of lutites. Nature 299, 715–717.

Nesbitt, H.W., Young, G.M., 1984. Prediction of some weathering trends of plutonic and volcanic rocks based on thermodynamic and kinetic considerations. Geochimica et Cosmochimica Acta 48, 1523–1534.

Nesbitt, H.W., Young, G.M., McLennan, S., Keays, R., 1996. Effects of chemical weathering and sorting on the petrogenesis of siliciclastic sediments, with implications for provenance studies. The Journal of Geology 104, 525–542.

Nielsen, C.B., Groffman, P.M., Hamburg, S.P., Driscoll, C.T., Fahey, T.J., Hardy, J.P., 2001. Freezing Effects on Carbon and Nitrogen Cycling in Northern Hardwood Forest Soils. Soil Science Society of America Journal 65 (6), 1723.

Ni, J., 2002. Carbon storage in grasslands of China. Journal of Arid Environments 50 (2), 205–218.

Niu, F., Lin, Z., Liu, H., Lu, J., 2011. Characteristics of thermokarst lakes and their influence on permafrost in Qinghai–Tibet Plateau. Geomorphology 132 (3-4), 222–233.

Ohtsuka, T., Hirota, M., Zhang, X., Shimono, A., Senga, Y., Du, M., Yonemura, S., Kawashima, S., Tang, Y., 2008. Soil organic carbon pools in alpine to nival zones along an altitudinal gradient (4400–5300m) on the Tibetan Plateau. Polar Science 2 (4), 277–285.

Ouyang, X.-J., Zhou, G.-Y., Huang, Z.-L., Liu, J.-X., Zhang, D.-Q., Li, J., 2008. Effect of Simulated Acid Rain on Potential Carbon and Nitrogen Mineralization in Forest Soils. Pedosphere 18 (4), 503–514.

Parker, A., 1970. An index of weathering for silicate rocks. Geological Magazine 107, 501–504.

Parton, W.J., Schimel, D., Ojima, D.S., Cole, C.V., 1994. A general model for soil organic matter dynamics: sensitivity to litter chemistry, texture and management, in: Bryant, R.B., Arnold, R.W. (Eds.), Quantitative modeling of soil forming processes. Proceedings of a symposium … in Minneapolis, Minnesota, 2 Nov. 1992. SSSA special publication 39. Soil Science Soc. of America, Madison, Wis, pp. 147–167.

Parton, W.J., Stewart, J.W.B., Cole, C.V., 1988. Dynamics of C, N, P and S in grassland soils: a model. Biogeochemistry 5 (1), 109–131.

Pei, S., Fu, H., Wan, C., Chen, Y., Sosebee, R.E., 2006. Observations on Changes in Soil Properties in Grazed and Nongrazed Areas of Alxa Desert Steppe, Inner Mongolia. Arid Land Research and Management 20 (2), 161–175.

Percival, H.J., Parfitt, R.L., Scott, N.A., 2000. Factors controlling soil carbon levels in New Zealand grasslands: is clay content important? Soil Science Society of America Journal 64 (5), 1623–1630.

Ping, C.-L., Qiu, G., Zhao, L., 2004. The periglacial environment of China, in: Kimble, J. (Ed.), Cryosols. Permafrost-Affected Soils. Springer, Berlin, pp. 275–291.

Post, E., Forchhammer, M.C., Bret-Harte, M.S., Callaghan, T.V., Christensen, T.R., Elberling, B., Fox, A.D., Gilg, O., Hik, D.S., Hoye, T.T., Ims, R.A., Jeppesen, E., Klein, D.R., Madsen, J., McGuire, A.D., Rysgaard, S., Schindler, D.E., Stirling, I., Tamstorf, M.P., Tyler, N.J., van der Wal, R., Welker, J., Wookey, P.A., Schmidt, N.M., Aastrup, P., 2009. Ecological Dynamics Across the Arctic Associated with Recent Climate Change. Science 325 (5946), 1355–1358.

Post, W.M., Emanuel, W.R., Zinke, P.J., Stangenberger, A.G., 1982. Soil carbon pools and world life zones. Nature 298 (5870), 156–159.

Qi, F., Guoduong, C., Masao, M., 2001. The carbon cycle of sandy lands in China and its global significance. Climatic Change 48 (4), 535–549.

Qiu, J., 2008. China: The third pole. Nature 454 (7203), 393–396.

Raghubanshi, A., 1992. Effect of topography on selected soil properties and nitrogen mineralization in a dry tropical forest. Soil Biology and Biochemistry 24 (2), 145–150.

Raich, J.W., Potter, C.S., 1995. Global patterns of carbon dioxide emissions from soils. Global Biogeochem. Cycles 9 (1), 23–36.

Raich, J.W., Schlesinger, W.H., 1992. The global carbon dioxide flux in soil respiration and its relationship to vegetation and climate. Tellus B 44, 81–99.

Raich, J.W., Tufekcioglu, 2000. Vegetation and soil respiration: correlations and controls. Biogeochemistry 48, 71–90.

Reichstein, M., Beer, C., 2008. Soil respiration across scales: The importance of a model–data integration framework for data interpretation. J. Plant Nutr. Soil Sci. 171 (3), 344–354.

Reichstein, M., Rey, A., Freibauer, A., Tenhunen, J., Valentini, R., Banza, J., Casals, P., Cheng, Y., Grünzweig, J.M., Irvine, J., Joffre, R., Law, B.E., Loustau, D., Miglietta, F., Oechel, W., Ourcival, J.-M., Pereira, J.S., Peressotti, A., Ponti, F., Qi, Y., Rambal, S., Rayment, M., Romanya, J., Rossi, F., Tedeschi, V., Tirone, G., Xu, M., Yakir, D., 2003. Modeling temporal and large-scale spatial variability of soil respiration from soil water availability, temperature and vegetation productivity indices. Global Biogeochem. Cycles 17 (4), n/a.

Rezapour, S., Jafarzadeh, A.A., Samadi, A., Oustan, S., 2010. Distribution of iron oxides forms on a transect of calcareous soils, north-west of Iran. Archives of Agronomy and Soil Science 56 (2), 165–182.

Robinson, C.H., 2002. Controls on decomposition and soil nitrogen availability at high latitudes. Plant and Soil 242, 65–81.

Rodrigo, A., Recous, S., Neel, C., Mary, B., 1997. Modelling temperature and moisture effects on C-N transformations in soils: comparison of nine models. Ecological Modelling 102, 325–339.

Rumpel, C., Kögel-Knabner, I., 2011. Deep soil organic matter—a key but poorly understood component of terrestrial C cycle. Plant Soil 338 (1-2), 143–158.

Rustad, L.E., Campbell, J.L., Marion, G.M., Norby, R.J., Mitchell, M., Hartley, A.E., Cornelissen, J.H.C., Gurevitch, J., 2001. A meta-analysis of the response of soil respiration, net nitrogen mineralization, and aboveground plant growth to experimental ecosystem warming. Oecologia 126 (4), 543–562.

Saito, M., Kato, T., Tang, Y., 2009. Temperature controls ecosystem CO2 exchange of an alpine meadow on the northeastern Tibetan Plateau. Global Change Biology 15 (1), 221–228.

Satti, P., Mazzarino, M.J., Gobbi, M., Funes, F., Roselli, L., Fernandez, H., 2003. Soil N dynamics in relation to leaf litter quality and soil fertility in north-western Patagonian forests. Journal of Ecology 91 (2), 173–181.

Sauer, D., Wagner, S., Brückner, H., Scarciglia, F., Mastronuzzi, G., Stahr, K., 2010. Soil development on marine terraces near Metaponto (Gulf of Taranto, southern Italy). Quaternary International 222 (1-2), 48–63.

Savage, K., Davidson, E.A., Richardson, A.D., 2008. A conceptual and practical approach to data quality and analysis procedures for high-frequency soil respiration measurements. Functional Ecology 22 (6), 1000–1007.

Scheffer, F., Schachtschabel, P., Blume, H.-P., 2002. Lehrbuch der Bodenkunde, 15th ed. Spektrum Lehrbuch. Spektrum, Akad. Verl., Heidelberg [u.a.], XIV, 593 S.

Schimel, D., Parton, W., Kittel, T., Ojima, D., Cole, C., 1990. Grassland biogeochemistry: Links to atmospheric processes. Climatic Change 17, 13–25.

Schimel, D.S., Braswell, B.H., Holland, E.A., McKeown, R., Ojima, D.S., Painter, T.H., Parton, W.J., Townsend, A.R., 1994. Climatic, edaphic, and biotic controls over storage and turnover of carbon in soils. Global Biogeochem. Cycles 8 (3), 279–293.

Schlesinger, W.H., 1997. Biogeochemistry: an analysis of global change. Academic Press, San Diego.

Schlesinger, W.H., Andrews, J.A., 2000. Soil respiration and the global carbon cycle. Biogeochemistry 48, 7–20.

Schlichting, E., Blume, H.-P., 1962. Art und Ausmaß der Veränderungen des Bestandes mobiler Oxyde in Böden aus jungpleistozänem Geschiebemergel und ihren Horizonten. J. Plant Nutr. Soil Sci. 96, 144–156.

Schlütz, F., Lehmkuhl, F., 2009. Holocene climatic change and the nomadic Anthropocene in Eastern Tibet: palynological and geomorphological results from the Nianbaoyeze Mountains. Quaternary Science Reviews 28 (15-16), 1449–1471.

Schuur, E.A.G., Bockheim, J., Canadell, J.G., Euskirchen, E., Field, C.B., Goryachkin, S.V., Hagemann, S., Kuhry, P., Lafleur, P.M., Lee, H., Mazhitova, G., Nelson, F.E., Rinke, A., Romanovsky, V.E., Shiklomanov, N., Tarnocai, C., Venevsky, S., Vogel, J.G., Zimov, S.A., 2008. Vulnerability of Permafrost Carbon to Climate Change: Implications for the Global Carbon Cycle. BioScience 58 (8), 701.

Schuur, E.A.G., Vogel, J.G., Crummer, K.G., Lee, H., Sickman, J.O., Osterkamp, T.E., 2009. The effect of permafrost thaw on old carbon release and net carbon exchange from tundra. Nature 459 (7246), 556–559.

Schwertmann, U., 1964. Differenzierung der Eisenoxide des Bodens durch Extraktion mit Ammoniumoxalat-Lösung. J. Plant Nutr. Soil Sci. 105, 194–202.

Scurlock, J.M.O., Hall, D.O., 1998. The global carbon sink: a grassland perspective. Global Change Biol 4 (2), 229–233.

Shaver, G.R., Billings, W.D., Chapin III, F.S., Giblin, A.E., Nadelhoffer, K.J., Oechel, W.C., Rastetter, E.B., 1992. Global change and the carbon balance of Arctic ecosystems. BioScience 42, 433–441.

Shaver, G.R., Giblin, A.E., Nadelhoffer, K.J., Thieler, K.K., Downs, M.R., Laundre, J.A., Rastetter, E.B., 2006. Carbon turnover in Alaskan tundra soils: effects of organic matter quality, temperature, moisture and fertilizer. J Ecology 94 (4), 740–753.

Shaw, M.R., Harte, J., 2001. Response of nitrogen cycling to simulated climate change: differential responses along a subalpine ecotone. Global Change Biol 7 (2), 193–210.

Shur, Y.L., Jorgenson, M.T., 2007. Patterns of permafrost formation and degradation in relation to climate and ecosystems. Permafrost Periglac. Process. 18 (1), 7–19.

Song, G., Li, L., Pan, G., Zhang, Q., 2005. Topsoil organic carbon storage of China and its loss by cultivation. Biogeochemistry 74 (1), 47–62.

Stahr, K., Rück, F., Gaiser, T., 1994. Soil Nitrogen – Reserves and mineralization as affected by climate, soil and landuse. Nova Acta Leopoldina, NF 70, 213–235.

Stevenson, F.J., Cole, M.A., 1999. Cycles of soil: Carbon, nitrogen, phosphorus, sulfur, micronutrients, 2nd ed. Wiley, New York, xviii, 427.

Stokstad, E., 2004. Defrosting the Carbon Freezer of the North. Science 304 (5677), 1618–1620.

Suarez, D.L., 2000. Impact of agriculture on CO_2 as affected by changes in inorganic carbon, in: Lal, R., Kimble, J., Eswaran, H., Stewart, B.A. (Eds.), Global climate change and pedogenic carbonates. CRC Press, Boca Raton, pp. 257–272.

Sugden, A., 2004. Ecology in the Underworld. Science 304 (5677), 1613.

Torrent, J., Cabedo, A., 1986. Sources of iron oxides in reddish brown soil profiles from calcarenites in southern Spain. Geoderma 37, 57–66.

Torrent, J., Liu, Q., Bloemendal, J., Barrón, V., 2007. Magnetic Enhancement and Iron Oxides in the Upper Luochuan Loess–Paleosol Sequence, Chinese Loess Plateau. Soil Science Society of America Journal 71 (5), 1570.

Torrent, J., Schwertmann, U., Schulze, D.G., 1980. Iron oxide mineralogy of some soils of two river terrace swquences in Spain. Geoderma 23, 191–208.

Vitousek, P.M., 1997. Human Domination of Earth's Ecosystems. Science 277 (5325), 494–499.

Wagner, D., Kobabe, S., Liebner, S., 2009. Bacterial community structure and carbon turnover in permafrost-affected soils of the Lena Delta, northeastern SiberiaThis article is one of a selection of papers in the Special Issue on Polar and Alpine Microbiology. Can. J. Microbiol. 55 (1), 73–83.

Wagner, M., 2005. Geomorphological and pedological investigations on the glacial history of the Kali Gandaki (Nepal Himalaya). GeoJournal 63 (1-4), 91–113.

Wang, B., French, H.M., 1994. Climate controls and high-altitude permafrost, Qinghai-Xizang (Tibet) Plateau, China. Permafrost Periglac. Process. 5 (2), 87–100.

Wang, B., French, H.M., 1995. Permafrost on the Tibet Plateau, China. Quaternary Science Reviews 14, 255–274.

Wang, G., Bai, W., Li, N., Hu, H., 2011. Climate changes and its impact on tundra ecosystem in Qinghai-Tibet Plateau, China. Climatic Change 106 (3), 463–482.

Wang, G., Ju, Q., Cheng, G., Lai, Y., 2002. Soil organic carbon pool of grassland soils on the Qinghai-Tibetan Plateau and its global implication. Science of The Total Environment 291 (1-3), 207–217.

Wang, G., Li, Q., Chang, G., Shen, Y., 2001. Climate change and its impact on the eco-environment in the source regions of Yangtze and Yellow Rivers in recent 40 years. Journal of Glaciology and Geocryology 23, 346–352.

Wang, G., Liu, L., Liu, G., Hu, H., Li, T., 2010. Impacts of grassland vegetation cover on the active-layer thermal regime, northeast Qinghai-Tibet Plateau, China. Permafrost Periglac. Process. 21 (4), 335–344.

Wang, G., Li, Y., Hu, H., Wang, Y., 2008a. Synergistic effect of vegetation and air temperature changes on soil water content in alpine frost meadow soil in the permafrost region of Qinghai-Tibet. Hydrol. Process. 22 (17), 3310–3320.

Wang, G., Li, Y., Wang, Y., Wu, Q., 2008b. Effects of permafrost thawing on vegetation and soil carbon pool losses on the Qinghai–Tibet Plateau, China. Geoderma 143 (1-2), 143–152.

Wang, G., Wang, Y., Li, Y., Cheng, H., 2007. Influences of alpine ecosystem responses to climatic change on soil properties on the Qinghai–Tibet Plateau, China. Catena 70 (3), 506–514.

Wang, G., Wang, Y., Qian, J., Wu, Q., 2006. Land Cover Change and Its Impacts on Soil C and N in Two Watersheds in the Center of the Qinghai-Tibetan Plateau. Mountain Research and Development 26 (2), 153–162.

Wang, J.-T., 1988. The steppes and deserts of the Xizang Plateau (Tibet). Plant Ecology 75, 135–142.

Wang, S., Jin, H., Li, S., Zhao, L., 2000. Permafrost degradation on the Qinghai-Tibet Plateau and its environmental impacts. Permafrost Periglac. Process. 11, 43–53.

Wang, S., Zhou, C., 2001. Estimation of soil organic carbon reservoir in China. J GEOGR SCI 11, 3–13.

Wang, W., Wang, Q., Lu, Z., 2009. Soil organic carbon and nitrogen content of density fractions and effect of meadow degradation to soil carbon and nitrogen of fractions in alpine Kobresia meadow. Sci. China Ser. D-Earth Sci. 52 (5), 660–668.

Wan, S., Norby, R.J., Ledford, J., Weltzin, J.F., 2007. Responses of soil respiration to elevated CO 2 , air warming, and changing soil water availability in a model old-field grassland. Global Change Biol 13 (11), 2411–2424.

Weischet, W., Endlicher, W., 2000. Regionale Klimatologie Teil 2. Schweizerbart'sche Verlangsbuchhandlung, Stuttgart.

Wiesmeier, M., Steffens, M., Kölbl, A., Kögel-Knabner, I., 2009. Degradation and small-scale spatial homogenization of topsoils in intensively-grazed steppes of Northern China. Soil and Tillage Research 104 (2), 299–310.

Wu, G.-L., Liu, Z.-H., Zhang, L., Chen, J.-M., Hu, T.-M., 2010a. Long-term fencing improved soil properties and soil organic carbon storage in an alpine swamp meadow of western China. Plant Soil 332 (1-2), 331–337.

Wu, H., Guo, Z., Gao, Q., Peng, C., 2009. Distribution of soil inorganic carbon storage and its changes due to agricultural land use activity in China. Agriculture, Ecosystems & Environment 129 (4), 413–421.

Wu, H., Guo, Z., Peng, C., 2003. Land use induced changes of organic carbon storage in soils of China. Global Change Biol 9 (3), 305–315.

Wu, J., Sheng, Y., Wu, Q., Wen, Z., 2010b. Processes and modes of permafrost degradation on the Qinghai-Tibet Plateau. Sci. China Ser. D-Earth Sci. 53 (1), 150–158.

Wu, R., Tiessen, H., 2002. Effect of Land Use on Soil Degradation in Alpine Grassland Soil, China. Soil Science Society of America Journal 66 (5), 1648.

Wu, S., Yin, Y., Zheng, D., Yang, Q., 2005. Climate change in the Tibetan Plateau during the last three decades. Acta Geographica Sinica 60, 3–11.

Wütherich, C., Möller, D., Thannheiser, D., 2000. Pflanzengesellschaften und Kohlenstoffhaushalt der höheren und der niederen Arktis. Geoöko 21, 103–119.

Wu, Z., 1980. Vegetation of China. Science Press, Beijing.

Xie, X., Yang, G.J., Wang, Z.R., Wang, J., 2010. Landscape pattern change in mountainous areas along an altitude gradient in the upper reaches of Shule River. Chinese Journal of Ecology 29, 1420–1426.

Xie, Z., Zhu, J., Liu, G., Cadisch, G., Hasegawa, T., Chen, C., Sun, H., Tang, H., Zeng, Q., 2007. Soil organic carbon stocks in China and changes from 1980s to 2000s. Global Change Biol 13 (9), 1989–2007.

Xue, X., Guo, J., Han, B., Sun, Q., Liu, L., 2009. The effect of climate warming and permafrost thaw on desertification in the Qinghai–Tibetan Plateau. Geomorphology 108 (3-4), 182–190.

Xu, S.X., Zhao, X.Q., Li, Y.N., Zhao, L., Yu, G.R., Sun, X.M., Cao, G.M., 2005. Diurnal and monthly variations of carbon dioxide flux in an alpine shrub on the Qinghai–Tibet Plateau. Chin.Sci.Bull. 50, 539–543.

Yan, C., Song, X., Zhou, Y., Duan, H., Li, S., 2009. Assessment of aeolian desertification trends from 1975's to 2005's in the watershed of the Longyangxia Reservoir in the upper reaches of China's Yellow River. Geomorphology 112 (3-4), 205–211.

Yang, M., Nelson, F.E., Shiklomanov, N.I., Guo, D., Wan, G., 2010a. Permafrost degradation and its environmental effects on the Tibetan Plateau: A review of recent research. Earth-Science Reviews 103 (1-2), 31–44.

Yang, M., Wang, S., Yao, T., Gou, X., Lu, A., Guo, X., 2004a. Desertification and its relationship with permafrost degradation in Qinghai-Xizang (Tibet) plateau. Cold Regions Science and Technology 39 (1), 47–53.

Yang, S., Jung, H.-S., Li, C., 2004b. Two unique weathering regimes in the Changjiang and Huanghe drainage basins: geochemical evidence from river sediments. Sedimentary Geology 164 (1-2), 19–34.

Yang, Y., Fang, J., Ji, C., Han, W., 2009a. Above- and belowground biomass allocation in Tibetan grasslands. Journal of Vegetation Science 20, 177–184.

Yang, Y., Fang, J., Ji, C., Ma, W., Su, S., Tang, Z., 2010b. Soil inorganic carbon stock in the Tibetan alpine grasslands. Global Biogeochem. Cycles 24 (4), n/a.

Yang, Y., Fang, J., Smith, P., Tang, Y., Chen, A., Ji, C., Hu, H., Rao, S., Tan, K., He, J.-S., 2009b. Changes in topsoil carbon stock in the Tibetan grasslands between the 1980s and 2004. Global Change Biology 15 (11), 2723–2729.

Yang, Y., Fang, J., Tang, Y., Ji, C., Zheng, C., He, J.-S., Zhu, B., 2008. Storage, patterns and controls of soil organic carbon in the Tibetan grasslands. Global Change Biol 14 (7), 1592–1599.

Yang, Y.H., Fang, J.Y., Guo, D.L., Ji, C.J., Ma, W.H., 2010c. Vertical patterns of soil carbon, nitrogen and carbon: nitrogen stoichiometry in Tibetan grasslands. Biogeosciences Discuss. 7 (1), 1–24.

Yang, Z., Ouyang, H., Zhang, X., Xu, X., Zhou, C., Yang, W., 2011. Spatial variability of soil moisture at typical alpine meadow and steppe sites in the Qinghai-Tibetan Plateau permafrost region. Environ Earth Sci 63 (3), 477–488.

Yao, T., Liu, X., Wang, N., Shi, Y., 2000. Amplitude of climatic changes in Qinghai-Tibetan Plateau. Chin.Sci.Bull. 45 (13), 1236–1243.

Yi, S., Zhou, Z., Ren, S., Xu, M., Qin, Y., Chen, S., Ye, B., 2011. Effects of permafrost degradation on alpine grassland in a semi-arid basin on the Qinghai–Tibetan Plateau. Environ. Res. Lett. 6 (4), 45403.

Zeller, V., Bahn, M., Aichner, M., Tappeiner, U., 2000. Impact of land-use change on nitrogen mineralization in subalpine grasslands in the Southern Alps. Biology and Fertility of Soils 31 (5), 441–448.

Zhang, F., Wang, T., Xue, X., Han, B., Peng, F., You, Q., 2010. The response of soil CO2 efflux to desertification on alpine meadow in the Qinghai–Tibet Plateau. Environ Earth Sci 60 (2), 349–358.

Zhang, J.H., Liu, S.Z., Zhong, X.H., 2006. Distribution of soil organic carbon and phosphorus on an eroded hillslope of the rangeland in the northern Tibet Plateau, China. Eur J Soil Science 57 (3), 365–371.

Zhang, J., Wang, J.T., Chen, W., Li, B., Zhao, K., 1988. Vegetation of Xizang (Tibet). Science Press, Beijing.

Zhang, Y., Ohata, T., Kadota, T., 2003. Land-surface hydrological processes in the permafrost region of the eastern Tibetan Plateau. Journal of Hydrology 283 (1-4), 41–56.

Zhang, Y., Tang, Y., Jiang, J., Yang, Y., 2007a. Characterizing the dynamics of soil organic carbon in grasslands on the Qinghai-Tibetan Plateau. SCI CHINA SER D 50 (1), 113–120.

Zhang, Y., Tang, Y., Jiang, J., Yang, Y., 2007b. Characterizing the dynamics of soil organic carbon in grasslands on the Qinghai-Tibetan Plateau. Sci. China Ser. D-Earth Sci. 50 (1), 113–120.

Zhao, L., Cheng, G., Li, S., Zhao, X., Wang, S., 2000. Thawing and freezing processes of active layer in Wudaoliang region of Tibetan Plateau. Chin.Sci.Bull. 45, 2181–2187.

Zhao, L., Ping, C.-L., Yang, D., Cheng, G., Ding, Y., Liu, S., 2004. Changes of climate and seasonally frozen ground over the past 30 years in Qinghai–Xizang (Tibetan) Plateau, China. Global and Planetary Change 43 (1-2), 19–31.

Zheng, D., Zhang, Q., Wu, S., 2000. Mountain geoecology and sustainable development of the Tibetan Plateau. The GeoJournal library 57. Kluwer Academic Publishers, Dordrecht, Boston, xii, 393.

Zhou, H., Zhao, X., Tang, Y., Gu, S., Zhou, L., 2005. Alpine grassland degradation and its control in the source region of the Yangtze and Yellow Rivers, China. Grassland Science 51 (3), 191–203.

Zhou, X.M., 2001. "Kobresia" Meadow ecosystem in China. Science and Technology Press, Beijing.

Zimov, S.A., Schuur, E.A.G., Chapin III, F.S., 2006. Permafrost and the Global Carbon Budget. Science 312 (5780), 1612–1613.

Manuscript 1

Pedogenesis, permafrost, and soil moisture as controlling factors for soil nitrogen and carbon contents across the Tibetan Plateau

Global Change Biology (2009), 15 (12): 3001 - 3017

Frank Baumann[1], Jin-Sheng He[2], Karsten Schmidt[1], Peter Kühn[1], Thomas Scholten[1]

[1]Institute of Geography, Chair of Physical Geography, University of Tübingen, Rümelinstrasse 19-23, 72070 Tübingen, Germany

[2]Department of Ecology, College of Urban and Environmental Sciences, Peking University, 100871 Beijing, China

Abstract

We investigated the main parameters [e.g. mean annual air temperature, mean annual soil temperature, mean annual precipitation, soil moisture (SM), soil chemistry and physics] influencing soil organic carbon (C_{org}), soil total nitrogen (N_t) as well as plant available nitrogen (N_{min}) at 47 sites along a 1,200 km transect across the high-altitude and low-latitude permafrost region of the central-eastern Tibetan Plateau. This large-scale survey allows testing the hypothesis that beside commonly used ecological variables, diversity of pedogenesis is another major component for assessing carbon (C) and nitrogen (N) cycling. The aim of the presented research was to evaluate consequences of permafrost degradation for C and N stocks and hence nutrient supply for plants, as the transect covers all types of permafrost including heavily degraded areas and regions without permafrost. Our results show that SM is the dominant parameter explaining 64% of C_{org} and 60% of N variation. The extent of the effect of SM is determined by permafrost, current aeolian sedimentation occurring mostly on degraded sites, and pedogenesis. Thus, the explanatory power for C and N concentrations is significantly improved by adding $CaCO_3$ content (P = 0.012 for C_{org}; P = 0.006 for N_t) and soil texture (P = 0.077 for C_{org}; P = 0.015 for N_t) to the model. For soil temperature, no correlations were detected indicating that in high-altitude grassland ecosystems influenced by permafrost, SM overrides soil temperature as the main driving parameter at landscape scale. It was concluded from the current study that degradation of permafrost and corresponding changes in soil hydrology combined with a shift from mature stages of pedogenesis to initial stages, have severe impact on soil C and plant available N. This may alter biodiversity patterns as well as the development and functioning of the ecosystems on the Tibetan Plateau.

1 Introduction

The Tibetan Plateau is a key area concerning environmental evolution of the earth at regional as well as global scales and proves to be particularly sensitive to global warming (Yao *et al.*, 1995; Liu & Zhang, 1998; Liu & Chen, 2000). It is the youngest, largest and highest plateau in the world, comprising an area of more than 2.4 million km^2 with an average altitude exceeding 4,000 m a.s.l.

The Tibetan Plateau represents the largest high-altitude and low-latitude permafrost area on earth with 54.3% of its total surface affected by permafrost (Cheng, 2005). Mainly due to the low-latitudes, this permafrost subtype is characterized by strong diurnal patterns, high radiation on the surface as well as a distinct geothermal gradient (Wang & French, 1994). Permafrost degradation processes were found to have been even more enhanced over the past decades compared with high latitude-low altitude permafrost regions (Yang *et al.*, 2004). The proposed decay of Tibetan permafrost (Wang *et al*., 2000; Böhner & Lehmkuhl, 2005) will have a strong impact on soil hydrology, leading to severe changes in soil moisture-temperature regimes (Zhang *et al.*, 2003). Thus, there is a direct link to soils, which are the basic resources life in terrestrial ecosystems depends on and of particular importance for the global C cycle (Schimel, 1995; Sudgen *et al.*, 2004). Global environmental change, largely caused by human activities, affects climate as well as soils, and consequently reassigns their role in ecosystem functioning (Vitousek *et al.*, 1997; Chapin *et al.*, 2000).

The key ecosystem attributes likely to impart feedback on climate change in this alpine grassland ecosystem are soil organic carbon (C_{org}) and soil nitrogen (N) stocks (Rodrigo *et al.*, 1997; Wang *et al*., 2007). Many types of grasslands are highly productive, species-rich and consequently among the most responsive of terrestrial ecosystems to climate change, bearing on a global scale 10% of the terrestrial ecosystem's carbon (C) (Schimel *et al.*, 1990; IPCC, 2001). Vegetation of the investigated region consists mainly of alpine meadow and alpine steppe grassland spreading over 60% of the plateau's total surface which corresponds to an area of 1.6 x 10^8 ha and equals 40% of the national Chinese grassland area (Wu, 1980). The alpine meadows of the Tibetan Plateau currently act as a C sink (Kato *et al.*, 2004). Approximately 33.52 Pg C is stored in organic compounds, in which the alpine meadow and steppe ecosystem is responsible for 23.24 Pg (Wang *et al.*, 2002) and hence retains the highest amount of C_{org} and total nitrogen (N_t) in Chinese soils (23.44%), which accounts for 2.5% of the global pool (Wang & Zhou, 1999; Ni, 2002). Therefore, periglacial environments of Central China play a major role in the global C and N cycle, especially due to the pronounced sensitivity of this region to climate change. Considerable losses in soil organic matter and N_t of heavily degraded ecosystems have been observed over the past 20-40 years on the Tibetan Plateau (Wang *et al.*, 2001, 2007; Yang *et al.*, 2009), indicating a significant modification of soil C and N cycles. This makes it essential to get a better under-

standing of the main parameters influencing C and N dynamics and consequently ecosystem functioning in the Tibetan grasslands.

On landscape scale, it is a common approach in ecology to use correlations between control variables, such as climate and topography, and dependent variables, such as vegetation composition and soil parameters (e.g. Wang *et al.*, 2002; Yang *et al.*, 2008). These correlations are also used as basis for modeling feedback interactions of ecosystems on climate change (Burke *et al.*, 1997) as the results of laboratory incubations are not easy to evaluate since incubation conditions are difficult to reproduce and to compare in natural environments (Rodrigo *et al.*, 1997). Most studies concerning stock dynamics in grassland ecosystems, particularly with respect to alpine steppe and meadows, have been carried out solely on a local scale. For example, Fisk *et al.* (1998) showed topographically related soil moisture (SM) patterns as the fundamental control on N cycling and production of biomass in alpine tundra ecosystems. Soil forming factors, as substrate composition and relief position, were considered only in few other studies on C and N dynamics of steppe ecosystems (e.g. Dodd *et al.*, 2000; Hook & Burke, 2000; Dharmakeerthi *et al.*, 2005).

Generally, soil temperature is considered as a key factor of many terrestrial biochemical processes like soil respiration, decomposition of organic matter, N mineralization, denitrification, plant productivity and nutrient uptake by plants (e.g. Raich & Potter, 1995; Lindroth *et al.*, 1998; Rustad *et al.*, 2001; Shaw & Harte, 2001; Callesen *et al.*, 2003; Shaver *et al.*, 2006). However, as major parts of the research area in Tibet, particularly alpine steppes, are moisture-limited, SM has to be taken into account as another crucial parameter (Reichstein *et al.*, 2003).

The main objective of our study was to investigate on a landscape scale the influence of pedogenesis on C and N stocks supplementary to the above-mentioned generally used ecological parameters like climate, temperature, moisture conditions, vegetation, topography and hydrology. We hypothesize that diversity patterns of pedological features across a changing landscape are crucial to assess C and N dynamics more precisely.

2 Materials and methods

2.1 Environmental settings along the transect

During an expedition in summer 2006, launched in cooperation with Peking University, China and University of Tübingen, Germany, along a transect of about 1,200 km length and 200 km width in the central-eastern part of the Tibetan Plateau from Xining to Lhasa, botanical, ecological and pedological settings have been investigated at 47 sites. The transect is situated between 91 to 101°E latitude and 30 to 36°N longitude with an eastern section from Xining to Yushu and a western part from Golmud to Lhasa (Fig. 1).

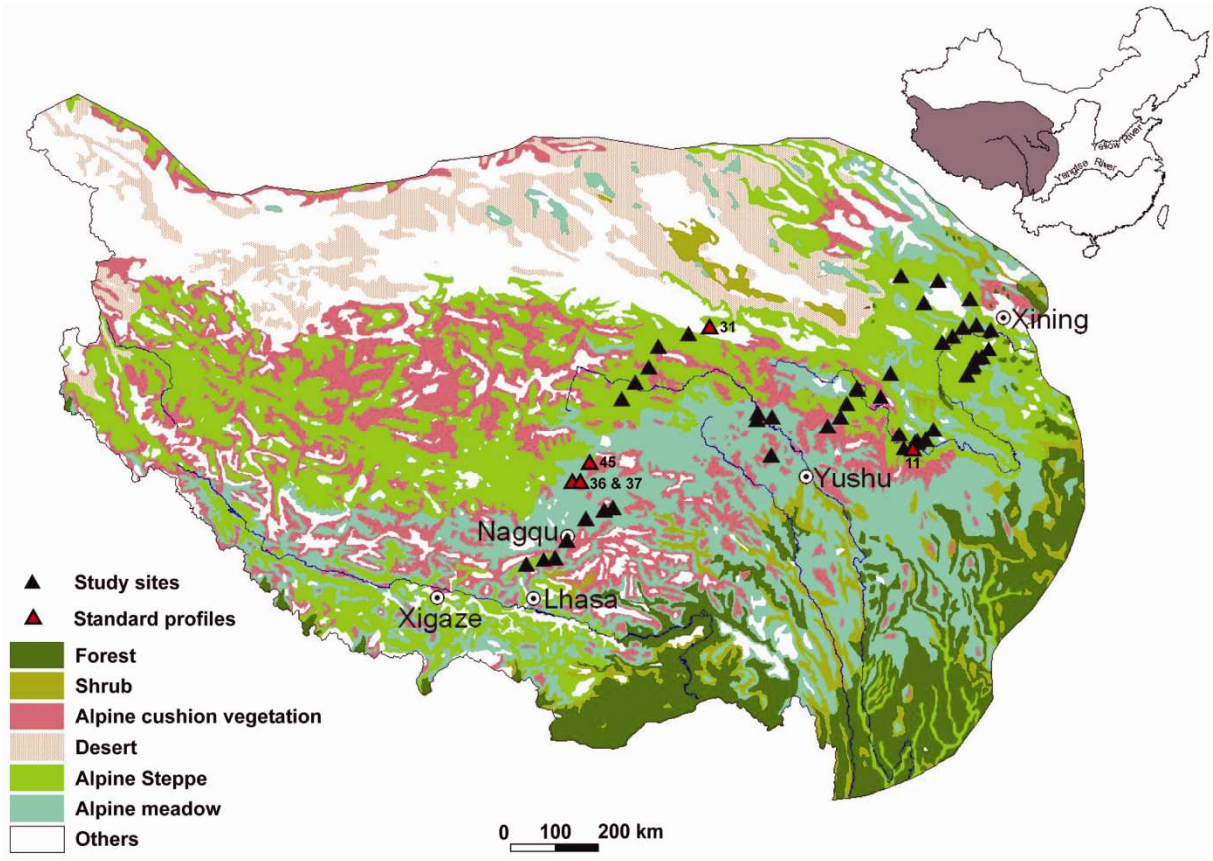

Fig.1 Vegetation map of the Tibetan Plateau, adapted from the Vegetation Map of China (Hou, 1982), showing study sites and standard soil profiles representing the most important soil groups.

Our research is mainly concentrated on plateau grassland areas largely excluding the high mountain regions. The east-west stretching mountain ranges have a major influence by marking important barriers for the relatively moist and warm tropical Indian monsoon coming from the south. The influence of the Asian monsoon decreases westwards (Harris, 2006), leading to both higher temperature and precipitation in the south and east of the plateau. More than 80% of the annual precipitation is occurring during the summer months from July until September ranging from 218 to 600 mm mean annual precipitation (MAP). Mean annual air temperature (MAT) varies from -5.75 to 2.57°C, mean annual evaporation from 1204 to 1327 mm (Yao *et al.*, 2000; Wang *et al.*, 2001; Zhang *et al.*, 2003).

The permafrost characteristics closely follow the mean annual soil temperature (MAST) gradient (Wang & French, 1994; Ping *et al.*, 2004). The depth of the active layer increases from north to south and overall with lower altitude, averaging around 1-2 m in continuous permafrost (Wang *et al.*, 2000; Cheng & Wu, 2007). The diurnal fluctuation may reach 25 - 40°C manifesting frequent daily freeze-thaw cycles and relating consequences for C and N stocks (Ping *et al.*, 2004).

Soils in the study area can be characterised by young development, frequent polygenetic formation and strong degradation features affected by cryogenic or erosive processes. This leads to a high diversity and variety of substrates, geomorphological processes and soil forming factors.

In many soil profiles, relict and mainly humic horizons can be observed. On steep upper slopes Leptic Cambisols and Leptosols are evident, whereas Gleysols are frequent next to rivers or lakes. Gelic Gleysols, Gelic Cambisols, and Permagelic/Gelic Histosols are predominantly developed on permafrost sites. In cold alpine meadow areas, felty turf-like topsoils mainly containing organic residuals are developed and described as Afe-horizons (Kaiser, 2004) having on average high soil organic C contents. This horizon is covering a wide range of different soil types.

Alpine *Kobresia* meadow ecosystems are the most widely distributed vegetation types on the plateau (Zhou, 2001) occurring at elevations ranging from 3200 to 5200 m asl (Kato *et al.*, 2004). The main species are *Kobresia pygmaea*, *Kobresia humilis*, *Polygonum gentiana,* and *Saussurea* sp. In wetlands *Kobresia littledalei*, *Kobresia tibetica*, *Carex lanceolata,* and *Carex muliensis* occur. Alpine steppe vegetation consists mainly of *Stipa purpurea*, *Stipa subsessiliflora* and *Carex moorcroffiana* (Chang, 1981).

2.2 Field methods

Detailed field investigations included soil profile description according to FAO (2006) and IUSS Working Group WRB (2006). Soil sampling was split into three parts: horizon-wise sampling for pedogenesis using soil pits; schematic sampling conducted by drilling at three depth-increments (0-5, 5-10, and 10-20 cm) for C and N analysis; volumetric samples at equal depths for bulk density and gravimetric water content determination.

This was accompanied by on-site extraction of mineralized N (N_{min}) consisting of NO_3-N (nitrate) and NH_4-N (ammonium). At each site four schematic samples of each depth-increment were mixed. The macroscopic root material and other organic compounds were removed. An aliquot of 10 g of homogenized soil was used for extraction with 50 mL 1 M KCl for 60 min immediately after sampling stirred with a glass stirrer every 10 min and then filtered through Whatman No. 42 cellulose filter paper into 100 mL PE-vials. Samples were conserved with 2 mL HCl (30%). For recalculating the contents in dry soil, the gravimetric water content was used.

SM was supplementary determined directly in the field by TDR-probes (Delta-T Devices Ltd,Cambridge, UK) for all pedogenetic horizons as well as for the depth increments. Above- and belowground biomass was investigated at a 1 m^2 sampling square at each site by clipping and digging out the roots. The same method was used to describe plant species composition.

Soil temperature was measured with buried temperature data loggers (Hobo U12, Onset Computer Corporation, Pocasset, MA, USA) at an interval of 1 h starting in July 2006 for 1 year.

2.3 Laboratory analysis

Grain size analysis was done by combined pipette and sieving method (seven fractions, Koehn, DIN 19683-1). Color description was carried out with Munsell Soil Color Charts. Electrical conductivity was determined in bi-distilled H_2O while pH was measured in both 0.01 M $CaCl_2$ and bi-distilled H_2O potentiometrically. $CaCO_3$ was analyzed volumetrically. Soil-N_t and -C_{org} was measured with heat combustion (VARIO EL III, Elementar, Hanau, Germany). C bound in $CaCO_3$ was subtracted from the total amount of C (C_t) quantified with CN analysis to get the proportion of organic C (C_{org}). The KCl-extractions for N_{min}-analysis were measured photometrically (CFA SAN Plus, Skalar, Breda, the Netherlands). Water content was determined gravimetrically by taking the skeleton content into account.

2.4 Data analysis and statistical applications

The investigated soil profiles were sorted into different groups based on field observations, soil description and laboratory analysis of the profile pits and horizon-wise samples. In this context, pedogenesis is described by acidity, carbonate content and grain size distribution. Five sites were chosen as representative soil profiles out of 47 sites, under which the other research areas could be subordinated. For statistical analyses the whole dataset of 47 sites was used.

Climate data for each site was calculated based on linear models using latitude, longitude, and altitude as variables from 50-year averaged temperature and precipitation records (1951-2000) at 680 well-distributed climate stations across China (He *et al.*, 2006). For statistical approaches the results of the schematic sampling series was utilized with a sample size of n = 141. This dataset was split into the three sampling depths (0-5, 5-10, 10-20 cm). To examine dependencies, correlation and regression analyses were conducted for SM, MAST, MAT, MAP, soil texture, carbonate content ($CaCO_3$), and soil acidity (pH). To address multicollinearity, out of these predictors only variables with $R^2 < 0.5$ were used for regression analysis in the same model.

The significant relationships were included into a least squares (OLS) regression analysis. A general linear model (GLM) was used to describe the effects of the dependent parameters (vide supra) on the independent variables (C_{org}, N_t, NH_4^+ and NO_3^-). This single condition models where used to investigate the impact of each dependent variable based on correlation analysis and multiple linear model explanation. The differences of the contribution of site parameters were compared by one-way analysis of variance (ANOVA). For all dependent parameters multicollinearity was tested. The analyses were performed with SPSS 10.0 J for Windows and R software package (R Development Core Team, 2009).

3 Results

3.1 Pedogenesis

All investigated soil profiles were allocated to five different main soil groups, covering most soil types of the Tibetan Plateau (Table 1). These main soil groups represent different stages of maturity, from initial soil formation to long developed soils underlain by stable permafrost conditions. Soil development is often young and has been frequently disturbed or interrupted over time. Therefore, relict, mostly humic horizons can be observed in some profiles, representing phases of stability. The most important factor controlling these processes is recent active aeolian sedimentation, diluting the topsoil's chemical composition or burying the developed soils completely (cf. site 31). This explains the strong trend to accumulate carbonates and bases often also relocated to deeper horizons, recognizable by carbonate pseudo-mycelic structures. In the southern and eastern part, distinct weathering and enrichment of secondary Fe oxides in Bw horizons can be found disappearing to the north of the continuous permafrost zone. Strong gleyic or stagnic properties are evident towards the southern and eastern margin of the permafrost-affected area with increasing precipitation, although the permafrost table is deeper.

Table 1 Grouping of soil profiles

Pedological Unit	Abbreviation	*n*
Initially formed soils	IS	13
Regosols	RG	7
Cambisols	CM	11
Groundwater Influenced	GL	4
Permafrost Influenced	PF	12

The main differences between sites are substantially related to the permafrost regime. For instance, sites 36 and 37 are situated only 150 m from each other in the discontinuous permafrost zone south of Amduo on a small mountain pass (4900 m asl) (Fig. 2). Position 36 is primarily vegetated by *Kobresia parva* and *K. humilis* forming very felty topsoils, whereas site 37 is dominated by *K. tibetica* and *Carex* spp. community developing hummocks alternating with hollows (lower usually water-filled sectors). The distribution of the hummocks is inhomogeneous with an average diameter of 1.5 m and height of 40 cm. Permafrost could be detected at this site in 190 cm depth. No permafrost is evident in a depth of 240 cm at site 36.

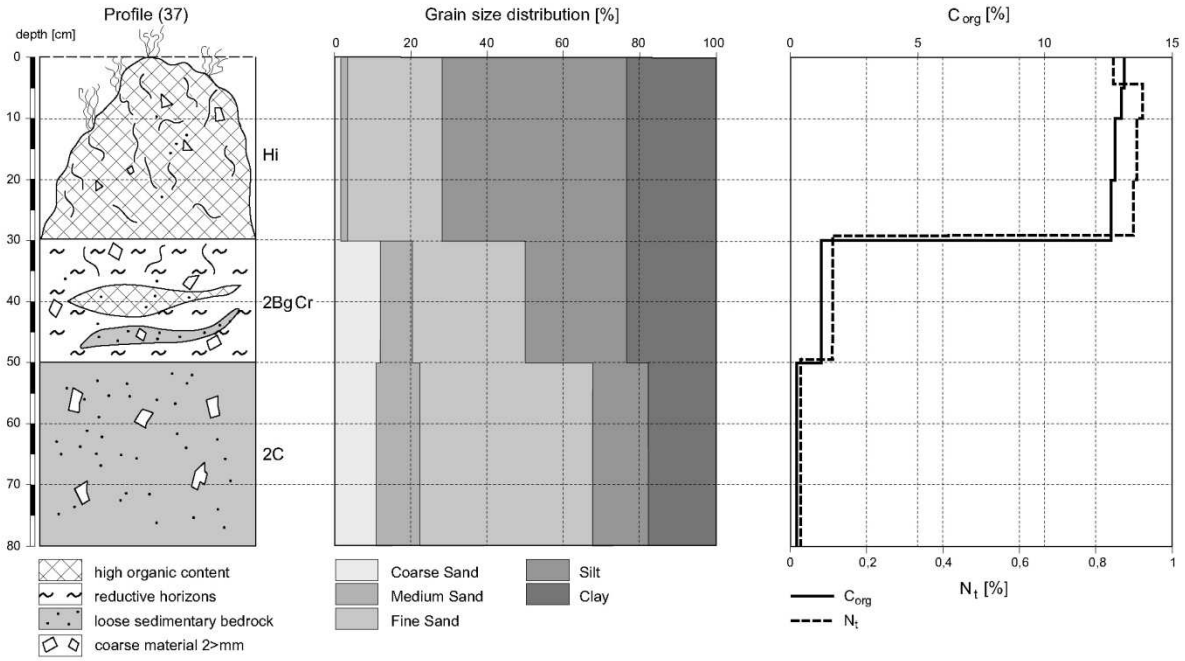

Site 37: Calcaric Gelic Histosol; 4,902 m asl; 32.18°N, 91.72°E; MAT -4.2°C; MAP 472 mm/a; upper middle slope; *Kobresia schoenoides, Carex spp., Oxytropis spp., Aster spp.*

Pedogenetic samples

Horizon	Depth [cm]	Munsell Color moist	Particles > 2 mm [%]	$CaCO_3$ [%]	pH [$CaCl_2$]	EC [µS cm^{-1}]	C:N ratio
nHcw	0-30	10YR3/2	2.1	0.6	6.8	388	14.1
2BgCr	30-49	10YR4/4	8.8	8.8	7.1	145	11.1
2C	49-80+	7.5YR5/4	8.1	0.4	7.0	54	8.0

Schematic samples

Depth [cm]	SM [vol. %]	Bulk density [g/cm³]	NH_4^+ [mg/kg]	NO_3^- [mg/kg]
0-5	4.4	0.48	7.49	0.23
5-10	11.1	0.40	8.31	0.22
10-20	11.6	0.45	6.21	0.21

Fig. 2a Comparison of sites 37 and 36 in discontinuous permafrost

Sites 45 and 31 (Fig. 3) show an example of the continuous permafrost area between Kunlun Shan and Tanggula Shan. Profile 45 (directly south of Tanggula Shan) is influenced by permafrost at a depth of 145 cm, whereas site 31 (close to Kunlun Shan) is exhibiting severe permafrost degradation features. This is typical for degraded permafrost areas with almost no C or N content due to recent aeolian sedimentation processes acting as a diluter (C_{org} < 0.9%; N_t < 0.06%). The micro-relief at profile 45 is comparable to site 37, although SM is much higher at site 45 due to its relief position in a depression compared to site 37 situated on a mountain pass. Additionally, there is abundant perennial water supply by melting water of nearby snow fields in the mountain range. Strong redoximorphic features can be related to the high groundwater table

due to present permafrost acting as an aquiclude. After heavier and longer rainfalls, the water table is reaching the ground level with only the vegetated bumps being outside the water.

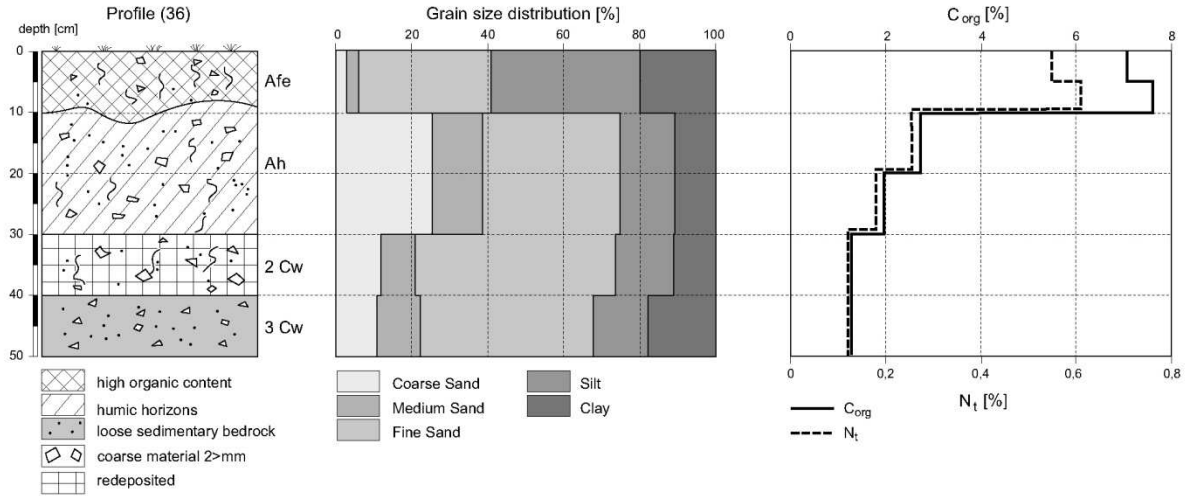

Site 36: Colluvic Regosol; 4,903 m asl; 32.18°N, 91.72°E; MAT -4.2°C; MAP 473 mm/a; middle slope; *Kobresia parva, Kobresia humilis, Stipa regeliana*

Pedogenetic samples

Horizon	Depth [cm]	Munsell Color moist	Particles > 2 mm [%]	$CaCO_3$ [%]	pH [$CaCl_2$]	EC [µS cm^{-1}]	C:N ratio
Afe	0-12	10YR2/2	9.2	0.4	6.9	350	12.7
Ah	12-24	5YR3/2	38.3	0.3	7.0	168	10,9
2Cw	24-41	5YR3/2	15.2	0.2	7.3	89	10,7
3Cw	41-50+	7.5YR5/4	8.5	0.4	7.0	54	8.0

Schematic samples

Depth [cm]	SM [vol. %]	Bulk density [g/cm^3]	NH_4^+ [mg/kg]	NO_3^- [mg/kg]
0-5	2.3	0.71	7.08	0.00
5-10	5.5	0.83	4.18	0.03
10-20	5.5	1.19	2.27	0.00

Fig. 2b *(Continued)*

3.2 Amount and distribution of C and N stocks

On a large scale, C and N stocks decrease from southeastern to northwestern regions corresponding to climate conditions and the influence of the southern tropical or eastern subtropical monsoon, respectively. Because no longitudinal trend can be observed, it is assumed that latitudinal climate effects are stronger. Related to vegetation patterns, stocks of alpine meadows are larger than of alpine steppes (Fig. 4).

Highly fluctuating C and N contents of topsoils can be observed on small spatial scales, mainly controlled by relief position and in particular by related permafrost distribution in discontinu-

ous permafrost areas (Fig. 2). The mineralized fraction of N at the investigated sites can be found almost exclusively as ammonia (NH_4^+), with the highest contents occurring at water saturated sites underlain by permafrost (Fig. 5). Highest C and N contents occur in permafrost and groundwater influenced soils, whereas the lowest amounts appear in initially formed soils with little soil genesis (Fig. 6). There is a clear trend to higher C and N stocks with an advanced degree of maturity of soil development observable, with increasing soil acidity, decreasing carbonate content (Fig. 5) and grain size distribution showing more fine-rich textures (Figs 2 and 3).

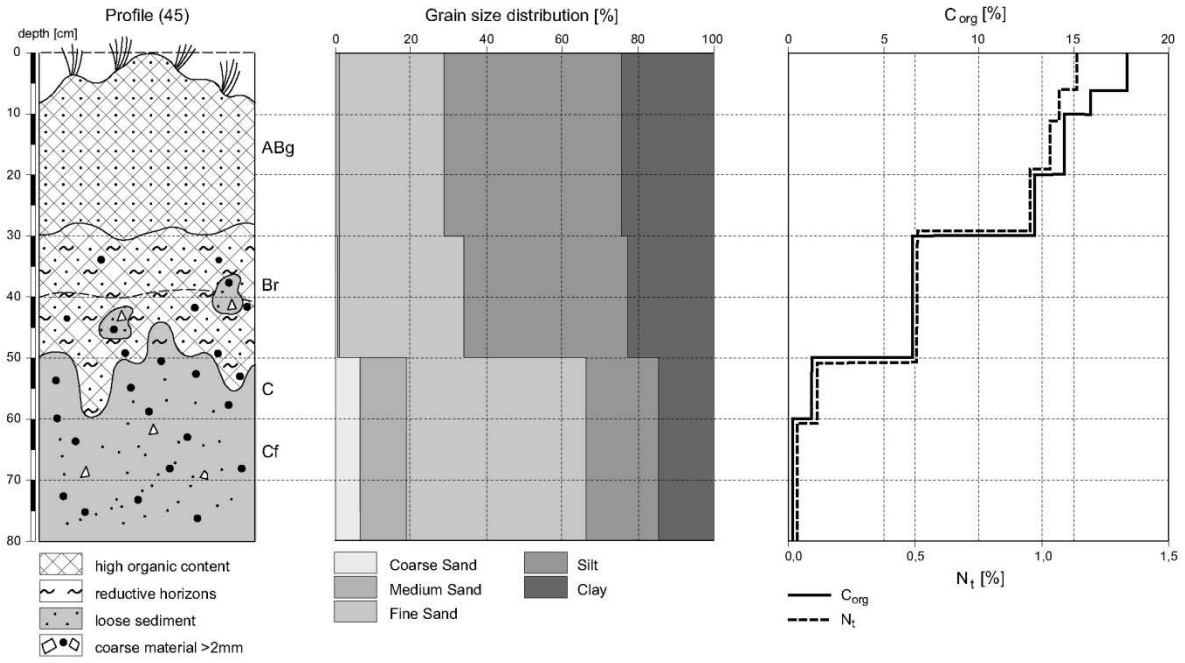

Site 45: Umbric Gleysol above Calcic Gelic Cryosol; 5,105 m asl; 32.58°N, 91.86°E; MAT -5.8°C; MAP 488 mm/a; river floodplain; Kobresia schoenoides, Kobresia humilis, Poa annua

Pedogenetic samples

Horizon	Depth [cm]	Munsell Color moist	Particles > 2 mm [%]	$CaCO_3$ [%]	pH [$CaCl_2$]	EC [µS cm^{-1}]	C:N ratio
ABg	0-25	10YR3/1	1.2	0.8	6.7	444	14.1
Br	25-48	10YR3/1	0.8	0.5	6.7	223	11.1
C	48-68	10YR7/5	0.4	8.2	6.9	108	8.0
Cf	68-150+	10YR7/5	0.3	8.2	7.0	110	7.3

Schematic samples

Depth [cm]	SM [vol. %]	Bulk density [g/cm^3]	NH_4^+ [mg/kg]	NO_3^- [mg/kg]
0-5	55.35	0.44	18.05	0.51
5-10	54.91	0.39	13.37	0.89
10-20	55.91	0.45	11.41	0.54

Fig. 3a Comparison of site 45 (continuous permafrost) and site 31 (degraded). The latter as an example of aeolian sediment input due to permafrost degradation.

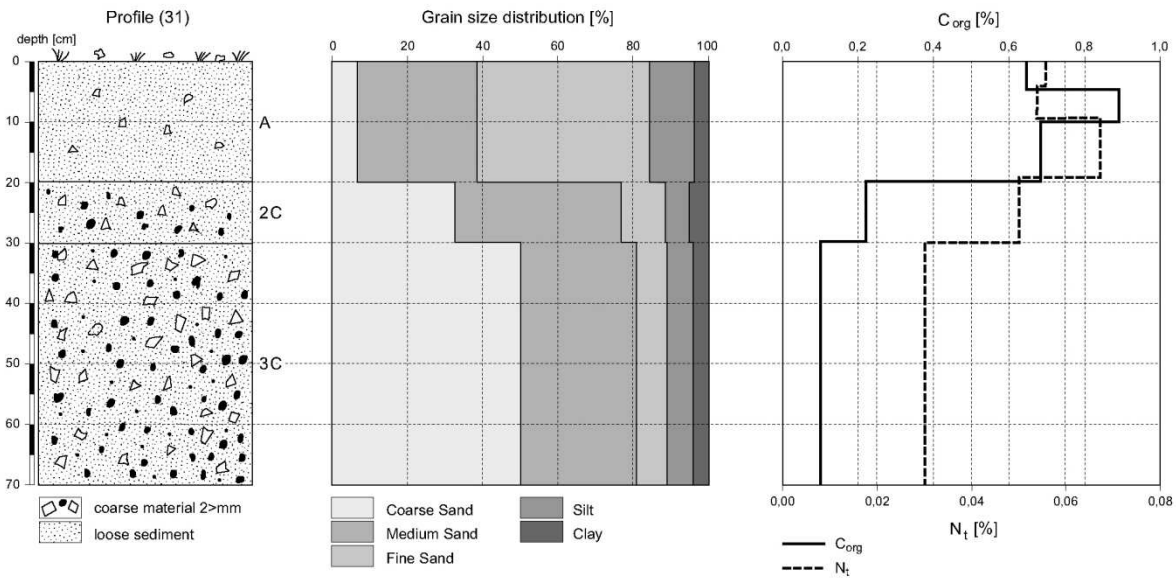

Site 31: Calcaric Regosol; 4,222 m asl; 35.74°N, 94.25°E; MAT -3.1°C; MAP 218 mm/a; plain valley bottom; Stipa purpurea, Kengylia thoroldiana, Carex spp.

Pedogenetic samples

Horizon	Depth [cm]	Munsell Color moist	Particles > 2 mm [%]	$CaCO_3$ [%]	pH [$CaCl_2$]	EC [µS cm^{-1}]	C:N ratio
A	0-17	10YR4/3	7.3	4.3	7.6	134	8.2
2C	17-30	10YR5/2	38.2	3.5	7.6	136	4.4
3C	30-70+	10YR5/2	45.2	4.8	7.6	126	3.3

Schematic samples

Depth [cm]	SM [vol. %]	Bulk density [g/cm^3]	NH_4^+ [mg/kg]	NO_3^- [mg/kg]
0-5	1.8	1.17	2.75	0.23
5-10	2.6	1.47	2.02	0.00
10-20	3.2	1.39	1.69	0.00

Fig. 3b *(Continued)*

3.3 C and N dynamics

Analyses of schematic soil samples show high significant correlations for SM and C contents as well as for SM and N contents (Table 2). Furthermore, significant, but relatively weakened relationships are evident for MAP, whereas no high significant correlations ($P < 0.01$) were found concerning MAT and MAST. The only exception marks the significant temperature dependency of NO_3^- stocks shown by the correlation coefficient after *Spearman*. For all three main fractions of soil texture (sand, silt and clay) also high significant relationships ($P < 0.01$) with C and N contents are evident, whereas only the sand fraction is negatively correlated. Both pH and carbonate content ($CaCO_3$) have negative relationships to the dependent variables.

Variables used as predictors for pedogenesis show strong relationships within the independent parameter set. Most importantly, this is true for MAP and SM (R^2 = 0.42, P < 0.001) as well as for pH and $CaCO_3$ (R^2 = 0.50, P < 0.001). But also other parameters correlate, for example soil texture and soil moisture. Interestingly, SM and MAST show a comparably weak negative correlation (Table 2).

The GLM suggests SM as the most important parameter explaining 64% of C_{org} variation. Slightly lower values can be identified for N_t (Fig. 7). Both C_{org} and N_t predictions can be significantly improved by adding $CaCO_3$ and sand contents to the model, explaining 65% and 64% of the variation, respectively (Table 3, Fig. 7). MAT as well as MAST has no influence on the model. Looking at the control parameters, SM explains 64%, MAP 20%, pH 38%, $CaCO_3$ 23% and sand 29% for C_{org}. Concerning N_t, SM accounts for 60%, MAP 27%, pH 24%, $CaCO_3$ 26% and sand for 35% of the variation. The best-fit model of the GLM regression can be expressed as follows:

(1) C_{org} [%] = 0.398 + 0.009SM - 0.004Sand - 0.018$CaCO_3$

(2) N_t [%] = 4.929 + 0.146SM - 0.248$CaCO_3$ - 0.040Sand

(3) NH_4^+ [mg/kg] = 4.321 + 0.135SM - 0.201$CaCO_3$

4 Discussion

4.1 Impact of pedogenesis and spatial heterogeneity of C_{org}, N_t and N_{min}

The landscape along the investigated transect is a patchwork of geochemically very diverse microecosystems that show variations in organic matter, nutrient stocks, plant communities and productivity. These differences are closely related to topographic position and permafrost distribution, particularly in areas affected by discontinuous permafrost (Fig. 2).

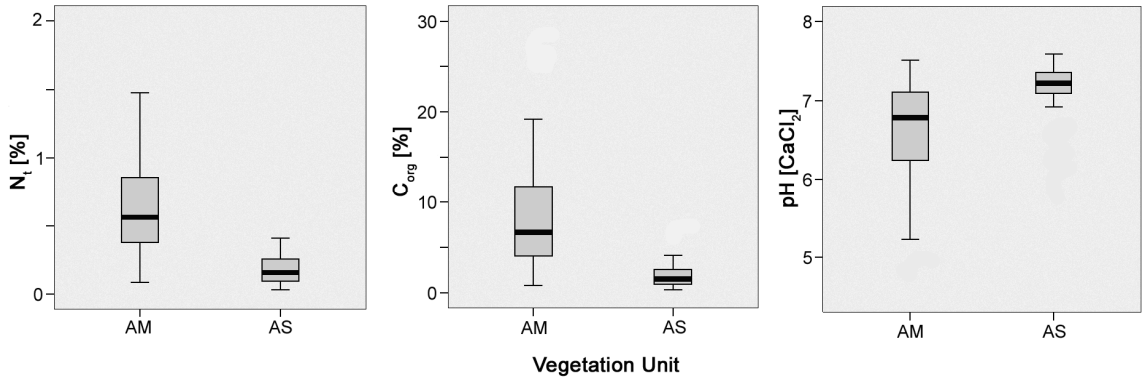

Fig. 4 Distribution for N_t, C_{org}, and soil acidity (pH) for main vegetation units: alpine meadow (AM) and alpine steppe (AS). Higher amounts of N_t and C_{org} and more acid conditions are noticeable in alpine meadow soils indicating a relationship between immature soil development and AS vegetation. The boxplots show median, 25% and 75% quartiles with the error bar indicating 5-95% range of the observation.

The main controlling mechanism of this heterogeneity on the Tibetan Plateau is related to soil hydrological regimes, reflecting different soil drainage classes.

The stage of soil development is an important co-variable to explain nutrient stocks in grassland ecosystems on the Tibetan Plateau (cf. Fig. 6). The lower amount of C and N in soils not influenced by permafrost, can be explained by shorter duration of pedogenesis, predominantly linked to different moisture regimes. Particularly at sites with initial soil formation, frequently affected by aeolian sedimentation, extremely low contents of C and N combined with a high spatial variability were observed. The airborne layers are composed of sandy and coarse-silty, mostly proximal generated material, often linked to direct (e.g. overgrazing, construction) (Zhang *et al.*, 2006) and indirect (climate change) human impact. These processes may be inferred from the status of pH and $CaCO_3$ contents: initially formed soils have highest pH values and carbonate contents with an opposite trend in more mature stages of pedogenesis (Fig. 5).

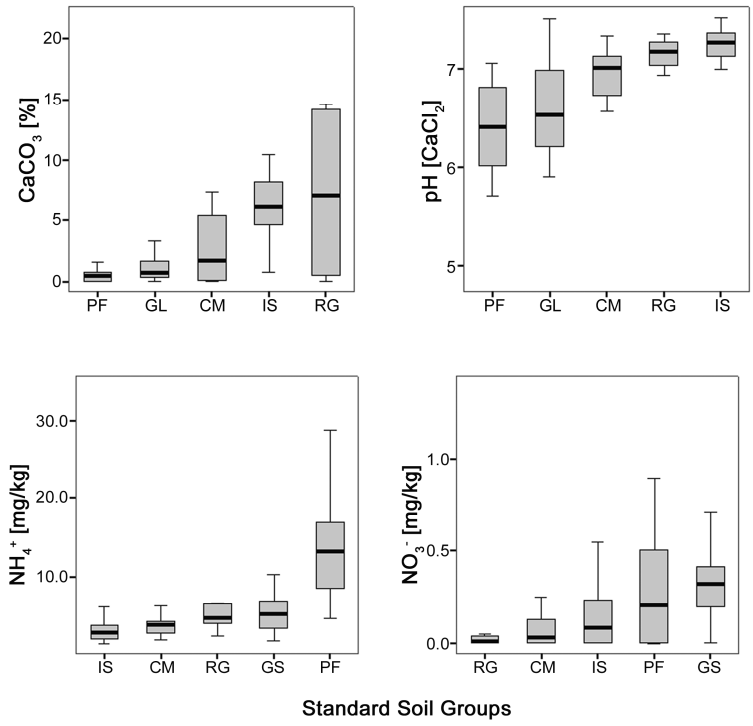

Fig. 5 $CaCO_3$, pH, NH_4^+, and NO_3^- related to standard soil groups. $CaCO_3$ and pH show an overall trend to higher soil acidity and respectively lower $CaCO_3$ content with increasing maturity of soil development. Order of soil groups according to increasing contens (abbreviations for standard soil groups see Fig. 6). The boxplots show median, 25% and 75% quartiles with the error bar indicating 5-95% rang of the observation.

Grain size distribution has a large influence on C and N stocks. Many studies found strong evidence for relationships between different soil textures and C_{org} (e.g. Parton *et al.*, 1994; Schimel *et al.*, 1994) often describing positive correlations between clay and C_{org} or N_t. The relationships between texture and dependent variables of our data show that sand and silt have the strongest impact, whereas clay is correlated to a much lower extent (Table 2). Thus, the ecosystem is dominated by sandy and silty grain size compositions. Sand and silt have an extremely high negative

relationship (R = -0,947**). Consequently, processes controlling the formation of these particular grain size distributions have to be different and thus, recent aeolian sedimentation contributes mainly fine sand rather than silty material to the surface layers. Contrarily, mature soils, which are silt-dominated, show clear positive correlations between the stage of pedogenesis and C stocks, i.e. these soils have higher N and C contents. Highly fluctuating C and N contents of topsoils can therefore be found on a small spatial scale.

NH_4^+ is an essential parameter when N mineralization and microbial activity is studied near saturation (Rodrigo *et al.*, 1997) that is the case at many permafrost influenced sites in our research area. Nitrate-N contents are mostly very low (e.g. Iwatsubo *et al.*, 1989). Aerobic nitrification is restricted at water contents near saturation and denitrification increases as soil water content increases. Ammonification works well even near saturation (Chapin *et al.*, 2002). The high microbial demands for these nutrients in comparable ecosystems may limit plant N availability in arctic and obviously in permafrost influenced soils (Nadelhoffer *et al.*, 1991). Furthermore, nitrate-N can be leached or denitrified especially from wet soils more easily than ammonium-N (Schlesinger, 1997). Although nitrate contents at our sites are low, the dataset shows a significant relationship of nitrate-N with temperature (Table 2), which can be explained by the strong temperature dependency of nitrification processes (Chapin *et al.*, 2002; Robinson, 2002). Overall, NH_4^+-N dominated N availability was highest on wet permafrost-influenced sites supporting the assumption that specific organic matter and moisture characteristics, not microclimatic factors, are responsible for the high N availability (Nadelhoffer *et al.*, 1991).

4.2 Main independent variables and their interactions

Except SM, $CaCO_3$ and sand no other variables were included in the GLM as they show no significant contribution to enhance the explanatory power of the model, despite high correlations of these parameters with the dependent variables (Table 3).

Nevertheless, it is comprehensible why MAP and pH were not included into the model. Generally, one would expect a strong relationship between SM and MAP. The relatively moderate correlation coefficient (R^2 = 0.45**) shows however, that other important environmental controls must be involved. In the study area, permafrost is the second, even more effective mechanism, determining SM content of soils emphasizing the role of permafrost for the ecosystem. Contrarily, MAT and MAST are highly correlated (R^2 = 0.91**), where MAST is modified only weakly by SM (R^2 = -0.29**). This means a more or less direct tracing of air into soil temperatures and explains the major difference of temperature and moisture regime features in high-altitude grassland ecosystems as well as why SM is such a powerful predictor for C and N stocks compared to temperature. $CaCO_3$ proves to be a more stable predictor compared to pH and was therefore

confirmed by ANOVA as a significant contributor to an improved model quality. As the two parameters are soil chemically closely linked, including one is sufficient for an appropriate prediction. Soil acidity as a selective single measurement in the laboratory is in contrast very labile and dependent on many general conditions, such as actual temperature and moisture contents in the field.

For estimating the average moisture regime, deeper layers prove to give a better estimation. The highest R^2 for SM occurs in the deeper increments between 5 and 20 cm (Fig. 7). Because of isolation effects of covering material, the average moisture content in lower layers is more stable than closer to the surface. The uppermost part is more susceptible for strong radiation, diurnal temperature differences and accentuated precipitation events characterizing the special climate conditions on the Tibetan Plateau. Therefore, the average of all depth increments is the most appropriate predictor for moisture regimes for calculating the GLM. This is mainly the case because the dataset consists of single measurements instead of continuous monitoring which makes it likely to pick extreme events for the measurements. Moreover, it has to be mentioned that 2006 was a comparably dry year which implies a general underestimation of SM content especially at wet sites leading to an overall undervaluation of the impact of SM on the model. Dry sites do not show as high variation in dry years as wet sites which are generally groundwater level dependent. Topsoils are drying out rather quickly due to commonly found coarse grain size compositions, especially at sites with fresh airborne sediment. At sites, where water is retained for example by permafrost, moisture supply is proportionally linked to the groundwater level which is in turn related to the amount of precipitation. Consequently, for the variable sand the opposite is true indicating the top layers as the strongest predictors. This reflects clearly the process of aeolian sedimentation being mainly responsible for the sand input.

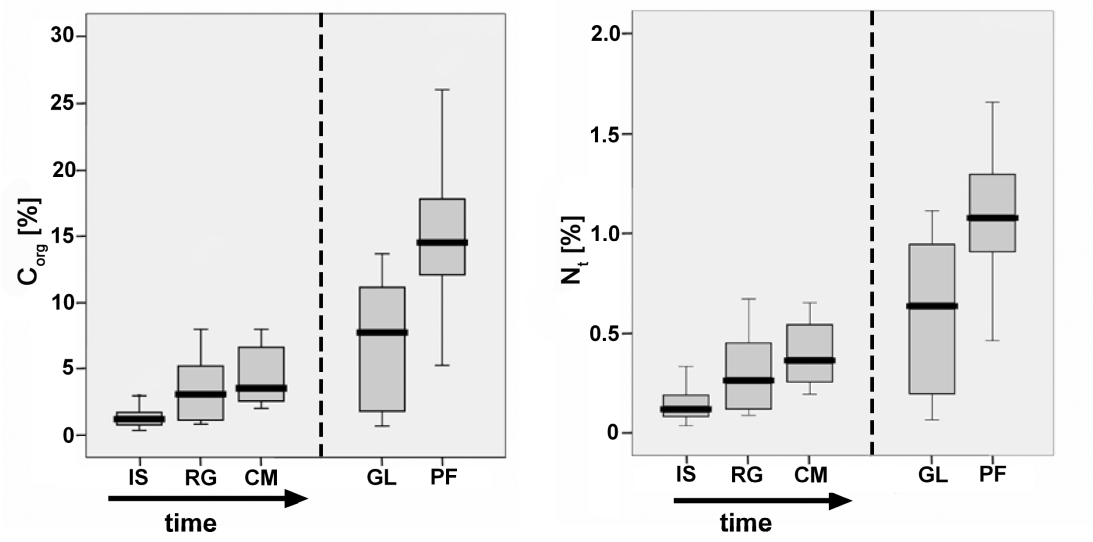

Fig. 6 C_{org} and N_t stocks related to the stage of pedogenesis. IS, initially formed soils; RG, Regosols; CM, Cambisols; GL, groundwater influenced; PF, permafrost influenced. The boxplots show median, 25% and 75% quartiles with the error bar indicating 5-95% rang of the observation.

Ecosystem ecology has usually focused on temperature and modeled soils mostly as an ecosystem feature whose attributes vary strongly by thermodynamic principles (Craine *et al.*, 1999). C and N stocks are assumed to decrease with increasing temperature due to enhanced decomposition processes because temperature sensitivity of decomposition is thought to be greater than of net primary productivity (Shaver *et al.*, 1992; Kirschbaum, 1995). By performing a spatially small scale study at Haibei Alpine Meadow Research Station located at the northeastern margin of the Tibetan Plateau, Kato *et al.* (2006) found no significant relation of seasonal averages of CO_2 exchange to moisture conditions. Therefore, warming climate conditions have positive effects on plant growth in alpine meadows or tundra and wet meadow ecosystems (cf. Kato *et al.*, 2006). The results of our transect study suggest however, that particularly nutrient supply is the crucial point limiting plant growth even when having higher temperatures. A major result of our transect study is the main control of nutrient supply by moisture conditions. Especially at sites where permafrost has been degraded or fresh airborne material was deposited, the proportion of plant available N dropped rapidly. Therefore, rising temperatures have even an indirect negative effect by accelerating permafrost decay, thus lowering SM and therewith plant available nutrient contents. The resulting drainage increases soil aeration and soil respiration rates by improving the oxygen supply to microorganisms. Similar results for soil respiration are evident for northern peatlands showing close linkages to the water table (Moore & Knowles, 1989). Furthermore, parameters affecting photosynthesis and whole-plant C gain (e.g. SM and nutrient availability), are correlated strongly to C_{org} contents in soils (Craine *et al.*, 1999). Therefore, understanding the N cycle is crucial to get an appropriate understanding of the complete ecosystem's feedback mechanisms.

Recent research has also shown that changes in moisture and drainage conditions will have serious impact on N and C cycling of soils in particular ecosystems (Johnson *et al*., 1996; Rodrigo *et al.*, 1997; Hook & Burke, 2000; Janssens *et al.*, 2001; Robinson, 2002; Kato *et al.*, 2004; Shaver *et al.*, 2006). In our research area the impact of moisture has to be seen even more severe due to permafrost control of soil hydrological conditions in vast areas of the Tibetan Plateau. Higher SM together with improved C_{org} quality may lead to enhanced plant productivity and substrate availability in ecosystems and consequently to higher C and N contents in soils (Schimel *et al.*, 1994; Reichstein *et al.*, 2003; Reichstein & Beer, 2008) overshadowing the effect of temperature as shown also in a study about European forest ecosystems (Janssens *et al.*, 2001). Therefore, decomposition may be controlled by substrate quality and quantity as well as moisture rather than by low temperatures. Giardina & Ryan (2000) postulate relatively constant decomposition rates of organic C contained in forest mineral soils across a global-scale gradient in MAT. Their data show no direct influence of temperature limitations on microbial activity and no stimulation of decomposition by increased temperature alone. However, it is questionable if large scale

Table 2 Correlation matrix for the most important site variables

	Altitude [m asl]	MAT [°C]	MAST [°C]	MAP [mm/a]	SM [%]	pH [CaCl2]	$CaCO_3$ [%]	N_t [%]	C_{org} [%]	NH_4^+ [mg/kg]	NO_3^- [mg/kg]	Sand [%]	Silt [%]	Clay [%]
Altitude [m asl]		-0.75 **	-0.72 **	0.10	0.21 *	-0.26 **	-0.03	0.15	0.23 **	0.15	-0.24*	0.30	-0.34**	-0.08
MAT [°C]	-0.74 **		0.91 **	0.04	-0.29 **	0.11	-0.17 *	-0.14	-0.17 *	-0.15	0.14	-0.13	0.12	0.12
MAST [°C]	-0.72 **	0.89 **		0.09	-0.29**	0.05	-0.14	-0.18*	-0.20*	-0.17	0.13	-0.07	0.08	0.04
MAP [mm/a]	0.08	-0.04	0.01		0.42 **	-0.56 **	-0.51 **	0.49 **	0.43 **	0.29 **	-0.13	-0.38 **	0.39**	0.21 *
SM [%]	0.12	-0.27 **	-0.12 *	0.43 **		-0.49 **	-0.33 **	0.75 **	0.73 **	0.60 **	0.05	-0.48 **	0.55**	0.15
pH [$CaCl_2$]	-0.21 *	0.15	0.06	-0.61 **	-0.46 **		0.50 **	-0.53 **	-0.53 **	-0.43 **	0.17	0.26 *	-0.28**	-0.09
$CaCO_3$ [%]	-0.05	-0.07	0.01	-0.56 **	-0.35 **	0.64 **		-0.50 **	-0.47 **	-0.37 **	-0.05	0.15	-0.11	-0.17
N_t [%]	-0.01	-0.02	-0.03	0.54 **	0.60 **	-0.61 **	-0.61 **		0.95 **	0.72 **	-0.00	-0.59 **	0.60**	0.33 **
C_{org} [%]	0.05	-0.04	-0.05	0.53 **	0.59 **	-0.63 **	-0.61 **	0.99 **		0.82 **	-0.02	-0.52 **	0.53**	0.31 **
NH_4^+ [mg/kg]	0.08	-0.15	-0.12	0.38 **	0.55 **	-0.53 **	-0.47 **	0.84 **	0.85 **		0.01	-0.33 **	0.35**	0.15
NO_3^- [mg/kg]	-0.25 **	0.27 **	0.34 **	0.02	0.03	0.09	-0.11	0.24 *	0.23 *	0.23 *		-0.19	0.19	0.11
Sand [%]	0.35 **	-0.22 *	-0.15	-0.17	-0.47 **	0.25*	0.27 **	-0.66 **	-0.63 **	-0.45 **	-0.15		-0.95**	-0.71 **
Silt [%]	-0.39 **	0.16	0.12	0.21	0.56 **	-0.28 **	-0.24 *	0.65 **	0.61 **	0.48 **	0.12	-0.91 **		0.45 **
Clay [%]	-0.10	0.16	0.09	0.12	0.23 *	-0.14	-0.24 *	0.47 **	0.46 **	0.27 **	0.13	-0.76 **	0.45 **	

Product-moment correlation coefficients (Pearson) are shown in the upper triangle; rank correlation coefficients (Spearman) in the lower part. The level of significance is marked.

(**$P < 0.01$; *$P < 0.05$; others $P > 0.05$)

MAP, mean annual precipitation; MAT, mean annual temperature; MAST, mean annual soil temperature; SM, soil moisture.

studies across various climates (cf. Giardina & Ryan, 2000) are feasible due to potential (co-) variations of parameters by large magnitude. Therefore, it was proposed to interpret the data under the aspect that other factors rather override the temperature effect, than negating the fundamental relationship of temperature to C and N cycling (Reichstein & Beer, 2008). The difficulty of multicollinearity within the independent parameter set presented was mentioned above. Nevertheless, our study was performed in a clearly defined ecosystem compared to global datasets. For the GLM, parameters were selected appropriately and the correlation between MAT and SM was comparably weak. Yang *et al.* (2008) found similar patterns and controls of C_{org} in Tibetan grasslands. C_{org} density increased with SM, clay and silt content, but only on a low level with MAT. Although, it seems possible that taking annual average temperature data is rather difficult as the climate shows strong diurnal patterns. Moreover, studies from northern Alaska showed insensitivity to temperature between 3° and 9°C but a doubled effect in arrange between 9° and 15°C (Nadelhoffer *et al.*, 1991). Thus, temperature insensitivity of investigated sites on the Tibetan Plateau can be partly caused by the low range of MAT between -5.8° and 2.6°C and range of average July temperatures from 4.9° to 13.8°C. Recent studies in plant physiology also highlight the importance of plant adaptation to the low temperature resulting in a moderate modification of leaf chemical traits and photosynthesis by temperature and precipitation (He *et al.*, 2006).

Our study shows that other factors than temperature are more important between sites at regional and continental scales (cf. Janssens *et al.*, 2001). Summarizing, soil temperature is more likely to account for seasonal and diurnal variations (Kato *et al.*, 2006), not so much when comparing intersite relationships as in the presented study. Temperature dependency may rather be relevant for ecosystems when SM or other factors are not limiting or altering the relationship between temperature and soil processes (Craine *et al.*, 1999; Reichstein *et al.*, 2003).

4.3 Permafrost degradation and its impact on ecosystem functioning

Under present climate conditions, two processes refer to permafrost degradation and corresponding low C and N contents in soils of the Tibetan plateau: (i) a higher mineralization rate under warmer and drier conditions, (ii) the deposition of aeolian sediments. Hence, under increasing temperatures and decreasing annual precipitation, sequestration of large amounts of C can be expected in areas with permafrost (cf. Figs 3 and 6; Shaver *et al.*, 2006; Zimov *et al.*, 2006). In case of amplified permafrost degradation during warmer climate conditions in the future (Liu & Chen, 2000; Wang *et al.,* 2000), a strong increase in areas with recent aeolian sedimentation of blown out material can be expected. Additionally, the mineralization of bound organic matter can be assumed over the period of only some decades for the light fraction of organic C fractions (Hirota *et al.*, 2006; Wang *et al.*, 2008).

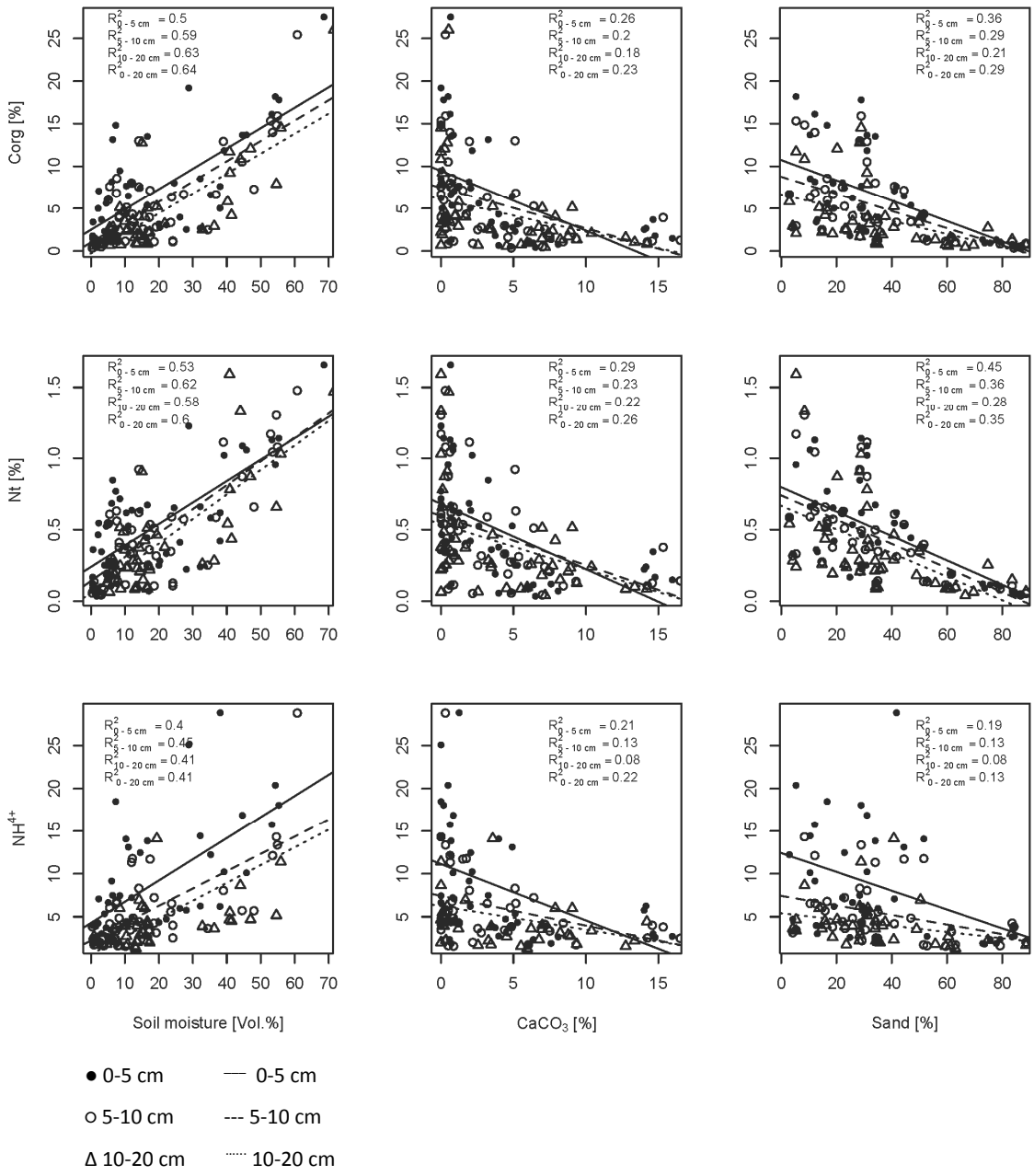

Fig. 7 Relationships between dependent and independent variables with the highest impact on the regression model. The three different depth increments are shown on the graphs.

Semi-natural systems like alpine grasslands on the Tibetan Plateau are generally limited in available plant nutrients. Thus, the productivity of alpine grassland ecosystems is determined by the available nitrogen pool, the amount of nitrogen input as well as by nitrogen fixation (Körner, 1999), modified by water availability to plants over the year (Gründling & Scholten, 2006). Hence, plants' nutrients availability is closely linked to the degradation processes. This is a major issue to address in terms of climate change when discussing about how higher vegetation could potentially sequestrate C lost by enhanced decomposition (Hungate *et al.*, 2003) and how the system will behave under elevated CO_2 conditions (Morgan, 2002). Our results indicate a rapid decrease of plant available N leading to the assumption, that the general nutrient situation

may limit plant growth even more severely than the changing direct environmental parameters in the first place (cf. Fig. 5).

Table 3 Summary of the general linear model (GLM) and ANOVA indicating the integrative effects of soil moisture (SM), $CaCO_3$ and texture for the depth of 0-20 cm

Source	Estimate	SE	*t*-value	Significance Pr (>|*t*|)	MS	*F*-value	Significance Pr (>*F*)
Dependent Variable: C_{org} (0-20 cm); Multiple R^2 = 0.65; Residual SE = 0.198 on 35 df							
SM	0.009	0.003	3.546	0.00113	374.75	52.423	0.000000019
Sand	-0.004	0.002	-2.497	0.01737	23.76	3.324	0.07685
$CaCO_3$	-0.018	0.008	-2.425	0.02059	49.63	6.943	0.01245
Dependent Variable: N_t (0-20 cm); Multiple R^2 = 0.64; Residual SE = 2.638 on 36 df							
SM	0.146	0.033	4.447	0.00008	1.93	49.360	0.000000035
$CaCO_3$	-0.248	0.091	-2.728	0.00979	0.34	8.673	0.005708
Sand	-0.040	0.022	-1.847	0.07292	0.25	6.514	0.015227
Dependent Variable: NH_4^+ (0-20 cm); Multiple R^2 = 0.48; Residual SE = 2.731 on 35 df							
SM	0.135	0.032	4.209	0.00017	205.19	27.515	0.0000076
$CaCO_3$	-0.201	0.097	-2.083	0.04461	32.36	4.340	0.04461

SE, standard errors; MS, mean square; df, degree of freedom.

5 Conclusions

Three basic features characterize soil genesis on the Tibetan Plateau: young stage of development, frequent polygenetic formation, and strong degradation phenomena triggered by diverse erosive and cryogenic processes. The soil development stage is an important predictor for C and N contents in these soils. This is emphasized by significant contributions of $CaCO_3$ and sand to the GLM, which are used to describe pedogenesis.

However, the results imply that SM is the major controlling parameter of C and N stocks in high altitude grassland ecosystems influenced by permafrost, explaining 65% of C_{org} and 64% of N_t variations, respectively. As MAP and SM show only a moderate correlation compared to the very high relationship between MAT and MAST, it can be concluded that SM is closely linked to permafrost. Consequently, C and N stocks and ecosystem functioning are predominantly affected by permafrost, aeolian sedimentation and the stage of soil development. Permafrost and aeolian sedimentation are also a function of relief position, parent material, human impact, and seasonal climatic fluctuations. Given a shift to drier and warmer climatic conditions, the Tibetan Plateau could change from a net C sink to a net source, implying that C loss by respiration is higher than C fixation connected to enhanced photosynthesis activity.

Including SM as a major factor will be crucial for developing large scale models evaluating C and N dynamics on the Tibetan Plateau. Nevertheless, we infer from our results, that SM tends to

explain intersite variations on landscape scale, whereas ST rather accounts for seasonal or diurnal fluctuations in these particular ecosystems.

6 Acknowledgements

The authors would like to thank members of the Peking University expedition team, particularly Wang Liang, Yang Kuo, Liang Cunzhu, Ma Wenhong, Shen Tong, Wu Yi, Mou Shanmin and Qi Shanxue. This research was supported by the National Natural Science Foundation of China (NSFC Grant 30670322 and 30870381 to J.S.H.) and a graduation fellowship from the state of Baden-Württemberg, Germany (Grant No. VI 4.2 – 7631.2/Baumann). We thank V. Häring, C. Dörfer, J. Daumann and K. Drechsel for assistance with the laboratory works. Michael Scherer-Lorenzen, ETH Zürich, Switzerland, supported us with laboratory equipment.

7 References

Böhner J, Lehmkuhl F (2005) Climate and environmental change modelling in central and high asia. *Boreas*, **34**, 220-231.

Burke IC, Lauenroth WK, Parton WJ (1997) Regional and temporal variation in net primary production and nitrogen mineralization in grasslands. *Ecology*, **78**, 1330-1340.

Callesen I, Liski J, Raulund-Rasmussen K, Olsson MT, Tau-Strand L, Vsterdas L, Westman CJ (2003) Soil carbon stores in Nordic well-drained forest soils-relationships with climate and texture class. *Global Change Biology*, **9**, 358-370.

Chang DHS (1981) The vegetation zonation of the Tibetian Plateau. *Mountain Research and Development*, **1**, 29-48.

Chapin FS III, Matson PA, Mooney H (2002) *Principles of terrestrial ecosystem ecology.* Springer-Verlag, New York.

Chapin FS III, Zavaleta ES, Eviner VT, Naylor RL (2000) Consequences of changing biodiversity. *Nature*, **405**, 234-242.

Cheng G (2005) Permafrost studies in the Qinghai-Tibet Plateau for road construction. *Journal of Cold Regions Engineering*, **19**, 19-29.

Cheng G, Wu T (2007): Responses of permafrost to climate change and their environmental significance, Qinghai-Tibet Plateau. *Journal of Geophysical Research*, **112**, F02S03, doi: 10.1029/2006JF000631.

Craine JM, Wedin DA, Chapin FS III (1999) Predominance of ecophysiological controls on soil CO_2 flux in a Minnesota grassland. *Plant and Soil*, **207**, 77-86.

Dharmakeerthi RS, Kay BD, Beauchamp EG (2005) Factors contributing to changes in plant available nitrogen across a variable landscape. *Soil Science Society of America Journal*, **69**, 453-462.

Dodd MB, Lauenroth WK, Burke IC (2000) Nitrogen availability through a coarse-textured soil profile in the shortgrass steppe. *Soil Science Society of America Journal*, **64**, 391-398.

FAO (2006) *Guidelines for Soil Description,* 4th edn. FAO, Rome.

Fisk MC, Schmidt SK, Seastedt TR (1998) Topographic patterns of above- and belowground production and nitrogen cycling in alpine tundra. *Ecology*, **79**, 2253-2266.

Giardina CP, Ryan MG (2000) Evidence that decomposition rates of organic carbon in mineral soil do not vary with temperature. *Nature*, **404**, 858-861.

Gründling R, Scholten T (2006) The role of pedodiversity and the impact of historical land use for ecosystem functioning (biodiversity) in grassland ecosystems. In: *Proceedings of the International ESSC Congress on 'Soil and Water Conservation under Changing Land Use' in Lleida, Spain* (eds Martinez-Casasnovas JA, Pla Sentis I, Martin MCR, Solanes JCB), pp. 191-194.

Harris N (2006) The elevation history of the Tibetan Plateau and its implications for the Asian monsoon. *Palaeogeography, Palaeoclimatology, Palaeoecology*, **241**, 4-15.

He J-S, Wang Z, Wang X *et al.* (2006) A test of generality of leaf trait relationships on the Tibetan Plateau. *New Phytologist*, **170**, 835-848.

Hirota M, Tang Y, Hu Q *et al.* (2006) Carbon dioxide dynamics and controls in a deep-water wetland on the Qinghai-Tibetan Plateau. *Ecosystems*, **9**, 673-688.

Hook PB, Burke IC (2000) Biogeochemistry in a shortgrass landscape: control by topography, soil texture, and microclimate. *Ecology*, **81**, 2686-2703.

Hou HY (1982) *Vegetation Map of the People's Republic of China (1:4M).* Chinese Map Publisher, Beijing, China.

Hungate BA, Dukes JS, Shaw MR, Luo Y, Field CB (2003) Nitrogen and climate change. *Science*, **302**, 1512-1513.

IPCC (2001) *Climate Change 2001: The Scientific Basis.* Cambridge Univ. Press, Cambridge.

IUSS Working Group WRB (2006) *World reference base for soil resources 2006. World Soil Resources* Reports No. 103, FAO, Rome.

Iwatsubo G, Zheng X, Shidei T (1989) An ecological study of soils in the highlands of western Tibet. II. Vertical change from 3900 m to 5450 m in elevation. *Ecological Research*, **4**, 233-241.

Janssens IA, Lankreijer H, Matteucci G et al. (2001) Productivity overshadows temperature in determining soil and ecosystem respiration across European forests. *Global Change Biology*, **7**, 269-278.

Johnson LC, Shaver GR, Giblin AE, Nadelhoffer KJ, Rastetter ER, Laundre JA, Murray GL (1996) Effects of drainage and temperature on carbon balance of tussock tundra microcosms. *Oecologia*, **108**, 737-748.

Kaiser K (2004) Pedogeomorphological transect studies in Tibet: implications for landscape history and present-day dynamics. *Prace Geograficzne*, **200**, 147-165.

Kato T, Tang Y, Gu S *et al.* (2004) Carbon dioxide exchange between the atmosphere and an alpine meadow ecosystem on the Qinghai-Tibetan Plateau, China. *Agricultural and Forest Meteorology*, **124**, 121-134.

Kato T, Tang Y, Gu S, Hirota M, Du M, Li Y, Zhao X (2006) Temperature and biomass influences on interannual changes in CO_2 exchange in an alpine meadow on the Qinghai-Tibetan Plateau. *Global Change Biology*, **12**, 1285-1298.

Kirschbaum MUF (1995) The temperature dependence of soil organic matter decomposition, and the effect of global warming on soil organic C storage. *Soil Biology & Biochemistry*, **27**, 753-760.

Körner CH (1999) *Alpine Plant Life: Functional Plant Ecology of High Mountain Ecosystems*. Springer Verlag, Berlin.

Lindroth A, Grelle A, Morén AS (1998) Long-term measurements of boreal forest carbon balance reveal large temperature sensitivity. *Global Change Biology*, **4**, 443-450.

Liu X, Chen B (2000) Climatic warming in the Tibetan Plateau during recent decades. *International Journal of Climatology*, **20**, 1729-1742.

Liu XD, Zhang MF (1998) Contemporary climatic change of Qinghai-Xizang (Tibetan) Plateau and its response to greenhouse effect. *Chinese Geographical Science*, **8**, 289-298.

Moore TR, Knowles R (1989) The influence of watertable levels on methane and carbon dioxide emissions from peatland soils. *Canadian Journal of Soil Science*, **69**, 33–38.

Morgan SA (2002) Looking Beneath the Surface. *Science*, **298**, 1903-1904.

Nadelhoffer KJ, Giblin AE, Shaver GR, Laundre JA (1991) Effects of temperature and substrate quality on element mineralization in six artic soils. *Ecology*, **72**, 242-253.

Ni J (2002) Carbon storage in grassland of China. *Journal of Arid Environments*, **50**, 205-218.

Parton WJ, Schimel DS, Ojima DS, Cole CV (1994) A general model for soil organic matter dynamics: sensitivity to litter chemistry, texture and management. In: *Quantitative Modeling of Soil Farming Processes. SSSA Special Publication 39* (eds Bryant RB, Arnold RW) pp. 147-167. ASA, CSSA, and SSA, Madison, WI.

Ping CL, Qiu G, Zhao L (2004) The periglacial environment of China. In: *Cryosols. Permafrost-Affected Soils* (ed Kimble JM) pp. 275-291. Springer-Verlag, Berlin.

Raich JW, Potter CS (1995) Global patterns of carbon dioxide emissions from soils. *Global Biogeochemical Cycles*, **9**, 23-36.

R Development Core Team (2009) *R: A Language and Environment for Statistical Computing.* R Foundation for Statistical Computing, Vienna, Austria.

Reichstein M, Beer C (2008) Soil respiration across scales: the importance of a model-data integration framework for data interpretation. *Journal of Plant Nutrition and Soil Science*, **171**, 344-354.

Reichstein M, Rey A, Freibauer A *et al.* (2003) Modeling temporal and large-scale spatial variability of soil respiration from soil water availability, temperature and vegetation productivity indices. *Global Biogeochemical Cycles*, **17**, 15/1-15/15.

Robinson CH (2002) Controls on decomposition and soils nitrogen availability at high latitudes. *Plant and Soil*, **242**, 65-81.

Rodrigo A, Recous S, Neel C, Mary B (1997) Modelling temperature and moisture effects on C-N transformations in soils: comparison of nine models. *Ecological Modelling*, **102**, 325-339.

Rustad LE, Campbell JL, Marion GM *et al.* (2001) A meta-analysis of the response of soil respiration, net nitrogen mineralization, and aboveground plant growth to experimental ecosystem warming. *Oecologia*, **126**, 543-564.

Schimel DS (1995) Terrestrial ecosystems and the carbon cycle. *Global Change Biology*, **1**, 77-91.

Schimel DS, Braswell BH, Holland EA *et al*. (1994) Climatic, edaphic, and biotic controls over storage and turnover of carbon in soils. *Global Biogeochemical Cycles*, **8**, 279-293.

Schimel DS, Parton WJ, Kittel TGF, Ojima DS, Cole CV (1990) Grassland biogeochemistry: Links to atmospheric processes. *Climatic Change*, **17**, 13-25.

Schlesinger WH (1997) *Biogeochemsitry: An Analysis of Global Change.* Academic Press, San Diego.

Shaver GR, Billings WD, Chapin FS III, Giblin AE, Nadelhoffer KJ, Oechel WC, Rastetter EB (1992) Global change and the carbon balance of arctic ecosystems. *BioScience*, **42**, 433-441.

Shaver GR, Giblin AE, Nadelhoffer KJ, Thieler KK, Downs, MR, Laundre JA, Rastetter EB (2006) Carbon turnover in Alaskan tundra soils of organic matter quality, temperature, moisture and fertilizer. *Journal of Ecology*, **94**, 740-753.

Shaw MR, Harte J (2001) Response of nitrogen cycling to simulated climate change: differential responses along a subalpine ecotone. *Global Change Biology*, **7**, 193-210.

Stevenson FJ, Cole MA (1999) *Cycles of Soil.* New York.

Sudgen A, Stone R, Ash C (2004) Ecology in the underworld. *Science*, **304**, 1613.

Vitousek PM, Mooney HA, Lubchenco J, Melillo JM (1997) Human domination of the earth's ecosystems. *Science*, **277**, 494–499.

Wang B, French HM (1994) Climate controls and high-altitude permafrost, Qinghai-Xizang (Tibet) Plateau, China. *Permafrost and Periglacial Processes*, **5**, 87-100.

Wang G, Li Q, Cheng G, Shen Y (2001) Climate change and its impact on the eco-environment in the source regions of Yangtze and yellow Rivers in recent 40 years. *Journal of Glaciology and Geocryology*, **23**, 346-352.

Wang G, Li Y, Wang Y, Wu Q (2008) Effects of permafrost thawing on vegetation and soil carbon pool losses on the Qinghai-Tibet Plateau, China. *Geoderma*, **143**, 143-152.

Wang G, Qian J, Cheng G, Lai Y (2002) Soil organic carbon pool of grassland soils on the Qinghai-Tibetan Plateau and its global implication. *The Science of the Total Environment*, **291**, 207-217.

Wang G, Wang Y, Li Y, Cheng H (2007) Influence of alpine ecosystem responses to climatic change on soil properties on the Qinghai-Tibet Plateau, China. *Catena*, **70**, 506-514.

Wang S, Jin H, Li S, Zhao L (2000) Permafrost degradation on the Qinghai-Tibet Plateau and its environmental impacts. *Permafrost and Periglacial Processes*, **11**, 43-53.

Wang S, Zhou C (1999) Estimating soil carbon reservoir of terrestrial ecosystem in China. *Geographical Research*, **18**, 349-356.

Wu ZY (1980) *Vegetation of China.* Science Press, Beijing.

Yang M, Wang S, Yao T, Gou X, Lu A, Guo X (2004) Desertification and its relationship with permafrost degradation in Qinghai-Xizang (Tibet) plateau. *Cold Regions Science and Technology*, **39**, 47-53.

Yang Y, Fang J, Tang Y, Ji C, Zheng C, He J-S, Zhu B (2008) Storage, patterns and controls of soil organic carbon in the Tibetan grasslands. *Global Change Biology*, **14**, 1592-1599.

Yang YH, Fang JY, Smith P *et al.*(2009) Changes in topsoil carbon stock in the Tibetan grasslands between the 1980s and 2004. *Global Change Biology*, **15**, doi:10.1111/j.1365-2486.2009.01924.x.

Yao T, Liu X, Wang N (2000) Amplitude of climatic changes in Qinghai-Tibetan Plateau. *Chinese Science Bulletin*, **45**, 98-106.

Yao T, Lonnie G, Thompson LG, Mosley-Thompson E, Yang Z (1995) Recent warming as recorded in the Qinghai-Tibet cryosphere. *Annals of Glaciology*, **21**, 196-200.

Zhang JH, Liu SZ, Zhong XH (2006) Distribution of soil organic carbon and phosphorus on an eroded hillslope of the rangeland in the northern Tibet Plateau, China. *European Journal of Soil Science*, **57**, 365-371.

Zhang Y, Ohata T, Kodata T (2003) Land-surface hydrological processes in the permafrost region of the eastern Tibetan Plateau. *Journal of Hydrology*, **283**, 41-56.

Zhou XM (2001) *"Kobresia" Meadow ecosystem in China.* Science and Technology Press, Beijing.

Zimov SA, Schuur EAG, Chapin FS III (2006) Permafrost and the global carbon budget. *Science*, **312**, 1612-1613.

Manuscript 2

Soil Respiration in Tibetan Alpine Grasslands: Belowground Biomass and Soil Moisture, but Not Soil Temperature, Best Explain the Large-Scale Patterns

PLoS ONE (2012), 7 (4): e34968

Yan Geng[1,2], Yonghui Wang[1], Kuo Yang[1], Shaopeng Wang[1], Hui Zeng[1,3], Frank Baumann[4], Peter Kuehn[4], Thomas Scholten[4], Jin-Sheng He[1,2]

[1]Department of Ecology, College of Urban and Environmental Sciences, and Key Laboratory for Earth Surface Processes of the Ministry of Education, Peking University,Beijing, China

[2]Key Laboratory of Adaptation and Evolution of Plateau Biota, Northwest Institute of Plateau Biology, Chinese Academy of Sciences, Xining, China

[3]Shenzhen Key Laboratory of Circular Economy, Shenzhen Graduate School, Peking University, Shenzhen, China

[4]Department of Geoscience, Physical Geography and Soil Science, University of Tuebingen, Tuebingen, Germany

Abstract

The Tibetan Plateau is an essential area to study the potential feedback effects of soils to climate change due to the rapid rise in its air temperature in the past several decades and the large amounts of soil organic carbon (SOC) stocks, particularly in the permafrost. Yet it is one of the most under-investigated regions in soil respiration (Rs) studies. Here, Rs rates were measured at 42 sites in alpine grasslands (including alpine steppes and meadows) along a transect across the Tibetan Plateau during the peak growing season of 2006 and 2007 in order to test whether: (1) belowground biomass (BGB) is most closely related to spatial variation in Rs due to high root biomass density, and (2) soil temperature significantly influences spatial pattern of Rs owing to metabolic limitation from the low temperature in cold, high-altitude ecosystems. The average daily mean Rs of the alpine grasslands at peak growing season was 3.92 μmol CO_2 m^{-2} s^{-1}, ranging from 0.39 to 12.88 μmol CO_2 m^{-2} s^{-1}, with average daily mean Rs of 2.01 and 5.49 μmol CO_2 m^{-2} s^{-1} for steppes and meadows, respectively. By regression tree analysis, BGB, aboveground biomass (AGB), SOC, soil moisture (SM), and vegetation type were selected out of 15 variables examined, as the factors influencing large-scale variation in Rs. With a structural equation modeling approach, we found only BGB and SM had direct effects on Rs, while other factors indirectly affecting Rs through BGB or SM. Most

(80%) of the variation in Rs could be attributed to the difference in BGB among sites. BGB and SM together accounted for the majority (82%) of spatial patterns of Rs. Our results only support the first hypothesis, suggesting that models incorporating BGB and SM can improve Rs estimation at regional scale.

1 Introduction

Soil respiration (Rs) is the major pathway for carbon (C) exiting terrestrial ecosystems and plays a central role in global carbon cycles [1–3]. Because soil is the largest carbon pool in terrestrial ecosystems, containing more than 1500 Pg C (1 PG = 10^{15} g) [4– 6], small change in the rate of Rs may have a profound impact on atmospheric CO_2 concentration, exerting positive feedbacks to global warming [2,7–9]. Therefore, it is important to understand and be able to predict how Rs responds to environmental variation and climate change.

Rs has been a major research theme, particularly since the beginning of 1990s [2,6,10–16]. Many studies in a variety of ecosystems have been devoted to evaluation of various influencing factors, including microbial activity [17–19], C allocation [20,21], root dynamics [22], and regulators such as temperature, soil moisture, soil texture and other climatic and soil variables [23,24]. Nevertheless, synthetic analyses of existing data show a substantially huge heterogeneity in Rs, for which reason we require comprehensive datasets before being able to discuss the uncertainties that may arise owing to differences in intensity of sampling in different ecosystems [25].

It has been well documented that Rs varies greatly with time and space [25]. With the advanced equipment for high-frequency records of Rs, temperature, moisture and other variables (e.g. [26]), within-site temporal patterns of Rs can be relatively easily obtained. However, to address patterns of ecosystem C cycling at regional scale, to predict responses of Rs to future climate change based on mechanistic data, and to scale-up from specific sites to vegetation biomes, studies on Rs need to move beyond within-site variations in soil temperature and soil moisture and to incorporate differences among broad ecosystem types [6,27,28]. At regional scale, patterns of biogeochemical cycling of different ecosystem types are governed by at least five independent controls or so-called state factors, i.e. climate, parent material, topography, biota, and time [3,29]. Hence, factors closely associated with Rs within-ecosystem and among-ecosystems are not identical. However, compared with the plenty of studies on temporal variations, relatively fewer publications have explored in-depth the regional patterns of Rs and the factors revolving around Rs process (but see [30]).

The Tibetan Plateau is one of the most under-studied regions for Rs research, despite its essential role in the global C cycles. Due to rough natural conditions, only a few studies have measured Rs. Some in alpine steppe [31], some in alpine meadow [32–35], and others in cropland [36].

Alpine grassland accounts for 62% of the total area of the plateau, out of which 32% is alpine steppe, and 30% alpine meadow [37]. Alpine grassland is of special interest because of the high C density [38,39] and potential feedbacks to climate warming [40]. We previously estimated that SOC storage in the top one meter in these alpine grasslands was 7.4 Pg C, with an average density of 6.5 kg m^{-2} [39]. Moreover, the Tibetan Plateau is the largest high-altitude and low-latitude permafrost area on the earth, with over 50% of its total surface in permafrost [41,42]. The observed rapid rises in air temperature [43], degradation of the permafrost and the associated changes in soil hydrology in the last several decades [42,44,45] will seriously impact the C cycles [34,46]. The high-altitude ecosystems, low-latitude permafrost, unique vegetation composition and physiological adaptation to the extreme environments, as well as the relatively low intensity of human disturbance motivated us to focus on carbon cycle and the effects of global climate change on natural ecosystems of the Tibetan Plateau.

The primary objective of this study is to investigate large-scale spatial patterns of Rs and to examine their responses to naturally occurring environmental gradients in order to identify factors most closely associated with Rs in such extreme environments. We hypothesized that:

(1) Belowground biomass is most related to large-scale variations in Rs, because alpine grasslands have a high root biomass density [47]. As a result autotrophs will contribute a large proportion of the total respiratory CO_2 efflux.

(2) Soil temperature is another important influential factor for alpine grassland Rs. This is because low growing-season temperature is a limiting factor for physiological processes in high-altitude grassland ecosystems [48,49]. Therefore, it is predicted that Rs increases with increasing soil temperature.

These two hypothesis were tested in a transect study across alpine grasslands on the Tibetan Plateau. The measurement of Rs in this vast, remote, high-altitude area complements the existing data and help to estimate the global C flux from soils.

2 Materials and Methods

2.1 Ethics Statement

No specific permits were required for the described field studies in the Tibetan Plateau. The research sites are not privately-owned or protected in any way and field studies did not involve endangered or protected species.

2.2 Study sites

This study was conducted during two expeditions in late July and early August of 2006 and 2007, in collaboration with University of Tuebingen, Germany. Out of the 51 sites, 42 were selected for soil respiration measurements along a transect which stretches from latitudes of 30.31 to 37.69°N and longitudes of 90.80 to 101.48°E, and elevations from 2925 to 5105 m a.s.l. (Table 1, Fig. 1).

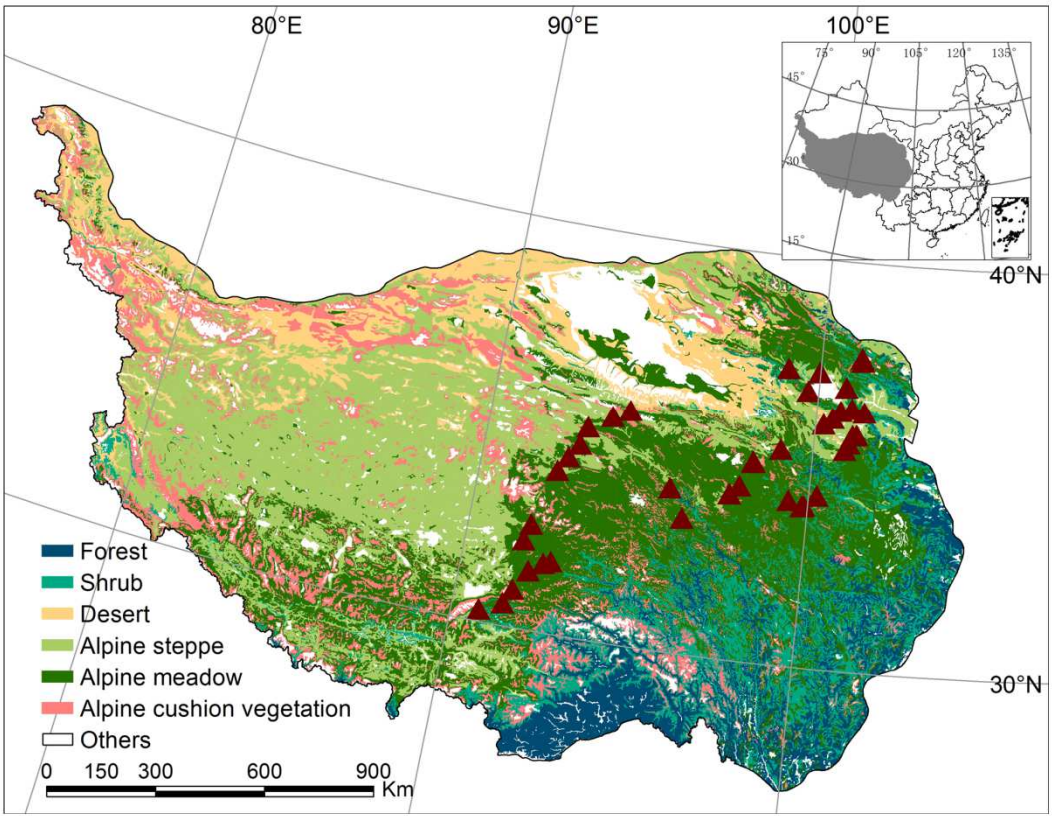

Fig. 1 Vegetation map of the sampling sites, selected from the Vegetation Map of China [80]. Triangles represent sampling sites.

Mean annual air temperature (MAT) and mean annual precipitation (MAP) range from -5.75 to 2.57°C and 218 to 604 mm yr^{-1}, respectively. The vegetation represents alpine grassland, including the two main ecosystem types, alpine meadow and alpine steppe [49,50]. Out of the 42 sites, 23 were alpine meadows and 19 alpine steppes. Alpine meadows are dominated by perennial tussock grasses such as *Kobresia pygmaea* and *K. tibetica*, while alpine steppes are dominated by short and dense tussock grasses such as *Stipa purpurea*; both ecosystem types have extensive distributions. The sites were selected by visual inspection of the vegetation, aiming to sample sites subject to minimal grazing and other anthropogenic disturbances.

Table 1 Description of 42 sites where soil respiration measurements were taken.

Site	Latitude	Longitude	Altitude [m]	MAT [°C]	GST [ºC]	MAP [mm yr^{-1}]	GSP [mm yr^{-1}]	Rs [μmol m^{-2} s^{-1}]	Vegetation
QZ01	36.37	101.48	3454	-1.83	7.33	466	326	4.35	Meadow
QZ02	35.80	101.30	3302	0.03	8.98	475	328	5.27	Meadow
QZ03	35.78	101.17	3263	0.39	9.37	466	322	3.26	Steppe
QZ04	35.58	101.08	3416	-0.37	8.50	488	336	2.87	Steppe
QZ06	35.41	100.97	3517	-0.79	7.99	501	346	4.07	Meadow
QZ07	34.24	100.25	4282	-4.23	3.96	604	414	5.09	Meadow
QZ08	33.96	99.88	4053	-2.11	6.06	580	395	4.08	Meadow
QZ11	33.94	99.83	4156	-2.77	5.38	589	402	5.15	Meadow
QZ13	34.06	99.40	4231	-3.22	5.05	568	389	12.9	Meadow
QZ14	34.92	98.21	4267	-3.96	4.96	464	326	5.06	Meadow
QZ15	34.89	98.23	4224	-3.63	5.27	462	325	2.14	Steppe
QZ17	34.28	97.88	4667	-5.74	2.84	522	364	9.32	Meadow
QZ18	33.32	96.28	4506	-2.89	5.48	482	333	6.00	Meadow
QZ19	34.01	95.80	4201	-1.60	7.15	390	274	3.58	Steppe
QZ22	34.06	97.60	4700	-5.55	2.97	523	365	2.46	Meadow
QZ23	35.29	99.01	4217	-4.48	4.47	478	336	1.19	Steppe
QZ24	36.01	100.25	3109	1.63	10.92	393	274	1.59	Steppe
QZ25	36.17	100.51	2925	2.57	11.93	380	264	0.89	Steppe
QZ26	36.36	100.74	3233	0.08	9.43	409	287	2.19	Steppe
QZ27	36.44	101.09	3486	-1.94	7.32	446	314	5.36	Meadow
QZ28	36.95	100.86	3130	-0.01	9.62	372	265	2.52	Steppe
QZ29	37.26	99.98	3215	-0.55	9.39	319	233	1.78	Steppe
QZ30	37.28	98.99	3437	-1.61	8.48	290	216	4.04	Steppe
QZ31	35.74	94.25	4222	-3.14	6.70	218	170	2.17	Steppe
QZ32	35.52	93.74	4564	-5.01	4.80	238	185	0.39	Steppe
QZ33	35.17	93.04	4682	-5.41	4.31	234	182	0.75	Steppe
QZ34	34.72	92.89	4801	-5.75	3.76	348	249	4.23	Meadow
QZ35	33.99	92.35	4654	-4.22	4.94	336	248	1.24	Steppe
QZ36	32.18	91.72	4903	-4.18	4.12	473	327	2.79	Meadow
QZ38	31.45	92.02	4494	-0.25	7.94	480	341	1.12	Meadow
QZ40	31.77	92.62	4605	-2.05	5.89	523	361	3.03	Meadow
QZ41	31.69	92.41	4596	-1.92	6.00	511	355	3.99	Meadow
QZ42	30.94	91.66	4756	-2.76	5.45	539	371	1.90	Steppe
QZ43	30.56	91.45	4506	-0.53	7.32	507	359	5.94	Meadow
QZ44	30.31	90.80	4324	1.23	8.81	442	326	1.99	Steppe
QZ45	32.58	91.86	5105	-5.75	2.77	488	331	4.59	Meadow
QZ46	34.37	92.61	4656	-4.56	4.78	327	241	1.78	Steppe
QZ47	36.78	99.67	3391	-1.00	8.72	348	251	8.25	Meadow
QZ48	37.61	101.31	3196	-1.53	7.74	363	309	7.26	Meadow
QZ49	37.61	101.31	3196	-2.12	7.19	364	311	10.6	Meadow
QZ50	37.69	101.28	3268	-1.89	7.67	313	270	5.32	Meadow
QZ51	37.28	98.99	3437	-1.61	8.48	290	216	1.99	Steppe

MAT, Mean annual temperature; GST, growing season temperature; MAP, mean annual precipitation; GSP, growing season precipitation; Rs, daily mean soil respiration rate.

2.3 Field measurements

At each site, we conducted (1) measurement of plant biomass after surveying the entire plant community, (2) collections of soil samples at three depths (0–5, 5–10, and 10–20 cm) using soil corer, followed by volumetric samples at equal depths for bulk density and gravimetric water

content determinations, (3) on-site extraction of soil mineralized N (N_{min}) consisting of nitrate (NO_3-N) and ammonium (NH_4-N), and (4) measurement of soil respiration rates.

Plant biomass measurement. We harvested aboveground biomass (AGB) in three plots (1 x 1 m^2) and belowground biomass (BGB) in three soil pits (0.5 x 0.5 m^2) described in Yang et al. [47]. Biomass samples were dried using a custom-built portable oven in the field, and oven-dried at 60°C to a constant weight, and weighed to the nearest 0.01 g upon returning to the laboratory.

Soil property measurement. Soil sampling procedures, soil bulk density (SBD), soil total N (STN) and SOC measurements have been detailed elsewhere [39]. On-site extraction of N_{min} was carried out using a custom-designed equipment which could perform on-site extraction without any disturbances. In brief, 10 g of homogenized soil was extracted with 50 ml 1 mol KCl for 60 minutes immediately after sampling, filtered through Whatman No. 42 cellulose filter paper into 100 ml PE-vials, and conserved by acidification with 3 ml hydrochloric acid (HCl, 30%) [38].

Soil respiration measurement. At each site, seven PVC soil collars (10 cm inside diameter and 5 cm in height) were installed 2–3 cm into the soil along a straight line at one-meter intervals. Rs (CO_2 efflux) was measured with a Li-6400 infrared gas analyzer equipped with the 6400-09 soil flux chamber (Li-Cor Inc, Lincoln, NE, USA). The protocol recommended by LiCor (LI-6400-09 manual) was changed to five observations of 10 μmol mol^{-1} (for steppes) and 30 μmol mol^{-1} (for meadows) per measurement. Typically, soil respiration rates were measured 3–4 times during 4–5 hours from 10:00 to 16:00 (Beijing Standard Time) when soil respiration peaked. To obtain the diurnal pattern, we also measured the complete diurnal variation of soil respiration at nine sites (Fig. 2). We then calculated the ratios of instant Rs from 10:00 to 16:00 to the daily mean Rs for the nine sites. Using these ratios, we calculated daily mean Rs of non-diurnal sites according to similarity in community composition and closeness in distance. On average, diurnal courses of soil respiration were measured every four to five sites. Soil temperature at 10 cm was monitored simultaneously with soil respiration measurement using the attached soil temperature probe. Air temperature was measured with the temperature probe of Li-6400 infrared gas analyzer.

2.4 Laboratory analysis

Dried soil samples were grounded using a ball mill (NM200, Retsch, Germany). Total C and N concentrations were determined on 5–6 mg aliquot of the homogenously grounded material for each sample using an elemental analyzer (2400 II CHNS/O Elemental Analyzer, Perkin-Elmer, Boston, MA, USA) with a combustion temperature of 950°C and a reduction temperature of 640°C. Soil inorganic carbon (SIC) was measured volumetrically using an inorganic carbon analyzer (Calcimeter 08.53, Eijkelkamp, Netherland). Thus SOC was calculated as the difference be-

tween STC and SIC. Soil pH was determined in both 0.01 M $CaCl_2$ and bi-distilled H_2O potentiometrically, but only those of water solution were used in the current study. The KCl-extractions for N_{min}-analysis were measured photometrically using a Continuous Flow Analyzer (SAN Plus, Skalar, Netherlands). Soil moisture (SM) was determined gravimetrically by taking the skeleton content into account.

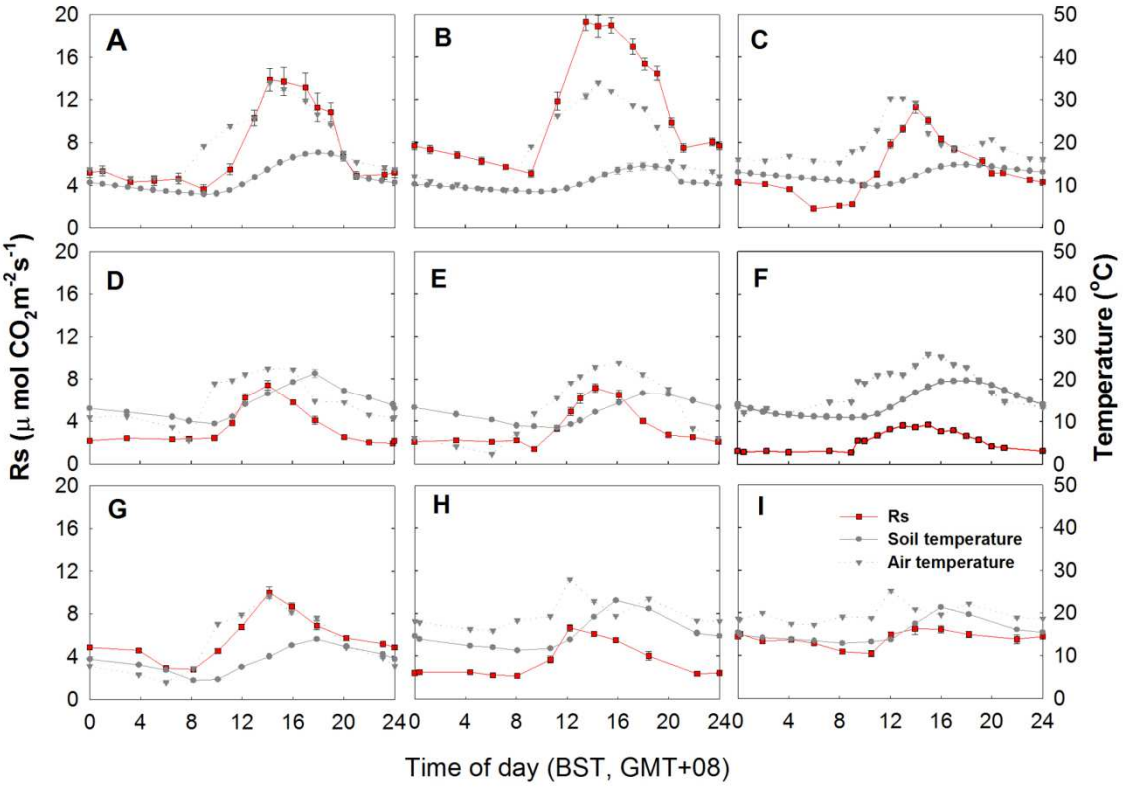

Fig. 2 Diurnal changes of soil respiration rate, soil temperature and air temperature. Complete diurnal courses of soil respiration were measured for seven alpine meadows and two alpine steppes on the Tibetan Plateau. Vertical bars indicate the standard error of the measurement mean (n = 5–7) for each time. (A), Haibei, *Kobresia* and *Festuca* mixed meadow; (B), Haibei, *Kobresia tibetica* meadow; (C), Haibei, *Kobresia pygmaea* meadow; (D) Naqu, *Kobresia pygmaea* meadow; (E) Naqu, *Kobresia tibetica* meadow; (F) Tianjun, *Stipa purpurea* steppe; (G) Fenghuoshan, *Kobresia pygmaea* meadow; (H) Qumalai, *Kobresia pygmaea* meadow; (I) Qumalai, *Festuca* steppe.

2.5 Climate data and statistical analysis

At each site, we installed temperature data loggers (Hobo U12, Onset Computer Corporation, Pocasset, MA) in July 2006 to measure soil temperature (– 10 cm) at 1 h interval. We revisited these sites in July or August in 2007, 2008 and 2009 to download the recorded temperature data. Based on those measurements mean annual soil temperature (MAST) of each site was calculated. The climate data used in this study were calculated based on linear models using latitude, longitude, and altitude as variables from 55-year averaged temperature and precipitation records (1951–2005) at 680 well-distributed climate stations across China [48,51,52].

The variables to explain the spatial variation of soil respiration consist of (1) soil properties,

measured by SOC, SM, MAST, soil C/N ratio, SBD, soil acidity (pH), soil texture (sand content, clay content), and N_{min}, (2) average climate, encompassing growing season temperature (GST), growing season precipitation (GSP), and (3) plant community characteristics, including vegetation type (VT, meadow or steppe), AGB and BGB (Table 2). We used regression tree analysis [53], as implemented in the SAS statistical software package version 8.01 [54], to screen important variables influencing soil respiration, as tree-based modeling is an exploratory data analytic technique for summarizing multivariable and uncovering its structure in large datasets [55]. We selected *F* test's *p*-value as splitting criterion, and set observations required for a split search at 5. Our sample size (42 sites) doesn't allow us to do cross validation, but when we set the *F* test significant level at 0.20, the tree developed was adequate in complexity (depth) and explanation (R^2). From the relative importance in the regression tree which was calculated as the cumulative variance reduction at each split for a particular independent variable, five variables with the importance values greater than 0.4 were screened out, i.e. AGB, BGB, VT, SOC, and SWC (Table 2).

Table 2 Variables included in the regression tree analysis and their importance value.

Variable	*n*	Mean	SD	Range	Importance in regression tree
Soil organic carbon (SOC, %)	42	5.25	4.79	0.339-19.4	1.0000
Aboveground biomass (AGB, g m^{-2})	42	119	100	29.9-530	0.8997
Belowground biomass (BGB, g m^{-2})	42	1816	1957	202-9393	0.8889
Vegetation type (VT)	42	-	-		0.4577
Soil moisture (SM, v/v, %)	42	38.3	50.2	0.44-220	0.4383
Growing season temperature (GST, ^{o}C)	42	6.67	2.25	2.77-11.93	0.1719
Mean annual soil temperature (MAST, ^{o}C)	42	17.0	5.53	–1.12-8.14	0.1621
Growing season precipitation (GSP, mm yr^{-1})	42	306	61.5	170-414	0.0000
Soil temperature (ST, ^{o}C)	42	17.0	5.53	6.30-31.55	0.0000
Soil C/N ratio (C/N, g g^{-1})	39	12.1	2.85	7.97-20.1	0.0000
Soil bulk density (SBD, g cm^{-3})	38	0.94	0.32	0.31-1.65	0.0000
pH	38	7.3	0.52	6.0-8.1	0.0000
Sand content (%)	37	42.3	18.4	20.0-80.0	0.0000
Clay content (%)	37	7.60	6.59	3.0-24	0.0000
Available nitrogen (mmol l^{-1})	37	0.080	0.046	0.026-0.218	0.0000

To address how these variables affect soil respiration both directly and indirectly is challenging because variables measured in field are cross-correlated [11,14,28]. Structural equation modelling (SEM) [56–58] has been used in recent studies to explicitly evaluate the causal relationships among multiple interacting variables (e.g. [59– 61]). SEM aims to account for the roles of multiple variables in a single analysis, providing mechanisms behind the overall patterns by partitioning direct from indirect effects that act through other components of the system. We used SEM here to partition the total effect of variables on soil respiration into direct effects and indirect effects. A path model was developed to relate soil respiration to AGB, BGB, VT, SOC, and SWC, based on theoretical knowledge of the major factors associated with soil respiration at ecosystem level [3]. The model was fitted using EQS 6.1 for Windows [62].

As the results of SEM are dependent on correctly specifying theoretical causal relationships between variables prior to analysis [56,58], the initial theoretical model was modified to improve the fit between model and data. The final model was strong: Bentler's comparative fit index (CFI) = 0.96, Bentler-Bonett normed fit index (NFI) = 0.95. Furthermore, R-squares for Rs, AGB, BGB are very high in the path model.

3 Results

3.1 Overall soil respiration

Across 42 sites, the daily mean Rs of alpine grassland at peak growing season was 3.92 μmol CO_2 m^{-2} s^{-1}, and ranged from 0.39 to 12.88 μmol CO_2 m^{-2} s^{-1} (Table 1), with a coefficient of variation (CV) of 69.1%. The daily mean Rs of steppes was 2.01 μmol CO_2 m^{-2} s^{-1} (ranged from 0.39 to 4.04), while Rs of meadows, 5.49 μmol CO_2 m^{-2} s^{-1} (ranged from 1.12 to 12.88), was approximately two and half times that of the steppes. Although the meadows had a significantly higher Rs than steppes, their CV were similar, being 48.9 and 47.1% for meadow and steppe, respectively.

Large diurnal variations in Rs were observed, although the diurnal patterns were generally similar for meadow and steppe (Fig. 2), both exhibiting the highest Rs during the time from 12:00 to 14:00 BST. Rs and their climatic, community and soil properties for the important ecosystem types, such *as Kobresia pygmaea* meadow, *K. tibetica* meadow, species-rich meadow (mixed-species meadow), and *Stipa* spp. steppe are lised in Table 3. *K. tibetica* meadow had the highest Rs, while *Stipa* steppe had the lowest Rs.

3.2 Factors associated with spatial variations in soil respiration

Based on regression analysis, five variables with an importance value greater than 0.4383 were selected (Table 2), and thus were included in the development of the structural equation models. Other variables had negligible or no impact on soil respiration.

When all five variables were entered into the model, a tree with AGB, vegetation type, and SOC as explanatory variables was developed (Fig. 3B), while BGB and SM were excluded from the model because of the close correlations between BGB and AGB, and SM and vegetation type. When BGB and SM were entered into the model, another tree was developed (Fig. 3A). Both trees are significantly more than a random tree (P<0.001), explaining 86% (Fig. 3A) or 76% (Fig. 3B) of the variance in Rs rate.

Table 3 Soil respiration, community biomass, and soil properties, and climatic variables in different ecosystem types.

Variable	*n*	Mean	SD	*n*	Mean	SD	*n*	Mean	SD	*n*	Mean	SD	*n*	Mean	SD
	***Kobresia humilis* meadow**			***Kobresia tibetica* meadow**			***Stipa* spp. steppe**			**Mixed-specie meadow**			**Others**		
Rs (μmol m^{-2} s^{-1})	11	4.36	1.52	4	9.34	3.49	12	2.18	0.95	3	6.93	1.52	12	2.68	1.49
SOC (%)	11	6.23	3.61	4	11.51	2.54	12	1.96	1.07	3	8.82	6.50	12	4.66	5.68
AGB (g m^{-2})	11	107	65	4	285	188	12	78	40	3	253	114	12	84	41
BGB (g m^{-2})	11	2390	1261	4	5852	2682	12	528	272	3	3299	2051	12	862	619
SM (g water g^{-1} dry soil)	11	32.2	20.4	4	125.1	26.3	12	7.0	4.2	3	45.4	37.7	12	44.6	68.3
GST (^{o}C)	11	6.28	1.46	4	4.46	2.10	12	7.61	2.20	3	8.48	0.66	12	6.38	2.64
Soil MAT ((^{o}C))	11	3.37	1.61	4	0.91	1.88	12	3.80	2.36	3	3.66	0.31	12	2.72	3.09
GSP (mm yr^{-1})	11	351	42	4	349	35	12	257	55	3	296	40	12	301	59
C/N (g g^{-1})	10	13.75	3.20	3	15.19	0.77	12	10.36	1.16	2	11.79	1.56	12	11.81	3.10
BD (g cm^{-3})	10	0.79	0.20	3	0.44	0.01	12	1.14	0.24	2	0.74	0.20	12	1.00	0.35
pH	8	6.9	0.59	3	6.8	0.32	12	7. 7	0.26	3	7.4	0.09	12	7.3	0.53
Sand content (%)	10	34.6	6.0	3	31.0	4.5	12	55.7	23.7	2	37.5	9.2	10	36.1	13.5
Clay content (%)	10	8.2	6.0	3	4.0	3.8	12	5.1	3.7	2	12.5	12.0	10	9.4	8.7
Available N (mmol l^{-1})	10	0.11	0.05	3	0.12	0.03	11	0.05	0.02	2	0.15	0.02	11	0.06	0.04

Rs, daily mean soil respiration rate; SOC, soil organic carbon content; AGB, above-ground biomass; BGB, below-ground biomass, SM, soil moisture; GST, growing season temperature; MAT, Mean annual temperature, GSP, growing season precipitation; SBD, soil bulk density; n, number of sampling sites; SD, standard deviation.

These analyses indicated that BGB, SOC, SM, AGB, and vegetation types are biotic and abiotic factors that are most closely associated with large-scale variations in soil respiration. For the first tree (Fig. 3A), in the areas with BGB>3102 g m^{-2}, only SM had a statistically significant influence on soil respiration rate; while in the areas with BGB<3102 g m^{-2}, both SOC and SM had a detectable effect. For the second tree (Fig. 3B), when AGB>167 g m^{-2}, soil respiration rate was not significantly affected by vegetation type or SOC; by contrast, when AGB<167 g m^{-2}, soil respiration rate was influenced by both vegetation type and SOC.

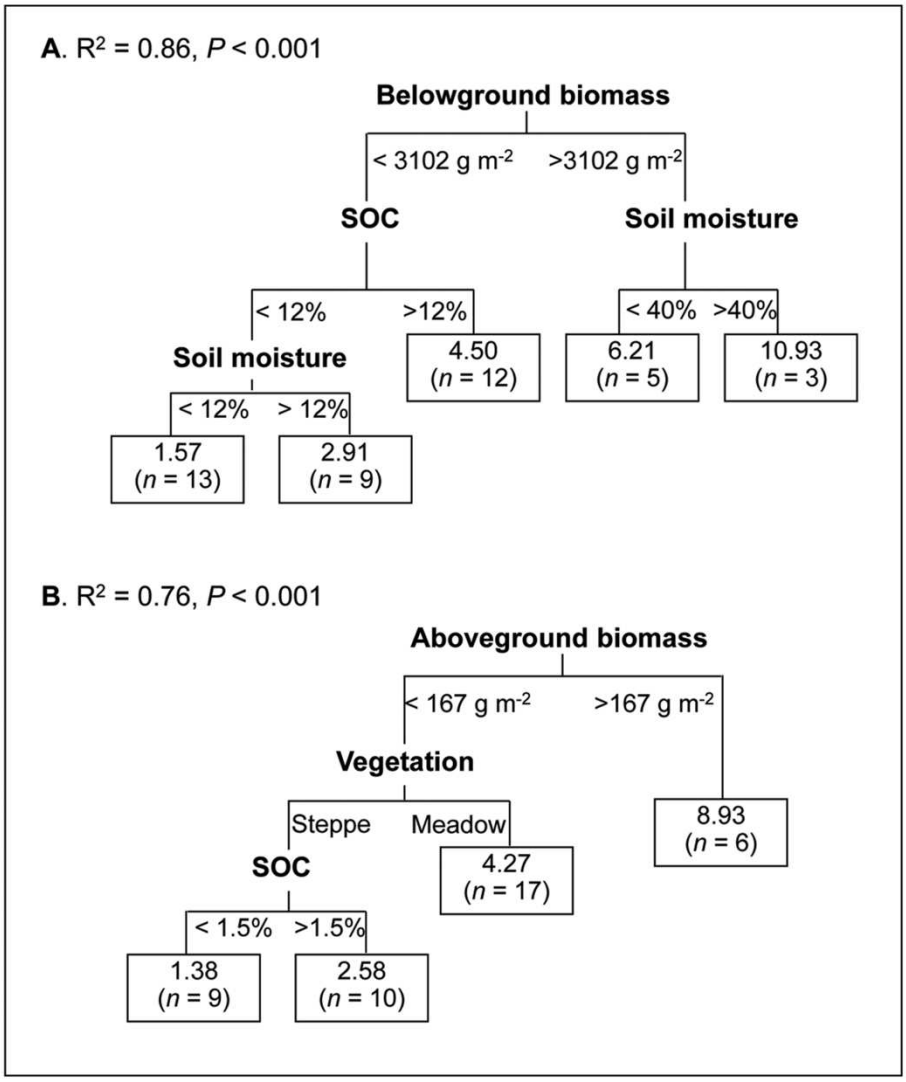

Fig. 3 Regression tree showing generalized relationships between daily mean soil respiration rate and environmental variables. Relationships between soil respiration rate and belowground biomass, soil organic carbon content (SOC) and soil moisture (A), aboveground biomass, vegetation type, and SOC (B). Branches are labelled with criteria used to segregate data. Values in terminal nodes represent mean soil respiration rate of sites grouped within the cluster. The tree explained 86% (A) and 76% (B) of the variance in soil respiration rate, which is significantly more than a random tree (P<0.001). n = number of plots in the category.

3.3 Structural equation modeling to explain variations in soil respiration

From the scatter plots and the box plot (Fig. 4), each of the selected variables such as AGB, BGB, SM, SOC and vegetation type was closely related to Rs. However, because these five variables were intercorrelated, these apparent relationships combined both direct and indirect correlations. Thus, we further used SEM to explicitly evaluate the causal relationships among these interacting variables.

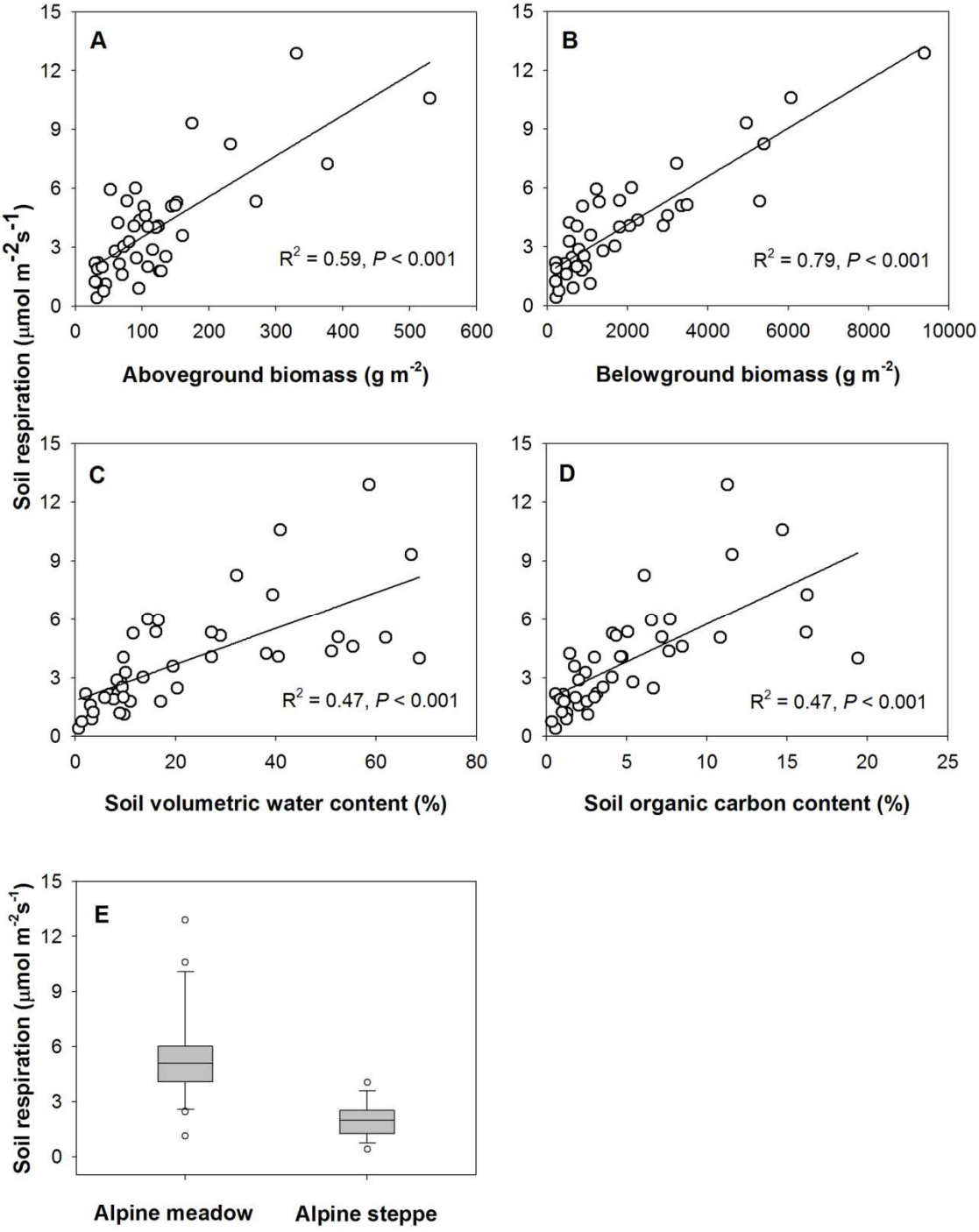

Fig. 4 Scatterplots and box plot for daily mean soil respiration rate versus biotic and abiotic factors. Relationships between soil respiration rate and aboveground biomass (A), belowground biomass (B), soil moisture (C), soil organic carbon content (D), and vegetation type (E).

The final SEM explained 82.1% of the variation in Rs (Fig. 5). Direct, indirect and total effects of the variables are summarized in Table 4. Increasing BGB and SM were strongly associated with increases in Rs, indicating that Rs could be well-predicted from these two variables (R^2 = 0.82). Even though there were significant bivariate relationships between AGB, SOC and Rs, they only had strong indirect positive effects on RS. Vegetation type had only an indirect effect on Rs (0.379) through its direct effect on BGB and its indirect effect on SOC and AGB. The rank of total effects, in decreasing order, was: BGB, AGB, SOC, vegetation type, and SM (Table 4).

It is also evident that, from the SEM (Fig. 5), BGB can well be predicted from vegetation type and AGB, explaining 71.8% of the variation. Moreover, SOC explained about 50% of the variations in AGB.

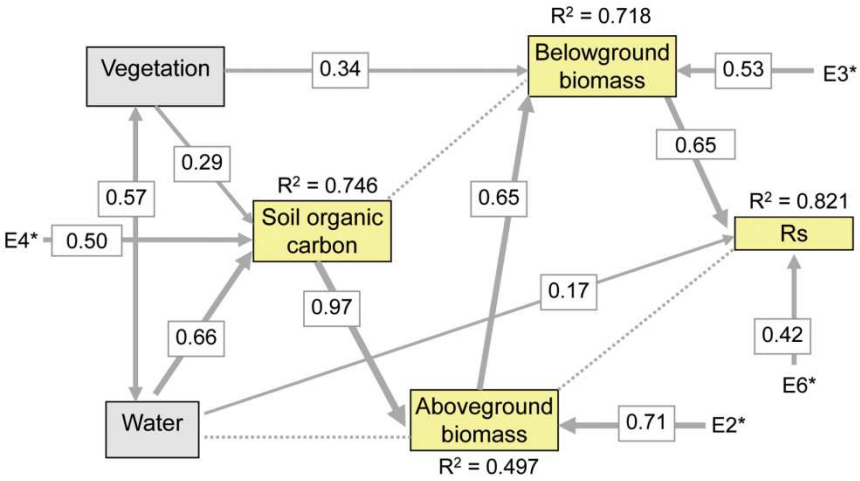

Fig. 5 Final structural equation model for soil respiration. Non-significant paths are showed in dashed lines. The thickness of the solid arrows reflects the magnitude of the standardized SEM coefficients. Standardized coefficients are listed on each significant path.

4 Discussion

One common feature of natural grasslands is the climate, usually characterized by periodic droughts [63]. For a specific region, it may also be associated with basic parameters such as soil characteristics, frequent fires, grazing pressure and human activities. Chinese grasslands are generally distributed in three different regions: temperate grassland on the Inner Mongolian Plateau, alpine grassland on the Tibetan Plateau, and mountain grassland in the Xinjiang mountain areas [64]. Tibetan alpine grasslands, which are associated with cold climate of the high altitudes [49], differ from tropical and temperate grasslands. Yet, they are poorly documented in C cycles. Our survey on the large-scale patterns of Rs was preliminary, but the trend and relationships were clear.

Table 4 Total direct and indirect effects in the structural model. These effects were calculated using standardized path coefficients.

Variable	Direct effect	Indirect effect	Total
Rs			
Belowground biomass	0.654	-	0.654
Aboveground biomass	0.191ns	0.427	0.618
Soil organic carbon	-	0.586	0.586
Vegetation type	-	0.397	0.397
Soil moisture	0.165	0.175ns	0.335
Belowground biomass			
Aboveground biomass	0.652	-	0.652
Soil organic carbon	-0.021ns	0.634	0.613
Vegetation type	0.345	0.179	0.524
Soil moisture	-	0.175ns	0.175ns
Aboveground biomass			
Soil organic carbon	0.971	-	0.971
Vegetation type	-	0.283	0.283
Soil moisture	-0.355ns	0.644	0.29
Soil organic carbon			
Vegetation type	0.292	-	0.292
Soil moisture	0.663	-	0.663

4.1 Magnitude of soil respiration of alpine grasslands

Large differences were observed between Rs from two vegetation types, alpine meadow and alpine steppe, being about two and half times greater in the alpine meadows. The daily mean Rs rates measured in alpine meadows (5.49 μmol CO_2 m^{-2} s^{-1} by daily average) are similar to previously reported results. For example, Cao et al. [32] reported that during peak growing season (Mid-July or August), daily Rs was 4.4 and 3.2 μmol CO_2 m^{-2} s^{-1} for light and heavy grazed meadows on the north-eastern edge of the Plateau. Li and Sun [33] reported a range of Rs from 0.93 to 8.02 μmol CO_2 m^{-2} s^{-1} during growing season in their recently published results. However, the only study from the alpine steppe by Zhang et al. [31], with a daily mean Rs rate of 0.38 μmol CO_2 m^{-2} s^{-1} at peak growing season, and an annual mean soil respiration rate of 0.248 μmol CO_2 m^{-2} s^{-1} using a closed static chamber-gas chromatograph method in a *Stipa purpurea* and *Carex moocroftii* community, was at the lower end of our measurement. The Rs rates of alpine steppe from this study (2.01 μmol CO_2 m^{-2} s^{-1} by daily average) are similar to the temperate steppe on the Inner Mongolia Plateau [23,65–69].

Consequently, the question arises: why is there such a difference in Rs rates between the two main grassland types, alpine meadow and alpine steppe? We suggest biological differences in standing biomass and productivity as well as physical differences in soil water availability were the major factors affecting Rs. On average, AGB (proxy of aboveground productivity) and BGB of the typical *Kobresia* meadows were much greater than the typical *Stipa* steppe (Table 3). Fur-

thermore, SM of alpine meadow was also much higher than *Stipa* steppe. These high BGB and SM in alpine meadows significantly increased Rs rate.

The alpine grasslands of the Tibetan Plateau are sometimes called alpine tundra, despite their different species composition and environmental conditions compared to arctic tundra. Nevertheless, Tibetan alpine grassland and arctic tundra share some common features, such as large below ground standing biomass (averaging 1658 g m^{-2} for arctic tundra in Alaska [70], and 1816 g m^{-2} on the Tibetan Plateau in current study), relatively large soil C density [39,40], relatively high soil moisture (particularly in alpine meadow), and influences of permafrost. These characteristics mean that they are more responsive to global warming than other ecosystems, because their soils have the potential to release significant amounts of carbon-based greenhouse gases [46,71,72].

4.2 Factors associated with the large-scale patterns of soil respiration

Our analysis showed that among biotic and abiotic factors, BGB and SM together well explained the spatial patterns of peak growing-season Rs, accounting for 82% of the variation among 42 sampling sites. The important role of SM for Rs is in good accordance with results from other studies on soil nitrogen and carbon contents across the Tibetan Plateau [39]. Most of the variation in Rs could be attributed to the difference in BGB among sites (80%), with a small proportion further explained by SM (2%, SM entered after BGB in general linear models, because BGB and SM covaried). Thus, the results support our first hypothesis that BGB is most closely associated with the large-scale variations in Rs. This finding implies that autotrophic Rs (including plant roots and closely associated organisms) contributes a large proportion to total Rs, or/and autotrophic Rs is strongly related to heterotrophic Rs in these alpine grassland ecosystems.

A few studies with data compilation have addressed the general patterns of Rs across biomes. For example, on a global scale, Raich & Schlesinger [6] found Rs is positively correlated with MAT and MAP, as well as a close correlation between mean annual net primary productivity (NPP) of different vegetation biomes and their mean annual Rs. Bond-Lamberty & Thomson [25] built a global database of Rs from 3379 records spanning publication years 1963–2008, and found MAT, MAP and leaf area index together explained approximately 41% of the observed variability in annual Rs. Across the northern hemisphere, Hibbard et al. [28] found Rs and soil temperature are closely correlated for the deciduous and mixed forests, but not for non-forest biomes. These across-biome patterns of Rs are generally controlled by climate and NPP. Furthermore, Mahecha et al. [73] approximated the sensitivity of terrestrial ecosystem respiration to MAT across 60 sites worldwide, and offers substantial evidence for a general temperature sensitivity of soil respiration. Within the grassland biome, aboveground net primary productivi-

ty (ANPP, approximation to AGB of peak growing season as in this study) was shown to be positively correlated with Rs rate [12]. Craine et al. [27] also reported in Minnesota grasslands that both AGB and BGB are positively correlated with Rs. These previous studies in grasslands are consistent with the current results, since we observed a positive correlation between AGB, BGB and Rs as well. The novel part of our study is that we found only BGB and SM had direct effects on Rs at regional scale, with other factors indirectly affecting Rs through BGB or SM. It is also evident that factors most closely associated with Rs within-biome and across biomes are different.

In contrast, intra-annual variation in Rs at individual sites are mainly explained by soil temperature and soil moisture, but not by ANPP or AGB [74]. Temporal variations of Rs have been well simulated by using the continuous records of temperature and moisture [75]. Our measurements, across altitudes from 2925 to 5105 m and mean soil temperature (–10 cm) of midday (10:00 to 16:00 BST) from 6.3 to 31.6°C (the highest soil temperature of 31.6°C was recorded in an alpine steppe at 2925 m) during the field measurement exhibited that soil temperature did not have a strong effect on Rs across study sites. For example, *Kobresia tibetica* meadow on permafrost with a soil temperature of 6.3°C still had a daily mean Rs rate as high as 5.1 μmol CO_2 m^{-2} s^{-1}. Our results from the Tibetan grassland do not support the second hypothesis that Rs increases with increasing soil temperature in alpine grassland, but support the argument by Hibbard et al. [28] that within-site robust relationships with temperature and/or moisture are not adequate to characterize soil CO_2 effluxes across space, because for regional variation BGB is the most important factor.

4.3 Separating direct and indirect factors influencing soil respiration

In the present study, we used regression tree analysis [53] and SEM [56–58] as new approaches to conduct variable selection, to identify direct and indirect factors, and to determine the extent to which these factors may constrain Rs. To our knowledge, the efficiency of these approaches has not been evaluated empirically in soil respiration research.

Traditionally, stepwise selection and linear regression are used to identify and rank the limiting factors in Rs studies. However, when performing stepwise selection, closely covariated parameters cannot be selected simultaneously in the final model, because the explanatory power would not increase when a closely related variable is included. In our case, when BGB retain in the model, AGB will not be selected due to their close correlation. As a matter of fact, AGB has a strong indirect effect through BGB on Rs. This problem can be solved by a regression tree analysis which has the advantage to rank the limiting factors based on their importance [55].

Field studies examining ecosystem responses to climatic and other environmental changes typically use naturally occurring climatic gradients. However, some studies have realized the limitations of correlation method in analyzing factors influencing Rs [12,76]. For example, Rs rates vary significantly among major plant biomes, suggesting that vegetation type influences the rate of soil respiration. Nevertheless, the correlations among climatic factors, vegetation distributions, and Rs make cause-effect arguments difficult [12]. Burke et al. [76] raised the issue that there are inherent problems with utilizing simple statistical relationships of spatial variability as a foundation for understanding ecosystem function, because complex covariance along the gradient occurs across large spatial scales, leading to the problem that actual and apparent controlling factors may be confounded. Without field experiments, which are difficult to conduct across numerous sites, and without simulation of ecological processes, which need to be based on mechanistic data, SEM is one option. The quantitative procedure in the current study showed that the direct factors influencing Rs at large-scale were BGB and SM, AGB, SOC and vegetation type only had indirect influences despite their significant correlations with Rs. This holistic approach is appropriate in across-site comparisons of ecosystem structure and function.

4.4 Limitations of the current study

In the present study the soil PVC collars were installed only one hour before measurement due to the low accessibility of most sites, while the placement of collars are at least 24 hour prior to measurement in most Rs studies. Although the insertion of collars may cause unrealistic readings of soil CO_2 efflux because of the high fluxes after collar installation, fluxes stabilize after 10–30 min [77,78]. In addition, our measurement of Rs followed the same procedure throughout our survey. Therefore the error introduced by soil disturbance could be treated as a systematic error which is weak.

Complete diurnal courses were obtained at nine sites, whereas for most of our sites soil respiration were measured 3–4 times during 4–5 hours when Rs peaked. We acknowledge that soil respiration is a dynamic process that may not be well represented by a few replicated measurements during several hours of a day. However, we found average midday Rs rates of the nine sites were well correlated with their daily mean Rs. Furthermore, we calculate daily mean Rs of each site by extrapolating the nine diurnal courses to all 42 sites according to community composition and closeness in distance. This extrapolation might add uncertainty to the estimates of daily mean Rs. Nevertheless, sites of similar vegetation composition and closest in distance generally share comparable features of geology, climate, soil and vegetation, which in combination are the major determinants of soil respiration.

The main objective of this study is to investigate the large-scale regional patterns of Rs in the Tibetan Plateau. Rs of 42 sites were measured during peak growing season of late July and early August. Measurements over a time span of one month may lead to problems as spatial variation of Rs could interfere with temporal changes. However, a four-year observation on soil CO_2 efflux in Haibei Alpine Grassland Research Station of Northwest Institute of Plateau Biology, the Chinese Academy of Sciences (3200 m a.s.l.) revealed that Rs values peak and stabilize in late July and early August (unpublished data by YHW and JSH). This phenomenon was observed in north America as well [79]. Therefore, compared with the large variation of Rs across the plateau, the temporal interference should be minor.

4.5 Conclusions and implications

Our understanding of the controls and magnitudes of regional Rs is limited by the uncertainties due to spatial heterogeneity of vegetation across regional environmental gradients. In the current study, we moved beyond within-site differences in soil temperature and moisture to incorporate differences among broad ecosystem types (e.g. biomes). We can conclude with certainty that BGB is the factor most closely associated with Rs rate at regional scale for the grassland ecosystems, suggesting that in future we could develop models for Rs from plant standing biomass, which has a much larger database with wider biogeographic coverage, particularly in remote areas, such as the Tibetan Plateau. We acknowledge that only Rs rates during peak growing season were measured in the current study. Therefore, intensive measurements should be taken on a few sites across environmental gradients to develop more precise prediction models for annual Rs. Our results also have the implication that if we take Rs rates at peak growing season as a parameter of ecosystem metabolic activity, then compared with the plant physiology at individual level, ecosystem metabolism is not so much influenced by temperature itself. Furthermore, our results imply that a shift from alpine meadow to steppe due to changes of soil hydrological properties as a consequence of permafrost degradation will significantly alter Rs.

5 Acknowledgments

The authors are grateful to members of the Peking University expedition team, particularly Tong Shen, Wenhong Ma, Cunzhu Liang, Liang Wang, Yi Wu, Shanmin Mou and Shanxue Qi for assistance with field measurement, to Bernhard Schmid of University of Zurich, Switzerland, for statistical advice, and to Jingyun Fang and Dan Flynn for helpful comments.

6 References

1. Schlesinger WH (1997) Biogeochemistry: an analysis of global change. San Diego: Academic Press. 588 p.
2. Schlesinger WH, Andrews JA (2000) Soil respiration and the global carbon cycle. Biogeochemistry 48: 7–20.
3. Chapin FS, III, Matson PA, Mooney H (2002) Principles of terrestrial ecosystem ecology. New York: Springer-Verlag. 529 p.
4. Amundson R (2001) The carbon budget in soils. Annu Rev Earth Pl Sc 29: 535–562.
5. Eswaran H, van der Berg E, Reich P (1993) Organic carbon in soils of the world. Soil Sci Soc Am J 57: 192–194.
6. Raich JW, Schlesinger WH (1992) The global carbon dioxide flux in soil respiration and its relationship to vegetation and climate. Tellus B 44: 81–99.
7. Davidson EA, Janssens IA (2006) Temperature sensitivity of soil carbon decomposition and feedbacks to climate change. Nature 440: 165–173.
8. Luo YQ (2007) Terrestrial carbon-cycle feedback to climate warming. Annu Rev Ecol Evol S 38: 683–712.
9. Melillo JM, Steudler PA, Aber JD, Newkirk K, Lux H, et al. (2002) Soil warming and carbon-cycle feedbacks to the climate system. Science 298: 2173–2176.
10. Bond-Lamberty B, Thomson A (2010) Temperature-associated increases in the global soil respiration record. Nature 464: 579–582.
11. Luo YQ, Zhou XH (2006) Soil respiration and the environment. San Diego: Academic Press. 319 p.
12. Raich JW, Tufekcioglu A (2000) Vegetation and soil respiration: Correlations and controls. Biogeochemistry 48: 71–90.
13. Rustad LE, Campbell JL, Marion GM, Norby RJ, Mitchell MJ, et al. (2001) A meta-analysis of the response of soil respiration, net nitrogen mineralization, and aboveground plant growth to experimental ecosystem warming. Oecologia 126: 543–562.
14. Ryan MG, Law BE (2005) Interpreting, measuring, and modeling soil respiration. Biogeochemistry 73: 3–27.
15. Subke J-A, Inglima I, Cotrufo MF (2006) Trends and methodological impacts in soil CO_2 efflux partitioning: A metaanalytical review. Global Change Biol 12: 1–23.

16. Xu M, Qi Y (2001) Spatial and seasonal variations of $Q_{(10)}$ determined by soil respiration measurements at a Sierra Nevadan forest. Global Biogeochem Cy 15: 687–696.

17. Allison SD, Czimczik CI, Treseder KK (2008) Microbial activity and soil respiration under nitrogen addition in Alaskan boreal forest. Global Change Biol 14: 1156-1168.

18. Fierer N, Colman BP, Schimel JP, Jackson RB (2006) Predicting the temperature dependence of microbial respiration in soil: A continental-scale analysis. Global Biogeochem Cy 20: GB3026.

19. Kutsch WL, Persson T, Schrumpf M, Moyano FE, Mund M, et al. (2010) Heterotrophic soil respiration and soil carbon dynamics in the deciduous Hainich forest obtained by three approaches. Biogeochemistry 100: 167–183.

20. Hörberg P, Nordgren A, Buchmann N, Taylor AFS, Ekblad A, et al. (2001) Large-scale forest girdling shows that current photosynthesis drives soil respiration. Nature 411: 789–792.

21. Wan S, Luo Y (2003) Substrate regulation of soil respiration in a tallgrass prairie: Results of a clipping and shading experiment. Global Biogeochem Cy 17: 1054.

22. Misson L, Gershenson A, Tang J, McKay M, Cheng W, et al. (2006) Influences of canopy-photosynthesis and summer rain pulses on root dynamics and soil respiration ina young ponderosa pine forest. Tree Physiol 26: 833–844.

23. Chen Q, Wang Q, Han X, Wan S, Li L (2010) Temporal and spatial variability and controls of soil respiration in a temperate steppe in northern China. Global Biogeochem Cy 24: 1–10.

24. Wan S, Norby RJ, Ledford J, Weltzin JF (2007) Responses of soil respiration to elevated CO_2, air warming, and changing soil water availability in a model old-field grassland. Global Change Biol 13: 2411–2424.

25. Bond-Lamberty B, Thomson A (2010) A global database of soil respiration data. Biogeosciences 7: 1915–1926.

26. Savage K, Davidson EA, Richardson AD (2008) A conceptual and practical approach to data quality and analysis procedures for high-frequency soil respiration measurements. Funct Ecol 22: 1000–1007.

27. Craine JM, Tilman D, Wedin D, Reich P, Tjoelkker M, et al. (2002) Functional traits, productivity and effects on nitrogen cycling of 33 grassland species. Funct Ecol 16: 563–574.

28. Hibbard KA, Law BE, Reichstein M, Sulzman J (2005) An analysis of soil respiration across northern hemisphere temperate ecosystems. Biogeochemistry 73: 29–70.

29. Jenny H (1941) Factors of soil formation. New York: McGraw-Hill. 229 p.

30. McCulley RL, Burke IC, Nelson JA, Lauenroth WK, Knapp AK, et al. (2005) Regional patterns in carbon cycling across the Great Plains of North America. Ecosystems 8: 106–121.

31. Zhang XZ, Shi PL, Liu YF, Ouyang H (2005) Experimental study on soil CO_2 emission in the alpine grassland ecosystem on Tibetan Plateau. Sci China Ser D 48: 218–224.

32. Cao G, Tang Y, Mo W, Wang Y, Li Y, et al. (2004) Grazing intensity alters soil respiration in an alpine meadow on the Tibetan plateau. Soil Biol Biochem 36: 237–243.

33. Li G, Sun S (2011) Plant clipping may cause overestimation of soil respiration in a Tibetan alpine meadow, Southwest China. Ecol Res 26: 497–504.

34. Lin X, Zhang Z, Wang S, Hu Y, Xu G, et al. (2011) Response of ecosystem respiration to warming and grazing during the growing seasons in the alpine meadow on the Tibetan Plateau. Agric For Meteor 151: 792–802.

35. Wang JF, Wang GX, Hu HC, Wu QB (2010) The influence of degradation of the swamp and alpine meadows on CH_4 and CO_2 fluxes on the Qinghai-Tibetan Plateau. Environ Earth Sci 60: 537–548.

36. Shi PL, Zhang XZ, Zhong ZM, Ouyang H (2006) Diurnal and seasonal variability of soil CO_2 efflux in a cropland ecosystem on the Tibetan Plateau. Agric For Meteor 137: 220–233.

37. Hou XY (1982) Vegetation map of the People's Republic of China (1:4M). Beijing: Chinese Map Publisher.

38. Baumann F, He J-S, Schmidt K, Ku¨hn P, Scholten T (2009) Pedogenesis, permafrost, soil temperature and soil moisture as controlling factors for soil nitrogen and carbon contents across the Qinghai-Tibetan Plateau. Global Change Biol 15: 3001–3017.

39. Yang YH, Fang JY, Tang YH, Ji CJ, Zheng CY, et al. (2008) Storage, patterns and controls of soil organic carbon in the Tibetan grasslands. Global Change Biol 14: 1592–1599.

40. Zimov SA, Schuur EAG, Chapin FS, III (2006) Permafrost and the global carbon budget. Science 312: 1612–1613.

41. Cheng GD (2005) Permafrost studies in the Qinghai-Tibet Plateau for road construction. J Cold Reg Eng 19: 19–29.

42. Nan ZT, Li SX, Cheng GD (2005) Prediction of permafrost distribution on the Qinghai-Tibet Plateau in the next 50 and 100 years. Sci China Ser D 48: 797–804.

43. Wu S, Yin Y, Zheng D, Yang Q (2005) Climate change in the Tibetan Plateau during the last three decades. Acta Geogr Sin 60: 3–11.

44. Zhao L, Ping CL, Yang DQ, Cheng GD, Ding YJ, et al. (2004) Changes of climate and seasonally frozen ground over the past 30 years in Qinghai-Xizang (Tibetan) Plateau, China. Global Planet Change 43: 19–31.

45. Böhner J, Lehmkuhl F (2005) Environmental change modeling for Central and High Asia:Pleistocene, present and future scenarios. Boreas 34: 220–231.

46. Cheng GD, Wu TH (2007) Responses of permafrost to climate change and their environmental significance, Qinghai-Tibet Plateau. J Geophys Res Earth Surface 112.

47. Yang YH, Fang JY, Ji CJ, Han WX (2009) Above- and belowground biomass allocation in Tibetan grasslands. J Veg Sci 20: 177–184.

48. He JS, Wang ZH, Wang XP, Schmid B, Zuo WY, et al. (2006) A test of the generality of leaf trait relationships on the Tibetan Plateau. New Phytol 170: 835–848.

49. Zhang J, Wang JT, Chen W, Li B, Zhao K (1988) Vegetation of Xizang (Tibet). Beijing: Science Press. 589 p.

50. Wang JT (1988) The steppes and deserts of the Xizang Plateau (Tibet). Plant Ecol 75: 135–142.

51. Fang JY, Piao SL, Tang ZY, Peng CH, Ji W (2001) Interannual variability in net primary production and precipitation. Science 293: 1723.

52. He JS, Wang X, Flynn DFB, Wang L, Schmid B, et al. (2009) Taxonomic, phylogenetic, and environmental trade-offs between leaf productivity and persistence. Ecology 90: 2779–2791.

53. Breiman L, Friedman J, Olshen R, Stone C (1984) Classification and regression trees. Belmont: Wadsworth International Group. 358 p.

54. SAS Institute (1999) SAS/STAT User's guide, Version 8.01 (On-line Docs). Cary, NC: SAS Institute.

55. De'ath G, Fabricius KE (2000) Classification and regression trees: a powerful yet simple technique for ecological data analysis. Ecology 81: 3178–3192.

56. Grace JB (2006) Structural equation modeling and natural systems. Cambridge: Cambridge University Press. 365 p.

57. Grace JB, Pugesek BH (1977) A structural equation model of plant species richness and its application to a coastal wetland. Am Nat 149: 436–460.

58. Shipley B (2002) Cause and correlation in biology: A user's guide to path analysis, structural equations and causal inference. Cambridge: Cambridge University Press. 317 p.

59. Grace JB, Keeley JE (2006) A structural equation model analysis of post-fire plant diversity in California shrublands. Ecol Appl 16: 503–514.

60. Lamb EG (2008) Direct and indirect control of grassland community structure by litter, resources, and biomass. Ecology 89: 216–225.

61. Shipley B, Lechowicz MJ, Wright IJ, Reich PB (2006) Fundamental trade-offs generating the worldwide leaf economics spectrum. Ecology 87: 535–541.

62. Bentler PM (2006) EQS 6 Structural equations program manual. Encino, CA: Multivariate Software, Inc.

63. Ripley EA (1992) Grassland climate. In: Coupland RT, ed. Natural grasslands: Introduction and western hemisphere. Amsterdam: Elsevier. pp 151–182.

64. Wu ZY (1980) Vegetation of China. Beijing: Science Press. 1382 p.

65. Dong YS, Qi YC, Liu JY, Geng YB, Domroes M, et al. (2005) Variation characteristics of soil respiration fluxes in four types of grassland communities under different precipitation intensity. Chin Sci Bull 50: 583–591.

66. Li LH, Wang QB, Bai YF, Zhou GS, Xing XR (2000) Soil respiration of a Leymus chinensis grassland stand in the Xilin River Basin as affected by over-grazing and climate. Acta Phytoecol Sin 24: 680–686.

67. Qi Y, Dong Y, Domroes M, Geng Y, Liu L, et al. (2006) Comparison of CO_2 effluxes and their driving factors between two temperate steppes in Inner Mongolia, China. Adv Atmos Sci 23: 726–736.

68. Wang G, Du R, Kong Q, Lu D (2004) Experimental study on soil respiration of temperate grassland in China. Chin Sci Bull 49: 642–646.

69. Yan L, Chen S, Huang J, Lin G (2010) Differential responses of auto- and heterotrophic soil respiration to water and nitrogen addition in a semiarid temperate steppe. Global Change Biol 16: 2345–2357.

70. Dennis JG (1977) Distribution patterns of belowground standing crop in arctic tundra at Barrow, Alaska. Arct Alp Res 9: 113–127.

71. Billings WD, Luken JO, Mortensen DA, Peterson KM (1982) Arctic tundra: A source or sink for atmospheric carbon dioxide in a changing climate? Oecologia 53: 7–11.

72. Nobrega S, Grogan P (2008) Landscape and ecosystem-level controls on net carbon dioxide exchange along a natural moisture gradient in Canadian low arctic tundra. Ecosystems 11: 377–396.

73. Mahecha MD, Reichstein M, Carvalhais N, Lasslop G, Lange H, et al. (2010) Global convergence in the temperature sensitivity of respiration at ecosystem level. Science 329: 838–840.

74. Dornbush ME, Raich JW (2006) Soil temperature, not aboveground plant productivity, best predicts intra-annual variations of soil respiration in central Iowa grasslands. Ecosystems 9: 909–920.

75. Raich JW, Potter CS, Bhagawati D (2002) Interannual variability in global soil respiration, 1980–94. Global Change Biol 8: 800–812.

76. Burke IC, Lauenroth WK, Parton WJ (1997) Regional and temporal variation in net primary production and nitrogen mineralization in grasslands. Ecology 78: 1330–1340.

77. Davidson EA, Savage K, Verchot LV, Navarro R (2002) Minimizing artifacts and biases in chamber-based measurements of soil respiration. Agric For Meteor 113: 21–37.

78. Norman JM, Kucharik CJ, Gower ST, Baldocchi DD, Crill PM, et al. (1997) A comparison of six methods for measuring soil-surface carbon dioxide fluxes. J Geophys Res 102: 28771–28778.

79. Zhou X, Wan S, Luo Y (2007) Source components and interannual variability of soil CO_2 efflux under experimental warming and clipping in a grassland ecosystem. Global Change Biol 13: 761–775.

80. Editorial Board of Vegetation Map of China (2001) Vegetation Atlas of China (1:1,000,000). Beijing: Science Press. 260 p.

Manuscript 3

Storage, patterns, and control of soil organic carbon and nitrogen in the northeastern margin of the Qinghai-Tibetan Plateau

Environmental Research Letters (2012), 7: 035401

Wenjie Liu[1], Shengyun Chen[1], Xiang Qin[1], Frank Baumann[2,], Thomas Scholten[2], Zhaoye Zhou[1], Weijun Sun[1], Tongzuo Zhang[3], Jiawen Ren[1] and Dahe Qin[1]

[1]Qilian Shan Station of Glaciology and Ecologic Environment, State Key Laboratory of Cryospheric Sciences, Cold and Arid Regions Environmental and Engineering Research Institute, Chinese Academy of Sciences, Lanzhou 730000, People's Republic of China

[2]Institute of Geography, Chair of Physical Geography and Soil Science, University of Tübingen, Rümelinstrasse 19-23, Tübingen 72070, Germany

[3]Northwest Institute of Plateau Biology, Chinese Academy of Sciences, Xining 810001, People's Republic of China

Abstract

This study tested the hypothesis that soil organic carbon (SOC) and total nitrogen (TN) spatial distributions show clear relationships with soil properties and vegetation composition as well as climatic conditions. Further, this study aimed to find the corresponding controlling parameters of SOC and TN storage in high-altitude ecosystems. The study was based on soil, vegetation and climate data from 42 soil pits taken from 14 plots. The plots were investigated during the summers of 2009 and 2010 at the northeastern margin of the Qinghai–Tibetan Plateau.

Relationships of SOC density with soil moisture, soil texture, biomass and climatic variables were analyzed. Further, storage and vertical patterns of SOC and TN of seven representative vegetation types were estimated. The results show that significant relationships of SOC density with belowground biomass (BGB) and soil moisture (SM) can be observed. BGB and SM may be the dominant factors influencing SOC density in the topsoil of the study area. The average densities of SOC and TN at a depth of 1 m were about 7.72 kg C m^{-2} and 0.93 kg N m^{-2}. Both SOC and TN densities were concentrated in the topsoil (0–20 cm) and fell exponentially as soil depth increased. Additionally, the four typical vegetation types located in the northwest of the study area were selected to examine the relationship between SOC and environmental factors (temperature and precipitation). The results indicate that SOC density has a negative relationship with temperature and a positive relationship with precipitation diminishing with soil depth. It was con-

cluded that SOC was concentrated in the topsoil, and that SOC density correlates well with BGB. SOC was predominantly influenced by SM, and to a much lower extent by temperature and precipitation. This study provided a new insight in understanding the control of SOC and TN density in the northeastern margin of the Qinghai–Tibetan Plateau.

1 Introduction

Soils play an important role in the global carbon cycle. The soil organic carbon (SOC) pool has been estimated to be approximately three times the size of the atmospheric pool, and about four times the size of the biotic pool (Janzen 2004, Lal 2004). Minor changes in SOC storage could result in a significant alteration of atmospheric CO_2 concentration (Davidson and Janssens 2006, Post *et al* 2009). Climate warming may have its largest positive feedback effects in high-latitude ecosystems that contain large pools of partially decomposed soil carbon accumulated under cold and moist conditions (Melillo *et al* 2002). A recent study (Tarnocai *et al* 2009) reported that the northern permafrost region contains approximately 1670 Pg of SOC, which accounts for approximately 50% of the estimated global belowground organic carbon pool. If these soils undergo both warming and drying, they have the potential to lose large amounts of carbon as CO_2/CH_4 to the atmosphere (Davidson *et al* 2000). Similarly, soils in high-altitude ecosystems have also been considered to play an important role in the global SOC cycle due to their high SOC density (Davidson and Janssens 2006). High-altitude soils play a critical role in the global terrestrial carbon cycle due to low temperature and potential sensitivity to climate warming (Davidson and Janssens 2006, Zimov *et al* 2006, Yang *et al* 2008, Post *et al* 2009, Schuur *et al* 2009).

A better understanding of the patterns and controls of SOC storage in high-altitude ecosystems is important to evaluate soil roles in the global terrestrial carbon cycle and potential feedbacks to global climatic change (Baumann *et al* 2009, Yang *et al* 2010). Many studies have addressed the characteristics of SOC pools and their control factors in high-altitude ecosystems. Studies include the soil C stock (Wang *et al* 2002, Tian *et al* 2007, Yang *et al* 2008) and its change trends (Piao *et al* 2006, Tan *et al* 2010), as well as CO_2 flux (Xu *et al* 2005, Kato *et al* 2006). However, due to limited field observations and large spatial heterogeneity, the storage and distribution patterns of SOC in high-altitude ecosystems remain largely uncertain (Tao *et al* 2006, Yang *et al* 2008). The latter may be caused by a number of environmental factors showing high variations across a landscapes at large and small spatial scales. Variations include low temperature, permafrost, soil texture, and waterlogging (Hobbie *et al* 2000, Schuur *et al* 2008, Yang *et al* 2010). Therefore, extensive field soil surveys are expected to provide improved assessments of SOC storage, as well as vertical and spatial patterns of SOC.

The Qinghai–Tibetan Plateau (QTP), with its unique vegetation types and climate conditions, is

the largest high-altitude ecosystem on earth. It represents an ideal region for the study of carbon cycles and the corresponding feedback interactions to global climatic change. Spatial distribution and temporal dynamics of SOC storage have been partly researched in this region (Wang *et al* 2002, Tao *et al* 2006, Yang *et al* 2010). However, few studies in the QTP ecosystem have addressed the vertical distribution of SOC (Tao *et al* 2006), total nitrogen (TN) and its stoichiometry (C:N ratio), and the environmental controls of the above-stated features (Tian *et al* 2007, Baumann *et al* 2009, Yang *et al* 2010). All of the above-described studies focused on the central QTP, while little work has been done on the northeastern margin of the QTP. The northeastern margin of the QTP is mainly influenced by the Asian monsoon system, the influence of which decreases westwards. The relatively moist and warm tropical Indian monsoon coming from the south is held back by big east–west stretching mountain ranges. Accordingly, there is a relatively high annual temperature (Xie *et al* 2010) and low precipitation in comparison to the characteristics of the southeastern QTP. Moreover, the geomorphological situation consists of complex mountain topography (Sheng *et al* 2010) compared to vast flat plateau-like areas interrupted by mountain ranges in the central QTP. The combined climate and topography conditions of the northeastern QTP give the region a large range of vegetation and soil types (Chen *et al* 2011).

Previous studies have reported significant climate warming in this area over the past 30 years (see e.g. Zhao *et al* 2004). Further, in the past 15 years, large areas of frozen soil have seriously degraded (Xie *et al* 2010). This has had a great impact on the soil environment and vegetation composition. Specifically, active layer thickness and soil temperature changes in permafrost altered the transfer processes of soil temperature and water conditions. Consequently, the stability of the vegetation and soil environment in the northeastern QTP was affected (Zhang *et al* 2003, Qin and Ding 2009, Yi *et al* 2011). The working hypothesis for this study was that SOC and TN distributions show clear relationships with selected soil parameters, vegetation composition, and climatic conditions. We then established SOC and TN density for each vegetation type and estimated SOC and TN storage. Overall, we examined how environmental factors affect the vertical distributions and spatial patterns of SOC and TN density.

2 Materials and methods

2.1 Study location and site description

The study area is located in the upstream regions of the Shule River Basin on the northeastern margin of the QTP. Altitudes range from 2100 to 5750 m, and the study region has an area of $\sim 1.25 \times 10^4$ km^2 (Xie *et al* 2010). This area belongs to the continental arid desert climate region. It has low average annual temperatures, little rainfall, and high evaporation (Sheng *et al* 2010). The mean annual temperature is approximately –5°C the annual precipitation range is ~100–300 mm (Chen *et al* 2011), and annual evaporation is about 1200 mm (Xie *et al* 2010). Due to

the indirect influence of glaciers in the region, significant small scale temperature and precipitation gradients were observed, especially at the four plots in the northwestern part of study area (table 1).

Table 1 Dominant plants, soil type, mean annual temperature (MAT), mean annual precipitation (MAP) of different vegetation types.

Vegetation Types [area, km^2]	Sampling Plots	Dominant plants (Chen *et al* 2011)	Soil types	MAT [°C]	MAP [mm]
ASM (227)	SLP3	*Kobresia tibetica, Carex parva*	Bog soils	–4.5	417
DG (598)	SLP9	*Saussurea arenaria, Ajania pallasiana*	Cold caclic soils	–4.8	422
AM (803)	SLP1	*Kobresia capillifolia, Carex moorcroftii*	Felty soils	–4.7	419
	SLP4	*Carex moorcroftii, Stipa purpurea*	Frigid caclic soils	–4.8	417
	SLP5	*Kobresia robusta, Artemisia nanschanica*	Cold caclic soils	–5.2	400
	SLP2	*Kobresia pygmaea, Carex moorcroftii*	Cold caclic soils	–6.0	476
D (182)	SB1	*Salsola passerine, Allium spp*.	Gray-brown desert soils	6.3	67
DS (3,174)	SB2	*Stipa breviflora, Artemisia hedinii*	Brown pedocals	2.7	89
AS (1,794)	SLP6	*Stipa purpurea, Saussurea arenaria*	Frigid caclic soils		
	SLP7	*Stipa purpurea, Leymus secalinus*	Frigid caclic soils	–4.3	400
	SLP8	*Stipa purpurea, Leontopodium leonto-podioides*	Cold caclic soils	–3.5 –2.5	368 324
	SB3	*Stipa purpurea, Leontopodium leonto-podioides*	Cold caclic soils	–0.3	168
PV (5,674)[a]	SB4	*Rhodiola quadrifida, Poa annua*	Frigid frozen soils	–5.0	205
	SB5	*Poa annua, Saussurea arenaria*	Frigid frozen soils	–5.6	209

ASM: alpine swamp meadow; DG: desertified grassland; AM: alpine meadow; D: desert; DS: desert steppe; AS: alpine steppe; PV: periglacial vegetation.
[a] The area included the bareland.

Our sampling campaign was conducted along a transect that traversed the typical vegetation and soil types within the study area. A total of 14 plots were selected among the gradients (figure 1). Plots SB1 and SB2 are located outside the boundary of the upstream regions of the Shule River Basin. We chose these plots because of their good accessibility and similarity in terms of vegetation characteristics and soil texture distributions to those throughout the boundary area.

2.2 Soil samples collection and analysis, and biomass survey

To estimate SOC and TN storage and patterns in typical vegetation types within the altitude gradients, we sampled 42 soil pits from 14 plots (i.e., two or three soil pits at each plot). The plots were located at the northeastern margin of the QTP (figure 1), and sampling occurred during the summer months (July and August) of 2009 and 2010. At each sampling plot, three soil pits were excavated to collect samples for analyses of soil physical and chemical properties. Soil samples of each pit were collected schematically at depths of 0–10, 10–20, 20–30, 30–40, 40–60, 60–80 and 80–100 cm. Five subsamples for each depth layer were randomly collected and mixed into a composite sample, then packed in bags and brought to the laboratory. In the sample plot, three replicates of volumetric soil samples for each soil depth were collected using a cutting ring (volume of 100 g cm^{-3}) to determine bulk density. Soil moisture (SM) was measured gravimetrically

after 24 h drying at 105°C. The volume of rock fragments (coarser than 2 mm) was determined by submerging moist rock fragments and recording the volume of displaced water. For larger rock fragments (>50 mm), volume was determined by visual estimation.

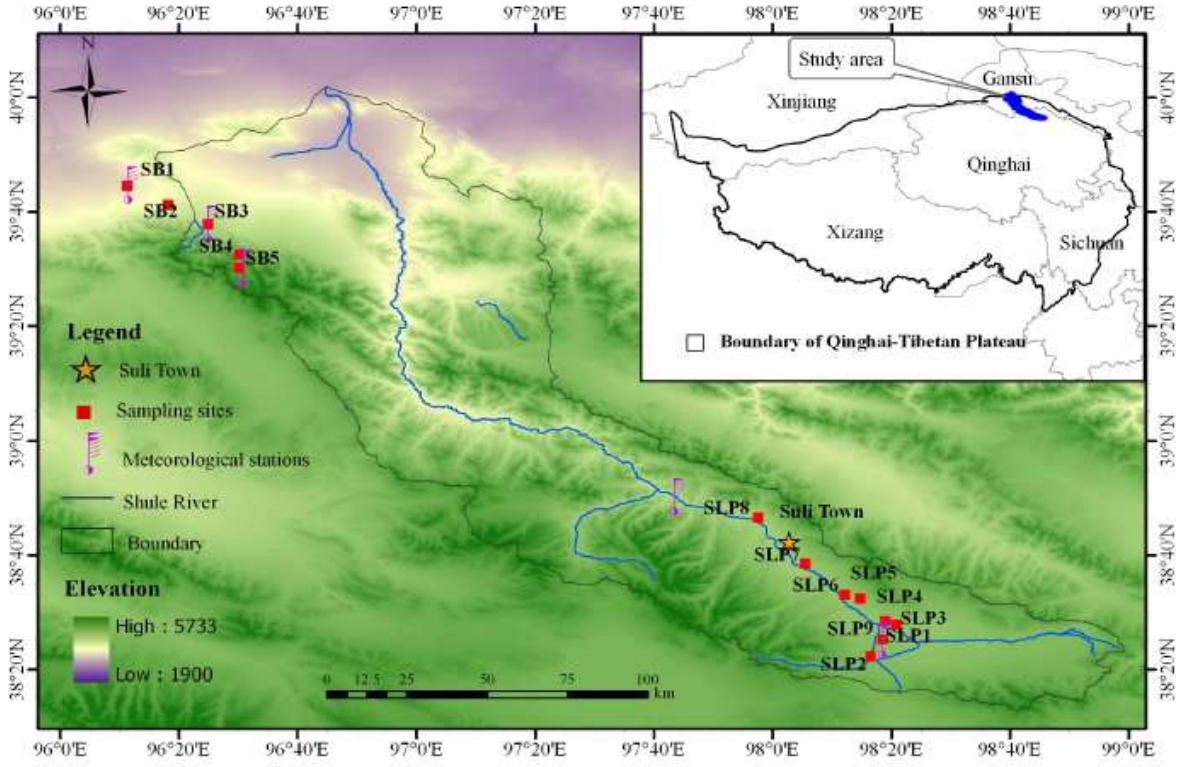

Fig. 1 Spatial distribution of sampling sites of typical vegetation in the upper area of the Shule River Basin

Soil samples were air-dried and then hand-sieved through a 2 mm screen to remove roots, litter and stone. A subsample of the air-dried sample was ground to pass through a 0.25 mm sieve and was then analyzed for SOC and TN. SOC was determined by dichromate oxidation using the Walkley–Black procedure (Nelson and Sommers 1982). TN was measured using the micro-Kjeldhal procedure (ISSCAS 1978). Soil particle size distribution was determined by the wet sieve method (Chaudhari *et al* 2008).

All plants in five quadrats (0.5m x 0.5 m) at each plot were harvested to measure aboveground biomass (AGB). Because recent studies have shown that 90% of roots in alpine grasslands are concentrated in the top 30 cm (Yang *et al* 2009, Chen *et al* 2011), we collected the belowground biomass (BGB) only to a depth of 0–40 cm. At each plot, BGB were drilled with an auger at depths of 0–10, 10–20, 20–30 and 30–40 cm. Each sample was repeated five times. Stones and other debris were removed, and the samples were packed in bags and brought to the laboratory. Each soil section was washed with a different pore-size sieve. Biomass samples were oven-dried at 80°C to a constant weight. BGB was determined by the sum of biomass at depths of 0–10, 10–20, 20–30 and 30–40 cm.

We took photos of each plot using a multi-spectral camera before collecting biomass, to obtain NDVI values, using Tetracam Agricultural Digital Camera (ADC, Tetracam Inc., Chatsworth, CA,

USA), with resolution of 2048 pixels × 1536 pixels. The ADC records three bands, i.e. near infrared, red and green, which are approximately equal to the fourth, third and second bands of the Landsat thematic mapper (TM). The pictures were then processed using a calibration file (the file was provided by ADC company according to measured reflectance values of green (G), red (R) and near infrared (NIR) for our multi-spectral pictures) in PixelWrench2 software. NDVI = (NIR − R)/(NIR + R) were further derived (Yi *et al* 2011).

2.3 Climate data, vegetation composition and soil types

Datasets of mean annual temperature (MAT) and mean annual precipitation (MAP) were derived from the climatic data of the northeastern margin of the QTP for the period of 2008–10. Data corresponding to the five plots were obtained and spatially interpolated from records of a nearby meteorological station (figure 1). Based on NDVI values for each vegetation type, vegetation types (figure 2) were grouped using a vegetation map interpreted by TM remote sensing data acquired on 16 July 2010.

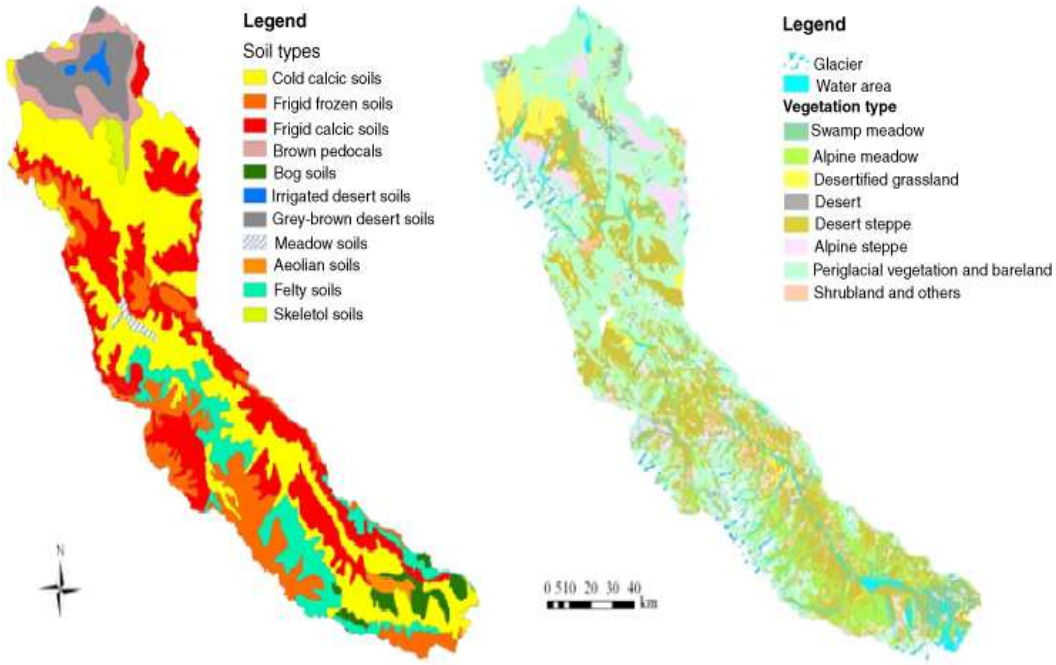

Fig. 2 Distribution of vegetation and soil types in the research area of the northeastern QTP.

We selected seven typical vegetation types as being representative of the sampling sites to examine differences in vertical distributions of SOC, TN and C:N stoichiometry among the distinct vegetation types. Vegetation type and its size, dominant plants, soil type and climate are shown in table 1. The spatial distribution of vegetation types in the northeastern margin of the QTP is complex; however, it is related to corresponding precipitation and temperature conditions. More details of the representative plants have been described in Chen *et al* (2011). Generally, those

soils may be described by their young development and strong degradation features, which are triggered by cryogenic processes or soil erosion. Consequently, a broad variety of soil formation factors is evident in the study area. According to the Chinese soil classification system, the main soil types in this area were (soil types according to WRB classification (IUSS Working Group WRB 2006) are given in parentheses): frigid calcic soils (Chernozems, Kastanozems); bog soils (gleysols, histosols, gelic gleysols, gelic histosols, umbric cambisols); brown pedocals (leptic to haplic cambisols); gray-brown desert soils (regosols (arenosols and leptosols)); frigid frozen soils (cryosols, gelic cambisols, gelic histosols); cold calcic soils (kastanozems); and felty soils (kastanozems or cambisols, frequently with felty turf-like topsoil). These felty turf-like topsoils contain large amounts of organic residuals and are widespread in cold alpine meadow areas (Kaiser 2004). The soil type data set (figure 2) was provided by Environmental and Ecological Science Data Center for West China, National Natural Science Foundation of China (http://westdc.westgis.ac.cn).

2.4 Vertical distribution of SOC and TN

The calculation of SOC density for each soil profile was obtained using equation (1).

$$\mathrm{SOCD} = \sum_{i=1}^{n} h_i \mathrm{BD}_i \mathrm{SOC}_i (1 - C_i)/100 \quad (1)$$

where SOCD, h_i, BD_i, SOC_i, and C_i are SOC density (kg m^{-2}), soil thickness (cm), bulk density (g cm^{-3}) SOC (g kg^{-1}), and volume percentage of the soil particles fraction >2 mm at layer *i*, respectively. Vertical distribution of TN was described analogously. The SOC density for each interval in the top 1 m were summed, and then to be multiplied by area of each vegetation type to obtain the storage of SOC and TN, and last the storage of SOC and TN for each vegetation type (seven typical vegetation types) to be summed to obtain the total study area SOC and TN storage. The C:N ratios were calculated using mass ratios.

Each dataset of topsoil (0–20 cm) was split into the two sampling depths (0–10, 10–20 cm), and statistical analysis was utilized with the 28 sample sizes. Linear regression and correlation analyses were conducted to evaluate the relationship between SOC content and soil acidity (pH), bulk density, SM, altitude, MAT, MAP, soil texture, AGB and BGB. A general linear mode (GLM) was used to describe the effects of the dependent parameters (*vide supra*) on the independent variables (SOC and TN density). These single condition models were used to investigate the impact of each dependent variable based on correlation analysis and multiple linear model explanation. The statistical analyses were conducted with SPSS software (version 11.5) and SAS software package (version 8.2). The $P < 0.05$ level was considered to be significant.

3 Results

3.1 Storage of SOC and TN

AGB, BGB and SOC density for all vegetation types are listed in table 2. As shown, AGB and BGB exhibited large differences among the vegetation types. Average SOC densities ranged from 4.39 to 19.84 kg m^{-2} for a thickness of 1 m in the different vegetation types.

Table 2 SOC density (SOCD) and TN density (TND), aboveground biomass (AGB) and belowground biomass (BGB) in the top 1 m of different vegetation types.

Vegetation Types	SOCD [kg m^{-2}]	TND [kg m^{-2}]	AGB [g m^{-2}]	BGB (0-10,10-20 cm)[a] [g m^{-2}]
Alpine swamp meadow (ASM)	19.84±1.81	2.34±0.55	168.48±0.94	12,261.09±299.20 (66%, 19%)
Desertified grassland (DG)	6.24±1.73	0.75±0.29	16.27±5.95	472.78 ±165.40 (47%, 52%)
Alpine meadow (AM)	8.70±1.19	0.81±0.08	54.29±9.21	1,391.27±599.17 (75%, 17%)
Desert (D)	4.39±0.71	0.68±0.06	107.18±26.71	1,006.21±506.61 (51%, 31%)
Desert steppe (DS)	7.09±0.65	0.99±0.14	41.86±3.06	1,860.35±171.43 (64%, 22%)
Alpine steppe (AS)	9.24±1.11	1.07±0.21	56.42±48.43	1,505.79±344.29 (65%, 21%)
Periglacial vegetation (PV)	9.46±1.77	1.15±0.16	70.58±26.27	819.97±40.94 (62%, 26%)

[a] The values in bracket were the proportions of BGB in the 0-10cm and 10-20 cm layer relative to the content of the entire 40 cm soil layer for each vegetation type, respectively.

Within the study area, the total C and N storage in the top 1 m were about 96.08 Tg (1 Tg = 10^{12} g) and 11.61 Tg, respectively. According average densities were 7.72 kg C m^{-2} and 0.93 kg N m^{-2}. In addition, average SOC densities were 8.11, 19.84, 7.09, 4.39, 9.24, 8.39 and 6.13 kg m^{-2} for a thickness of 1 m in frigid calcic soils, bog soils, brown pedocals, gray-brown desert soils, frigid frozen soils, cold calcic soils and felty soils, respectively (table 3).

Table 3 SOC density (SOCD) and TN density (TND) in the top 1 m of different soil types.

Soil Types (Chinese soil classification)	SOCD [kg m^{-2}]	TND [kg m^{-2}]
Frigid calcic soils	8.11±1.25	0.84±0.16
Bog soils	19.84±1.81	2.34±0.55
Brown pedocals	7.09±0.65	0.99±0.14
Gray-brown desert soils	4.39±0.71	0.68±0.06
Frigid frozen soils	9.46±1.77	1.15±0.16
Cold calcic soils	8.39±1.67	0.96±0.14
Felty soils	6.13±1.72	0.80±0.01

Figure 3 illustrates the SOC and TN density in soil profiles for each vegetation type. The proportions of SOC below the 40 cm soil layer were 25%, 28% and 23% for alpine swamp meadow, desertified grassland and alpine meadow. Both SOC and TN density in different vegetation soils decreased as soil depth increased (figure 3).

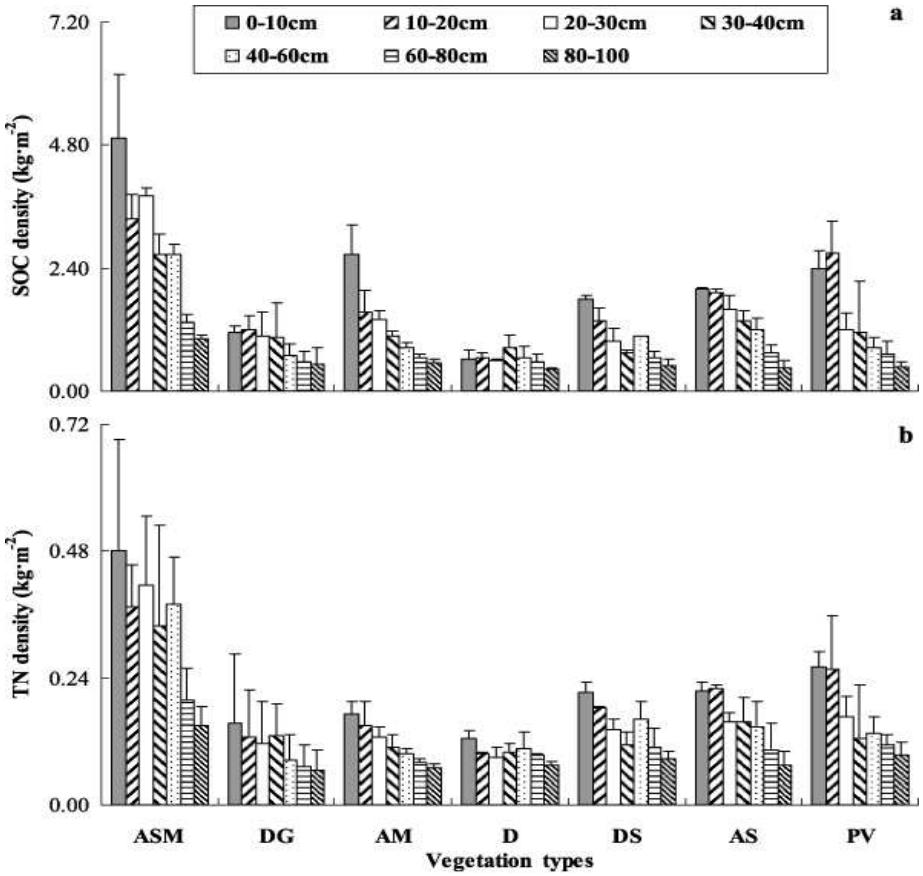

Fig. 3 Soil organic carbon (SOC) density (a) and total N (TN) density (b) in soil profiles of different vegetation types. (ASM: alpine swamp meadow, DG: desertified grassland, AM: alpine meadow, D: desert, DS: desert steppe, AS: alpine steppe, PV: periglacial vegetation). Error bars express standard deviation from the mean.

Similarly, a higher proportion of TN density in the upper layer was observed in all of the vegetation type soils. The average values for the seven different vegetation types were about 43% of total SOC and about 39% of total TN at 0–20 cm soil depth (figure 4).

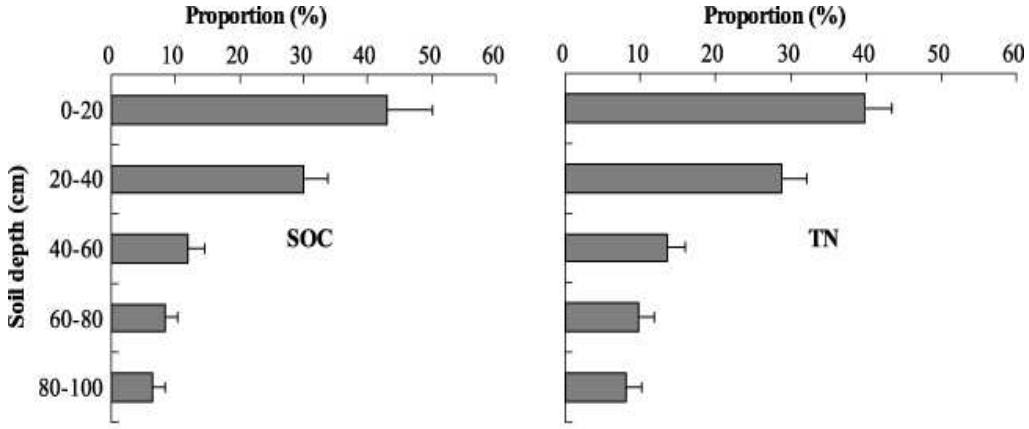

Fig. 4 Averaged profiles (all vegetation types) for SOC and TN proportional distributions in the top 100 cm of soil in the northeastern margin of the QTP. Error bars express standard deviation from the mean.

Soil C:N ratios ranged from 5 to 11 and exhibited a decreasing trend with soil depth in most vegetation types. However, the C:N ratios were relatively smooth in desertified grassland and desert (figure 5).

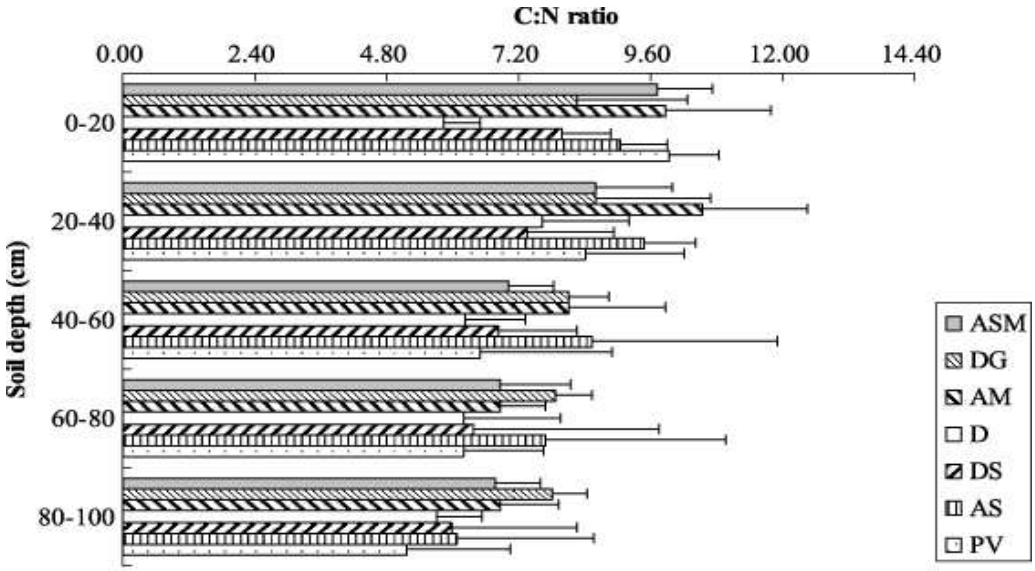

Fig. 5 Variations of C:N ratios among the soil profiles of different vegetation types in the northeastern margin of the QTP (ASM: alpine swamp meadow, DG: desertified grassland, AM: alpine meadow, D: desert, DS: desert steppe, AS: alpine steppe, PV: periglacial vegetation). Error bars express standard deviation from the mean.

3.2 Relationship of SOC with biomass, soil moisture, soil texture and climatic variables

A significant relationship between SOC density and SM (0-20 cm) was characterized by a linear function of SOC = 0.12 x moisture + 2.42 (R = 0.71, P < 0.01, n = 14). The correlation matrix for the 14 plots variables show significant correlations between SOC content in the topsoil (0-10 and 10-20 cm) and BGB (R = 0.73, P < 0.01). There was a significant relationship between SOC in the topsoil and AGB (R = 0.44, P = 0.02) (table 4). As an indicator for soil development processes, soil texture correlates with SOC and TN, showing a significant relationship between SOC content and soil clay fraction (R = 0.54, P < 0.01). There is a significant relationship between BGB and SM (R = 0.69, P < 0.01). The best-fit model of the GLM regression can be expressed as follows:

(2) SOC = 0.571SM + 0.292clay + 0.049AGB (R^2 = 0.91, P < 0.01)

(3) TN = 0.043SM + 0.054clay + 0.005AGB (R^2 = 0.94, P < 0.01).

With the exception of SM, soil clay fraction and AGB, no other variables were included in the GLM. The SM (accounted for 54% of variation) was the most important parameter for SOC content, whereas the soil clay fraction (accounted for 43% of variation) was the most important parameter for TN content.

Table 4 Correlation matrix for the fourteen plots variables (soil parameter dataset was split into two sampling depths: 0-10 and 10-20 cm).

	SOC [g kg^{-1}]	TN [g kg^{-1}]	pH value	BD [g cm^{-3}]	SM [%]	Altitude [m]	MAT [°C]	MAP [mm]	Sand [%]	Silt [%]	Clay [%]	AGB [kg m^{-2}]	BGB [kg m^{-2}]
SOC [g kg^{-1}]	1												
TN [g kg^{-1}]	0.93**	1											
pH value	-0.10	-0.16	1										
BD [g cm^{-3}]	-0.19	-0.27	0.19	1									
SM [%]	0.71**	0.69**	-0.06	-0.12	1								
Altitude [m]	0.29	0.14	0.16	0.39*	0.44*	1							
MAT [°C]	-0.26	-0.11	-0.14	-0.41*	-0.47*	-0.99**	1						
MAP [mm]	0.07	-0.02	0.03	0.33	0.48**	0.69**	-0.79**	1					
Sand [%]	-0.11	-0.31	0.17	0.46*	-0.10	0.66**	-0.65**	0.40*	1				
Silt [%]	-0.08	0.11	-0.12	-0.46*	-0.09	-0.72**	0.72**	-0.49**	-0.96**	1			
Clay [%]	0.54**	0.69**	-0.23	-0.31	0.52**	-0.27	0.25	-0.05	-0.75**	0.54**	1		
AGB [kg m^{-2}]	0.44*	0.46*	-0.01	0.02	0.33	-0.05	0.06	-0.20	0.30	-0.13	0.12	1	
BGB [kg m^{-2}]	0.73**	0.72**	-0.01	-0.15	0.69**	0.18	-0.20	0.05	0.51**	0.05	-0.08	0.58**	1

SOC: soil organic carbon; TN: total nitrogen; BD: bulk density; SM: soil moisture; MAT: mean annual temperature; MAP: mean annual precipitation; AGB: aboveground biomass; BGB: belowgro biomass; *, ** indicate significant effects at $p<0.05$ and 0.01, respectively.

3.3 Relationship of SOC and climate variables in the four vegetation types of the northwestern region of the study area

For the following vegetation types in the northwestern part of the study area: desert (SB1), desert steppe (SB2), alpine steppe (SB3) and periglacial vegetation (SB4) (figure 1), the proportion of SOC below the 40 cm soil layer decreased as temperature decreased and precipitation increased (desert > desert steppe > alpine steppe > periglacial vegetation). SOC density in the topsoil decreased as temperature increased, but increased as precipitation increased. Correlations of SOC with climate parameters diminished as soil depth increased (table 5).

4 Discussion

4.1 SOC and TN storage estimation and their significance

The total of C and N storage for the top 1 m were approximately 96.08 and 11.61 Tg in the upstream regions of the Shule River Basin in the northeastern margin of the QTP. Further, the average density of SOC was 7.72 kg m^{-2}, which was higher than the average density of 6.52 kg m^{-2} for the whole QTP (Yang *et al* 2008). We found the lowest SOC density of 4.39 kg m^{-2} in areas with desert (D) vegetation type (gray-brown desert soils) (table 2). This was lower than the average value for desert globally (6.20 kg m^{-2}) (Jobbágy and Jackson 2000), while both densities were higher than the average SOC density of gray-brown desert soils (1.24 kg m^{-2}) in Qinghai Province (Wang *et al* 2002). The highest SOC density was found in alpine swamp meadow (19.84 kg m^{-2}). This value was lower than that in the central QTP (49.88 kg m^{-2}) (Wang *et al* 2002) with the same soil type of bog soil. Wu *et al* (2003) have reported an average SOC density of 9.47 kg m^{-2} in China's alpine meadow vegetation, whereas Yang *et al* (2008) published an average SOC density of 9.05 kg m^{-2} for the alpine meadows in the whole QTP. Both of the above recorded density values for alpine meadows were higher than those found in our study (8.70 kg m^{-2}). However, for alpine steppe, Wu and Yang reported lower SOC densities (7.48 and 4.38 kg m^{-2}) than the densities we found (9.24 kg m^{-2}). These differences could be an effect of the significant spatial heterogeneity across the QTP (Baumann *et al* 2009). Although the vegetation type was uniform, soil types and climate conditions were very different, thus playing a critical role in determining the SOC density distributions (Ravindranath and Ostwald 2008). Further, our study concentrates on the northeastern margin of the QTP. Previous studies involve several uncertainties for average C density estimation of different vegetation types of the QTP, such as limited data to extrapolate over large areas and use different geostatistical algorithms (Wang *et al* 2002, Yang *et al* 2008). This indicates that an estimation of SOC storage for the entire QTP requires more field data and a finer sampling raster.

4.2 Vertical distributions of SOC, TN

The proportions of the first 0–20 cm interval related to the total content of the 1 m profile (43% of total SOC and 39% of total TN) are lower than the comparable proportions that Yang *et al* (2010) found in alpine grasslands on the central QTP (49% of total SOC and 43% of TN) (figure 4). The results of our study are consistent with those published by Jobbágy and Jackson (2000) (42% and 38% for SOC and TN at global ecosystems, respectively). The distribution of SOC and TN concentrated in the surface soil layer could be caused by their shallower root distribution (Jobbágy and Jackson 2000, Yang *et al* 2010). The distribution of relative BGB in 0–10 cm and 10–20 cm in this study (table 2) also supports this hypothesis. Due to this shallow root allocation in alpine ecosystems (see e.g. Yang *et al* 2009), comparably little SOC can be sequestered in deeper soil layers. Consequently, SOC storage in deep layers can be not as high as in woodland ecosystems (see e.g. Sommer *et al* 2000). In other words, because of even higher inputs of organic material, SOC and TN levels are generally concentrated in topsoil (Li and Zhao 2001).

The vertical distribution of SOC for the seven vegetation types generally showed that SOC density in 20 cm interval decreased as soil depth increased (figure 3). This agrees with observations on the entire QTP (Yang *et al* 2010), and with those of other ecosystems (Jobbágy and Jackson 2000). However, the soil depth of 20–40 cm revealed the highest SOC density (the sum of SOC density in 20–30 and 30–40 cm soil layer) in desert-type vegetation (figure 3). Litter fallen on the soil surface and turnover of fine roots are regarded as the main pathways of SOC input in natural ecosystems (Li and Zhao 2001). Thus potential explanations for this high SOC content include: (1) a small amount of AGB input; and the BGB inputs in the 20–40 cm soil layer were similar to those of the 0–20 cm layer in desert-type vegetation (data not shown); and (2) more organic matter was decomposed in the topsoil with relatively higher temperature and lower precipitation in desert-type vegetation soils (table 1). Another possible reason is the frequently observed high sediment input (e.g. aeolian sedimentation), where fine sand and silts are deposited on top, frequently burying the humic horizons of former soil formation underneath the fresh sediment.

Table 5 Correlations between the vertical distribution of SOC density and climatic variables of four vegetation types (D, DS, AS, and PV) with significant climatic gradients.

	MAT		MAP	
Depth [cm]	**Linear Equation [*Y*]**	**Correlation Coefficient [*R*]**	**Linear Equation [*Y*]**	**Correlation Coefficient [*R*]**
0–20	$0.32X_1+3.65$	0.97*	$0.02\ X_2+0.35$	0.93*
0–60	$0.44\ X_1+6.99$	0.86	$0.03\ X_2+2.03$	0.90
0-100	$0.46\ X_1+8.19$	0.85	$0.04\ X_2+2.99$	0.89

MAT: mean annual temperature; MAP: mean annual precipitation; *Y*: total SOC density for given soil depth; X_1: temperature; X_2: precipitation; *R* is correlation coefficient; * indicate significant effects at $p < 0.05$.

Importantly, the above-described process of active aeolian sedimentation is closely linked to permafrost degradation. Such degradation is often triggered by direct (e.g. overgrazing, construction) (Zhang *et al* 2006, Dai et al 2011) and indirect (climate change) human impact. It hence not only helps to explain the occurrence of SOC in deeper soil layers at desert vegetation plots, but also provides evidence for the vertical distribution of plant available nutrients. The main parameters that have to be considered are dilution caused by the ongoing sediment input, and the changes in soil temperature and moisture regimes linked to decomposition of organic material (Baumann *et al* 2009). The latter are particularly important if permafrost is degraded, leading to a thicker active layer and consequently to lower SM contents in accordant relief positions.

4.3 C:N ratio and its vertical distributions

C:N ratios of most vegetation types (except desertified grassland and desert) displayed decreasing trends with increasing soil depth (figure 5), which was consistent with previous study results (Callesen *et al* 2007). This is because there is more recalcitrant material with slower decomposition rates and lower C:N ratios in deep soil than in topsoil (Post *et al* 1985, Trumbore 2000). The C:N ratios (mass ratio) in this study ranged from 5 to 11. This result was consistent with previous results for similar regional conditions in the eastern QTP in which C:N ratio ranged from 6 to 14 (Xue *et al* 2009). The overall C:N ratios for our study area (especially at 0–20 cm depth) were low, and were thus similar to results in the central QTP (Yang *et al* 2010), and slightly lower than results in the frigid highland climate zone of China (11.66 ± 0.94) (Tian *et al* 2008). However, C:N ratios in this study were far lower than C:N ratios (17.40) in frigid highland climate zones outside China, summarized from Post *et al* (1985). Post *et al*'s high values may have resulted from some of the soil samples containing a humified litter layer that had a higher C:N ratio than soil (Tian *et al* 2008). Compared to the overall C:N ratios in frigid highland climate zones of China, our study area has relatively cold winters (freeze-thaw cycle) and warm summers (high temperature). This favors organic matter decomposition and nutrient release. Nevertheless, the low vegetation coverage in the northeast margin of the QTP (Xie *et al* 2010) implied the relatively low organic matter input. Therefore, we conclude that high mineralization ability and low amounts of litter returning in soil may be the cause of lower C:N ratios.

4.4 SOC density and its main influencing factors

SOC concentration depends on the balance between organic matter input and organic matter loss from soil (Zhuang *et al* 2007). Our results showed a higher correlation coefficient between SOC in the topsoil and BGB than between SOC and AGB, and a significant correlation between

AGB and BGB (table 4). Although equation (2) indicated that AGB was a stable predictor for SOC content, BGB is most likely the main resource and dominant factor for SOC density in the topsoil in our study area. A study by Hui and Jackson (2006) reported that about 70% of net primary production of vegetation in alpine ecosystems is distributed in the belowground parts of plants. Consequently, these parts are an important source of SOC. In addition, our results showed that ratios of BGB:AGB were very high (with an average of 32). The high BGB:AGB ratio is an effect of long-term adaptation of alpine grasslands to extreme environments, a common feature of alpine grasslands all over the world (Mokany *et al* 2006). Therefore, when estimating SOC storage and its temporal dynamics in high-altitude grassland ecosystems, the influence of BGB on SOC is an important factor to examine.

Although more than 90% of BGB in alpine grasslands has been shown to be concentrated in the top 30 cm of soil (Yang *et al* 2009), about 27% of SOC was distributed lower than 40 cm in our investigation area (figure 4). Accordingly, the main part of BGB was distributed much closer to the surface than was SOC. This pattern was originally observed in humid grasslands (Weaver *et al* 1935) and has been confirmed in other grasslands (Jobbágy and Jackson 2000). Decreasing SOC turnover with depth (Trumbore 2000) implies higher SOC accumulation rates in deeper soil layers. Another important reason for these observations is the migration of SOC as a result of leaching, which can lead to C enrichment often consisting of a more persistent and stable soil C pool rather than close to the surface (Guggenberger and Kaiser 2003, Strahm *et al* 2009, Rumpel and Kögel-Knabner 2011).

Equation (2) indicated that SM was a stable predictor for SOC. Importantly, significant relationships between SOC density and SM ($R = 0.71$, $P < 0.01$) were evident on a landscape scale in our study. Other studies have also reported similar patterns of SOC interrelationships in high-altitude ecosystems (Hobbie *et al* 2000, Baumann *et al* 2009, Yang *et al* 2010). It is likely that higher SM, together with improved SOC quality, leads to higher plant productivity and substrate availability in ecosystems. Thus, this leads to higher SOC and TN contents in related soils (Schimel *et al* 1990, Reichstein *et al* 2003, Reichstein and Beer 2008). This is particularly so in potentially dry regions (Giardina and Ryan 2000).

Frozen soils and their degradation patterns have direct and indirect impacts on SM conditions, and consequently these patterns affect vegetation and carbon sequestration in periglacial environments. Permafrost degradation is directly associated with soil hydrology, leading to severe changes in soil moisture–temperature regimes, and hence affecting the nutrient supply of plants (Zhang *et al* 2003). Plant biomass productivity and community coverage (Jorgenson *et al* 2001, Wang *et al* 2007), and structure and function of vegetation (Cheng and Wang 1998) are all directly interrelated. There was no direct correlation between MAT and SOC (table 4), but there is a significant negative correlation between MAT and soil moisture. It implied that permafrost was

a crucial factor to influence SM and SOC in study area. An increase in air temperature would cause the surface soil to be desiccated (as the permafrost degradation), which may result in a decrease of SOC in this region. In addition, vegetation would evolve to other species' composition, altering SOC storage and patterns. Consequently, differences in vertical distribution of SOC and TN as presented in our study help to better understand response and feedback mechanisms of SOC and TN in high-altitude ecosystems related to potential vegetation changes under the scope of global warming.

4.5 Decreasing influence of MAT and MAP on SOC with soil depth

In order to examine the relationship between SOC and climate variables, a subgroup of four vegetation types located in the northwestern part of our study area was selected (figure 1). Our results agree well with those published by Jobbágy and Jackson (2000) and Post *et al* (1982), showing that SOC density generally increases with increasing precipitation and decreasing temperature. Interestingly, we found high correlations of SOC with climatic factors in the top 0–20 cm, diminishing with the increase of soil depth (table 5). These findings are consistent with data from alpine ecosystems located in the central QTP (Tian *et al* 2007, Yang *et al* 2010). Other studies (Jobbágy and Jackson 2001, Tian *et al* 2007) have indicated that the importance of these controlling mechanisms changes with depth, thus climate effects are predominantly seen in layers close to the surface. This may be due to increasing proportions of slow-cycling SOC fractions in deep soil (Jobbágy and Jackson 2000, Rumpel and Kögel-Knabner 2011). Yang *et al* (2010) reported three reasons for this diminishing relationship: (1) slower-cycling SOC in deep soil layers; (2) soil buffering capacity reducing the effects of environmental influences in deep soil layers; and (3) a narrower range of SOC content in deep soil layers.

5 Conclusions

The SOC is concentrated in the topsoil and correlates well with BGB, which is the main resource and dominant parameter affecting SOC density in the topsoil. Moreover, SM retention is important for plant growth and ultimately for SOC formation in the study area. Soil texture is a critical factor for water retention in soil; e.g. sandy soils have low available water capacity and silty clay substrates have a high potential to hold water. According to our results, it can be assumed that SM is influenced even more by varying soil texture or the evidence of permafrost than by changing amounts of precipitation between years or over the main vegetation period. Degradation of permafrost under the scope of global warming leads to severe changes of SM conditions, and has a great influence on SOC storage patterns.

SOC in the upper parts of the topsoil is closely related to climatic factors (temperature and pre-

cipitation), and shows a diminishing relationship with soil depth in the four vegetation types of the northwestern study area. This indicates that SOC in the surface layer is vulnerable and should be strictly protected to minimize the risk of a potentially large carbon release. It is also important to mention that the dependent variables are interrelated, particularly SM and BGB.

Since decomposition of SOC is associated with permafrost degradation, feedback mechanisms between permafrost and soil water dynamics are key aspects of future development of the QTP ecosystem under climate change conditions. These feedback mechanisms are not yet sufficiently understood. Planned future work characterizing permafrost type and SOC pools at these plots (e.g. at 10 year intervals) will provide an opportunity to further assess vegetation and soil C dynamics.

6 Acknowledgment

This work was supported by the Global Change Research Program of China (2010CB951404), the National Natural Science Foundation of China (No. 41171054, 40901040), the Foundation for Excellent Youth Scholars, the Freedom Project (No. SKLCS-ZZ-2012-02-02) and the Open-Ended Fund (No. SKLCS 10-08) of the State Key Laboratory of Cryospheric Sciences, Cold and Arid Regions Environmental and Engineering Research Institute, Chinese Academy of Sciences, the China Postdoctoral Science Foundation (201104347). We are grateful to Professor Baisheng Ye for providing meteorological data. We thank the two anonymous reviewers for valuable suggestions and comments on the manuscript.

7 References

Baumann F, He J, Schmidt K, Kühn P and Scholten T 2009 Pedogenesis, permafrost, and soil moisture as controlling factors for soil nitrogen and carbon contents across the Tibetan Plateau *Glob. Change Biol.* 15 3001–17

Callesen I, Raulund-Rasmussen K, Westman C J and Tau-Strand L 2007 Nitrogen pools and C:N ratios in well-drained Nordic forest soils related to climate and soil texture *Boreal Environ. Res.* 12 681–92

Chaudhari S K, Singh R and Kundu D K 2008 Rapid textural analysis for saline and alkaline soils with different physical and chemical properties *Soil Sci. Soc. Am. J.* 72 431–41

Chen S Y, Liu W J, Ye B S, Yang G J, Yi S H, Wang FG, Qin X, Ren J W and Qin D H 2011 Species diversity of the vegetation in relation to biomass and environmental factors in the upper area of the Shule River *Acta Pratacult. Sin.* 20 70–83

Cheng G and Wang G 1998 Eco-environment changes and causal analysis of headwater region in

Qinghai–Xizang plateau *J. Adv. Earth Sci.* 13 (Suppl.) 24–31

Dai F, Su Z, Liu S and Liu G 2011 Temporal variation of soil organic matter content and potential determinants in Tibet, China *Catena* 85 288–94

Davidson E A and Janssens I A 2006 Temperature sensitivity of soil carbon decomposition and feedbacks to climate change *Nature* 440 165–73

Davidson E A, Trumbore S E and Amundson R 2000 Soil warming and organic carbon content *Nature* 408 789–90

Giardina C P and Ryan M G 2000 Evidence that decomposition rates of organic carbon in mineral soil do not vary with temperature *Nature* 404 858–61

Guggenberger G and Kaiser K 2003 Dissolved organic matter in soil: challenging the paradigm of sorptive preservation *Geoderma* 113 293–310

Hobbie S E, Schimel J P, Trumbore S E and Randerson J R 2000 Controls over carbon storage and turnover in high-latitude soils *Glob. Change Biol.* 6 196–210

Hui D and Jackson R B 2006 Geographical and interannual variability in biomass partitioning in grassland ecosystems: a synthesis of field data *New Phytol.* 169 85–93

ISSCAS (Institute of Soil Sciences, Chinese Academy of Sciences) 1978 *Physical and Chemical Analysis Methods of Soils* (Shanghai: Shanghai Science Technology Press) pp 7–59

IUSS Working Group WRB 2006 World reference base for soil resources 2006 *World Soil Resources Reports No. 103* 2nd edn (Rome: FAO)

Janzen H H 2004 Carbon cycling in earth systems: a soil science perspective *Agric. Ecosyst. Environ.* 104 399–417

Jobbágy E G and Jackson R B 2000 The vertical distribution of soil organic carbon and relation to climate and vegetation *Ecol. Appl.* 10 423–36

Jobbágy E G and Jackson R B 2001 The distribution of soil nutrients with depth: global patterns and imprint of plants *Biogeochemistry* 53 51–77

Jorgenson M T, Racine C H, Walters J C and Osterkamp T E 2001 Permafrost degradation and ecological changes associated with a warming in central Alaska *Clim. Change* 48 551–79

Kaiser K 2004 Pedogeomorphological transect studies in Tibet: implications for landscape history and present-day dynamics *Pr. Geogr.* 200 147–65

Kato T, Tang Y H, Gu S, Hirota M, Du M Y, Li Y N and Zhao X Q 2006 Temperature and biomass influences on interannual changes in CO2 exchange in an alpine meadow on the Qinghai–Tibetan Plateau *Glob. Change Biol.* 12 1285–98

Lal R 2004 Soil carbon sequestration to mitigate climate change *Geoderma* 123 1–22

Li Z and Zhao Q G 2001 Organic carbon content and distribution in soils under different land uses in tropical and subtropical China *Plant Soil* 231 175–85

Melillo J M, Steudler P A, Aber J D, Newkirk K, Lux H, Bowles F P, Catricala C, Magill A, Ahrens T and Morrisseau S 2002 Soil warming and carbon-cycle feedbacks to the climate system *Science* 298 2173–6

Mokany K, Raison R J and Prokushkin A S 2006 Critical analysis of root: shoot ratio in terrestrial biomes *Glob. Change Biol.* 12 84–96

Nelson D W and Sommers L E 1982 Total carbon, organic carbon, and organic matter *Methods of Soil Analysis Part II* ed A L Page (Madison, WI: American Society of Agronomy) pp 539–79

Piao S L, Fang J Y and He J S 2006 Variations in vegetation net primary production in the Qinghai-Xizang Plateau China from 1982 to 1999 *Clim. Change* 74 253–67

Post E *et al* 2009 Ecological dynamics across the arctic associated with recent climate change *Science* 325 1355–8

Post W M, Emanuel W R, Zinke P J and Stangenberger A G 1982 Soil carbon pools and world life zones *Nature* 298 156–9

Post W M, Pastor J, Zinke P J and Stangenberger A G 1985 Global patterns of soil nitrogen storage *Nature* 317 613–6

Qin D H and Ding Y J 2009 Cryospheric changes and their impacts: present, trends and key issues *Adv. Clim. Change Res.* 5 187–95

Ravindranath N H and Ostwald M 2008 Carbon inventory methods—handbook for greenhouse gas inventory, carbon mitigation and roundwood production projects *Advances in Global Change Research* (Heidelberg: Springer)

Reichstein M and Beer C 2008 Soil respiration across scales: the importance of a model-data integration framework for data interpretation *J. Plant Nutr. Soil Sci.* 171 344–54

Reichstein M *et al* 2003 Modeling temporal and large-scale spatial variability of soil respiration from soil water availability, temperature and vegetation productivity indices *Glob. Biogeochem. Cycles* 17 1–15

Rumpel C and Kögel-Knabner I 2011 Deep soil organic matter—a key but poorly understood component of terrestrial C cycle *Plant Soil* 338 143–58

Schimel D, Parton W J, Kittel T G F, Ojima D S and Cole C V 1990 Grassland biogeochemistry: links to atmospheric processes *Clim. Change* 17 13–25

Schuur E A G, Vogel J G, Crummer K G, Lee H, Sickman J O and Osterkamp T E 2009 The effect of permafrost thaw on old carbon release and net carbon exchange from tundra *Nature* 459 556–9

Schuur E AG *et al* 2008 Vulnerability of permafrost carbon to climate change: Implications for the global carbon cycle *BioScience* 58 701–14

Sheng Y, Li J, Wu J C, Ye B S and Wang J 2010 Distribution patterns of permafrost in the upper area of Shule River with the application of GIS technique *J. China Univ. Min. Technol.* 39 32–9

Sommer R, Denich M and Vlek P L G 2000 Carbon storage and root penetration in deep soils under small-farmer land-use systems in the Eastern Amazon region, Brazil *Plant Soil* 219 231–41

Strahm B D, Harrison R B, Terry T A, Harrington T B, Adams A B and Footen P W 2009 Changes in dissolved organic matter with depth suggest the potential for postharvest organic matter retention to increase subsurface soil carbon pools *Forest Ecol. Manag.* 258 2347–52

Tan K, Ciais P, Piao S L, Wu X P, Tang Y H, Vuichard N, Liang S and Fang J Y 2010 Application of the ORCHIDEE global vegetation model to evaluate biomass and soil carbon stocks of Qinghai–Tibetan grasslands *Glob. Biogeochem. Cycles* 24 GB1013

Tao Z, Shen C D, Gao Q Z, Sun YM, Yi W X and Li Y N 2006Soil organic carbon storage and vertical distribution of alpine meadow on the Tibetan Plateau *Acta Geogr. Sin.* 61 720–8

Tarnocai C, Canadell J G, Schuur E A G, Kuhry P, Mazhitova G and Zimov S 2009 Soil organic carbon pools in the northern circumpolar permafrost region *Glob. Biogeochem. Cycles* 23 1–11

Tian Y Q, Ouyang H, Song M H, Niu H S and Hu Q W 2007 Distribution characteristics and influencing factors of soil organic carbon in alpine ecosystems on Tibetan Plateau transect *J. Zhejiang Univ.* 33 443–9

Tian Y Q, Ouyang H, Xu X L, Song M H and Zhou C P 2008 Distribution characteristics of soil organic carbon storage and density on the Qinghai–Tibet Plateau *Acta Ped. Sin.* 45 933–42

Trumbore S E 2000 Age of soil organic matter and soil respiration: radiocarbon constraints on belowground C dynamics *Ecol. Appl.* 10 399–411

Wang G X, Qian J, Cheng G D and Lai Y M 2002 Soil organic carbon pool of grassland soils on the Qinghai–Tibetan Plateau and its global implication *Sci. Total Environ.* 291 207–17

Wang G X, Wang Y B, Li Y S and Cheng H Y 2007 Influences of alpine ecosystem responses to climatic change on soil properties on the Qinghai–Tibet Plateau, China *Catena* 70 506–14

Weaver J E, Houghen V H and Weldon M D 1935 Relation of root distribution to organic matter in prairie soil *Bot. Gaz.* 96 389–420

Wu H B, Guo Z T and Peng C H 2003 Distribution and storage of soil organic carbon in China *Glob. Biogeochem. Cycles* 17 1048

Xie X, Yang G J, Wang Z R and Wang J 2010 Landscape pattern change in mountainous areas along an altitude gradient in the upper reaches of Shule River *Chin. J. Ecol.* 29 1420–6

Xu S X, Zhao X Q, Li Y N, Zhao L, Yu GR, Sun X M and Cao G M 2005 Diurnal and monthly variations of carbon dioxide flux in an alpine shrub on the Qinghai–Tibet Plateau *Chin. Sci. Bull.* 50 539–43

Xue X J, Li Y N, Du M Y, Liu A H, Zhang F W and Wang J L 2009 Soil organic matter and total nitrogen changing with altitudes on the southern foot of eastern Qilian mountains *J. Glaciol. Geocryol.* 31 642–9

Yang Y H, Fang J Y, Guo D L, Ji CJ and Ma W H 2010 Vertical patterns of soil carbon, nitrogen and carbon: nitrogen stoichiometry in Tibetan grasslands *Biogeosci. Discuss.* 7 1–24

Yang Y H, Fang J Y, Ji CJ and Han W X 2009 Above-and belowground biomass allocation in Tibetan grasslands *J. Veg. Sci.* 20 177–84

Yang Y H, Fang J Y, Tang Y H, Ji J S and Zhu B 2008 Storage, patterns and controls of soil organic carbon in the Tibetan grasslands *Glob. Change Biol.* 14 1592–9

Yi S, Zhou Z, Ren S, Xu M, Qin Y, Chen S and Ye B 2011 Effects of permafrost degradation on alpine grassland in a semi-arid basin on the Qinghai–Tibetan Plateau *Environ. Res. Lett.* 6 045403

Zhang J H, Liu S Z and Zhong X H 2006 Distribution of soil organic carbon and phosphorus on an eroded hillslope of the rangeland in the northern Tibet Plateau, China *Eur. J. Soil Sci.* 57 365–71

Zhang Y, Ohata T and Kodata T 2003 Land-surface hydrological processes in the permafrost region of the eastern Tibetan Plateau *J. Hydrol.* 283 41–56

Zhao L, Ping C L, Yang D Q, Cheng G D, Ding Y J and Liu S Y 2004 Changes of climate and seasonally frozen ground over the past 30 years in Qinghai-Xizang (Tibetan) Plateau, China *Glob. Planet Change* 43 19–31

Zhuang Q L, Li Q, Jiang Y, Liang W J and Steinberger Y 2007 Vertical distribution of soil organic carbon in agroecosystems of Songliao Plain along a latitudinal gradient *Am.-Euras. J. Agric. Environ. Sci.* 2 127–32

Zimov S A, Schuur E A G and Chapin F S 2006 Permafrost and the global carbon budget *Science* 312 1612–3

Manuscript 4

Soil Organic Carbon Pools and Stocks in Permafrost-Affected Soils on the Tibetan Plateau

PLoS ONE (2013), 8 (2): e57024

Corina Dörfer[1], Peter Kühn[1], Frank Baumann[1], Jin-Sheng He[2], and Thomas Scholten[1]

[1]Department of Geosciences, Physical Geography and Soil Science, University of Tuebingen, Tuebingen, Germany

[2]Department of Ecology, College of Urban and Environmental Sciences, Peking University, Beijing, China

Abstract

The Tibetan Plateau reacts particularly sensitively to possible effects of climate change. Approximately two thirds of the total area is affected by permafrost. To get a better understanding of the role of permafrost on soil organic carbon pools and stocks, investigations were carried out including both discontinuous (site Huashixia, HUA) and continuous permafrost (site Wudaoliang, WUD). Three organic carbon fractions were isolated using density separation combined with ultrasonic dispersion: the light fractions (< 1.6 g cm^{-3}) of free particulate organic matter (FPOM) and occluded particulate organic matter (OPOM), plus a heavy fraction (> 1.6 g cm^{-3}) of mineral associated organic matter (MOM). The fractions were analyzed for C, N, and their portion of organic C. FPOM contained an average SOC content of 252 g kg^{-1}. Higher SOC contents (320 g kg^{-1}) were found in OPOM while MOM had the lowest SOC contents (29 g kg^{-1}). Due to their lower density the easily decomposable fractions FPOM and OPOM contribute 27 % (HUA) and 22 % (WUD) to the total SOC stocks. In HUA mean SOC stocks (0-30 cm depth) account for 10.4 kg m^{-2}, compared to 3.4 kg m^{-2} in WUD. 53 % of the SOC is stored in the upper 10 cm in WUD, in HUA only 39 %. Highest POM values of 36 % occurred in profiles with high soil moisture content. SOC stocks, soil moisture and active layer thickness correlated strongly in discontinuous permafrost while no correlation between SOC stocks and active layer thickness and only a weak relation between soil moisture and SOC stocks could be found in continuous permafrost. Consequently, permafrost-affected soils in discontinuous permafrost environments are susceptible to soil moisture changes due to alterations in quantity and seasonal distribution of precipitation, increasing temperature and therefore evaporation.

1 Introduction

The relationship between soil organic carbon (SOC) stocks and site characteristics has been well investigated in the temperate zones at local and regional scale (e.g. [1–4]), but much less studies exist about the role of SOC in high-cold alpine regions (e.g. [5–8]). Studies in Arctic regions have shown that permafrost-influenced alpine ecosystems are highly sensitive to global climate change [9]. Prevailing low temperatures and permanently low turn-over rates result in large SOC stocks, providing a great emission potential for greenhouse gases such as CO_2 and CH_4 [10–14]. Thus, an estimate of SOC stocks in their extent and distribution is essential to predict feedback of SOC on global climate change [4,1,3]. Furthermore, differentiation between carbon pools is necessary because various SOM fractions show large differences in their turn-over rates according to their mineral binding [15–17].

The Tibetan Plateau is a particularly sensitive area in terms of possible effects of global climate change. It is the largest and highest plateau on earth and covers an area of 2.5 million square kilometers with an average altitude of more than 4000 m a.s.l. comprising about a quarter of China's mainland [18]. On the Tibetan Plateau seasonally frozen soils are widespread [19]. Approximately two thirds of the total area is affected by permafrost [20]. Many studies focus on recent changes of the permafrost conditions on the Tibetan Plateau, attesting increasing permafrost temperatures, active layer thickness and rising degradation (e.g. [21–26]. Due to relatively high permafrost temperatures just below the freeze-thaw point, the so-called warm permafrost is more sensitive to global warming than the cold permafrost of higher latitudes [27]. The permafrost distribution is closely related to the characteristics of the land surface such as slope, exposure, vegetation distribution and snow cover. In this study permafrost is classified after the Chinese Permafrost Classification which differs from the classification of the International Permafrost Association (IPA). 50-90 % of permafrost is required for classifying discontinuous permafrost after IPA Permafrost Classification; 30-70 % is required after Chinese Permafrost Classification [28].

Recent soil ecological research mainly focuses on soil temperature as the main driving force for ecosystem processes (e.g. [3,29–31]). Baumann et al. [6] showed that nutrient availability is a limiting factor for plant growth as well, which in turn is controlled by soil moisture. Furthermore studies show soil moisture is the dominant parameter regarding to the spatial variation of SOC contents [6] and soil CO_2 efflux [32] on the landscape scale in permafrost influenced ecosystems. Zhao et al. [20] found a negative relationship between vegetation cover/biomass and active layer thickness in alpine meadow ecosystems. Permafrost favors the development of alpine meadow ecosystems, protecting in turn permafrost by their dense vegetation cover from degradation [33,34].

According to Wang et al. [5] about 33.52 Pg SOC are stored in grassland soils of the Tibetan Plateau down to a depth of 70 cm. Alpine meadow and alpine steppe soils have a share of 23.2 Pg, which represents 2.5 % of the global soil carbon pool [5]. Alpine meadows make up 38.2 % of total grassland soil carbon in Chinese grassland soils [35]. Wang et al. [33] estimated that the degradation of grassland is resulting in a loss of 57 % of SOC in heavy fractions (HF) and 84 % in light fractions (LF) from alpine meadow soils in Dari County (Qinghai Province). From 1986 to 2000 land cover changes have led to a loss of 1.8 Gg SOC and a mass loss of 65 % in the LF in the upper 30 cm [36].

Major objectives of this study are (1) to investigate SOC stocks and their affiliation to pools by density fractionation and (2) to examine interactions of SOC, soil moisture, and active layer thickness in permafrost-affected soils on the Tibetan Plateau. For comparing stocks and processes in soils affected by continuous and discontinuous permafrost adequately, sites with similar rainfall under varying temperatures were selected.

2 Materials and Methods

2.1 Study Sites

The study sites are located on the northeastern Tibetan Plateau, Qinghai Province, China and were investigated in May/June 2009 and 2010 (Fig. 1). Site HUA is situated near the settlement of Huashixia in Maduo County in the Yellow River catchment area, 4300 m a.s.l. The area is affected by the subtropical East Asian Monsoon, which transports air masses with high water vapor content from the lowlands to the Tibetan Plateau through the meridional flow furrows [37], leading to relatively high rainfall. The nearest climate station at Maduo shows a Mean Annual Air Temperature (MAAT) of -4.1 °C and a Mean Annual Precipitation (MAP) of 326 mm [38]. The catchment area of the Yellow River (Huang He) is characterized by discontinuous, unstable permafrost. The soils freeze to a depth of 2-3 m, while the upper limit of the permafrost lies in 4-7 m depth; so-called taliks have developed [39]. This vertical disconnection of the permafrost is widespread near the study site. The site is influenced by severe summer grazing with yak *(Bos grunniens)* and sheep *(Ovis aries)* and a temporary settlement by nomads.

Site WUD is located in the headwaters of the Yangtze River, in the middle between Wudaoliang and Tuotuohe next to the Qinghai-Tibet Highway. Precipitation decreases from SE to NW on the Plateau, but due to its location on the Fenghuo Shan mountains, site WUD is characterized by higher precipitation and lower temperatures as the surrounding area (MAP: 348 mm, MAAT: -5.75 °C, 4801 m a.s.l., [32]). The high elevation and the low influence of the South Asian Monsoon are responsible for the widespread continuous permafrost in that area [40] which is relatively poor in ice [39]. This also results in a shorter vegetation growth period compared to HUA. Dur-

ing the field campaign no grazing occurred. Nevertheless, the area is used only as late summer pasture due to extreme climate conditions. Generally, grazing is less intensive compared to HUA.

Fig. 1 Location of the study sites on the Tibetan Plateau.

The soils in both study areas are developed in sandy loess, mixed with coarser material derived from frost weathering processes. Poorly developed soils at site HUA are classified as gleyic Fluvisols, haplic Regosols and mollic Cryosols, whereas cambic Cryosols are common in WUD [41]. Alpine *Kobresia* meadow ecosystems are the most common vegetation types on the plateau [38] occurring at elevations ranging from 3200 to 5200 m a.s.l. [42]. At the study sites, particularly *Kobresia pygmaea* and *K. humilis* are widespread. Plant composition is similar at both sites, differing along the altitudinal gradient according to water supply. Strongly rooted, partly felty topsoils are common [43].

2.2 Field methods

During May and June in 2009, 11 soil profiles were sampled (HUA: 6, WUD: 5). All soil profiles were arranged along an elevation gradient and affected by permafrost with an active layer thickness less than 100 cm at both sites. At each site two soil profiles in footslope position, two soil profiles in lower mid-slope position and two (HUA) and one (WUD) soil profiles in upper mid-slope position were sampled. We set a high value on the comparability of both study sites in topographic position of the soil profiles, inclination of the slopes and vegetative cover. Soil sampling was split into three parts: horizon-wise sampling for pedogenesis and soil chemical analyses using soil pits, schematic sampling conducted by drilling at four depth-increments (0-5, 5-10, 10-20 and 20-30 cm, four replicates each) for C analysis and volumetric sampling at the same

depths for bulk density and gravimetric water content determination (three replicates each). Detailed description of soil profiles and pedogenic implications will be published elsewhere.

2.3 Laboratory analysis

All soil samples were air-dried and sieved to < 2 mm. The pH of the samples was measured in deionized water and in 0.01 M $CaCl_2$ solution at a solution:soil ratio of 2.5:1 with a glass electrode (Sentix 81, WTW, pH 340). $CaCO_3$ was analyzed gasvolumetrically on ground subsamples (Calcimeter, Eijkelkamp). Total C and N in bulk soil samples and density fractions were determined on ground subsamples by heat combustion with a CNS analyzer (Vario EL III, Elementar GmbH, Hanau, Germany). SOC in bulk soils and density fractions was calculated as the difference between soil total and soil inorganic carbon. Water content was determined by gravimetric water content analysis, corrected by the skeleton content (> 2 mm).

Density fractionation was carried out using sodium polytungstate, following the procedures of Grünewald et al. [44]. It is generally accepted that the density of OM is < 1.5 g cm^{-3}. After Golchin et al. [45] a density fractionation at 1.6 g cm^{-3} separates light organic fractions from mineral dominated heavy fractions under the assumption, that most mineral particles contain less than 20 % OM [46]. Three fractions were isolated: the light fractions free particulate organic matter (FPOM) and occluded particulate organic matter (OPOM) with a density < 1.6 g cm^{-3}, plus a heavy fraction of mineral associated organic matter (MOM) with a density of > 1.6 g cm^{-3}. FPOM was separated by floatation after gently shaking in a sodium polytungstate solution (soil:solution ratio 1:5) and centrifugation at 4,500 rpm for 20 min, followed by vacuum filtration. OPOM was separated after ultrasonic dispersion (58 J ml^{-1}) and centrifugation at 4,500 rpm for 15 min. Calibration of the ultrasonic output energy was carried out according to Roscoe et al. [47]. The remains (MOM) were washed three times to remove the salt. Due to soil inhomogeneity fractionation was carried out twice per sample. The dried and ground fractions were analyzed for C, N and SOC. The density solution was recycled after Six et al. [48]. SOC stocks for bulk soils and individual fractions were calculated down to a depth of 30 cm, according to Ohtsuka et al. [7]:

$$SOC[\mathrm{kg\ m^{-2}}] = 0.001 \cdot M \cdot \rho_B \cdot SOC \cdot (100 - S)$$

where M is the soil layer thickness, ρ_B is the bulk density (g cm^{-3}) of the soil, SOC is the soil organic carbon content (Mass%) and S is the skeleton content (Mass%).

3 Results

3.1 Soil organic carbon content and SOC/N ratios

The SOC content of bulk soil decreased with increasing depth at both sites (Fig. 2). In HUA (51 g kg^{-1}) significantly higher mean values were reached than in WUD (19 g kg^{-1}). Highest contents occurred in the OPOM fractions (320 g kg^{-1}), FPOM followed with 252 g kg^{-1}, while they were lowest in the MOM fractions (29 g kg^{-1}). The SOC contents in the FPOM decreased with depth, while there were increasing SOC values in the OPOM fractions. The SOC contents of the MOM fraction follow the same depth gradient as SOC in bulk soils at both sites.

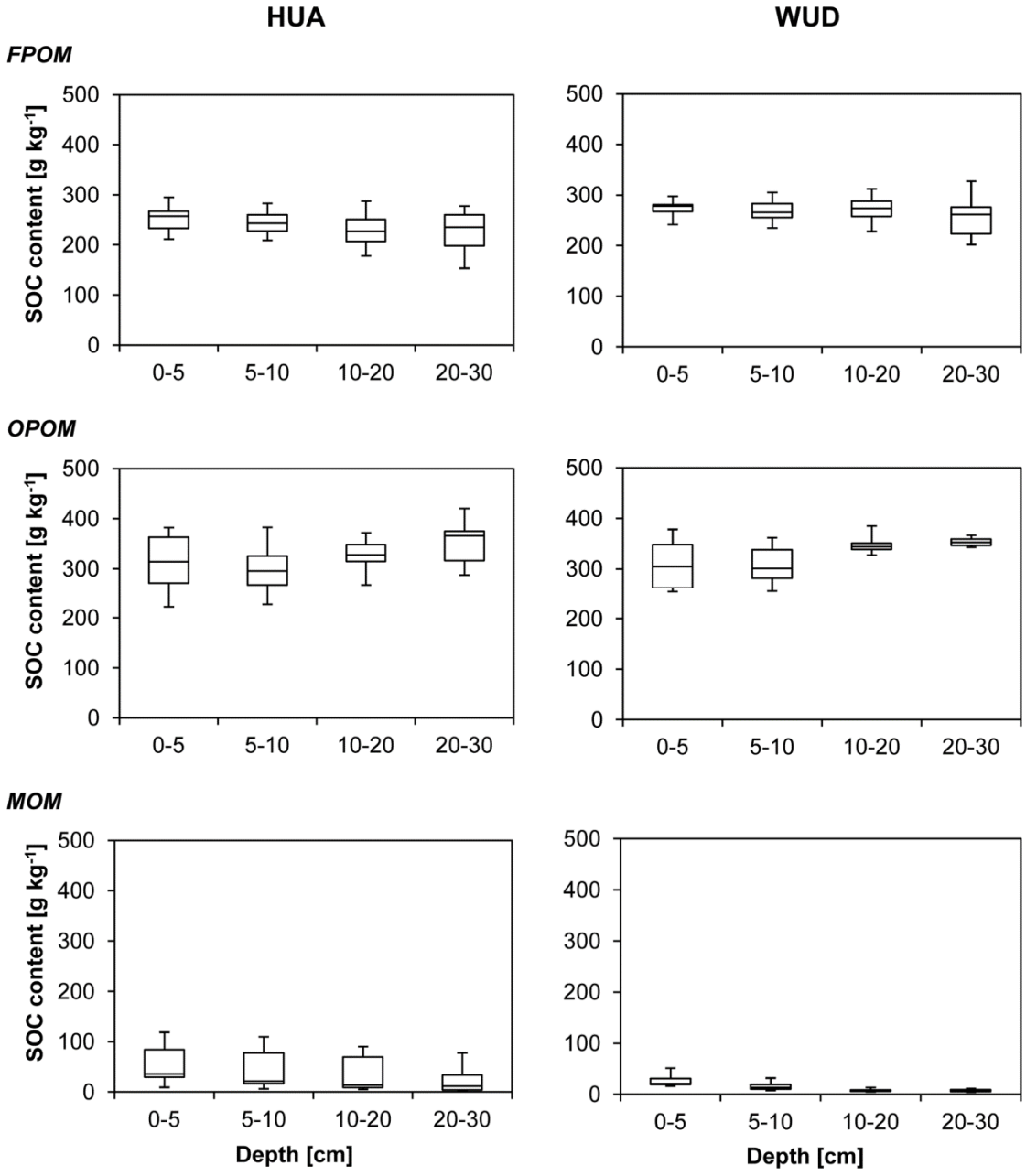

Fig. 2 Fractional soil organic carbon (SOC) contents of four different depth increments at Huashixia (HUA, left, n=40) und Wudaoliang (WUD, right, n=32).

Significantly higher SOC contents were found in this fraction on site HUA, showing a large variation. The mean recovery of SOC after density fractionation was 95 %.

SOC/N ratios of the bulk soils were relatively similar at both sites and decreased with depth (from 12 to 9) – except in extremely moist soils in HUA, where the SOC/N-ratios remained constant (13). The SOC/N ratios of the three fractions were remarkably different. Highest ratios were found in FPOM with a mean ranging from 15-36, followed by OPOM with 14-29. Generally, lower SOC/N ratios occurred in MOM fractions (3-12). We observed slightly rising SOC/N ratios with depth for the POM fractions in all soils, whereas ratios varied less with depth for the MOM fractions.

3.2 Soil organic carbon stocks of bulk soil and fractions

Total SOC stocks in HUA ranged from 1.9 kg m^{-2} to 19.3 kg m^{-2} up to 30 cm depth with a mean of 10.4 kg m^{-2} (Tab. 1). Significantly lower stocks were found in WUD ranging from 2.5 kg m^{-2} to 5.0 kg m^{-2} (mean: 3.4 kg m^{-2}).

Table 1 Max, Min, Mean values and standard deviations of total (A) and fractional (B) soil organic carbon stocks.

		HUA				WUD			
Depth [cm]		**FPOM**	**OPOM**	**MOM**	**Σ OM**	**FPOM**	**OPOM**	**MOM**	**Σ OM**
A. Total soil organic carbon stocks									
0-30	Mean [kg m^{-2}]	1.9	0.9	7.6	10.4	0.5	0.3	2.7	3.4
	SD	(2.1)	(0.9)	(4.5)	(7.1)	(0.2)	(0.1)	(0.6)	(0.8)
0-30	Max [kg m^{-2}]	5.0	2.4	12.9	19.3	0.7	0.4	3.9	5.0
0-30	Min [kg m^{-2}]	0.2	0.1	1.5	1.9	0.2	0.2	2.2	2.5
B. Fractional soil organic carbon stocks									
0-5	Mean [kg m^{-2}]	0.41	0.10	1.62	2.15	0.18	0.08	0.87	1.14
	SD	(0.25)	(0.05)	(0.58)	(0.83)	(0.10)	(0.03)	(0.19)	(0.29)
5-10	Mean [kg m^{-2}]	0.39	0.16	1.34	1.90	0.08	0.05	0.50	0.64
	SD	(0.38)	(0.13)	(0.79)	(1.24)	(0.04)	(0.01)	(0.16)	(0.20)
10-20	Mean [kg m^{-2}]	0.58	0.26	2.45	3.30	0.12	0.08	0.65	0.87
	SD	(0.75)	(0.31)	(1.77)	(2.60)	(0.08)	(0.03)	(0.27)	(0.37)
20-30	Mean [kg m^{-2}]	0.56	0.36	2.14	3.07	0.08	0.07	0.57	0.73
	SD	(0.80)	(0.46)	(1.71)	(2.88)	(0.05)	(0.02)	(0.18)	(0.24)

HUA: Huashixia (A: n=24; B: n=7), WUD: Wudaoliang (A: n=20; B: n=6). FPOM: free particulate organic matter, OPOM: occluded particulate organic matter, MOM: mineral-associated organic matter, Σ OM: Total organic matter. SD: standard deviation.

In line with the higher SOC contents, soils in HUA (0.41 kg m^{-2}) showed twice as high stocks as in WUD in the top 5 cm (Tab. 1). Fractional SOC stocks in particular depths were highest in the MOM fraction. In WUD, stocks decreased with depth for all three fractions whereas increasing SOC stocks in the OPOM fraction in 20-30 cm depth were evident compared to 10-20 cm depth at HUA.

Variations of the SOC stocks were much higher in HUA than in WUD, especially in the light POM fractions (Tab. 1).The POM fractions in HUA and WUD contributed 27 % and 22 % to the SOC stocks with 8 % in the OPOM fractions at both sites (Fig. 3). Comprising the different depth levels, 53 % of SOC is stored in the upper 10 cm in WUD. In HUA only 39 % is stored in the upper 10 cm and the portion of FPOM on SOC stocks remained constant with depth, while the portion of OPOM increased. The portion of FPOM on SOC stocks decreased slightly, whereas OPOM stocks increased with depth in WUD. The portion of MOM stock remained relatively constant at 77 %, thus slightly higher than in HUA.

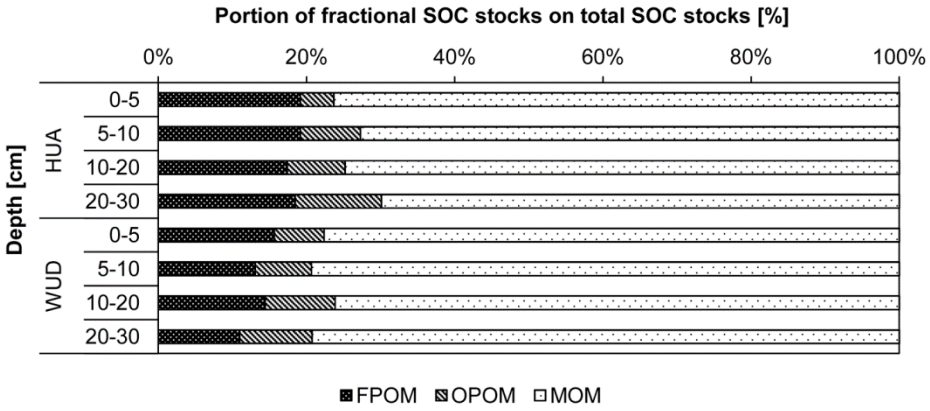

Fig. 3 Portion of fractional soil organic carbon (SOC) stocks on total soil organic carbon stocks in particular depth at Huashixia (HUA, top) and Wudaoliang (WUD, bottom).

3.3 Correlations between soil organic carbon stocks, active layer thickness and soil moisture

To assess the influence of soil hydrological properties on SOC stocks, active layer thickness and soil moisture content were taken into account. Since we did not reach the maximum active layer depth in May/June 2009, we used active layer and corresponding soil moisture data from August/September 2011. A significant correlation between SOC stocks and soil moisture can be confirmed for both study sites (Fig. 4). Soil moisture in HUA varies from 7 to almost 56 Vol. % with a high correlation of R^2=0.74 between SOC stocks and soil moisture. The range in WUD is smaller with values between 11 and 50 Vol. % soil moisture and a weak correlation (R^2=0.05).

An inverse correlation can be observed for active layer thickness and soil moisture (Fig. 5). The mean thaw depth at both locations is similar (HUA: 97 cm, WUD: 99 cm). Contrarily, the range differs distinctly, with a variation coefficient of 22.0 in HUA and 15.8 in WUD. The interrelation between active layer thickness and SOC stocks is positive for site HUA with R^2 = 0.77. For site WUD, similar significant correlations could not be detected.

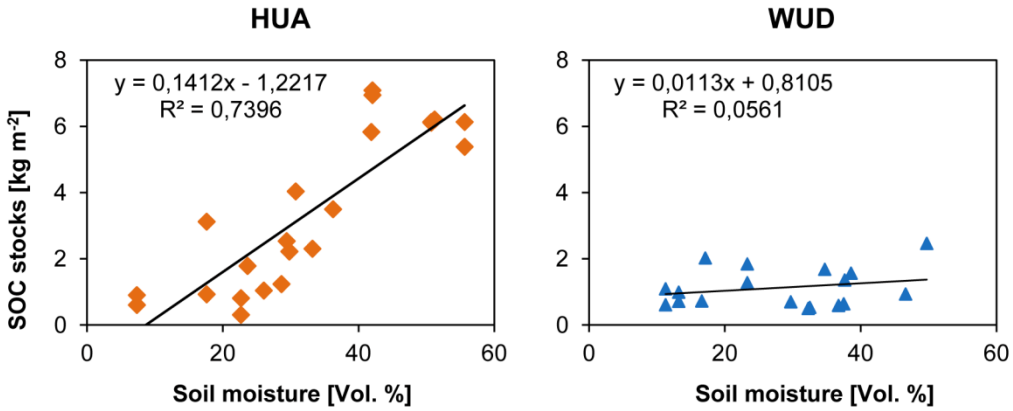

Fig. 4 Correlation between soil organic carbon (SOC) stocks and soil moisture in particular depth at Huashixia (HUA, left, n=24) and Wudaoliang (WUD, right, n=20).

4 Discussion

4.1 Soil organic carbon content

SOC contents decreased with soil depth at both locations in all soil profiles. At site HUA, however, much higher overall values were found than in WUD. The more humid, partly water logging conditions inhibit microbial decomposition processes [49] leading in combination with a more dense vegetation cover to a larger accumulation of organic matter.

Concerning the relative amount of OM fractions, our findings are in line with the results of Golchin et al. [50], who found higher SOC contents in the OPOM than in the FPOM and MOM fractions as well. Wang et al. [33] isolated a light fraction (LF) and a heavy fraction (HF) using a 1.8 g cm^{-3} density solution. In LF SOC contents of 290 g kg^{-1} (0-10 cm) and 260 g kg^{-1} (10-20 cm), for HF 30 g kg^{-1} (0-10 cm) and 40 g kg^{-1} (10-20 cm) were found. The comparably slightly lower SOC contents in the LF may reflect the influence of the MOM fraction. However, the comparison is difficult, because different density ranges for the fractionation were used [33].

SOC in FPOM and MOM decreased with depth, whereas the contents of the OPOM fractions increased slightly at both sites. Larger aggregates composed of coarse textured OPOM with a lower degree of decomposition were present in the depth increment 0-10 cm. A reduction of particle size with depth was clearly observable during the fractionation process. Even though the SOC content was relatively small compared with the POM fractions, the portion of total SOC stored in OPOM is large (Fig. 2).

4.2 OC/N ratios

OC/N ratios of bulk soil decreased with depth indicating a higher age and grade of humification in the subsoil [51]. SOC/N ratios in water-saturated soils in HUA remained relatively stable with

depth indicating inhibited decomposition processes. The highest SOC/N ratios with depth were found in the FPOM fraction followed by OPOM and MOM. Comparable results were reported by Grünewald et al. [44] and John et al. [52], who also observed decreasing SOC/N ratios with depth from FPOM > OPOM > MOM for all soils, indicating an increasing degree of OM degradation and humification. Golchin et al. [50] observed higher ratios for OPOM than for FPOM, whereas Kölbl and Kögel-Knabner [53] found no differences between both fractions.

OC/N ratios in FPOM showed little variations with depth, while the portion of carbon content decreases. Further, we observed a decrease in particle size in the POM fractions during the fractionation that may also contribute to a shift in the SOC/N ratio with depth. The very low SOC/N ratios in MOM fractions suggest a generally larger contribution of microbial biomass and, hence, stronger microbial decomposition of plant debris than for POM fractions. The contribution of inorganic N to the total N content – resulting in a very low SOC/N ratio – cannot be excluded.

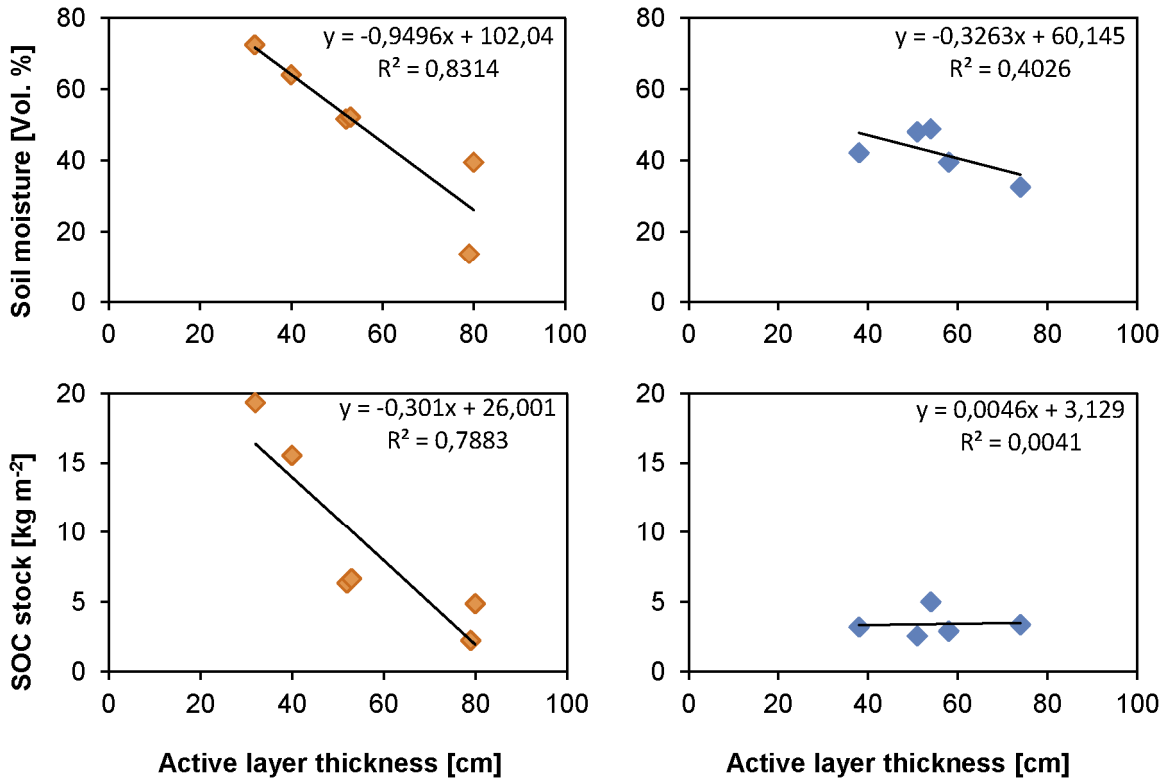

Fig. 5 Correlation between soil moisture and active layer thickness (top) and between soil organic carbon (SOC) stock and active layer thickness (bottom) at Huashixia (HUA, left, n=6) and Wudaoliang (WUD, right, n=5).

4.3 Soil and fractional organic carbon stocks

Our results on SOC stocks are in line with other published data on alpine meadow soils on the Tibetan Plateau [54,19,7,55] as well as on tundra soils in Siberia [56] at a depth of 0-30 cm (Tab. 2). In HUA mean SOC stocks of 10.4 kg m^{-2} were found, in WUD comparably low 3.4 kg m^{-2} (0-30 cm). Due to small-scale differences in substrate, soil moisture and hence vegetation cover,

carbon stocks differ more in HUA than in WUD. Highest stocks occurred in water saturated profiles at HUA (19.3 kg m^{-3}) whereas lowest stocks were found in dry profiles with a lower vegetation density in WUD (2.7 kg m^{-3}).

Table 2 Comparison of soil organic carbon (SOC) stocks in high-altitude and high-latitude permafrost-affected ecosystems.

Study	Mean SOC stocks [kg m^{-2}]	Depth [cm]	Ecosystem type	Region
Post et al. (1982) [4]	21.8	100	Tundra	
Gundelwein et al. (2007) [59]	30.7	100	Tussock Tundra	Siberia, Russia
Jobbágy and Jackson (2000) [1]	14.2	100	Tundra	Canada
Uhlirova et al. (2007) [56]	16.3	30	Tussock Tundra	Siberia, Russia
Wang et al. (2008) [54]	9.3	30	Alpine steppe	Tibetan Plateau, China
	9.8	30	Alpine meadow	Tibetan Plateau, China
	10.7	30	Alpine swamp meadow	Tibetan Plateau, China
Yang et al. (2008) [19]	6.2	30	Alpine meadow	Tibetan Plateau, China
Ohtsuka et al. (2008) [7]	2.6 to 13.7	30	Alpine meadow	Tibetan Plateau, China
Wang et al. (2002) [5]	53.1	75	Alpine meadow	Qinghai, China
	29.0	75	Alpine meadow	Tibet, China
Yang et al. (2010) [26]	9.2	40	Alpine meadow	Tibetan Plateau, China
	12.4	100	Alpine meadow	Tibetan Plateau, China
This study	3.4 to 10.4	30	Alpine meadow	Tibetan Plateau, China

Our results show that high soil moistures combined with low soil temperatures (due to the isolating effect of dense vegetation) lead to an increased accumulation of soil organic matter [57] and therefore higher SOC stocks than in drier soil profiles. SOC stocks decreased with depth, especially in WUD (Tab. 1).

The comparison of fractional SOC stocks with the results of other published research is challenging, as different density ranges and fractionation methods are used and the number of studies on the Tibetan Plateau is limited. Compared to other grassland ecosystems like steppe soils in Ukraine and Kazakhstan [58] and grassland soils in Saxony-Anhalt, Germany [52], in this study significantly higher portions of FPOM and OPOM on SOC stocks were found. About 18 % of the total contents in HUA and 14 % in WUD were contributed by the FPOM fraction. The OPOM portions were the same at both sites (8 %) and the MOM fractions contributed 74 and 78 % to the total SOC stocks (Fig. 3). Due to lower litter production in WUD, lower fraction masses and SOC contents led to lower portions of POM on total SOC stocks (Fig. 3). At site HUA the share of FPOM remained relatively constant with depth, while the stocks in WUD were decreasing. The share of OPOM increased at both sites with increasing depth. The increase in OPOM stocks was linked also to the increasing SOC content of the fractions with increasing depth.

The limitation of water caused a lower turnover of organic matter at very dry profile sites in HUA and WUD. This resulted in a relatively high share of FPOM on SOC with small portions of OPOM similar to desert soils investigated by Kadono et al. [58]. The largest FPOM and OPOM

shares were found in water-saturated profiles at site HUA with a contribution of 39 % of the POM fractions to the SOC stocks since further degradation of SOM is strongly inhibited there.

Our results are comparable to studies in Siberia [59] and the Tibetan Plateau [36,33]. Wang et al. [36] isolated a light and heavy fraction (1.85 g cm^{-3} density solution) without distinction between FPOM and OPOM. In this case only trends can be compared with our results. The LF contained 7 kg m^{-2} and thus about 37-44 % of SOC from 0-30 cm depth. Altogether, SOC stocks comprised 9.81 kg m^{-2} at a depth of 30 cm. Wang et al. [33] isolated LF and HF with a density range of 1.8 g cm^{-3}. They found a SOC stock of 7.5 kg m^{-2} at a depth of 0-20 cm, with 0.8 kg m^{-2} in LF and 2.8 kg m^{-2} in HF in the upper 10 cm. 0.4 kg m^{-2} in LF and 3.5 kg m^{-2} in HF were contained in 10-20 cm depth.

4.4 Correlation between organic carbon stocks, active layer thickness and soil moisture

Similar mean active layer thicknesses are evident at both sites, but significantly larger variations were observed in HUA. These spatial dynamics are related to small scale changes in substrate, bulk density, soil moisture values [6] and hence in vegetation coverage leading to larger active layer thicknesses. Patches of dense vegetation have an isolating effect, protecting permafrost from thawing [33,20] resulting in shallower active layer depths.

The detected thawing depths of 55-124 cm in HUA and 84-122 cm in WUD correspond to the range of the maximum thawing depths of 80-150 cm near WUD in September published by Wang et al. [36]. Yang et al. [19] and Baumann et al. [6] showed, that soil moisture affects significantly extension and distribution of carbon stocks on the Tibetan Plateau, as we found as well. Soil moisture, active layer thickness and carbon stocks correlated strongly at HUA (Fig. 4 and 5). As a consequence of the moist to water-saturated conditions and the dense vegetation cover, a higher amount of organic matter is accumulated in HUA compared to WUD, where a lower litter input due to the shorter growing season and drier conditions accelerating mineralization, are prominent. In WUD we found no correlation between soil moisture and SOC stocks as well as between SOC stocks and active layer thickness.

5 Conclusions

In this paper we investigated the interactions of SOC stocks and the proportion of light and heavy SOC fractions with soil moisture and active layer thickness in permafrost-affected soils on the Tibetan Plateau. Furthermore, the affiliation of SOC stocks into different SOC pools was examined. The research sites are located in both continuous (WUD) and discontinuous (HUA) permafrost areas.

SOC stocks, soil moisture, and active layer thickness correlated strongly in discontinuous permafrost, whereas no correlation between SOC stocks and active layer thickness and only a weak relation between SOC stocks and soil moisture could be detected for continuous permafrost. Organic carbon contents and SOC stocks were remarkably lower under continuous permafrost conditions. We conclude that drier soil conditions and a shorter vegetation period compared to areas with discontinuous permafrost account for this. Moreover, these soils contain higher portions of easily decomposable POM fractions.

Although the POM fractions comprise only a small portion of the organic carbon mass balance, they contribute a large proportion on SOC stocks due to their high SOC contents. These results show that different POM fractions play specific roles under the scope of climate change: light POM fractions have short turnover rates and are particularly vulnerable to increasing temperatures in terms of potential CO_2 and CH_4 emission from soils.

6 Acknowledgements

We thank Yang Xiaoxia and Mi Zhaorong (NWIPB, CAS, China) for supporting the field campaign and Christian Wolf, Kathrin Drechsel and Sabine Flaiz (University of Tuebingen, Germany) for their assistance during laboratory analyses.

7 References

1. Jobbágy EG, Jackson RB (2000) The vertical distribution of soil organic carbon and its relation to climate and vegetation. Ecological Applications 10 (2): 423–436.
2. Bockheim JG, Hinkel KM, Nelson FE (2003) Predicting Carbon Storage in Tundra Soils of Arctic Alaska. Soil Sci. Soc. Am. J 67 (3): 948–950. Available: https://www.crops.org/publications/sssaj/abstracts/67/3/948.
3. Callesen I, Listi J, Raulund-Rasmussen K, Olsson MT, Tau-Strand L, et al. (2003) Soil carbon stores in Nordic well-drained forest soils - relationships with climate and texture class. Global Change Biology 9: 358–370.
4. Post WM, Emanuel WR, Zinke PJ, Stangenberger AG (1982) Soil carbon pools and world life zones. Nature 298: 156–159.
5. Wang G, Qian J, Cheng G, Lai Y (2002) Soil organic carbon pool of grassland soils on the Qinghai-Tibetan Plateau and its global implication. The Science of the Total Environment 291: 207–217.

6. Baumann F, He J, Schmidt K, Kühn P, Scholten T (2009) Pedogenesis, permafrost, and soil moisture as controlling factors for soil nitrogen and carbon contents across the Tibetan Plateau. Global Change Biology 15 (12): 3001–3017. Available: http://dx.doi.org/10.1111/j.1365-2486.2009.01953.x.

7. Ohtsuka T, Hirota M, Zhang X, Shimono A, Senga Y, et al. (2008) Soil organic carbon pools in alpine to nival zones along an altitudinal gradient (4400–5300 m) on the Tibetan Plateau. Polar Science 2 (4): 277–285.

8. Zhang Y, Tang Y, Jiang J, Yang Y (2007) Characterizing the dynamics of soil organic carbon in grasslands on the Qinghai-Tibetan Plateau. Science in China Series D: Earth Sciences 50 (1): 113–120.

9. Luo T, Li W, Zhu H (2002) Estimated biomass and productivity of natural vegetation on the Tibetan plateau. Ecological Applications 12 (4): 980–997. Available: doi:10.1890/1051-0761(2002)012[0980:EBAPON]2.0.CO.

10. Kirschbaum MUF (1995) The temperature dependence of soil organic matter decomposition, and the effect of global warming on soil organic C storage. Soil Biology & Biochemistry 27 (6): 753–760.

11. Wagner D, Liebner S (2009) Global Warming and Carbon Dynamics in Permafrost Soils: Methane Production and Oxidation. In: Margesin R, editor. Permafrost Soils. Berlin / Heidelberg: Springer. pp. 219–236.

12. Tarnocai C, Canadell JG, Schuur EAG, Kuhry P, Mazhitova G, et al. (2009) Soil organic carbon pools in the northern circumpolar permafrost region. Global Biogeochem. Cycles 23 (2): GB2023. Available: http://dx.doi.org/10.1029/2008GB003327.

13. Grosse G, Romanovsky V, Jorgenson T, Anthony KW, Brown J, et al. (2011) Vulnerability and Feedbacks of Permafrost to Climate Change. Eos Trans. AGU 92 (9): 73–74. Available: doi:10.1029/2011EO090001.

14. Schuur EAG, Bockheim J, Canadell JG, Euskirchen E, Field CB, et al. (2008) Vulnerability of Permafrost Carbon to Climate Change: Implications for the Global Carbon Cycle. BioScience 58 (8): 701–714.

15. Torn MS, Trumbore SE, Chadwick OA, Vitousek PM, Hendricks DM (1997) Mineral control of soil organic carbon storage and turnover. Nature 389 (6647): 170–173. Available: http://dx.doi.org/10.1038/38260.

16. Trumbore S (2006) Carbon respired by terrestrial ecosystems – recent progress and challenges. Global Change Biology 12 (2): 141–153.

17. Lützow M, Kögel-Knabner I, Ekschmitt K, Flessa H, Guggenberger G, et al. (2007) SOM fractionation methods: Relevance to functional pools and to stabilization mechanisms. Soil Biology and Biochemistry 39: 2183–2207.

18. Du Zheng, Zhang Q, Wu S (2000) Mountain geoecology and sustainable development of the Tibetan Plateau. Dordrecht / Boston: Kluwer Academic Publishers.

19. Yang Y, Fang J, Tang Y, Ji C, Zheng C, et al. (2008) Storage, patterns and controls of soil organic carbon in the Tibetan grasslands. Global Change Biology 14: 1592–1599.

20. Zhao L, Cheng G, Li S, Zhao X, Wang S (2000) Thawing and freezing processes of active layer in Wudaoliang region of Tibetan Plateau. Chinese Science Bulletin 45: 2181–2187.

21. Kang SXY, You Q, Flügel W, Pepin N, Yao T (2010) Review of climate and cryospheric change in the Tibetan Plateau. Environ. Res. Lett. 5: 1–8.

22. Jin H, Zhao L, Wang S, Jin R (2006) Thermal regimes and degradation modes of permafrost along the Qinghai-Tibet Highway. Science in China Series D: Earth Sciences 49 (11): 1170–1183.

23. Yang M, Wang S, Yao T, Gou X, Lu A, et al. (2004) Desertification and its relationship with permafrost degradation in Qinghai-Xizang (Tibet) plateau. Cold Regions Science and Technology 39: 47–53.

24. Cheng G, Wu T (2007) Responses of permafrost to climate change and their environmental significance, Qinghai-Tibet Plateau. J. Geophys. Res 112: F02S03. Available: doi:10.1029/2006JF000631.

25. Nan Z, Li S, Cheng G (2005) Prediction of permafrost distribution on the Qinghai-Tibet Plateau in the next 50 and 100 years. Science in China Series D: Earth Sciences 48 (6): 797–804.

26. Yang M, Nelson FE, Shiklomanov NI, Guo D, Wan G (2010) Permafrost degradation and its environmental effects on the Tibetan Plateau: A review of recent research. Earth-Science Reviews 103 (1–2): 31–44. Available: http://www.sciencedirect.com/science/article/pii/S0012825210000826.

27. Wang B, French HM (1995) Permafrost on the Tibet Plateau, China. Quaternary Science Reviews 14: 255–274.

28. Zhang T (2005) Historical Overview of Permafrost Studies in China. Physical Geography 26 (4): 279–298. Available: http://dx.doi.org/10.2747/0272-3646.26.4.279.

29. Davidson EA, Janssens IA (2006) Temperature sensitivity of soil carbon decomposition and feedbacks to climate change. Nature 440 (7081): 165–173. Available: http://dx.doi.org/10.1038/nature04514.

30. Saito M, Kato T, Tang Y (2009) Temperature controls ecosystem CO2 exchange of an alpine meadow on the northeastern Tibetan Plateau. Global Change Biology 15: 221–228.

31. Kirschbaum MUF (2006) The temperature dependence of organic-matter decomposition – still a topic of debate. Soil Biology & Biochemistry 38: 2510–2518.

32. Geng Y, Wang Z, Liang C, Fang J, Baumann F, et al. (2012) Soil Respiration in Tibetan Alpine Grasslands: Belowground Biomass and Soil Moisture, but Not Soil Temperature, Best Explain the Large-Scale Patterns. PLoS ONE 7 (4): e34968. Available: 10.1371/journal.pone.0034968.

33. Wang WY, Wang QJ, Lu ZY (2009) Soil organic carbon and nitrogen content of density fractions and effect of meadow degradation to soil carbon and nitrogen of fractions in alpine Kobresia meadow. Science in China Series D: Earth Sciences 52 (5): 660–668. Available: http://dx.doi.org/10.1007/s11430-009-0056-5.

34. Geng Y, Wang Z, Liang C, Fang J, Baumann F, et al. (2012) Effect of geographical range size on plant functional traits and the relationships between plant, soil and climate in Chinese grasslands. Global Ecology and Biogeography: no. Available: http://dx.doi.org/10.1111/j.1466-8238.2011.00692.x.

35. Ni J (2002) Carbon storage in grasslands of China. Journal of Arid Environments 50: 205–218.

36. Wang G, Li Y, Hu H, Wang Y (2008) Synergistic effect of vegetation and air temperature changes on soil water content in alpine frost meadow soil in the permafrost region of Qinghai-Tibet. Hydrological Processes 22: 3310–3320.

37. Weischet W, Endlicher W (2000) Regionale Klimatologie Teil 2. Stuttgart: Schweizerbart‘sche Verlagsbuchhandlung.

38. Zhou H, Zhao X, Tang Y, Gu S, Zhou L (2005) Alpine grassland degradation and its control in the source regions of the Yangtze and the Yellow Rivers, China. Grassland Science 51: 191–203.

39. Jin H, Li S, Cheng G, Shaoling W, Li X (2000) Permafrost and climatic change in China. Global and Planetary Change 26: 387–404.

40. Wang G, Wang Y, Li Y, Cheng H (2007) Influences of alpine ecosystem responses to climatic change on soil properties on the Qinghai-Tibet Plateau, China. Catena 70 (3): 506–514.

41. IUSS Working Group WRB. 2007. World Reference Base for Soil Resources 2006, first update 2007. World Soil Resources Reports No. 103. FAO, Rome.

42. Kato T, Tang Y, Gu S, Cui X, Hirota M, et al. (2004) Carbon dioxide exchange between the atmosphere and an alpine meadow ecosystem on the Qinghai–Tibetan Plateau, China. Agricultural and forest meteorology 124 (1–2): 121–134. Available: http://www.sciencedirect.com/science/article/pii/S0168192304000024.

43. Kaiser K, Miehe G, Barthelmes A (2008) Turf-bearing topsoils on the central Tibetan Plateau, China: Pedology, botany, geochronology. Catena 73 (3): 300–311.

44. Grünewald G, Kaiser K, Jahn R, Guggenberger G (2006) Organic matter stabilization in young calcareous soils as revealed by density fractionation and analysis of lignin-derived constituents. Organic Geochemistry 37: 1573–1589.

45. Golchin A, Oades JM, Skemstad J, Clarke P (1994) Study of free and occluded organic matter in soils by 13C CP/ MAS NMR spectroscopy and scanning electron microscopy. Australian Journal of Soil Research (32): 285–309.

46. Christensen B (1992) Physical fractionation of soil and organic matter in primary particle size and density separates. Advances in Soil Science (20): 1–90.

47. Roscoe R, Buurman P, Velthorst EJ (2000) Disruption of soil aggregates by varied amounts of ultrasonic energy in fractionation of organic matter of a clay Latosol: carbon, nitrogen and d13C distribution in particle-size fractions. European Journal of Soil Science 51: 445–454.

48. Six J, Schultz PA, Jastrow JD, Merckx R (1999) Recycling of sodium polytungstate used in soil organic matter studies. Soil Biology & Biochemistry 31: 1193–1196.

49. Wagner D, Kobabe S, Liebner S (2009) Bacterial community structure and carbon turnover in permafrost-affected soils of the Lena Delta, northeastern Siberia. Canadian Journal of Microbiology 55 (1): 73–83. Available: http://dx.doi.org/10.1139/W08-121.

50. Golchin A, Oades JM, Skjemstad J, Clarke P (1995) Structural and dynamic properties of soil organic-matter as reflected by 13C natural-abundance, pyrolysis mass-spectrometry and solid-state 13C NMR-spectroscopy in density fractions of an oxisol under forest and pasture. Australian Journal of Soil Research 33: 59–76. Available: http://dx.doi.org/10.1071/SR9950059.

51. Callesen I, Raulund-Rasmussen K, Westman C, Tau-Strand L (2007) Nitrogen pools and C:N ratios in well-drained Nordic forest soils related to climate and soil texture. Boreal Environment Research 12 (6): 681–692.

52. John B, Yamashita T, Ludwig B, Flessa H (2005) Storage of organic carbon in aggregate and density fractions of silty soils under different types of land use. Geoderma 128: 63–79.

53. Kölbl A, Kögel-Knabner I (2004) Content and composition of free and occluded particulate organic matter in a differently textured arable Cambisol as revealed by solid-state 13C NMR spectroscopy. Journal of Plant Nutrition and Soil Science 167 (1): 45–53. Available: 10.1002/jpln.200321185.

54. Wang G, Li Y, Wang Y, Wu Q (2008) Effects of permafrost thawing on vegetation and soil carbon losses on the Qinghai-Tibet Plateau, China. Geoderma 143: 143–152.

55. Yang YH, Fang JY, Guo DL, Ji CJ, Ma WH (2010) Vertical patterns of soil carbon, nitrogen and carbon: nitrogen stoichiometry in Tibetan grasslands. Biogeosciences Discuss. 7: 1–24.

56. Uhlirova E, Santruckova H, Davidov SP (2007) Quality and potential biodegradability of soil organic matter preserved in permafrost of Siberian tussock tundra. Soil Biology & Biochemistry 39: 1978–1989.

57. Wang G, Wang Y, Qian J, Wu Q (2006) Land cover change and its impact on soil C and N in two watersheds in the center of the Qinghai-Tibetan Plateau. Mountain Research and Development 26 (2): 153–162.

58. Kadono A, Funakawa S, Kosaki T (2008) Factors controlling mineralization of soil organic matter in the Eurasian steppe. Soil Biology and Biochemistry 40 (4): 947–955. Available: http://www.sciencedirect.com/science/article/pii/S0038071707004567.

59. Gundelwein A, Müller-Lupp T, Sommerkorn M, Haupt ETK, Pfeiffer E, et al. (2007) Carbon in tundra soils in the Lake Labaz region of arctic Siberia. European Journal of Soil Science 58 (5): 1164-1174. Available: http://dx.doi.org/10.1111/j.1365-2389.2007.00908.x.

Manuscript 5

Organic and inorganic carbon in the topsoil of the Mongolian and Tibetan grasslands: pattern, control and implications

Biogeosciences (2012), 9: 2287 - 2299

Yue Shi[1], Frank Baumann[2,], Yinlei Ma[1], Chao Song[1*], Peter Kühn[2], Thomas Scholten[2], Jin-Sheng He[3]

[1]Department of Ecology, College of Urban and Environmental Sciences, and Key Laboratory for Earth Surface Processes of the Ministry of Education, Peking University, 5 Yiheyuan Rd., 100871 Beijing, China

[2]Department of Geoscience, Physical Geography and Soil Science, University of Tübingen, Rümelinstrasse 19-23, 72070 Tübingen, Germany

[3]Key Laboratory of Adaptation and Evolution of Plateau Biota, Northwest Institut of Plateau Biology, Chinese Academy of Sciences, 23 Xinning Rd., 810008 Xining, China

[*]now at: Department of Ecology and Evolutionary Biology, University of Kansas, Lawrence, KS 66045, USA

Abstract

Soil carbon (C) is the largest C pool in the terrestrial biosphere and includes both inorganic and organic components. Studying patterns and controls of soil C help us to understand and estimate potential responses of soil C to global change in the future. Here we analyzed topsoil data of 81 sites obtained from a regional survey across grasslands in the Inner Mongolia and on the Tibetan Plateau during 2006– 2007, attempting to find the patterns and controls of soil inorganic carbon (SIC) and soil organic carbon (SOC). The averages of inorganic and organic carbon in the topsoil (0–20 cm) across the study region were 0.38 % and 3.63 %, ranging between 0.00–2.92 % and 0.32–26.17 % respectively. Both SIC and SOC in the Tibetan grasslands (0.51 % and 5.24 % respectively) were higher than those in the Inner Mongolian grasslands (0.21 % and 1.61 %). Regression tree analyses showed that the spatial pattern of SIC and SOC were controlled by different factors. Chemical and physical processes of soil formation drive the spatial pattern of SIC, while biotic processes drive the spatial pattern of SOC. SIC was controlled by soil acidification and other processes depending on soil pH. Vegetation type is the most important variable driving the spatial pattern of SOC. According to our models, given the acidification rate in Chinese grassland soils in the future is the same as that in Chinese cropland soils during the past two

decades: 0.27 and 0.48 units per 20 yr in the Inner Mongolian grasslands and the Tibetan grasslands respectively, it will lead to a 30 % and 53 % decrease in SIC in the Inner Mongolian grasslands and the Tibetan grasslands respectively. However, negative relationship between soil pH and SOC suggests that acidification will inhibit decomposition of SOC, thus will not lead to a significant general loss of carbon from soils in these regions.

1 Introduction

The importance of soil carbon (C) in global C cycling has received considerable attention in recent decades (Schulze and Freibauer, 2005; Trumbore and Czimczik, 2008; Schlesinger and Andrews, 2000; Lal, 2004a). A soil C pool comprises two distinct components: soil organic carbon (SOC) and soil inorganic carbon (SIC). The latter includes lithogenic inorganic carbon (LIC), which comes from parent material, and pedogenic inorganic carbon (PIC), which is formed through the dissolution and precipitation of carbonate parent material. On a global scale, the estimated size of SOC in the 1-m depth is 1500 to 1600 Pg (Lal, 2004b; Monger and Gallegos, 2000; Batjes, 1996), and the size of SIC is 695 to 1738 Pg (Batjes, 1996; Eswaran et al., 1995).

C flux between the atmosphere and terrestrial ecosystems involves both SOC and SIC. The C flux between SOC pools and the atmosphere depends on biomass production, organic materials input and soil respiration (Schlesinger and Andrews, 2000; Valentini et al., 2000). SIC pools exchange C with the atmosphere through a series of physical and chemical reaction, such as C sequestration by carbonate formation or CO_2 release by acidification and leaching (Lal and Kimble, 2000; Lal, 2008; Ouyang et al., 2008). Given that global change has altered temperature, precipitation, nitrogen availability and many other environmental factors (Rockström et al., 2009; Vitousek, 1994), these changes are most likely to have great impact on soil carbon. As the largest C pool in terrestrial biosphere, even a minor change in soil carbon stocks could result in a significant alteration of atmospheric CO_2 concentration (Davidson and Janssens, 2006; Trumbore and Czimczik, 2008). Therefore, both SIC and SOC pools should be considered in order to more accurately predict future soil carbon dynamics.

In arid and semiarid regions, which cover as much as one-third of the Earth's surface, SIC pools and their dynamics are important as the rate of accumulation of SIC is generally higher than in other biomes (Lal, 2008). Grasslands are one of the most widespread ecosystems in arid and semiarid regions, containing about 20 % of global soil C stocks (Jobbagy and Jackson, 2000; Scurlock and Hall, 1998; Wang and Fang, 2009). Grasslands cover more than 40 % of China's land surface, ranging from temperate grasslands in arid/semi-arid regions to alpine grasslands on the Tibetan Plateau (Kang et al., 2007; Yang et al., 2010b; He et al., 2009). Because of the large spatial extend, Chinese grasslands have significant effects on regional and global carbon cycles

(Ni, 2002; Yang et al., 2010b). Moreover, Chinese grasslands face rapid environmental changes (Kang et al., 2007). In recent years, many studies have been conducted to investigate the pattern, controls and dynamic of SOC (e.g. Ni, 2002; Yang et al., 2010b; Wu et al., 2003; Yu et al., 2007; Xie et al., 2007; Baumann et al., 2009) as well as SIC (e.g. Yang et al., 2010a; Mi et al., 2008; Feng et al., 2002) in Chinese grasslands. SOC stocks are reported to range from 37.7 Pg (Xie et al., 2007) to 41.0 Pg (Ni, 2002) in Chinese grasslands, and about 16.7 Pg in northern China's grasslands (Yang et al., 2010b). On the scale of the whole of China, SOC densities are significantly influenced by temperature (Xie et al., 2007), while soil moisture and texture control SOC density in the Tibetan grasslands (Yang et al., 2008; Baumann et al., 2009). For SIC, total stocks of the top 1 m are estimated to vary from 53.3 Pg to 77.9 Pg (Wu et al., 2009; Mi et al., 2008; Li et al., 2007) in China. Yang et al. (2010a) estimated the SIC stock of the Tibetan grasslands to 15.2 Pg. Temperature and precipitation both show significant relationships with SIC density (Li et al., 2007; Mi et al., 2008; Yang et al., 2010a).

However, there are still some uncertainties evident in recent studies. Most of the researches focused on mean soil carbon stocks for soil at depths of 1 m or more, but little work, especially for SIC, has been devoted to investigate the patterns, controls and dynamics of carbon in the topsoil. The topsoil is the component of the soil system showing most rapid responses to environmental changes, such as alterations in temperature, precipitation and nitrogen deposition (Liao et al., 2009; Song et al., 2005). Changes in the topsoil are particularly important for exploring ecosystem response and functioning (Franzluebbers and Stuedemann, 2010). Moreover, recent studies spent large efforts in determining patterns, controls and dynamics of SOC, but there is less attention drawn on SIC in general (Eswaran et al., 2000; Mi et al., 2008). Consequently, we cannot simply use results of these studies to predict potential responses of soil carbon to future global changes. Further, some recent studies calculated SIC as the difference between soil total carbon (STC) and SOC (e.g. Yang et al., 2010a; Mikhailova and Post, 2006). However, the proportions of carbonates in soil total carbon are usually small (Chatterjee et al., 2009), thus this method without the direct measurement of SIC could produce a large relative error. Therefore, studies focused on SIC based on measured data help us to reduce the uncertainties of previous studies and to predict response of soil carbon to global changes.

In this study, we analyzed the topsoil data of 81 sites obtained from a regional survey across grasslands in Inner Mongolia and the Tibetan Plateau during 2006–2007. We attempt (1) to investigate the large-scale patterns of inorganic and organic carbon in the topsoil of grasslands in Inner Mongolia and on the Tibetan Plateau, (2) to examine the changes of SIC and SOC along naturally occurring environmental gradients in order to identify key controlling factors for SIC and SOC contents, and (3) to estimate potential responses of inorganic and organic carbon in the topsoil related to soil acidification.

2 Materials and methods

2.1 Study sites

This study was conducted in temperate grasslands in the Inner Mongolia and alpine grasslands on the Tibetan Plateau, during two expeditions in late July and early August of 2006 and 2007. We selected 81 sites along an approximately 4000 km long transect (longitude from 90.80 to 120.12° E, latitude from 30.31 to 50.19° N, and altitude from 549 to 5105 m a.s.l.) for soil and plant community sampling (Table 1, Fig. 1). Mean annual temperature (MAT) ranges from −5.8 to 4.1°C and mean annual precipitation (MAP) ranges from 148 to 604 mm. The sites along the transect represent natural zonal grassland vegetation, including the five main vegetation types: meadow steppe, typical steppe, desert steppe, alpine steppe and alpine meadow. Field sites were selected by visual inspection of the vegetation, aiming to select sampling sites subject to minimal grazing and other anthropogenic disturbances.

Table 1 Description of the study regions. Mean annual temperature (MAT), mean annual precipitation (MAP), growing season temperature (GST), growing season precipitation (GSP), Averaged topsoil pH, soil bulk density (SBD), soil moisture (SM) and soil total nitrogen (STN) of the sampling sites are shown.

	Overall	**Inner Mongolian grasslands**	**Tibetan grasslands**
No. of site	81	36	45
Longitude [°E]	90.80 - 120.12	111.83 - 120.12	90.80 - 101.48
Latitude [°N]	30.31 - 50.19	41.79 - 50.19	30.31 - 37.28
Altitude [m]	549 - 5105	549 - 1418	2925 - 5105
MAT [°C]	-5.8- 4.1	-2.6 - 4.1	-5.8 - 2.6
GST [°C]	1.5 - 16.9	11.2 - 16.9	1.5 - 11
MAP [mm yr^{-1}]	148 - 604	148 - 436	218 - 604
GSP [mm yr^{-1}]	115 - 402	115 - 343	133 - 402
Soil pH	5.2 - 8.2	5.7-8.2	5.2-7.6
SBD [g cm^{-3}]	0.25 - 1.63	0.94-1.63	0.25-1.43
SM [V/V %]	0.73 - 68.11	2.04-16.10	0.73-68.11
STN [g/g %]	0.04 - 1.52	0.05-0.45	0.04-1.52

2.2 Soil and biomass survey

Detailed field investigations included soil profile description according to FAO (2006) and IUSS Working Group WRB (2006). Soil sampling was split into two parts: schematic soil sampling by drilling at three depth increments (0–5, 5–10, and 10–20 cm) for SIC and SOC analyses, as well as volumetric sampling using a standard container (100 cm^3 in volume) at equal depths for soil bulk density (SBD) and gravimetric water content (equalling to soil moisture, SM) determination. The sampling protocol is described in Baumann et al. (2009).

Soil samples were air-dried, all live root material was removed and the remaining soil was grounded using a ball mill (NM200, Retsch, Germany). We measured soil inorganic carbon (SIC) volumetrically using an inorganic carbon analyzer (Calcimeter 08.53, Eijkelkamp, Netherland).

Soil total carbon (STC) was measured by dry combustion using an elemental analyzer (VARIO EL III, Elementar, Hanau, Germany) with a combustion temperature of 1150°C and a reduction temperature of 850°C. Soil organic carbon (SOC) was calculated as the difference between STC and SIC. The average concentration of SIC, SOC and STC of the top 20 cm was calculated using the data from the three layers with soil bulk density, and this average value was used as site level data. Soil pH was determined in both 0.01 M $CaCl_2$ and double distilled water potentiometrically. Results from these two methods showed a very strong linear relationship. Since using a $CaCl_2$ solution gives better repeatable results (Brady and Weil, 2002), the pH data from a $CaCl_2$ solution were used in the model. Soil total nitrogen was also determined using an elemental analyzer (PE 2400 II CHN elemental analyzer, Perkin-Elmer, Boston, Massachusetts, USA).

Additionally, we measured aboveground biomass (AGB) in three plots (1 × 1 m^2) and belowground biomass (BGB) in three soil pits (0.5 × 0.5 m^2) at each site. Biomass was measured by oven-drying at 60°C to a constant weight and weighting to the nearest 0.1 g.

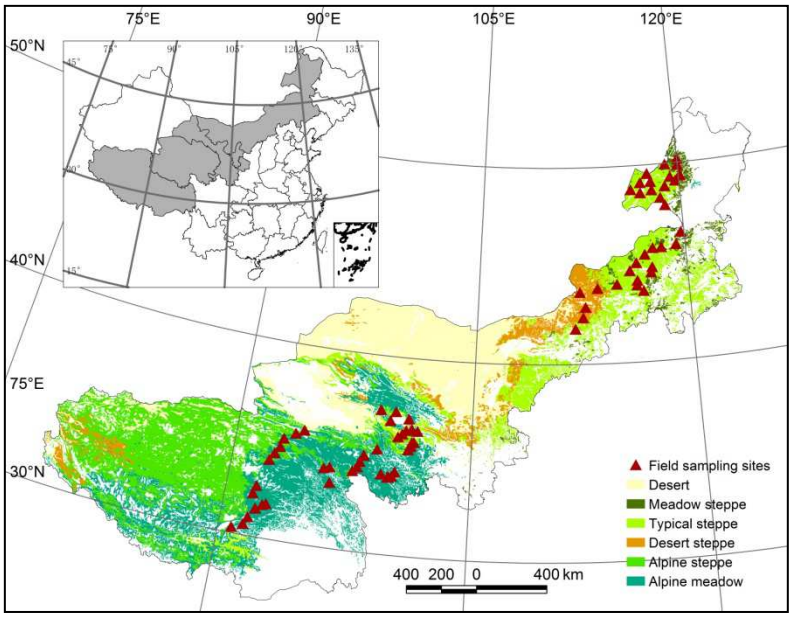

Fig. 1 Vegetation map of Chinese grasslands and location of sampling sites (1 : 1 000 000) (Chinese Academy of Sciences, 2001).

2.3 Climate data and statistical analyses

Climate data for each site was calculated based on linear models using latitude, longitude and altitude as predictors from 55-yr average temperature and precipitation records (1951–2005) at 680 climate stations across China (Fang et al., 2001; He et al., 2009). The calculation of potential evapotranspiration (PE) and actual evapotranspiration (AE) were based on Thornthwaite's method (Thornthwaite, 1948).

We used one-way ANOVA with Turkey's *post hoc* test to compare the effects of region, vegetation type, and soil depth on SIC, SOC and the ratio of SIC to STC (SIC/STC). We conducted classification and regression tree (CART) analyses, which can deal with both categorical and continuous variables simultaneously (Qian, 2009), to detect important variables influencing the patterns of SIC, SOC and SIC/STC. We selected the complexity parameter as split criterion, and set the observations required for a split search at 15. Climatic factors, including MAT, MAP, growing season temperature (GST, from April to August), growing season precipitation (GSP), AE, PE, as well as biotic factors including vegetation type (VT), AGB, and BGB were used in the tree models (Table 4). Since soil pH, SM, CO_2 partial pressure and water deficiency also influenced SIC, soil pH, SM, altitude (proxy of CO_2 partial pressure) as well as the ratio of MAP to PE (MAP/PE, an index of water deficiency) were incorporated into the CART analysis when we analysed SIC and SIC/STC. We did not include the overall grazing intensity as covariate in our model because our approach focuses on landscape scale stretching across regions with particular climate and geomorphology. Grazing patterns and grazing intensities are supposed to vary greatly in such diverse regions. Official data cannot be used to reflect the pattern since they are bound to county and provincial boundaries. Finally, for estimating the change of carbonates of the topsoil in the Inner Mongolian and Tibetan grasslands under the background of soil acidification, we built ordinary linear regression models for SIC and SIC/STC, using the most powerful explanatory variables in the CART analysis. SIC, SOC and SIC/STC were log transformation to achieve normal distribution (Fig. 2). All statistical analyses were performed using R 2.3.0 (R Development Core Team, 2011). The classification and regression trees were developed using the R package rpart.

3 Results

3.1 Overall patterns of SIC, SOC and SIC/STC

Frequency distributions of SIC, SOC and SIC/STC did not deviate significantly from log normal distributions ($P > 0.05$) neither at site level nor for each depth increment. At site level, the mean values of SIC, SOC and SIC/STC were 0.38 %, 3.58 % and 0.15, ranging between 0.00–2.92 %, 0.32–26.34 % and 0.00–0.65, with CV of 1.36, 1.19 and 1.26, respectively (Table 3). We did not find significant differences of SIC and SIC/STC among three soil depths ($P < 0.05$), while SOC in 0-5 cm was significantly higher than that in 10– 20 cm.

At site level, inorganic and organic carbon in the topsoil differed remarkably between the Inner Mongolian and Tibetan grasslands. The means of both SIC and SOC in the Tibetan grasslands (0.51 % and 5.24 % respectively) were higher ($P < 0.01$) than those in the Inner Mongolia grasslands (0.21 % and 1.61 %). However, SIC/STC had no significant difference between the Tibetan grasslands and the Inner Mongolian grasslands (0.18 and 0.11, $P = 0.54$). These patterns are also evident for the three soil depth increments (Table 3). Soil pH showed no significant difference

between the two regions, while soils in the Tibetan grasslands generally accounted for higher soil total nitrogen and SM but lower SBD compared to the Inner Mongolian grasslands (Table 2).

On the whole, vegetation type had significant effects on SIC, SOC and SIC/STC ($P < 0.01$). Generally, inorganic carbon was higher in alpine steppe soils than in meadow steppe and typical steppe soils. Organic carbon was higher in alpine meadow soils compared to desert steppe soils. SIC/STC was highest in the alpine steppe and lowest in the alpine meadow (Table 3).

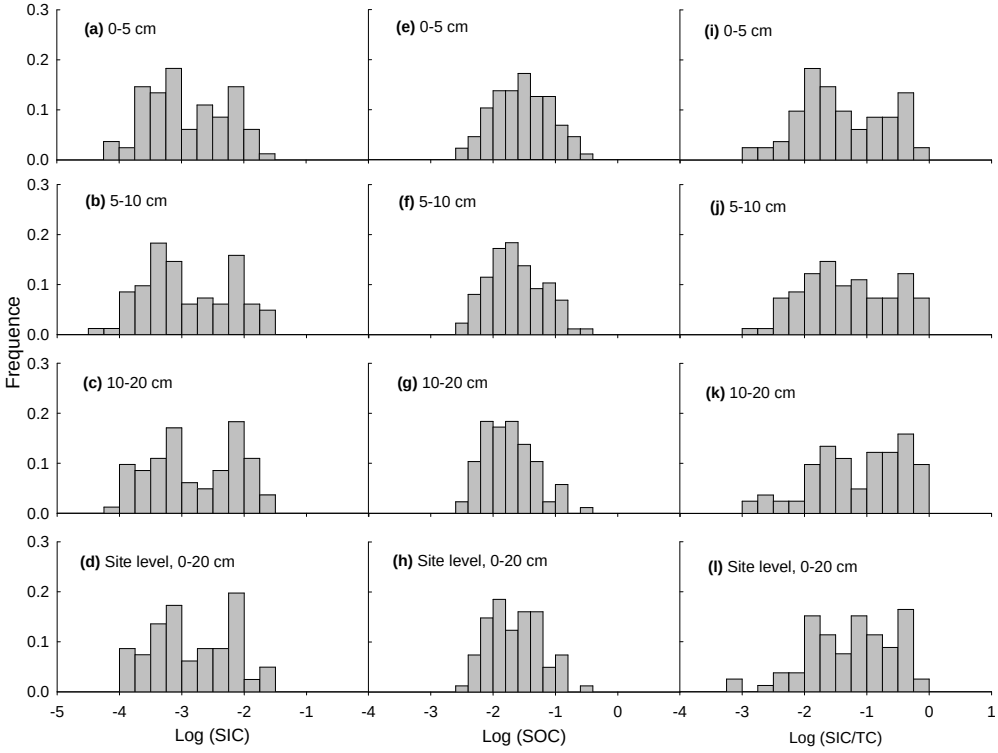

Fig. 2 Frequency distributions of SIC (**a-d**), SOC (**e-h**) and SIC/STC (**i-l**) in Chinese grasslands across all sampling sites at soil depths of 0-5 cm (**a, e, i**), 5-10 cm (**b, f, j**), 10-20 cm (**c, g, k**) and at site level (**d, h, l**). All distributions have no significant differences compared with normal distribution at $P < 0.05$.

3.2 Factors driving spatial variations of SIC and SOC

We developed regression tree models for SIC, SOC and SIC/STC (Fig. 3a–c). All three trees were significantly different from a random tree ($P < 0.05$). The trees for SIC, SOC and SIC/STC explained 69 %, 76 %, and 73 % of the variance, respectively. Tree models revealed that the spatial variations in SIC, SOC and SIC/STC were driven by very different factors (Table 4, Fig. 3).

For SIC (Fig. 3a), the tree model had an initial split on soil pH with a threshold of 7.0, implying that soil pH was the most important variable explaining the spatial variation of SIC. As pH increases above this threshold, MAT and PE represent two thermal factors that became common to affect SIC contents, indicating a negative relationship between SIC and thermal condition. In areas with pH below 7.0, MAP and SM, both reflecting water conditions, were included in the

model: carbonate in the topsoil was typically lower on average in low-precipitation (< 465 mm yr^{-1}) areas; in the areas with more precipitation, inorganic carbon was relatively high in soils with low moisture.

Table 2 Topsoil properties in the Inner Mongolian and Tibetan grasslands across sampling sites. Different letters indicate statistical significance at $P < 0.05$. SBD = soil bulk density; SM = soil moisture; STN = soil total nitrogen; CV = coefficient of variation.

		Inner Mongolian grass-lands	Tibetan grasslands
Soil pH	*n*	36	45
	Mean	6.9*a*	6.8*a*
	CV	0.10	0.09
	Range	5.7-8.2	5.2-7.6
SBD [g cm^{-3}]	*n*	36	45
	Mean	1.3*b*	0.95*a*
	CV	0.13	0.33
	Range	0.94-1.63	0.25-1.43
SM [V/V %]	*n*	32	44
	Mean	7.29*a*	20.95*b*
	CV	0.55	0.85
	Range	2.04-16.10	0.73-68.11
STN [g/g %]	*n*	36	45
	Mean	0.17*a*	0.44*b*
	CV	0.54	0.81
	Range	0.05-0.45	0.04-1.52

Vegetation type was the most important variable for SOC (Fig. 3b), explaining 49 % of the variations of SOC. Steppe soils had much lower organic carbon content than meadow soils. In the steppe, only GSP influenced SOC, with a trend that SOC increased with GSP. In the meadow, AGB and PE were involved. Lower AGB (< 95.4 g m^{-2}) corresponded to lower SOC; but when AGB was above this threshold, SOC decreased with increasing of PE.

Soil pH was the initial split variable with a threshold of 7.0 for SIC/STC (Fig. 3c). When soil pH increases above this threshold, AGB and MAT enter the model, while SM and BGB enter the model when pH is below this threshold. These environmental factors impact the spatial pattern of SIC/STC through influencing SIC and/or SOC.

Table 3 Statistical description of soil inorganic carbon (SIC), soil organic carbon (SOC) content and SIC to soil total carbon ratio (SIC/STC) in each depth increment in different regions and vegetation types. Different letters indicate statistical significance at $P < 0.05$. CV = coefficient of variation.

		SIC [%]				SOC [%]				SIC/STC			
		0-5cm	**5-10cm**	**10-20cm**	**Site level**	**0-5cm**	**5-10cm**	**10-20cm**	**Site level**	**0-5cm**	**5-10cm**	**10-20cm**	**Site level**
Overall	Mean	0.31	0.35	0.44	0.38	4.78	3.74	2.92	3.58	0.11	0.13	0.18	0.15
	CV	1.49	1.52	1.33	1.36	1.08	1.17	1.32	1.19	1.46	1.43	1.16	1.26
	Range	0.00-1.92	0.00-2.28	0.00-2.61	0.00-2.20	0.29-27.51	0.30-25.43	0.28-26.00	0.32-26.34	0.00-0.66	0.00-0.66	0.00-0.74	0.00-0.65
	n	87	87	87	81	87	87	87	81	87	87	87	81
Region													
Inner Mongolian grasslands	Mean	0.14*a*	0.18*a*	0.25*a*	0.22*a*	2.23*a*	1.58*a*	1.26*a*	1.61*a*	0.07*a*	0.09*a*	0.14*a*	0.11*a*
	CV	2.09	2.30	1.81	1.89	0.72	0.66	0.65	0.66	1.44	1.66	1.31	1.39
	Range	0.01-1.59	0.00-2.12	0.01-2.37	0.01-2.10	0.29-7.54	0.30-4.42	0.28-3.60	0.32-4.55	0.00-0.39	0.00-0.53	0.00-0.65	0.00-0.54
	n	39	39	39	36	39	39	39	36	39	39	39	36
Tibetan grasslands	Mean	0.45*b*	0.49*b*	0.58*b*	0.51*b*	6.84*b*	5.50*b*	4.27*b*	5.15*b*	0.15*a*	0.17*a*	0.21*a*	0.18*a*
	CV	1.18	1.19	1.07	1.10	0.89	0.95	1.11	0.99	1.30	1.27	1.06	1.16
	Range	0.00-1.92	0.00-2.28	0.00-2.61	0.00-2.20	0.41-27.51	0.35-25.43	0.45-26.00	0.45-26.34	0.00-0.66	0.00-0.66	0.00-0.74	0.00-0.65
	n	48	48	48	45	48	48	48	45	48	48	48	45
Vegetation													
Meadow steppe	Mean	0.06*ab*	0.04*ab*	0.16*ab*	0.11*a*	3.21*b*	2.46*b*	2.04*b*	2.43*b*	0.03*a*	0.02*a*	0.09*ab*	0.06*ab*
	CV	0.88	0.47	1.71	1.41	0.54	0.57	0.53	0.53	1.21	0.68	1.49	1.46
	Range	0.02-0.19	0.02-0.07	0.01-0.78	0.01-0.44	0.88-5.29	0.73-4.17	0.59-3.60	0.70-4.15	0.00-0.11	0.00-0.05	0.00-0.37	0.00-0.25
	n	7	7	7	7	7	7	7	7	7	7	7	7
Typical steppe	Mean	0.16*a*	0.21*a*	0.28*a*	0.24*a*	2.42*b*	1.64*ab*	1.25*ab*	1.65*ab*	0.05*a*	0.08*a*	0.12*ab*	0.09*ab*
	CV	2.23	2.36	1.93	2.02	0.64	0.52	0.51	0.55	1.81	1.79	1.46	1.52
	Range	0.01-1.59	0.00-2.12	0.01-2.37	0.01-2.10	0.69-7.54	0.57-4.418	0.48-3.51	0.59-4.55	0.00-0.39	0.00-0.50	0.01-0.63	0.01-0.51
	n	24	24	24	22	24	24	24	22	24	24	24	22
Desert steppe	Mean	0.23*ab*	0.31*abc*	0.44*ab*	0.39*ab*	1.07*a*	0.98*a*	0.80*a*	0.98*a*	0.17*b*	0.20*ab*	0.26*ab*	0.24*bc*
	CV	1.08	1.19	1.11	1.00	0.89	0.82	0.75	0.73	0.81	0.95	0.75	0.79
	Range	0.01-0.76	0.01-0.92	0.02-1.25	0.01-0.94	0.29-3.40	0.30-2.96	0.28-2.07	0.32-2.62	0.02-0.45	0.02-0.53	0.02-0.65	0.02-0.54
	n	10	10	10	9	10	10	10	9	10	10	10	9
Alpine steppe	Mean	0.71*c*	0.76*c*	0.83*b*	0.78*b*	2.42*b*	2.07*ab*	1.80*b*	1.97*ab*	0.29*b*	0.30*b*	0.34*b*	0.32*c*
	CV	0.82	0.90	0.89	0.88	0.72	0.63	0.61	0.65	0.75	0.77	0.68	0.69
	Range	0.00-1.92	0.04-2.28	0.01-2.61	0.02-2.20	0.41-6.24	0.35-4.33	0.45-4.00	0.45-4.19	0.00-0.66	0.01-0.66	0.01-0.74	0.01-0.65
	n	18	18	18	17	18	18	18	17	18	18	18	17
Alpine meadow	Mean	0.27*b*	0.31*bc*	0.39*ab*	0.30*ab*	10.02*c*	7.94*c*	6.03*c*	7.47*c*	0.05*a*	0.08*a*	0.11*a*	0.07*a*
	CV	1.63	1.51	1.27	1.25	0.61	0.71	0.92	0.76	2.01	2.01	1.53	1.66
	Range	0.00-1.698	0.00-1.75	0.00-1.71	0.00-1.68	1.07-27.51	0.82-25.43	0.69-26.00	0.81-26.34	0.00-0.40	0.00-0.63	0.00-0.67	0.00-0.55
	n	28	28	28	26	28	28	28	26	28	28	28	26

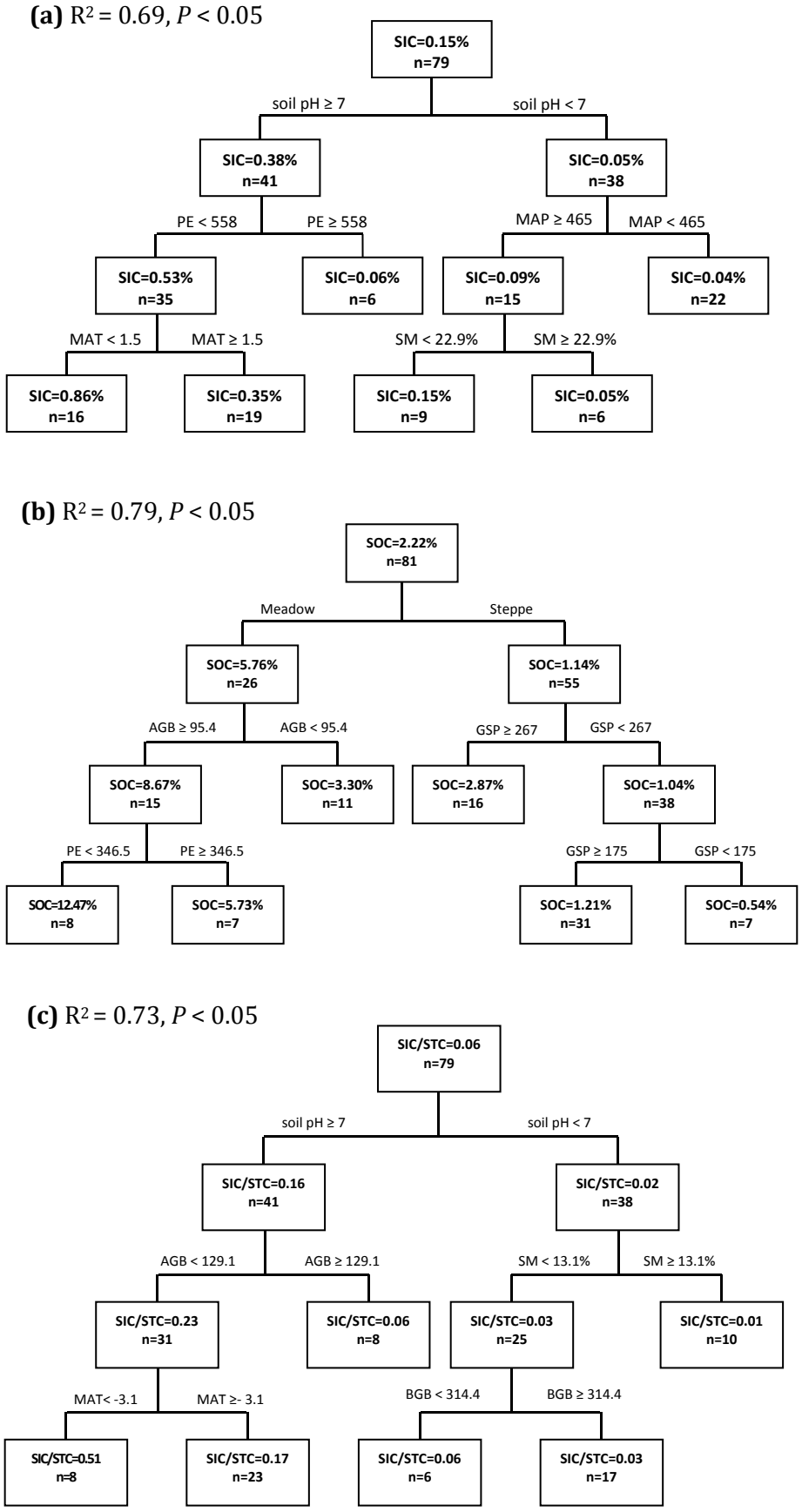

Fig. 3 Classification and regression trees of SIC **(a)**, SOC **(b)**, SIC/ STC **(c)**. Branches are labelled with criteria used to segregate data. Values in terminal nodes represent mean soil SIC **(a)**, SOC **(b)** and SIC/STC **(c)** of sites (0-20 cm) grouped within the cluster.

3.3 Empirical models for estimating the change of SIC

Regression trees showed that soil pH was the most important variable driving the pattern of both SIC and SIC/STC. Therefore, we built linear regression models to predict SIC and SIC/STC from soil pH (Fig. 4a–b).

SIC and SIC/STC were both correlated with soil pH positively ($P < 0.01$). The model for SIC had a slope of 0.58 with an R^2 of 0.29 (Fig. 4a), while the model for SIC/STC had a slope of 0.75 with an R^2 of 0.43 (Fig. 4b). The analysis showed that it was adequate to estimate SIC with the models, considering the sample size and spatial pattern. The results of these empirical models showed that 1-unit decrease in soil pH would lead to 73 % and 82 % decrease in SIC and SIC/STC respectively.

Furthermore, SIC/STC decreases faster than SIC when soil pH goes down, suggesting that SOC may also be affected by soil acidity. Thus, we did linear regression analyses to test the relationship between SOC and soil pH. The result showed a significant negative relationship between SOC and soil pH ($P < 0.05$), with a slope of −0.29 and an R^2 of 0.18 (Fig. 4c).

4 Discussion

4.1 Higher SIC and SOC in the Tibetan grasslands

Our results showed significantly higher concentrations for both SIC and SOC in the Tibetan grasslands than for those in the Inner Mongolian grasslands, at site level as well as for in each depth increment.

Across all the sites, SOC concentration is approximately 9 times as high as SIC concentration. The SIC content in our study, calculated with bulk density, had a mean value of 3.9 kg m^{-3} in 0–10 cm depth, which is lower than the average SIC content of 6 kg m^{-3} in the same depth increment in Chinese grasslands reported by Mi et al. (2008). Most likely, this is the case because the western Tibetan grasslands, which generally have higher SIC contents, were not included in our studies. Yang et al. (2010a) reported an average inorganic carbon density of 5.7 kg m^{-2} in the top 30 cm soil of the Tibetan grasslands, equal to 19.0 kg m^{-3} in 0–30 cm soil depth. Even considering different focused soil depth, their result is still much higher than the results of Mi et al. (2008) and the current study. The average organic carbon concentration in 0–20 cm soil depth in our study is 38.4 g kg^{-1}, close to the average value of 38.5 g kg^{-1} in Chinese grasslands reported by Xie et al. (2007).

Differences in soil formation and climatic conditions between Inner Mongolian grasslands and the Tibetan grassland may contribute to the above-described patterns. The fact that there was no significant difference between soil pH in Inner Mongolian and Tibetan grasslands suggests that higher SIC in the Tibetan grasslands may be due to basically two other reasons. Firstly,

compared with soils of the Inner Mongolian grasslands, soils of the Tibetan grasslands developed later thus parent material had stronger effects on soil characteristics, and carbonate migration is also lower (Xiong and Li, 1987). This would lead to higher LIC in the soil in the Tibetan grasslands. Secondly, due to higher elevation, CO_2 partial pressure is lower in the Tibetan grasslands (Körner, 2003). Lower temperature also induces lower soil respiration thus lower CO_2 partial pressure in the Tibetan grasslands soil (Kato et al., 2006). This influences the formation of pedogenic carbonate as presented in the following chemical equation:

(1) $Ca^{2+} + 2HCO_3^- \leftrightarrow CaCO_3 + H_2O + CO_2$

Consequently, lower CO_2 partial pressure will move the equilibrium towards more precipitation of carbonate (Nordt et al., 2000), benefitting the formation of PIC. Although this chemical reaction is well known, no studies considered CO_2 partial pressure as an important factor in determining the large-scale pattern of SIC. For the first time, our results showed that CO_2 partial pressure may play a key role in shaping topsoil carbonates in extreme high altitudinal environments.

The pattern of SOC could be attributed to climatic differences between these two regions. Low temperature leads to slower decomposition rates (Wu et al., 2003; Xie et al., 2007; Kirschbaum, 1995), and high precipitation causes high vegetation productivity (Jobbagy and Jackson, 2000; Wynn et al., 2006; Callesen et al., 2003). In addition, high moisture, and especially temporal water saturation in the Tibetan grasslands due to the frozen ground, also leads to slower decomposition rates (Baumann et al., 2009). All these factors contribute to the accumulation of organic carbon in the topsoil of the Tibetan grasslands.

Table 4 Variables included and selected in the regression tree analysis. Alt = altitude; MAT = mean annual temperature; GST = growing season temperature; MAP = mean annual precipitation; GSP = growing season precipitation; PE = potential evapotranspiration; AE = actual evapotranspiration; AP/PE = the ratio of MAP to PE; VT = vegetation type; AGB = aboveground biomass; BGB = belowground biomass; SBD = soil bulk density; SM = soil moisture.

				Variables used to build the tree models			Variables selected finally		
Variable	***n***	**Mean**	**SD**	**SIC**	**SOC**	**SIC/STC**	**SIC**	**SOC**	**SIC/STC**
Alt	80	2692	1692.4	Yes		Yes			
MAT	79	-1.1	2.42	Yes	Yes	Yes	Yes		Yes
GST	75	8.8	4.63	Yes	Yes	Yes			
MAP	79	384.0	113.66	Yes	Yes	Yes	Yes		
GSP	75	270.5	63.01	Yes	Yes	Yes		Yes	
PE	75	432.0	92.30	Yes	Yes	Yes	Yes	Yes	
AE	75	321.7	59.81	Yes	Yes	Yes			
AP/PE	74	1.0	0.43	Yes		Yes			
VT	81	-	-	Yes	Yes	Yes		Yes	
AGB	77	96.4	59.41	Yes	Yes	Yes		Yes	Yes
BGB	73	113.3	1515.15	Yes	Yes	Yes			
pH	81	6.88	0.563	Yes		Yes	Yes		Yes
SBD	81	1.11	0.315	Yes					
SM	76	15.2	15.27	Yes		Yes	Yes		Yes

4.2 Different controls on the large scale patterns of SIC and SOC

According to the tree models, carbonates and organic carbon in the topsoil were affected by different factors. The pattern of SIC could be well explained by climate, soil physical and chemical properties (including soil pH, PE, MAT, MAP and SM), while for SOC biotic and climatic factors were predominant (including vegetation type, AGB, PE and GSP).

In our research, soil pH is the most important factor for explaining the variation of SIC. Importantly, this strong relationship can be related to a decrease in HCO_3^- due to low pH as shown by the following equation:

(2) $CaCO_3 + 2H^+ \leftrightarrow Ca^{2+} + H^+ + HCO_3^- \leftrightarrow Ca^{2+} + CO_2 + H_2O$

Acidification induces the equilibrium towards the right, thus decreasing the formation of SIC (Lal and Kimble, 2000; Suarez, 2000). In our study, 42 % of the variation in SIC could be attributed to the differences of soil pH among the 81 sites. Within different pH ranges (pH < 7.0 or pH > 7.0), distinct environmental factors drive the finer pattern of SIC, indicating that SIC is influenced by different processes depending on soil pH. As pH increases above the threshold, thermal factors have stronger effects than other factors, showing negative relationships with SIC. This is consistent with results reported in other studies (Mi et al., 2008; Yang et al., 2010a). Temperature affects $CaCO_3$ equilibria through its effects on $CaCO_3$ solubility, evapotranspiration and leaching (Lal and Kimble, 2000), but it is not appropriate to attribute variation in SIC to temperature in our research. Temperature affects biological activity especially soil respiration positively (Davidson and Janssens, 2006; Raich and Schlesinger, 1992), which increases soil CO_2 partial pressure. Moreover, in our study region, temperature decreases with increasing elevation. Consequently, higher temperature means lower altitude and thus in turn higher CO_2 partial pressure. High CO_2 partial pressure inhibits the formation of carbonates in the topsoil (Eq. 1), leading to negative relationships between SIC and thermal factors. In the areas with pH < 7.0, SIC tends to be in a form of dissolved bicarbonate and the leaching process becomes more important, consequently water condition factors like MAP and SM entered the model. However, the result of our research showing that lower MAP is corresponding to lower SIC is in contrast to some other studies, in which SIC shows a decreasing trend along precipitation gradients (Mi et al., 2008; Nordt et al., 2000; Wang et al., 2010; Yang et al., 2010a). Further analysis suggested that most of those sites with MAP < 465mm were distributed in the Inner Mongolia, while those sites with MAP > 465 were all located on the Tibetan Plateau. Thus the positive SIC-precipitation relationship in this study may be caused by other confounding factors that were different between the two regions.

For SOC, steppe soils present much lower organic carbon contents than meadow soils. As the main resource of SOC, vegetation determines quantity, quality and distribution of SOC (Jobbagy

and Jackson, 2000; Poeplau et al., 2011; Quideau et al., 2001). In Chinese grasslands, meadow has higher productivity than steppe (Ma et al., 2010; Ni, 2004), which means more organic materials input into meadow soils compared to steppe sites. Moreover, alpine meadows occur under cold and humid environments. Consequently, decomposition of SOC is limited by temperature and temporal water saturation (Davidson and Janssens, 2006; Jobbagy and Jackson, 2000; Baumann et al., 2009).

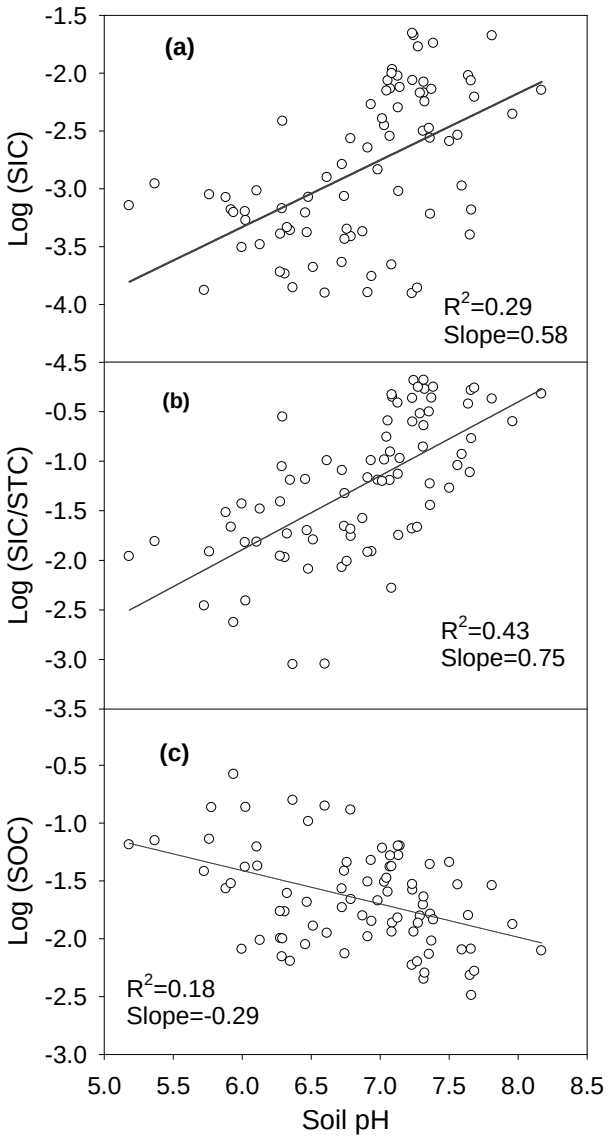

Fig. 4 Linear relationships of SIC **(a)**, SIC/STC **(b)** and SOC **(c)** with soil pH value in the topsoil. All regression lines were significant ($P < 0.05$).

These two interrelated processes (i.e. high input and low decomposition) both contribute to higher SOC in the meadow ecosystem. Within different vegetation types, finer patterns of SOC are driven by different processes. In meadows, AGB shows a strong effect on SOC. Because AGB reflects vegetation productivity (LeBauer and Treseder, 2008; Ni, 2004), the latter influences SOC content of the meadow sites by controlling the input of organic materials. When AGB in-

creases above the threshold, PE has a negative relationship with SOC. Although high temperature may stimulate plant production as temperature is an important limiting factor for vegetation growth in the alpine meadow (Piao et al., 2006), temperature-induced higher SOC decomposition overrides the resulting increase in C inputs, thus leading to a decrease of SOC. On the other hand, in steppe ecosystems, water conditions are the primary constraint to vegetation productivity (Heisler-White et al., 2008; Jobbagy et al., 2002; Sala et al., 1988). High GSP could stimulate plant production and increase soil C accumulation, thus precipitation is the most important variable in controlling SOC patterns in steppe ecosystems.

4.3 Decrease in SIC but increase in STC under soil acidification

Our study provides insights in estimating future change of SIC under the scope of soil acidification scenarios. During the past several decades, parts of Europe and Eastern North America suffered from significant acidification due to acid deposition (Bowman et al., 2008; Galloway et al., 2003). For example, in Europe soil pH decreased between 0.2 to 2 units over the past 17 to 110 yr (Stevens et al., 2009). China also has to face severe soil acidification problems due to increasing energy demand and excessive application of chemical fertilizer (Hicks et al., 2008; Larssen and Carmichael, 2000; Guo et al., 2010). Considering the important role of soil pH in controlling the pattern of SIC, soil acidification will have a great impact on topsoil's inorganic carbon stocks in the future.

Up to date, no studies have investigated the trend or extent of soil acidification in Chinese grasslands. However, soil pH records in croplands close to our study region provide circumstantial evidences to approximate the extent of soil acidification. From the 1980s to the 2000s, soil pH in croplands on the Loess Plateau and the Tibetan Plateau declined by 0.27 and 0.48 units respectively (Zhou et al., 2009; Guo et al., 2010). Assuming the acidification rate in croplands is the same as that in grasslands and remains the same in the next 20 yr, according to our linear regression models, acidification will lead to 30 % and 53 % decrease in SIC in the Inner Mongolian and Tibetan grasslands respectively.

Although acidification leads to a decrease in SIC, carbon stock in the topsoil will not necessarily decline with soil acidification. It can be assumed, that due to accumulation of SOC, STC is likely to rise with increasing acidity, backed up by the negative relationship between soil pH and SOC as well as the even faster decline of SIC/STC compared to SIC with decreasing soil pH. There are two ways this pattern can be explained. Firstly, acidification inhibits soil microbial activities and thus the SOC decomposition rate (Francis, 1986). Secondly, N deposition, a major cause of acidification, will lead to an increase of SOC inputs through increasing vegetation productivity (Neff et al., 2002), and may induce a decrease in microbial biomass and oxidase activity (Dalmonech et

al., 2010; Fisk and Fahey, 2001; Zak et al., 2008). Both of these will contribute to accumulation of SOC, thus leading to an increase in STC. Moreover, SIC only accounts for a very small proportion of STC on average. Therefore, soil acidification would not make a great impact on soil carbon.

4.4 Uncertainty of prediction

In the present study, the linear regression models with soil pH as independent variable were used to predict the future change of soil C under soil acidification scenario. Soil pH is the most important variable driving the large-scale pattern of SIC and SIC/STC. SOC also has a significant relationship with soil pH. These two facts suggest that our prediction could be helpful in understanding soil C change with acidification. However, some uncertainties remain in the prediction. The linear regression models were based on spatial relationships between soil pH and carbon content. Therefore, there may be some bias for predicting temporal soil carbon change using the models. Additionally, we used the acidification data in cropland near our study region since no other data is available to investigate the trend or extent of soil acidification in Chinese grasslands. This may also bring prediction errors.

Another limitation in our models could stem from ignoring the influences of grazing. The direct and indirect impact of grazing on soil parameters, such as bulk density, soil moisture and carbon contents have been described and discussed in various studies (Stavi et al., 2008; Wu et al., 2010; Hafner et al., 2012). At low grazing intensities, concentrated movements of livestock in areas with changing micro-topography on a small spatial scale mostly affect soil properties, often in a very complex way (Trimble and Mendel, 1995; Stavi et al., 2012). Since cattle tracks and pathways are obvious in field, we avoided taking samples from such places to minimize the grazing and other livestock-induced disturbances. Although sampling sites were selected against this background, nomadic pastoralism is ubiquitous in the Inner Mongolian and Tibetan grasslands, and can hardly be completely excluded. However, small-scale grazing variability in our study region may be not as pronounced as in other pasture grassland regions of the world for most of the investigated sites, as especially *Kobresia* dominated ecosystems have developed very stable felty topsoil horizons (Kaiser, 2004) that have formed during more than 6000 yr of nomadism (Schlütz and Lehmkuhl, 2009). What extent is grazing impacting on soil carbon in our study region is still difficult to quantify.

Further studies are needed to validate the robustness of the relationships between soil carbon and soil pH at different spatial and temporal scales. In particular, long-term multifactor experiments along environmental gradients might be useful to test these relationships. Moreover, the extents and trends of soil acidification in Chinese grasslands should also be investigated to give a more accurate prediction of soil carbon change in the future.

5 Conclusions

Through analyzing the topsoil data of 81 sites at three different depth increments obtained from a regional survey across grasslands in Inner Mongolia and the Tibetan Plateau during 2006–2007, we found that both SIC and SOC in the Tibetan grasslands were significantly higher than those in the Inner Mongolian grasslands. Higher SIC in the Tibetan grasslands may be due to higher LIC derived from parent material and more PIC formation caused by lower CO_2 partial pressure, whereas higher SOC in the Tibetan grasslands is caused by higher litter input and lower decomposition rates. At a large-scale, SIC and SOC were controlled by different environmental factors. SIC was mainly driven by chemical and physical processes, particularly by soil pH and other processes depending on soil pH. However, SOC was controlled by biotic processes such as vegetation type. Our results imply that given the acidification rate in Chinese grassland soils in the future, as has been the case in Chinese cropland soils during the past two decades, SIC will decrease by 30 % and 53 % in the Inner Mongolian grasslands and the Tibetan grasslands, respectively, in the next 20 yr. However, the negative relationship between soil pH and SOC suggests that acidification will inhibit decomposition of SOC, and thus will not lead to a significant general loss of carbon from soils in these regions.

6 Acknowledgements

The authors are grateful to Wenhong Ma, Kuo Yang for assistance with field sample collections, and Biao Zhu for helpful and constructive comments on the previous version of this manuscript. This study was supported by the Program of “One Hundred Talented People” of the Chinese Academy of Sciences (Grant No. KSCX2-YW-Z-0806), the National Natural Science Foundation of China (Grant No. 31025005 and 31021001), National Program on Key Basic Research Project (Grant No. 2010CB950602), and the “Strategic Priority Research Program” of the Chinese Academy of Sciences (Grant No. XDA05050304).

7 References

Batjes, N.: Total carbon and nitrogen in the soils of the world, Eur. J. Soil Sci., 47, 151–163, 1996.

Baumann, F., He, J. -S., Schmidt, K., Kühn, P., and Scholten, T.: Pedogenesis, permafrost, and soil moisture as controlling factors for soil nitrogen and carbon contents across the Tibetan Plateau, Global Change Biol., 15, 3001–3017, 2009.

Bowman, W. D., Cleveland, C. C., Halada, L., Hresko, J., and Baron, J. S.: Negative impact of nitrogen deposition on soil buffering capacity, Nat. Geosci., 1, 767–770, 2008.

Callesen, I., Liski, J., Raulund-Rasmussen, K., Olsson, M. T., Tau-Strand, L., Vesterdal, L., and

Westman, C. J.: Soil carbon stores in Nordic well-drained forest soils-relationships with climate and texture class, Global Change Biol., 9, 358–370, 2003.

Chatterjee, A., Lal, R., Wielopolski, L., Martin, M. Z., and Ebinger, M. H.: Evaluation of different soil carbon determination methods, Crit. Rev. Plant Sci., 28, 164–178, 2009.

Chinese Academy of Sciences: Vegetation Atlas of China, Science Press, Beijing, 2001.

Dalmonech, D., Lagomarsino, A., Moscatelli, M. C., Chiti, T., and Valentini, R.: Microbial performance under increasing nitrogen availability in a Mediterranean forest soil, Soil Biol. Biochem., 42, 1596–1606, 2010.

Davidson, E. A. and Janssens, I. A.: Temperature sensitivity of soil carbon decomposition and feedbacks to climate change, Nature, 440, 165–173, 2006.

Eswaran, H., Van den Berg, E., Reich, P., and Kimble, J.: Global soil carbon resources, in: Soils and Global Change, edited by: Lal, R., Kimble, J. M., Levine, E., and Stewart, B. A., CRC/Lewis Publishers, Boca Raton, 27–43, 1995.

Eswaran, H., Reich, P. F., Kimble, J. M., Beinroth, F. H., Padmanabhan, E., and Moncharoen, P.: Global carbon stocks, in: Global Climate Change and Pedogenic Carbonates, edited by: Lal, R., Kimble, J. M., Eswaran, H., and Stewart, B. A., CRC Press, Boca Raton, Florida, 15–25, 2000.

Fang, J. Y., Piao, S. L., Tang, Z. Y., Peng, C. H., and Wei, J.: Interannual variability in net primary production and precipitation, Science, 293, 1723, doi:10.1126/science.293.5536.1723a, 2001.

FAO: Guidelines for soil description, 4th Edn., FAO, Rome, 2006.

Feng, Q., Endo, K. N., and Cheng, G. D.: Soil carbon in desertified land in relation to site characteristics, Geoderma, 106, 21–43, 2002.

Fisk, M. C. and Fahey, T. J.: Microbial biomass and nitrogen cycling responses to fertilization and litter removal in young northern hardwood forests, Biogeochemistry, 53, 201–223, 2001.

Francis, A. J.: The ecological effects of acid deposition II: acid-rain effects on soil and aquatic microbial processes, Cell. Mol. Life Sci., 42, 455–465, 1986.

Franzluebbers, A. J. and Stuedemann, J. A.: Surface soil changes during twelve years of pasture management in the Southern Piedmont USA, Soil Sci. Soc. Am. J., 74, 2131–2141, 2010.

Galloway, J. N., Aber, J. D., Erisman, J. W., Seitzinger, S. P., Howarth, R. W., Cowling, E. B., and Cosby, B. J.: The nitrogen cascade, BioScience, 53, 341–356, 2003.

Guo, J. H., Liu, X. J., Zhang, Y., Shen, J. L., Han, W. X., Zhang, W. F., Christie, P., Goulding, K. W. T., Vitousek, P. M., and Zhang, F. S.: Significant acidification in major Chinese croplands, Science,

327, 1008–1010, 2010.

Hafner, S., Unteregelsbacher, S., Seeber, E., Lena, B., Xu, X., Li, X., Guggenberger, G., Miehe, G., and Kuzyakov, Y.: Effect of grazing on carbon stocks and assimilate partitioning in a Ti-betan montane pasture revealed by $^{13}CO_2$ pulse labeling, Global Change Biol., 18, 528–538, 2012.

He, J.-S., Wang, X., Flynn, D. F. B., Wang, L., Schmid, B., and Fang, J.: Taxonomic, phylogenetic, and environmental trade-offs between leaf productivity and persistence, Ecology, 90, 2779–2791, 2009.

Heisler-White, J. L., Knapp, A. K., and Kelly, E. F.: Increasing precipitation event size increases aboveground net primary productivity in a semi-arid grassland, Oecologia, 158, 129–140, 2008.

Hicks, W. K., Kuylenstierna, J. C. I., Owen, A., Dentener, F., Seip, H. M., and Rodhe, H.: Soil sensitivity to acidification in Asia: status and prospects, Ambio: A Journal of the Human Environment, 37, 295–303, 2008.

IUSS Working Group WRB: World reference base for soil resources 2006, FAO Rome, World Soil Resourses Reports. No. 103, 2006.

Jobbagy, E. G. and Jackson, R. B.: The vertical distribution of soil organic carbon and its relation to climate and vegetation, Ecol. Appl., 10, 423–436, 2000.

Jobbagy, E. G., Sala, O. E., and Paruelo, J. M.: Patterns and controls of primary production in the Patagonian steppe: a remote sensing approach, Ecology, 83, 307–319, 2002.

Kaiser, K.: Pedogeomorphological transect studies in Tibet: implications for landscape history and present-day dynamics, Prace Geograficzne, 200, 147–165, 2004.

Kang, L., Han, X. G., Zhang, Z. B., and Sun, O. J.: Grassland ecosystems in China: review of current knowledge and research advancement, Philos. T. R. Soc. B, 362, 997–1008, 2007.

Kato, T., Tang, Y., Gu, S., Hirota, M., Du, M., Li, Y., and Zhao, X.: Temperature and biomass influences on interannual changes in CO_2 exchange in an alpine meadow on the Qinghai-Tibetan Plateau, Global Change Biol., 12, 1285–1298, 2006.

Kirschbaum, M. U. F.: The temperature dependence of soil organic matter decomposition, and the effect of global warming on soil organic C storage, Soil Biol. Biochem., 27, 753–760, 1995.

Körner, C.: Alpine Plant Life: Functional Plant Ecology of High Mountain Ecosystems, Springer Berlin, Heidelberg, 2003.

Lal, R.: Soil carbon sequestration impacts on global climate change and food security, Science, 304, 1623–1627, 2004a.

Lal, R.: Agricultural activities and the global carbon cycle, Nutr. Cycl. Agroecosys, 70, 103–116, 2004b.

Lal, R.: Carbon sequestration, Philos. T. R. Soc. B, 363, 815–830, 2008.

Lal, R. and Kimble, J. M.: Pedogenic carbonates and the global carbon cycle, in: Global Climate Change and Pedogenic Carbonates, edited by: Lal, R., Kimble, J. M., Eswaran, H., and Stewart, B. A., CRC Press, Boca Raton, Florida, 1–14, 2000.

Larssen, T. and Carmichael, G. R.: Acid rain and acidification in China: the importance of base cation deposition, Environ. Pollut., 110, 89–102, 2000.

LeBauer, D. S. and Treseder, K. K.: Nitrogen limitation of net primary productivity in terrestrial ecosystems is globally distributed, Ecology, 89, 371–379, 2008.

Li, Z. P., Han, F. X., Su, Y., Zhang, T. L., Sun, B., Monts, D. L., and Plodinec, M. J.: Assessment of soil organic and carbonate carbon storage in China, Geoderma, 138, 119–126, 2007.

Liao, Q. L., Zhang, X. H., Li, Z. P., Pan, G. X., Smith, P., Jin, Y., and Wu, X. M.: Increase in soil organic carbon stock over the last two decades in China's Jiangsu Province, Global Change Biol., 15, 861–875, 2009.

Ma, W. H., He, J. -S., Yang, Y. H., Wang, X. P., Liang, C. Z., An-war, M., Zeng, H., Fang, J. Y., and Schmid, B.: Environmental factors covary with plant diversity-productivity relationships among Chinese grassland sites, Global Ecol. Biogeogr., 19, 233– 243, 2010.

Mi, N., Wang, S. Q., Liu, J. Y., Yu, G. R., Zhang, W. J., and Jobbagy, E.: Soil inorganic carbon storage pattern in China, Global Change Biol., 14, 2380–2387, 2008.

Mikhailova, E. A. and Post, C. J.: Effects of land use on soil inorganic carbon stocks in the Russian Chernozem, J. Environ. Qual., 35, 1384–1388, 2006.

Monger, H. C. and Gallegos, R. A.: Biotic and abiotic processes and rates of pedogenic carbonate accumulation, in: Global Climate Change and Pedogenic Carbonates, edited by: Lal, R., Kimble, J. M., Eswaran, H., and Stewart, B. A., CRC Press, Boca Raton, Florida, 2000.

Neff, J. C., Townsend, A. R., Gleixner, G., Lehman, S. J., Turnbull, J., and Bowman, W. D.: Variable effects of nitrogen additions on the stability and turnover of soil carbon, Nature, 419, 915–917, 2002.

Ni, J.: Carbon storage in grasslands of China, J. Arid. Environ., 50, 205–218, 2002.

Ni, J.: Estimating net primary productivity of grasslands from field biomass measurements in temperate northern China, Plant. Ecol., 174, 217–234, 2004.

Nordt, L. C., Wilding, L. P., and Drees, L. R.: Pedogenic carbonate transformations in leaching soil

system: implication for the global C cycle, in: Global Climate Change and Pedogenic Carbonates, edited by: Lal, R., Kimble, J. M., Eswaran, H., and Stewart, B. A., CRC Press, Boca Raton, Florida, 43–64, 2000.

Ouyang, X. J., Zhou, G. Y., Huang, Z. L., Liu, J. X., Zhang, D. Q., and Li, J.: Effect of simulated acid rain on potential carbon and nitrogen mineralization in forest soils, Pedosphere, 18, 503–514, 2008.

Piao, S. L., Fang, J. Y., and He, J. -S.: Variations in vegetation net primary production in the Qinghai-Xizang Plateau, China, from 1982 to 1999, Climatic Change, 74, 253–267, 2006.

Poeplau, C., Don, A., Vesterdal, L., Leifeld, J., Van Wesemael, B. A. S., Schumacher, J., and Gensior, A.: Temporal dynamics of soil organic carbon after land-use change in the temperate zone: carbon response functions as a model approach, Global Change Biol., 17, 2415–2427, 2011.

Qian, S. S.: Environmental and ecological statistics with R, Chapman & Hall, 2009.

Quideau, S. A., Chadwick, O. A., Benesi, A., Graham, R. C., and Anderson, M. A.: A direct link between forest vegetation type and soil organic matter composition, Geoderma, 104, 41–60, 2001.

R Development Core Team: R: a language and environment for statistical computing, R Foundation for Statistical Computing Vienna, Austria, 2011.

Raich, J. W. and Schlesinger, W. H.: The global carbon dioxide flux in soil respiration and its relationship to vegetation and climate, Tellus B, 44, 81–99, 1992.

Rockström, J., Steffen, W., Noone, K., Persson, A., Chapin, F. S., Lambin, E. F., Lenton, T. M., Scheffer, M., Folke, C., Schellnhuber, H. J., Nykvist, B., de Wit, C. A., Hughes, T., van der Leeuw, S., Rodhe, H., Sorlin, S., Snyder, P. K., Costanza, R., Svedin, U., Falkenmark, M., Karlberg, L., Corell, R. W., Fabry, V. J., Hansen, J., Walker, B., Liverman, D., Richardson, K., Crutzen, P., and Foley, J. A.: A safe operating space for humanity, Nature, 461, 472–475, 2009.

Sala, O. E., Parton, W. J., Joyce, L. A., and Lauenroth, W. K.: Primary production of the central grassland region of the United States, Ecology, 69, 40–45, 1988.

Schlesinger, W. H. and Andrews, J. A.: Soil respiration and the global carbon cycle, Biogeochemistry, 48, 7–20, 2000.

Schlütz, F., and Lehmkuhl, F.: Holocene climatic change and the nomadic Anthropocene in Eastern Tibet: palynological and geomorphological results from the Nianbaoyeze Mountains, Quaternary Sci. Rev., 28, 1449–1471, 2009.

Schulze, E. D. and Freibauer, A.: Carbon unlocked from soils, Nature, 437, 205–206, 2005.

Scurlock, J. M. O. and Hall, D. O.: The global carbon sink: a grassland perspective, Global Change

Biol., 4, 229–233, 1998.

Song, G. H., Li, L. Q., Pan, G. X., and Zhang, Q.: Topsoil organic carbon storage of China and its loss by cultivation, Biogeochemistry, 74, 47–62, 2005.

Stavi, I., Ungar, E. D., Lavee, H., and Sarah, P.: Grazing-induced spatial variability of soil bulk density and content of moisture, organic carbon and calcium carbonate in a semi-arid rangeland, Catena, 75, 288–296, 2008.

Stavi, I., Lavee, H., Ungar, E., and Sarah, P.: Grazing-induced modification of a semi-arid rangeland from a two-phase to a three-phase mosaic geo-ecosystem, Arid Land Research and Management, 26, 79–83, 2012.

Stevens, C. J., Dise, N. B., and Gowing, D. J.: Regional trends in soil acidification and exchangeable metal concentrations in relation to acid deposition rates, Environ. Pollut., 157, 313–319, 2009.

Suarez, D. L.: Impact of agriculture on CO_2 as affected by changes in inorganic carbon, in: Global Climate Change and Pedogenic Carbonates, edited by: Lal, R., Kimble, J. M., Eswaran, H., and Stewart, B. A., CRC Press, Boca Raton, Florida, 257–272, 2000.

Thornthwaite, C. W.: An approach toward a rational classification of climate, Geogr. Rev., 38, 55–94, 1948.

Treseder, K. K.: Nitrogen additions and microbial biomass: a meta-analysis of ecosystem studies, Ecol. Lett., 11, 1111–1120, 2008.

Trimble, S. W. and Mendel, A. C.: The cow as a geomorphic agent-a critical review, Geomorphology, 13, 233–253, 1995.

Trumbore, S. E. and Czimczik, C. I.: An uncertain future for soil carbon, Science, 321, 1455–1456, 2008.

Valentini, R., Matteucci, G., Dolman, A. J., Schulze, E. D., Rebmann, C., Moors, E. J., Granier, A., Gross, P., Jensen, N. O., Pilegaard, K., Lindroth, A., Grelle, A., Bernhofer, C., Grunwald, T., Aubinet, M., Ceulemans, R., Kowalski, A. S., Vesala, T., Rannik, U., Berbigier, P., Loustau, D., Guomundsson, J., Thorgeirsson, H., Ibrom, A., Morgenstern, K., Clement, R., Moncrieff, J., Montagnani, L., Minerbi, S., and Jarvis, P. G.: Respiration as the main determinant of carbon balance in European forests, Nature, 404, 861–865, 2000.

Vitousek, P. M.: Beyond global warming: ecology and global change, Ecology, 75, 1861–1876, 1994.

Wang, W. and Fang, J.: Soil respiration and human effects on global grasslands, Global Planet. Change, 67, 20–28, 2009.

Wang, Y. G., Li, Y., Ye, X. H., Chu, Y., and Wang, X. P.: Profile storage of organic/inorganic carbon in soil: from forest to desert, Sci. Total Environ., 408, 1925–1931, 2010.

Wu, H. B., Guo, Z. T., and Peng, C. H.: Distribution and storage of soil organic carbon in China, Global Biogeochem. Cy., 17, 1048, doi:10.1029/2001GB001844, 2003.

Wu, H. B., Guo, Z. T., Gao, Q., and Peng, C. H.: Distribution of soil inorganic carbon storage and its changes due to agricultural land use activity in China, Agr. Ecosyst. Environ., 129, 413–421, 2009.

Wu, G.-L., Liu, Z.-H., Zhang, L., Chen, J.-M., and Hu, T.-M.: Long-term fencing improved soil properties and soil organic carbon storage in an alpine swamp meadow of western China, Plant. Soil, 332, 331–337, 2010.

Wynn, J. G., Bird, M. I., Vellen, L., Grand-Clement, E., Carter, J., and Berry, S. L.: Continental-scale measurement of the soil organic carbon pool with climatic, edaphic, and biotic controls, Global Biogeochem. Cy., 20, GB1007, doi:10.1029/2005GB002576, 2006.

Xie, Z. B., Zhu, J. G., Liu, G., Cadisch, G., Hasegawa, T., Chen, C. M., Sun, H. F., Tang, H. Y., and Zeng, Q.: Soil organic carbon stocks in China and changes from 1980s to 2000s, Global Change Biol., 13, 1989–2007, 2007.

Xiong, Y. and Li, Q. D.: Soils of China, Science Press, Beijing, 1987 (in Chinese).

Yang, Y. H., Fang, J. Y., Tang, Y. H., Ji, C. J., Zheng, C. Y., He, J.-S., and Zhu, B. A.: Storage, patterns and controls of soil organic carbon in the Tibetan grasslands, Global Change Biol., 14, 1592–1599, 2008.

Yang, Y. H., Fang, J. Y., Ji, C. J., Ma, W. H., Su, S. S., and Tang, Z. Y.: Soil inorganic carbon stock in the Tibetan alpine grasslands, Global Biogeochem. Cy., 24, GB4022, doi:10.1029/2010GB003804, 2010a.

Yang, Y. H., Fang, J. Y., Ma, W. H., Smith, P., Mohammat, A., Wang, S. P., and Wang, W.: Soil carbon stock and its changes in northern China's grasslands from 1980s to 2000s, Global Change Biol., 16, 3036–3047, 2010b.

Yu, D. S., Shi, X. Z., Wang, H., Sun, W. X., Chen, J. M., Liu, Q. H., and Zhao, Y. C.: Regional patterns of soil organic carbon stocks in China, J. Environ. Manage., 85, 680–689, 2007.

Zak, D. R., Holmes, W. E., Burton, A. J., Pregitzer, K. S., and Talhelm, A. F.: Simulated atmospheric NO^{-}_{3} deposition increases soil organic matter by slowing decomposition, Ecol. Appl., 18, 2016–2027, 2008.

Zhou, Z., Du, S., and Liu, G.: Acidification of surface soil in croplands in the semiarid middle Tibet Plateau, China, 2009 International Conference on Environmental Science and Information Application Technology, 2009, 209–212, 2009.

Manuscript 6

Pedogenesis, permafrost, substrate and topography: Plot and landscape scale interrelations of weathering processes on the central-eastern Tibetan Plateau

Geoderma, submitted in September 2013

Frank Baumann[1], Karsten Schmidt[1], Corina Dörfer[1], Jin-Sheng He[2], Thomas Scholten[1], Peter Kühn[1]

[1]Department of Geosciences, Chair of Physical Geography and Soil Science, University of Tuebingen, Ruemelinstrasse 19-23, 72070 Tuebingen, Germany

[2]Department of Ecology, College of Urban and Environmental Sciences, Peking University, 100871 Beijing, China

Abstract

Weathering indices (WI) and pedogenic oxides ratios (POR) were used to describe patterns of weathering intensities and pedogenesis along climatic gradients, mainly affected by varying influences of the Asian and Indian Monsoon. These climate settings induce particular soil moisture (SM) conditions, in turn closely related to permafrost state, substrate, and topography. Nine sites with in total 30 soil profiles were examined along an eastern and a western transect across the central-eastern Qinghai-Tibet Plateau. Additionally, differences between four soil groups were analysed. According to our knowledge, the presented study is the first attempt of a comprehensive application of different WI and POR to substrates of currently permafrost-affected soils. It provides an evaluation of various tools in terms of chemically describing and differentiating the related processes to distinct environmental settings in low-weathering regions. We found that weathering trends along the climatic gradients could be clearly outlined by WI, whereas POR rather account for small scale variations, describing significant differences of pedogenesis between continuous and discontinuous permafrost conditions. Pyrophosphate soluble iron (Fep) proved to be useful for differentiating permafrost and ground water influenced soils, showing a strong correlation to total organic carbon (r=0.89). The chemical index of alteration (CIA) is the most suitable WI, whereas Ca-free CPA is more easily biased by salinity variations of topsoils at sites with negative water balance, thus pretending lower weathering intensities. Regression analyses for WI and POR with main independent variables underline the specific characteristics: climatic parameters best explain WI, while SM is dominant for POR. The ratio (Fed-Feo)/Fet proved as the most appropriate POR with 64% explained variation by a multiple linear regression model, implying significantly lower iron release with higher SM and pH values. Variation of

Fep can be explained by 63% with soil acidity being most important, followed by SM. Importantly, the presented research provides tools for investigating past and future stability or respective degradation processes of permafrost ecosystems on the Tibetan Plateau and may be applicable to other permafrost-affected environments.

1 Introduction

Pedogenesis and the state of soil development is considered to be an important predictor for soil organic carbon (TOC) and nitrogen contents of permafrost-affected soils on the Tibetan Plateau (Baumann et al., 2009). Soil development is closely associated with specific weathering intensities under distinct environmental conditions (Brady and Weil, 2008; Jenny, 1994). Hence, the presented research provides an approach to evaluate and differentiate pedogenesis by soil chemical properties in relation to their main influencing factors.

Chemical weathering processes release iron and other elements contained in primary minerals of bedrocks and sediments. Depending on various soil characteristics, such as soil moisture (SM), soil temperature (ST), soil acidity, and redox conditions, distinct pedogenic oxides (PO) are formed under a particular timeframe (Kämpf et al., 2011). By extracting fractions of PO with specific degrees of crystallisation, it is possible to determine intensity, duration, quality, and direction of pedogenic processes (McKeague, 1967; Mehra and Jackson, 1960; Schlichting and Blume, 1962; Schwertmann, 1964). Several pedogenic oxides ratios (POR) have been successfully applied to describe and relatively date geomorphological units (e.g. Aniku and Singer, 1990; Arduino et al., 1984; Mirabella and Carnicelli, 1992; Torrent et al., 1980) as well as soil weathering chronosequences and palaeosols (e.g. Buero and Schwertmann, 1987; Dahms et al., 2012; Diaz, 1989; Mahaney and Fahey, 1980; McFadden and Hendricks, 1985; Rezapour et al., 2010; Sauer et al., 2010; Torrent et al., 2007). However, only few soil surveys systematically investigated PO in periglacial environments and under the scope of current soil formation (Melke, 2007).

Weathering indices (WI) have been primarily developed for sedimentary geology (e.g. Cullers, 2000; McLennan, 1993; Yang et al., 2004). Many studies have adopted these tools for analysing and describing geomorphological units, loess layers and palaeosols (e.g. Bäumler, 2001; Bäumler and Zech, 2000; Buggle et al., 2011; Buggle et al., 2008; Gallet et al., 1998; Kühn et al., 2013; Wagner, 2005). Weathering intensities have been investigated in artic permafrost and glaciated areas (Bäumler, 2001; Melke, 2007; Wagner, 2005), whereas only little research has been done in dry permafrost areas like the Tibetan Plateau. Due to the cold and arid climate, low chemical weathering intensities are expected in periglacial environments (Brady and Weil, 2008; Fedo et al., 1995; McLennan, 1993).

The Tibetan Plateau extends over more than 2.4 million km² on an average altitude of 4000 m a.s.l., representing the largest high-altitude and low-latitude permafrost area on earth. It proved to be particularly sensitive in terms of global warming (Qiu, 2008) and land use changes (Yang et al., 2009). About 54% of the plateau's surface is directly influenced by permafrost (Cheng, 2005). Over the past decades, permafrost degradation processes can be more frequently observed with corresponding changes in soil moisture-temperature regimes (e.g. Cheng and Wu, 2007; Jin et al., 2000; Kang et al., 2010; Yang et al., 2010; Yang et al., 2011; Zhang et al., 2003) and desertification processes (Wang et al., 2011; Xue et al., 2009; Yan et al., 2009). Soil's properties are accordingly altered, reassigning their role in ecosystem functioning (Chapin III et al., 2000; Vitousek, 1997). This leads to instability and erosional features mainly triggered by widespread occurring loose sediments and sparse vegetation, which in turn is a result of lower soil moisture contents as a consequence of permafrost degradation (Baumann et al., 2009). Consequently, decreasing soil organic carbon contents can be observed (Dai et al., 2011).

Distinct climate gradients are evident across the research area (An et al., 2001), exhibiting clearly differing mean annual air temperature (MAT) and mean annual precipitation (MAP) as independent variables for soil weathering. Together with the above-described prerequisites and processes, the altering permafrost-affected ecosystems on the Tibetan Plateau provide an ideal compound to examine the use of POR and WI to describe weathering processes on both landscape scale and plot scale. In accordance to our present knowledge, this is the first study systematically analysing interdependencies of PO and WI in substrates subjected to current soil formation in permafrost environments across climate transects.

The primary objective of this study is to investigate the influence of permafrost on weathering intensity and pedogenesis. We hypothesise that:

(1) SM is a key variable for pedogenesis and weathering processes, mainly determined by permafrost characteristics, substrate, and topography.
(2) SM content is interrelated to distinct precipitation-temperature ratios and thus to specific permafrost distribution, caused by varying influences of monsoon systems between the eastern and western transect as well as along each transect.
(3) Intensity of weathering and pedogenesis can be described by WI, PO fractions and POR. These indicators are in turn all essentially related to independent moisture parameters showing clear differences along climate transects and specifically between continuous and discontinuous permafrost. By consideration of other independent parameters, WI and POR can be evaluated with regard to their validity in comparable environments.

2 Materials and methods

2.1 Environmental settings

Data presented in this paper were gathered during field work on the central-eastern Tibetan Plateau in the years 2006, 2007 and 2009 along an eastern and western transect, which both are north-south oriented (Fig. 1, Tab.1). Sites on the eastern transect (EAST) extend along 98.5°E and range from 34.3 to 35.3°N in the region between the settlements of Huashixia and Yushu, whereas the western transect (WEST) stretches along 92.2°E and ranges from 31.4 to 34.7°N between Wudaoliang and Nagqu.

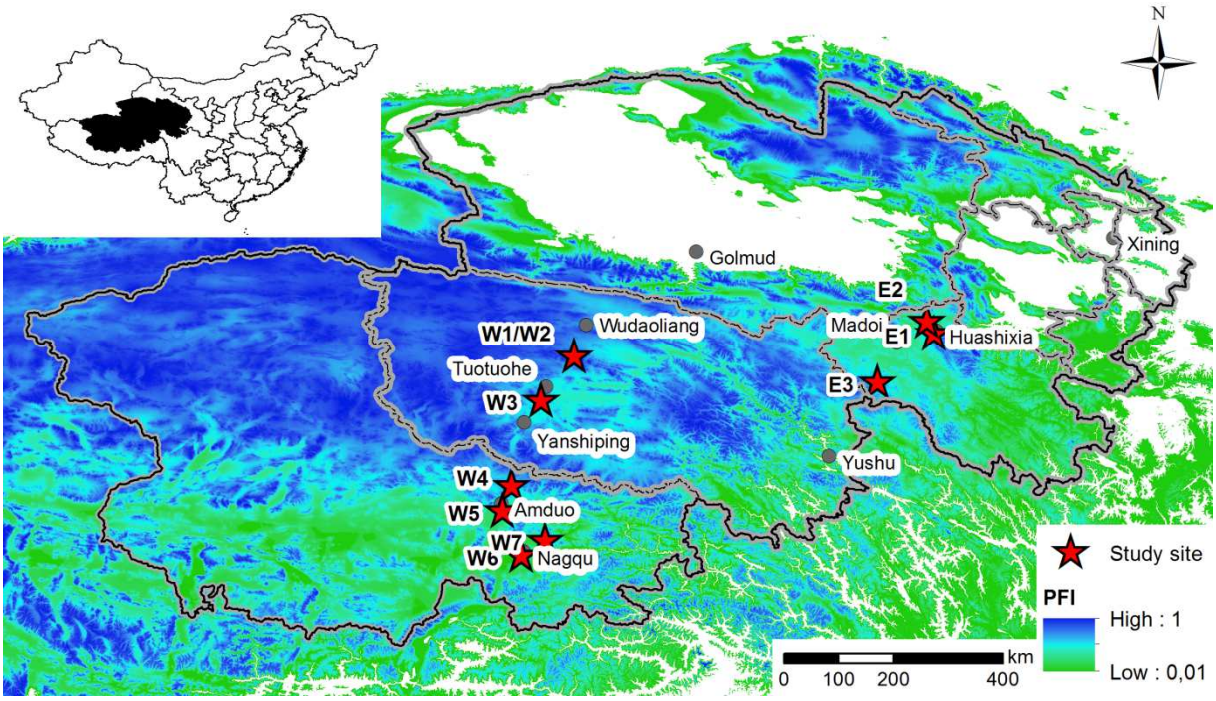

Fig. 1 Study sites split into transect EAST (E1-E3) and WEST (W1-W7).

MAT ranges from -3.5 to -5.7°C on the eastern transect and from -0.2 to -5.6°C on the western transect. Mean annual precipitation (MAP) varies from 458 to 521mm (EAST) and 285 to 510 mm (WEST) with 80% of the rainfall occurring during the summer months. Thus, two major climatic trends are evident in the research area: the subtropical East Asian Monsoon transporting comparably warm and moist air from the eastern lowlands to the eastern Tibetan Plateau during summer months decreasing westwards, and the Tropical Indian Monsoon influencing the Tibetan Plateau from the south (Domrös and Peng, 1988). The east-west oriented mountain ranges are important barriers for these airmasses. During the cold and dry winters, extratropical westerlies occur together with the prevailing Mongolian-Siberian high pressure system. Temperature and precipitation generally decreases from SE to NW, locally strongly influenced by topography and elevation. This explains the differences between sites E1 and E2 of EAST: they are geographically located next to each other but have pronounced climatic differences, which is caused by the Anyêmaqên mountain range located in the east. Site E2 is in lee position,

showing lower rainfall with higher temperatures compared to E1, where an east-west stretching furrow between the Anyêmaqên and Bayan Har Mountains locally leads to higher rainfall and lower temperatures. Site E3 is located southwards close to Bayan Har pass, explaining the lower MAT and higher MAP. Similar situations occur in WEST, with the Tanggula Mountains being the most eminent climatic divide. Evaporation ranges on average for the whole Tibetan Plateau between 1204 and 1327 mm (Wang and French, 1994), reaching 1478 mm in the headwaters of Yangtze River (Hu et al., 2009), 1264 mm in the headwaters of Yellow River around Maduo (Zhang et al., 2010) and 1770 mm in the area around Amduo (Feng and Zhu, 2009). Gao et al. (2006) provide evaporation values ranging from 1500 to 2300 mm for Nagqu County rising from SE to NW. Hence, evaporation largely exceeds precipitation in the whole research area.

Table 1 Main study sites

Location	Transect	Site name	Lat [°]	Lon [°]	Altitude [m asl]	MAT [°C]	MAP [mm]	Soil group	No. Profiles
Huashixia	East	E1	N 35.09937°	E 98.79250°	4310	-4.6	493	IS, GL, PF	6
Donggi Cona	East	E2	N 35.29432°	E 98.69263°	4095	-3.5	458	IS, CM, GL	4
Yushu	East	E3	N 34.28000°	E 97.88323°	4667	-5.7	522	PF	1
Wudaoliang West	West	W1	N 34.71560°	E 92.89029°	4804	-5.6	307	CM, GL,	5
Wudaoliang East	West	W2	N 34.73080°	E 92.89240°	4753	-5.2	285	PF	2
Tuotuohe	West	W3	N 33.98956°	E 92.34691°	4654	-4.2	336	IS	1
Tanggula	West	W4	N 32.58393°	E 91.86025°	5105	-5.8	488	PF	1
Amduo	West	W5	N 32.18068°	E 91.71571°	4903	-4.2	473	CM, PF	2
Nagqu West	West	W6	N 31.44857°	E 92.02182°	4494	-0.3	480	CM, GL	7
Nagqu East	West	W7	N 31.69285°	E 92.41270°	4596	-1.9	511	PF	1

Permafrost characteristics and distribution are closely linked to climatic patterns (Ping et al., 2004; Wang and French, 1994). Active layer thickness averages around 1-2 m, increasing from northwest to southeast and with decreasing altitude (Cheng and Wu, 2007; Wang et al., 2000). EAST is characterised by discontinuous and unstable permafrost conditions with a widespread vertical disconnection in the area around Huashixia. In these cases, soils freeze seasonally to a depth of 2-3 m with the upper limit of permafrost located in 4-7 m depth (Jin et al., 2000). This vertical freezing-gap is non-existent with higher elevation, as can be observed for the Bayan Har Shan site (E3). The western transect extends from continuous ice-poor permafrost in the area around Wudaoliang (W1/W2), to sporadic island permafrost in the region around Nagqu (W6/W7). Permafrost degradation, also caused by former construction activities, lead to the formation of numerous small depressions, where surface water accumulates or thermokarst lakes are formed (Niu et al., 2011). Moreover, desertification is a major consequence of permafrost degradation frequently observable in the research area (Xue et al., 2009).

Glacial aeolian loess-like sediments and sandy silts, being mainly of local origin (Feng et al., 2011), cover most slopes and terraces providing the main source material for pedogenesis (Schlütz and Lehmkuhl, 2009). Soil formation is closely related to permafrost conditions and topography (Baumann et al., 2009). It is subjected to broad ranges of substrates and geomorpho-

logical processes, frequently interrupted by fresh, mainly aeolian sedimentation and cryogenic (solifluction) or erosive processes. This often leads to buried, mainly humic horizons. Only weakly developed and frequently polygenetic formed soils on slopes and terraces (Leptosols, Leptic Cambisols, Haplic Regosols, Mollic Cryosols), as well as Gleysols and Gelic Gleysols occur in depressions next to rivers or lakes (Kaiser, 2004; Kaiser et al., 2007). This instability is enhanced by intense precipitation during the summer months leading to fluvial erosion and alluvial accumulation also by laminar sheet floods along gentle slopes (cf. site E2), whereas aeolian erosion and re-deposition is forced in such areas during winter triggered by the dry winter monsoon and sparse vegetation (Dietze et al., 2012; Xue et al., 2009). Under more stable conditions (cf. site W1/W2), Cambic Cryosols and well-developed Cambisols are evident, mirroring specific permafrost and climate conditions. The most widespread vegetation types are alpine *Kobresia* meadow and alpine steppe. Particularly in alpine meadow ecosystems, felty topsoils with a high root density are common (Kaiser et al., 2008).

2.2 Field methods

The sampling sets can be generally divided into an eastern (EAST) and western (WEST) transect (Fig. 1). Along each transect main sites and support sites were established. Main sites consist of several soil profiles, arranged along soil catenas, while support sites usually comprise only one soil profile (Tab. 1). Thus, both the variation within sites and along transects is represented. Each soil profile was described according to FAO (2006) and IUSS Working Group WRB (2006). Soil sampling was split into three parts: horizon-wise sampling to determine all relevant parameters for description of weathering and pedogenesis using soil pits; schematic sampling by drilling at three depth-increments (0-5, 5-10, and 10-20 cm) for C and N analysis and basic soil parameters as interpolation points between soil pits in catenas; volumetric samples at equal depths for bulk density and gravimetric water content determination. SM was additionally determined directly in the field by TDR-probes (Delta-T Devices Ltd., Cambridge, UK) for all pedogenic horizons as well as for depth increments.

2.3 Laboratory analyses

All soil samples were air-dried and sieved to < 2mm. Grain size analysis was conducted by combined pipette and sieving method (7 fractions, Koehn, DIN 19683-1). Electrical conductivity (EC) was measured in bi-distilled H_2O, whereas pH was determined in 0.01 M $CaCl_2$ potentiometrically. $CaCO_3$ was analysed gas-volumetrically on ground subsamples. Total organic carbon (TOC) was measured with heat combustion (VARIO EL III, Elementar, Hanau, Germany). C bound in $CaCO_3$ was subtracted from the total amount of C (TC) quantified with the CNS analyser to obtain

the proportion of organic C (TOC). Water content was quantified gravimetrically and corrected by the skeleton content (> 2mm).

Total element contents were determined by X-ray fluorescence. The results constitute the basis for the calculation of weathering indices and the determination of Fet. Pedogenic Fe-oxides (Fed) were extracted by dithionite-citrate-bicarbonate (DCB) solution (Mehra and Jackson, 1960); non crystallised and poorly crystallised Fe-oxides, hydroxides and associated gels (Feo) were extracted by acid ammonium oxalate solution (Schwertmann, 1964); and Fe-oxides and metalorganic compounds mainly bound in organic matter (Fep) by 0.1 M pyrophosphate solution (Bascomb, 1968; McKeague, 1967). All extractions were analysed with inductively coupled plasma optical emission spectrometry (ICP-OES), using Optima 5300 DV, PerkinElmer, Waltham, USA.

2.4 Weathering indices

The following weathering indices (WI) were calculated and compared. PI calculates on atomic proportions; all other WI on molar proportions of the total elemental contents.

(1) *Parker index (PI):* $PI = (Na_a/0.35 + Mg_a/0.9 + K_a/0.25 + Ca_a/0.7) \times 100$;
where X_a = % element X/atomic weight of X.

PI calculates the amount of alkali and alkaline earth cations lost and subsequently leached by mineral hydrolysis. The strength of the element-oxygen bond in the primary minerals element contents are considered by weighting the element contents by a corresponding factor (Bäumler, 2001). This factor is resulting from Nicholls' values of bond strength which accounts for the probability of an element to get mobilized (Parker, 1970).

The PI's major drawback is not to consider comparably immobile reference phases, such as Al_2O_3 for measuring relative shifts of composition of relevant mineral components. Moreover, it is assumed that all Ca is contributed by silicate minerals leading to inaccuracies, if larger carbonate contents are evident. The index decreases with weathering intensity and soil development.

(2) *Kronberg & Nesbitt Index (KN)* (Kronberg and Nesbitt, 1981):
Index A = $(SiO_2 + CaO + K_2O + Na_2O) / (Al_2O_2 + SiO_2 + CaO + K_2O + Na_2O)$

Index B = $(CaO + K_2O + Na_2O) / (Al_2O_3 + CaO + K_2O + Na_2O)$

Index A (abscissa) accounts for the relative enrichment of Al and Si oxide phases and inversely measures the leaching of Na, K and Ca. The selective accumulation of Al and Si provides information, if chemical weathering (Al enrichment; index calculates against 0) or physical weathering (Si enrichment; index calculates against 1) is prevailing.

Index B (ordinate) evaluates the degree of feldspar breakdown indicating the alteration of feldspar and formation of clay minerals. Consequently, the index also decreases with increasing weathering intensity. The main disadvantage of this index as well as for the PI is that CaO is not corrected for the carbonate content.

(3) Weathering index for carbonate-rich sediments (Feng, 1997):
FENG = $(Al_2O_3 + Fe_2O_3) / (Na_2O + K_2O + MgO + P_2O_5)$

(Feng) (1997) factored out Ca to avoid the above-described biases of carbonate and included instead Mg and P as critical determinants. This index increases during soil development and weathering processes.

(4) Chemical index of alteration (CIA) (Nesbitt and Young, 1982):
CIA = $[Al_2O_3/(Al_2O_3+Na_2O+CaO^*+K_2O)] \times 100$

(5) Chemical index of weathering (CIW) (Harnois, 1988):
CIW = [Al2O3/(Al2O3+Na2O+CaO*)]*100

(6) Plagioclase index of alteration (PIA) (Fedo et al., 1995):
PIA = $[(Al_2O_3-K_2O)/(Al_2O_3+CaO^*+Na_2O-K_2O)] \times 100$

CIA, CIW and PIA are all based on the similar assumption that feldspar is the most abundant and reactive mineral, whereas phyllosilicates (olivine, pyroxene, amphibole) are proportionally less evident (Nesbitt and Young, 1982). The indices are generally based on the ratio of non-mobile Al to unstable alkali metals and alkaline, thus giving a quantitative measurement of feldspar breakdown. It is important to note, that removal of K from K-feldspar is lower than removal rates of Na and Ca from plagioclase, because plagioclase is more sensitive for weathering than K-feldspar (Nesbitt and Young, 1984; Nesbitt et al., 1996).

However, it is frequently discussed, if K should be used for calculation of WI as it generally shows no consistency during different weathering intensities (e.g. Buggle et al., 2011). This is predominantly caused by the possible absorption of K by clay minerals and the stronger bond by sorptive complexes of soils than for Na or Ca. This may lead to enrichment of K if weathering is weak or vice versa to depletion of K under stronger weathering conditions (Buggle et al., 2011; Harnois, 1988). Accordingly, CIW is the K-free equivalent of CIA, albeit not accounting for the aluminium associated with the K-feldspar. Thus CIW values could be mistakenly high for K-feldspar-rich rocks, whether they are chemically altered or not (Fedo et al., 1995). Respectively, PIA can be used as an index, when only plagioclase weathering needs to be investigated. Importantly, all three indices are calculated with CaO*, considering only the silicate-bound Ca (Fedo et al., 1995).

CIA data can be displayed in A-CN-K diagrams to display weathering and sorting properties of aluminosilicates (for further explanations see Fig. 3; McLennan, 1993; Nesbitt and Young, 1984; Nesbitt et al., 1996). Numeric values increase with weathering intensity; low values indicate low or absence of chemical alteration as it can be observed under cool or arid conditions (Fedo et al., 1995).

(7) Chemical proxy of alteration (CPA) (Buggle et al., 2011; Cullers, 2000):
CPA (CIW') = $[Al_2O_3/(Al_2O_3+Na_2O)] \times 100$

CPA (CIW') tries to avoid all above-discussed biases of carbonate Ca and K-fixation, regarding Na and Al as the most suitable pair of elements to describe weathering intensities (Buggle et al., 2011; Cullers, 2000). Overall, K release is small compared to Na release caused by stronger weathering resistance of K phases such as K-feldspar and clay minerals. This leads to the assumption, that K plays a minor role in the cold climate of the Tibetan Plateau, making this WI a meaningful alternative for our research.

2.5 Pedogenic oxides ratios

Pedogenic oxides are amorphous and crystalline Fe- Mn-, Al- and Si-oxides, that are formed by chemical weathering and the related genesis of minerals occurring in both soils and sedimentary rocks (Kämpf et al., 2011). For this study, we assessed pedogenic Fe-oxides (PO) by using several differences and ratios (POR) of the following Fe-fractions to describe the intensity and direction of soil formation processes (Blume and Schwertmann, 1969; Schlichting and Blume, 1962):

- Fet: total iron content (Fe_2O_3)
- Fed: pedogenic (free), well-crystallised iron oxides, hydroxides and oxyhydroxides
- Feo: poorly-crystallised, active and amorphous oxides, hydroxides and oxyhydroxides
- Fep: metalorganic compounds and organically bound Fe (Bascomb, 1968; McKeague, 1967)

The following ratios and differences (POR) were used (for detailed discussion see subchapter 3.2):

- Fed/Fet: measure for iron release from weathering of primary Fe-bearing minerals (Blume and Schwertmann, 1969; Mirabella and Carnicelli, 1992); the proportion of Fed is higher, the longer and the more intensely weathering processes are persisting
- (Fed-Feo)/Fet: measure for weathering intensities (Alexander, 1985; Arduino et al., 1984); ratio is higher with increasing weathering intensity
- Feo/Fed: degree of activity (Schwertmann, 1964); high ratio indicates high proportion of amorphous oxides, usually showing strong recent weathering of primary silicates in still poorly-developed soils, whereas a low degree of activity refers to dominating well-crystallised iron oxides in comparably more developed soils, both in terms of timeframe and intensity; homogenous substrate for soil formation is an essential precondition for using this ratio
- Fet-Fed: silicate-bound iron in relation to complete iron (Torrent and Cabedo, 1986)
- Fed-Feo: indicates well-crystalised iron oxides (see (Fed-Feo)/Fet)

2.6 Data analyses and statistical applications

All investigated soil profiles (TOTAL), both main and support sites, were allocated to EAST and WEST, respectively. In order to get a better understanding of small-scale pedogenetic processes, one representative main site of each transect was selected for detailed comparison and for establishing continuous catenas. The two sites were chosen in respect of similar geomorphological preconditions, such as relief, hydrology and exposure: Huashixia (E1; HUA) for the eastern transect and Wudaoliang (W1/W2; WUD) for the western transect. TOTAL was bulked into four different soil groups (SG) based on field soil descriptions and laboratory analyses: initially formed soils (IS), Cambisols (CM), groundwater influenced soils (GL), permafrost affected soils (PF).

Mean annual air temperature (MAT) and mean annual precipitation (MAP) were calculated based on linear models. Latitude, longitude, and altitude were used as explanatory variables from 50-year averaged temperature and precipitation records (1951-2000) at 680 well-distributed climate stations across China (Fang et al., 2001; He et al., 2009; He et al., 2006).

For all sampling groups (TOTAL, EAST, WEST, HUA, WUD, and each SG), the same statistical approaches were conducted. Pearson product moment correlation was performed for WI, PO and their independent variables. The latter include MAT, MAP, SM, ST, pH, $CaCO_3$, TOC, and soil texture classes. On this basis, simple linear regression analyses were performed. Differences between sampling groups were analysed by an independent two-tailed Student's t-test. On the basis of an F-test it was decided, whether t-test for equal or unequal variances had to be performed. A multiple linear regression approach (MLR) was used to describe the most meaningful linear effects of independent variables on the dependent parameters PO and POR for each sampling group separately. All independent variables were tested for multicollinearity before multiple linear regression analyses were conducted. Thus, we excluded all variables for a single PO/POR with a high interaction ratio ($r > 0.6$; c.f. Tab. 3 – cross-correlation analysis) from the further analysis to avoid interpretations errors. Based on high correlation values, we decided to take only the variable with the most linear relationship to our dependent variable into account. This analysis was done for each sampling group separately.

For diagram construction and statistical analyses SigmaPlot 12 was used. Regression analyses were performed with R software package (R Development Core Team, 2009).

3 Results and Discussion

3.1 Weathering indices (WI)

3.1.1 Synopsis of weathering indices

Calculated WI are shown in multi-panel Fig. 2, together with the most significant POR as well as $CaCO_3$ and NaCl contents. Essentially, three groups of WI can be separated: PI and KN; CIA, CIW and PIA; as well as CPA and FENG. Curves for PI and KN B show close dependency to $CaCO_3$ contents, since Ca was not corrected for these indices, which makes their interpretation difficult (cf. subchapter 2.4). At sites, where carbonate contents do not vary much (cf. site W1), PI and KN B are basically comparable to the other indices.

For all investigated sites, CIA, CIW and PIA plot largely parallel with no differences in indicating the tendency of weathering or changes of layers within soil profiles. Accordingly, consideration of K does not make any difference for the investigated region, which is mainly due to the stronger weathering resistance of K phases, particularly in periglacial regions with overall low weathering intensities (Buggle et al., 2011; Cullers, 2000). Similarly, feldspars are mainly represented by plagioclases as can be proved by the A-CN-K diagrams (Fig. 3, Fedo et al., 1995).

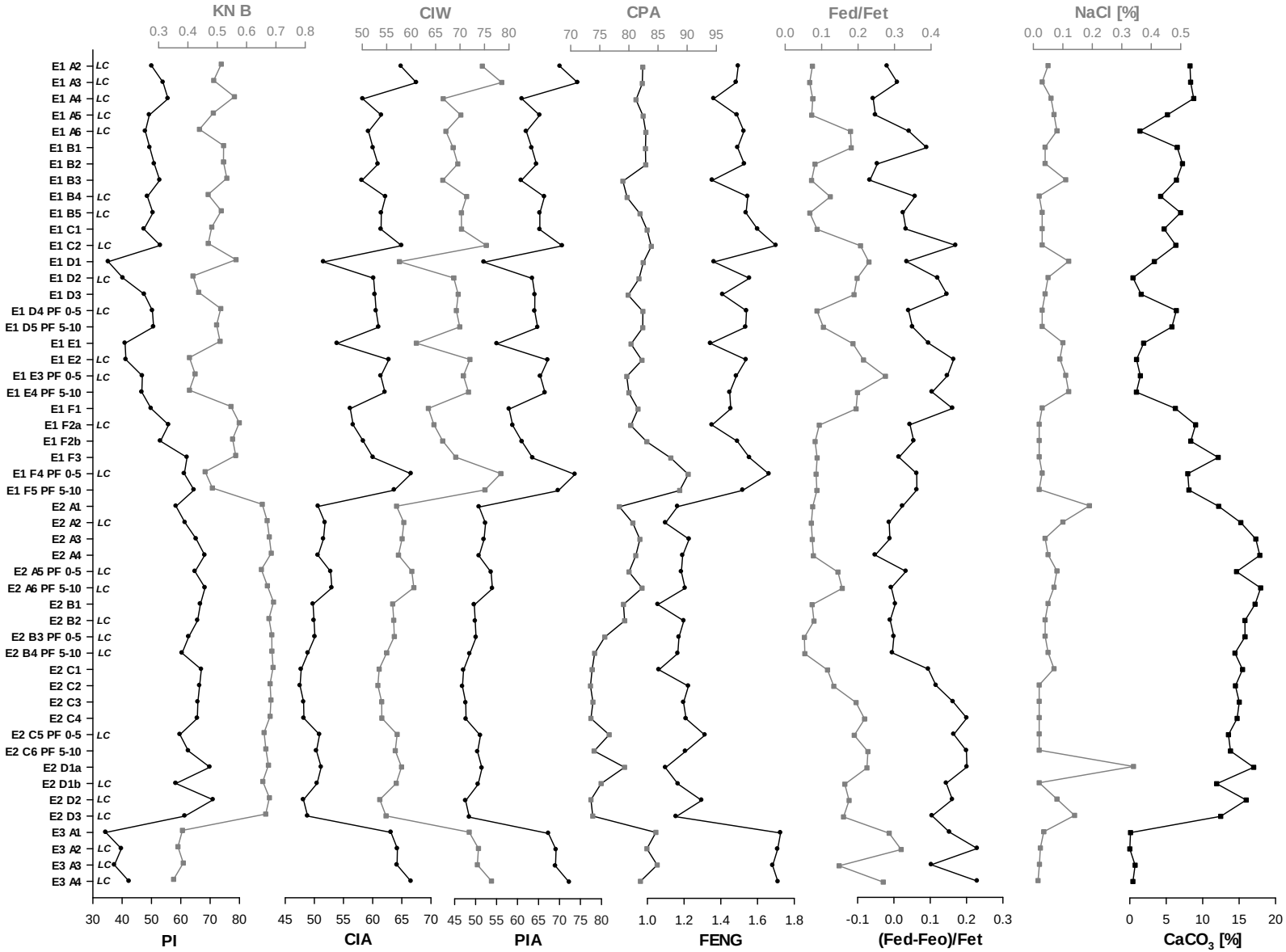

Fig. 2a Parallel plots of WI for transect EAST (Fig. 2a) and WEST (Fig. 2b). WI grouped according to similar characteristics: PI/KN B, CIA/CIW/PIA, CPA/FENG. The most significant l together with NaCl and $CaCO_3$ contents are plotted. Changes of layers are indicated by "*LC*". Sites are ordered for each transect from N to S.

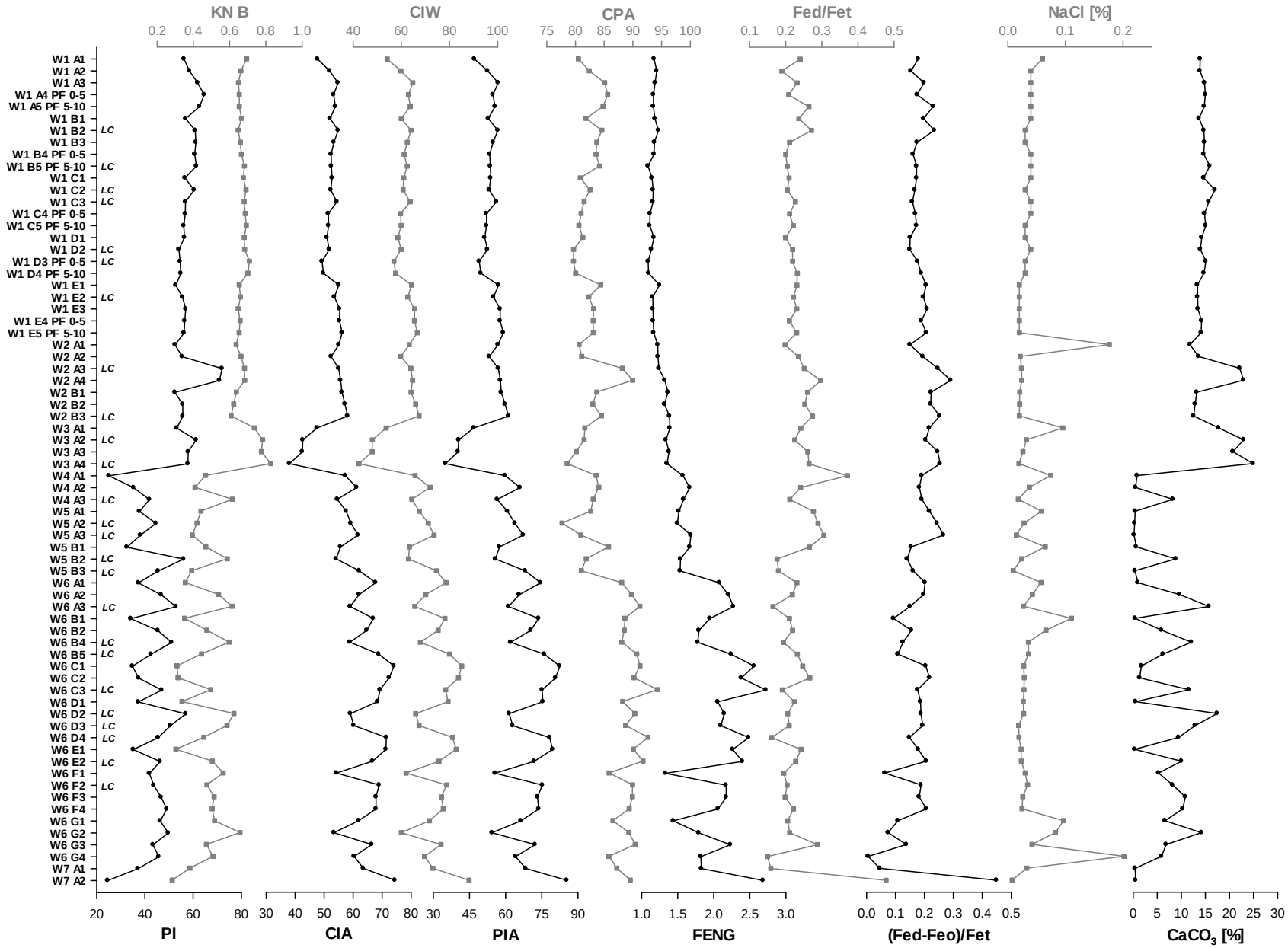
KN B
ClW
CPA
Fed/Fet
NaCl [%]
W1 A1
W1 A2
W1 A3
W1 A4 PF 0-5
W1 A5 PF 5-10
W1 B1
W1 B2 LC
W1 B3
W1 B4 PF 0-5
W1 B5 PF 5-10 LC
W1 C1
W1 C2 LC
W1 C3 LC
W1 C4 PF 0-5
W1 C5 PF 5-10
W1 D1
W1 D2 LC
W1 D3 PF 0-5 LC
W1 D4 PF 5-10
W1 E1
W1 E2 LC
W1 E3
W1 E4 PF 0-5
W1 E5 PF 5-10
W2 A1
W2 A2
W2 A3 LC
W2 A4
W2 B1
W2 B2
W2 B3 LC
W3 A1
W3 A2 LC
W3 A3
W3 A4 LC
W4 A1
W4 A2
W4 A3 LC
W5 A1
W5 A2 LC
W5 A3 LC
W5 B1
W5 B2 LC
W5 B3 LC
W6 A1
W6 A2
W6 A3 LC
W6 B1
W6 B2
W6 B4 LC
W6 B5 LC
W6 C1
W6 C2
W6 C3 LC
W6 D1
W6 D2 LC
W6 D3 LC
W6 D4 LC
W6 E1
W6 E2 LC
W6 F1
W6 F2 LC
W6 F3
W6 F4
W6 G1
W6 G2
W6 G3
W6 G4
W7 A1
W7 A2
PI
CIA
PIA
FENG
(Fed-Feo)/Fet
CaCO3 [%]

Fig. 2b

Because CaO* was used for these indices, curves are not directly linked to $CaCO_3$ contents, thus offering more reliable results than PI and KN for the investigated substrates. Hereafter, CIA is mentioned representatively for all CIA, CIW and PIA.

Ca-free indices CPA and FENG show better differentiation for some sites where other indices plot relatively homogenous (e.g. W2). Nevertheless, the depth function of CPA for other profiles is overall smoother and does not show extreme peaks, such as in E1 A, E1 D or E1 E. Since increased salinity occurs especially in topsoils of sites with negative water balance (Scheffer et al., 2002), a misinterpretation of CPA may happen with the result of an overall underestimated weathering intensity due to higher Na contents (Buggle et al., 2011). The higher sensitivity to recent climate conditions is related to the exclusive use of Al and Na for calculation of the CPA, thus giving Na a higher relative importance.

Changes of substrate layers in soil profiles indicated by amplitudes of WI were compared to soil physical and chemical analyses (grain size distribution and skeleton content, carbonate content, TOC). Accordingly, reasonable and verified layer changes are marked in Fig. 2 (LC). WI generally indicate weathering trends with soil depth, but also layering (e.g. E1). However, CPA depicts some problems with salinity in several topsoil horizons (e.g. W2 A1, W3 A1, W6 B1, W6 G1). The most pronounced and partly contradictory results of CIA and Ca-free indices can be observed in the area around Nagqu (W6): here, well-developed soils on sporadic permafrost and seasonally frozen ground are influenced by a stronger Tropical Monsoon. Site W6 A is highlighting this issue very clearly with opposite weathering trends indicated by both WI groups. Importantly, NaCl enrichment is not very pronounced at this site, but confirming the trend of CPA. The CIA decreases with depth, indicating a lower weathering intensity; this is supported by a simultaneously increasing $CaCO_3$ content with soil depth. Moreover, (Fed-Feo)/Fet suggests the same tendency. Similar observations can be discussed exemplary for the change of layer in horizon W6 C3 and for profile W6 E, although salinity has also no influence at these sites. These results show, that CIA is a most reliable index, if laboratory data of $CaCO_3$ contents are available for the calculation of CaO*.

Frequently, lower weathering intensities in the top horizons are evident. One explanation is the high organic content and felty structure built up by fine roots in topsoils of *Kobresia* meadows (Kaiser et al., 2008). These turf-like horizons comprise proportionally less in-situ weathered mineral soil material, often disconnected from the organo-mineral soil body, additionally acting easily as a trap for fresh airborne sediments. In most cases, comparably fresh aeolian sediment input on top of the profiles is evident, which is mainly derived from rather proximal source areas affected by strong permafrost degradation processes leading to layering (Baumann et al., 2009; Yang et al., 2010).

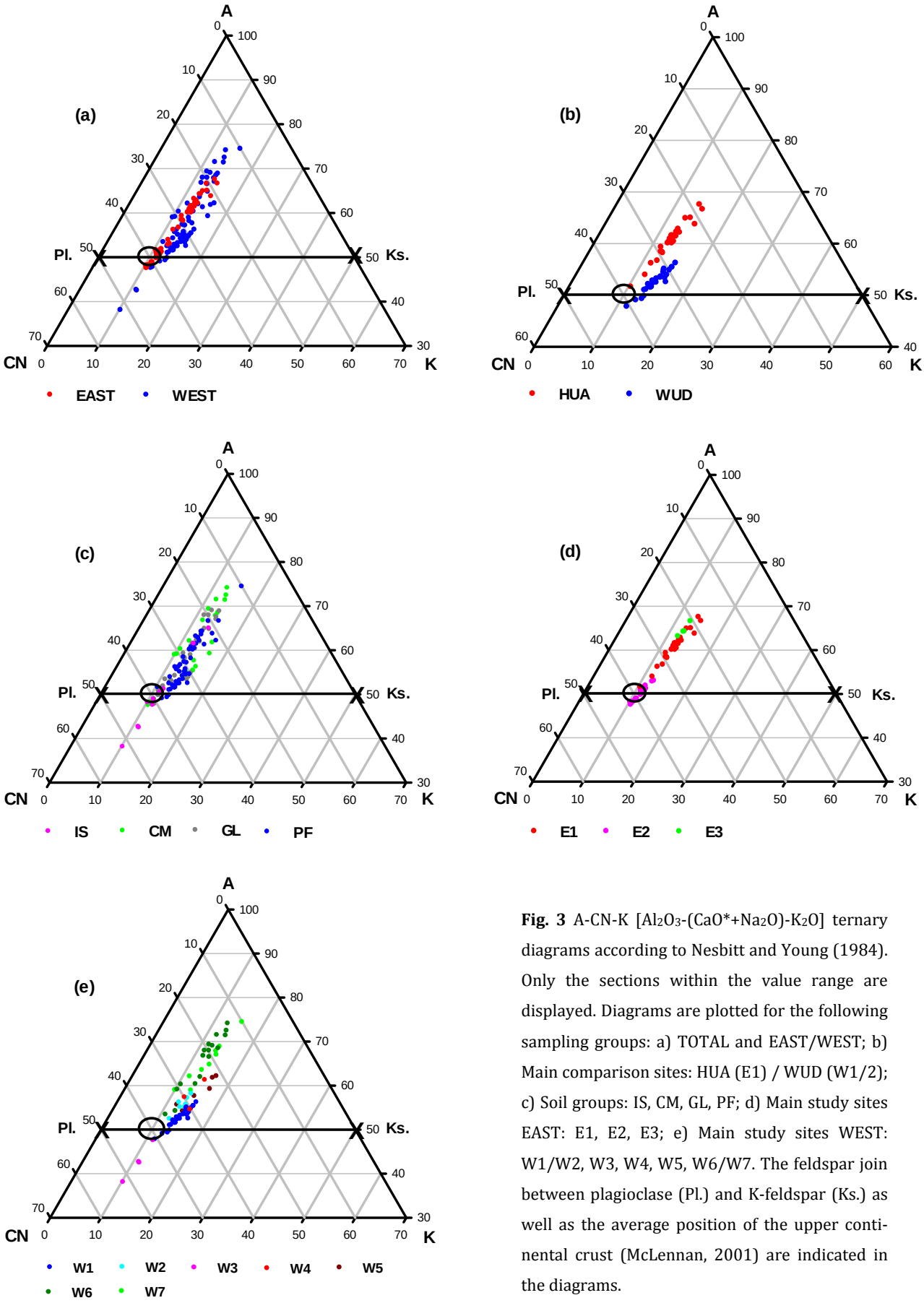

Fig. 3 A-CN-K [Al_2O_3-(CaO*+Na_2O)-K_2O] ternary diagrams according to Nesbitt and Young (1984). Only the sections within the value range are displayed. Diagrams are plotted for the following sampling groups: a) TOTAL and EAST/WEST; b) Main comparison sites: HUA (E1) / WUD (W1/2); c) Soil groups: IS, CM, GL, PF; d) Main study sites EAST: E1, E2, E3; e) Main study sites WEST: W1/W2, W3, W4, W5, W6/W7. The feldspar join between plagioclase (Pl.) and K-feldspar (Ks.) as well as the average position of the upper continental crust (McLennan, 2001) are indicated in the diagrams.

One has to be aware, that sorting effects of different substrates can also account for shifts of weathering indices, even though no differences of weathering intensities are evident (Nesbitt et al., 1996). Nevertheless, variation of substrate composition mostly shows no extremes in the research area, neither in agents, nor in texture. Profile E1 A provides a good example of the above mentioned possibilities of changes in depth functions due to layering: weathering intensity increases from horizon E1 A2 to E1 A3. This is mainly caused by layering, with higher aeolian derived silt content in the topsoil. Abrupt transitions to lower weathering intensities can also be explained by layering: the substrate of horizon E1 A4 consists of fluvial deposits with a high content of coarse material (>2 mm). In profiles E1 D and E1 E these characteristics are also evident, with higher silt contents and organic matter contents in the topsoils.

POR are easily influenced by strong short-term redox processes overprinting rather long-term weathering processes (Fiedler and Sommer, 2004). Thus, the depth function for (Fed-Feo)/Fet is hardly reasonable interpretable of soil horizons influenced by redox processes. Accordingly, Price and Velbel (2003) comment the use of Fe for WI critically due to the change in solubility when Fe^{3+} changes valence to Fe^{2+} (cf. FENG). Accordingly, Al-based WI can be regarded as more appropriate. The depth functions of profile W1 A can be best explained by a mixed influence of redox processes and permanently frozen horizons, because layering could not be identified.

Site W2 is crucial for the discussion of different characteristics of WI. The depth function of CPA is very similar to that of $CaCO_3$ and well corresponding to POR, whereas other indices show much smaller magnitudes and do not indicate all layer changes. However, the high salinity of horizon W2 A1 lowers the CPA. Generally, this supports the idea that related to environmental conditions; it should be a site-specific decision, which WI is most appropriate. All in all, the CIA plots the most comprehensible results.

Specific climatic trends and site conditions are traced very clearly by the plots (higher MAT and MAP from N to S and W to E) when comparing EAST and WEST. While the oscillation of the depth functions is generally high in the zone of discontinuous permafrost of EAST, sites located in regions with continuous permafrost conditions (W1 and W2) show only very small changes in weathering intensities due to stable temperature-moisture (Zhang et al., 2003) as well as sedimentary conditions (Baumann et al., 2009). The influence of the Tropical Monsoon is increasing further south on the western transect (sporadic permafrost mixed with seasonally frozen ground at W6-W7), with higher MAT and MAP (Domrös and Peng, 1988). This climate trend leads again to higher oscillations of the depth function of WI along WEST in southern direction. Data of EAST also gives an impression of different weathering dynamics at sites where permafrost has been degraded (E2) with clearly more homogenous conditions and lower weathering intensity caused by different soil moisture interrelations (Baumann et al., 2009; Xue et al., 2009).

3.1.2 A-CN-K ternary plots and chemical index of alteration (CIA)

CIA is the most reliable WI with the highest explanatory power. The elements used for calculation of the CIA can be plotted in A-CN-K ternary diagrams, visualising scattering in-between sampling groups (Nesbitt et al., 1996). This gives information with regard to weathering intensity and homogeneity of source material (Fig. 3; Buggle et al., 2011). This provides also a basis to decide, if results of the sampling groups can be compared and interpreted together as well as brought into the context for a common discussion. Supplementary to the diagrams, descriptive statistics for the A-K, CN-K and A-CN joins were calculated to gain average values of weathering intensities and a measure of dispersion for the indicators (Tab. 4; McLennan, 1993). Generally speaking, the A-K join is a measure for weathering intensity and can be equalled with CIA values, whereas the CN-K join displays the source material and its homogeneity (shift along the feldspar join). The degree of parallelism to the A-CN join indicates to what extend other minerals than plagioclases are the source of the weathering lines (Nesbitt and Young, 1984; Nesbitt et al., 1996).

TOTAL exhibits a wide range of weathering intensities (Fig. 3a). Interestingly, almost 25% of the samples plot below or only slightly above the feldspar join, indicating essentially no weathering processes. Moreover, other minerals, such as amphiboles or pyroxenes derived from mafic-ultramafic rocks are relevant in the unweathered material besides feldspars (Nesbitt and Young, 1984). Half of the samples are not or only slightly weathered, whereas the second quartile and the maximum value highlight sites with comparably intense weathering conditions. The median of the CN-K join shows a small shift from the UCC (upper continental crust) average towards K-feldspar, but with plagioclase being predominant (Tab. 4).

The two main investigation sites are compared in Fig. 3b. HUA (E1) reflects with clearly higher range and variance of weathering intensities the more diverse conditions in discontinuous permafrost environments. It shows a distinct feldspar weathering line with no results below the feldspar join. As indicated by the higher median, there is – compared to TOTAL – an enhanced weathering intensity evident. WUD (W1 and W2) reveals overall very low weathering intensities, being on average clearly below TOTAL with a maximum showing no distinct weathering signs (Nesbitt and Young, 1982). The range and variance is much smaller than in HUA underlining the above-mentioned lower weathering intensity and higher homogeneity of site characteristics in continuous permafrost landscapes. The CN-K join indicates very homogenous parent material with low scattering (cf. standard deviation and variance) and the mean reveals a shift towards K-feldspar compared to HUA. The two main sites thus can be explicitly differentiated in terms of parent material. The parallelism to the A-CN join differs between HUA and WUD.

Table 2 Descriptive statistics of selected parameters; ordered by parameters for comparison between sampling groups.

Group	Para-meter	n	Range	Mean	Var.	Std. Dev.	Min	1. Q	Med.	3. Q	Max	Skew-ness	Kurtosis	Std. Error	C. I. of mean
TOTAL	SM	95	72.40	36.17	294.34	17.16	4.00	21.15	39.70	48.50	76.40	-0.10	-0.71	1.76	3.50
EAST	SM	38	70.20	43.29	251.25	15.85	6.20	35.25	47.30	52.63	76.40	-0.35	0.07	2.57	5.21
WEST	SM	57	67.50	31.43	270.82	16.46	4.00	15.20	32.50	44.10	71.50	0.05	-0.93	2.18	4.37
HUA	SM	21	70.20	49.94	215.72	14.69	6.20	45.30	50.00	53.90	76.40	-0.92	3.19	3.21	6.69
WUD	SM	18	21.30	43.21	44.82	6.70	32.00	40.75	44.15	46.98	53.30	-0.32	-0.75	1.58	3.33
IS	SM	10	29.80	16.63	72.07	8.49	6.20	12.30	15.05	19.54	36.00	1.26	2.40	2.68	6.07
CM	SM	20	29.60	18.26	97.93	9.90	4.00	11.40	16.40	25.65	33.60	0.33	-1.22	2.21	4.63
GL	SM	29	48.40	44.04	135.60	11.64	10.40	43.60	48.00	50.00	58.80	-1.73	2.59	2.16	4.43
PF	SM	36	59.20	45.21	182.48	13.51	17.20	37.55	42.85	53.30	76.40	0.48	0.25	2.25	4.57
TOTAL	$CaCO_3$	126	24.92	10.13	38.76	6.23	0.00	5.81	12.12	14.75	24.92	-0.19	-0.88	0.55	1.10
EAST	$CaCO_3$	52	17.96	8.95	33.43	5.78	0.00	4.60	8.31	14.54	17.96	-0.05	-1.33	0.80	1.61
WEST	$CaCO_3$	74	24.73	10.96	41.33	6.43	0.19	6.31	13.37	14.81	24.92	-0.34	-0.59	0.75	1.49
HUA	$CaCO_3$	28	11.74	5.76	10.82	3.29	0.45	3.00	6.36	8.16	12.19	-0.02	-0.63	0.62	1.28
WUD	$CaCO_3$	28	3.63	14.64	0.65	0.81	13.36	14.10	14.70	15.05	16.99	0.67	1.45	0.15	0.31
IS	$CaCO_3$	10	20.21	15.48	44.66	6.68	4.71	12.06	16.50	19.97	24.92	-0.31	-0.77	2.11	4.78
CM	$CaCO_3$	26	17.26	9.54	39.19	6.26	0.19	1.44	13.13	14.18	17.45	-0.64	-1.39	1.23	2.53
GL	$CaCO_3$	38	17.56	10.50	23.16	4.81	0.40	6.55	10.57	14.73	17.96	-0.15	-1.05	0.78	1.58
PF	$CaCO_3$	52	22.95	9.12	44.19	6.65	0.00	1.33	10.42	14.70	22.95	-0.07	-1.25	0.92	1.85
HUA	TOC	28	18.13	3.32	15.51	3.94	0.15	1.08	2.29	3.38	18.28	2.67	7.99	0.74	1.53
WUD	TOC	28	5.83	1.26	1.59	1.26	0.41	0.62	0.85	1.09	6.24	2.80	8.76	0.24	0.49
IS	TOC	10	3.16	0.74	0.87	0.93	0.00	0.19	0.36	0.88	3.16	2.29	5.82	0.29	0.67
CM	TOC	26	7.15	1.44	2.85	1.69	0.24	0.42	0.75	1.85	7.39	2.22	5.40	0.33	0.68
GL	TOC	38	12.43	2.32	6.12	2.47	0.19	1.03	1.55	2.47	12.62	2.74	8.43	0.40	0.81
PF	TOC	52	18.23	3.23	17.57	4.19	0.05	0.65	1.20	3.84	18.28	1.85	2.96	0.58	1.17
HUA	Sand	23	67.52	24.23	267.40	16.35	7.01	14.57	17.65	30.20	74.53	1.76	3.07	3.41	7.07
WUD	Sand	21	25.99	25.20	62.23	7.89	13.09	17.35	26.11	30.72	39.08	0.08	-1.22	1.72	3.59
IS	Sand	9	77.23	60.33	612.55	24.75	10.30	52.74	67.07	74.53	87.53	-1.06	0.92	8.25	19.02
CM	Sand	25	66.33	38.04	397.45	19.94	8.44	23.52	31.24	53.85	74.77	0.66	-0.86	3.99	8.23
GL	Sand	37	50.98	23.53	162.75	12.76	5.69	14.27	20.98	29.00	56.67	1.06	0.60	2.10	4.25

Table 2 continued

Group	Para-meter	n	Range	Mean	Var.	Std. Dev.	Min	1. Q	Med.	3. Q	Max	Skew-ness	Kurtosis	Std. Error	C. I. of mean
PF	Sand	43	63.28	24.30	184.80	13.59	4.35	16.18	20.36	29.03	67.63	1.56	3.08	2.07	4.18
HUA	Silt	23	56.73	55.28	277.97	16.67	16.81	44.39	62.27	67.23	73.54	-0.94	-0.35	3.48	7.21
WUD	Silt	21	15.65	58.65	24.34	4.93	49.05	53.50	59.82	62.56	64.70	-0.51	-1.23	1.08	2.25
IS	Silt	9	62.34	28.35	432.11	20.79	8.74	16.81	20.10	33.48	71.08	1.29	1.08	6.93	15.98
CM	Silt	25	47.02	41.84	175.26	13.24	14.62	37.82	41.27	52.80	61.64	-0.54	-0.34	2.65	5.47
GL	Silt	37	51.91	54.90	179.30	13.39	26.15	42.34	57.49	65.72	78.06	-0.29	-1.04	2.20	4.47
PF	Silt	43	57.45	54.22	193.53	13.91	14.56	50.27	59.82	62.53	72.01	-1.43	1.21	2.12	4.28
HUA	Clay	23	43.74	20.50	131.53	11.47	8.67	14.04	17.94	19.85	52.41	2.02	3.50	2.39	4.96
WUD	Clay	21	15.10	16.15	19.47	4.41	8.62	12.86	15.78	18.92	23.72	0.13	-0.78	0.96	2.01
IS	Clay	9	14.97	11.33	34.88	5.91	3.73	4.97	13.36	15.17	18.70	-0.08	-1.76	1.97	4.54
CM	Clay	25	28.91	20.12	93.32	9.66	6.30	10.62	19.42	28.80	35.21	0.11	-1.55	1.93	3.99
GL	Clay	37	37.43	21.57	78.22	8.84	7.44	15.70	19.45	28.93	44.87	0.64	-0.10	1.45	2.95
PF	Clay	43	43.79	21.48	81.74	9.04	8.62	17.34	19.83	23.80	52.41	1.80	4.32	1.38	2.78
TOTAL	Fe p	125	2.52	0.36	0.22	0.47	0.02	0.07	0.17	0.43	2.54	2.28	5.32	0.04	0.08
EAST	Fe p	51	1.91	0.44	0.21	0.46	0.02	0.11	0.29	0.57	1.92	1.63	2.48	0.06	0.13
WEST	Fe p	74	2.51	0.31	0.23	0.48	0.03	0.07	0.15	0.29	2.54	2.86	8.37	0.06	0.11
HUA	Fe p	27	1.85	0.53	0.22	0.47	0.02	0.15	0.43	0.76	1.86	1.15	1.04	0.09	0.19
WUD	Fe p	28	0.44	0.17	0.01	0.11	0.06	0.11	0.14	0.18	0.50	1.62	2.22	0.02	0.04
IS	Fe p	10	0.38	0.08	0.01	0.11	0.03	0.04	0.04	0.07	0.41	3.06	9.53	0.04	0.08
CM	Fe p	26	0.55	0.13	0.02	0.13	0.03	0.06	0.09	0.15	0.57	2.47	6.30	0.03	0.05
GL	Fe p	37	1.85	0.44	0.15	0.39	0.05	0.18	0.35	0.53	1.90	2.07	4.99	0.06	0.13
PF	Fe p	52	2.52	0.48	0.36	0.60	0.02	0.11	0.18	0.62	2.54	1.70	2.17	0.08	0.17
TOTAL	Fe o	125	7.95	2.18	2.93	1.71	0.19	0.99	1.45	2.95	8.14	1.39	1.40	0.15	0.30
EAST	Fe o	51	6.74	2.78	3.31	1.82	0.42	1.38	2.33	3.89	7.16	0.70	-0.43	0.25	0.51
WEST	Fe o	74	7.95	1.76	2.28	1.51	0.19	0.84	1.29	1.92	8.14	2.25	5.68	0.18	0.35
HUA	Fe o	27	5.60	3.30	2.90	1.70	1.18	2.00	2.93	4.57	6.78	0.58	-0.87	0.33	0.67
WUD	Fe o	28	1.66	1.33	0.16	0.40	0.71	1.15	1.29	1.47	2.37	0.61	0.56	0.08	0.16
IS	Fe o	10	2.13	0.98	0.55	0.74	0.19	0.46	0.65	1.48	2.33	0.93	-0.60	0.23	0.53

Table 2 continued

Group	Para-meter	n	Range	Mean	Var.	Std. Dev.	Min	1. Q	Med.	3. Q	Max	Skew-ness	Kurtosis	Std. Error	C. I. of mean
CM	Fe o	26	2.95	1.13	0.52	0.72	0.46	0.73	0.81	1.15	3.40	1.87	3.20	0.14	0.29
GL	Fe o	37	7.35	3.58	4.09	2.02	0.79	1.51	3.37	5.15	8.14	0.38	-0.77	0.33	0.67
PF	Fe o	52	6.57	1.94	1.55	1.25	0.22	1.23	1.44	2.15	6.78	1.75	3.81	0.17	0.35
TOTAL	Fe d	125	17.48	7.38	10.15	3.19	1.39	5.39	6.91	8.98	18.87	0.67	0.71	0.28	0.56
EAST	Fe d	51	13.22	5.55	8.84	2.97	1.39	3.33	5.05	7.18	14.61	1.15	1.11	0.42	0.84
WEST	Fe d	74	14.49	8.65	7.21	2.69	4.38	6.79	7.88	10.30	18.87	1.30	2.03	0.31	0.62
HUA	Fe d	27	12.17	5.82	8.36	2.89	2.44	3.61	5.17	7.73	14.61	1.27	1.84	0.56	1.14
WUD	Fe d	28	4.79	7.36	1.33	1.15	5.90	6.64	6.94	7.88	10.69	1.42	2.08	0.22	0.45
IS	Fe d	10	7.43	6.43	5.18	2.28	3.75	5.08	5.69	6.78	11.18	1.23	1.01	0.72	1.63
CM	Fe d	26	11.06	8.68	8.44	2.90	3.30	6.93	8.30	10.67	14.36	0.11	-0.55	0.57	1.17
GL	Fe d	37	14.25	6.40	13.14	3.63	1.39	3.04	6.65	8.55	15.64	0.55	-0.35	0.60	1.21
PF	Fe d	52	15.31	7.62	8.55	2.92	3.56	5.94	6.85	8.50	18.87	1.60	3.57	0.41	0.81
TOTAL	Fe t	125	41.23	38.50	84.81	9.21	19.58	31.61	37.72	44.31	60.81	0.40	-0.62	0.82	1.63
EAST	Fe t	51	34.99	39.30	75.55	8.69	25.82	32.11	40.95	44.01	60.81	0.33	-0.17	1.22	2.45
WEST	Fe t	74	37.96	37.95	91.56	9.57	19.58	31.24	34.67	44.76	57.54	0.48	-0.77	1.11	2.22
HUA	Fe t	27	34.93	44.26	56.54	7.52	25.88	41.37	43.33	47.37	60.81	0.21	1.06	1.45	2.98
WUD	Fe t	28	11.79	33.55	10.28	3.21	27.78	31.08	33.16	35.46	39.57	0.38	-0.42	0.61	1.24
IS	Fe t	10	34.49	33.01	104.16	10.21	19.58	27.51	29.45	39.42	54.07	1.02	0.68	3.23	7.30
CM	Fe t	26	31.72	39.88	132.65	11.52	23.92	28.39	33.83	50.48	55.64	0.09	-1.89	2.26	4.65
GL	Fe t	37	31.72	41.50	55.24	7.43	25.82	37.20	40.62	44.55	57.54	0.28	0.00	1.22	2.48
PF	Fe t	52	40.13	36.73	67.18	8.20	20.68	30.98	34.58	41.18	60.81	0.97	1.27	1.14	2.28

While HUA is only slightly oblique towards the A-K join, WUD differs much stronger in the same direction indicating that also other minerals than plagioclase are involved in the weathering processes particularly at WUD.

Scattering along the CN-K join of the two main sites and TOTAL indicates homogenous conditions of source materials within the sites HUA and WUD. Compared to their standard deviation and variance, scattering of TOTAL can still be considered as moderate. Thus the results of TOTAL can be well discussed and interpreted to observe general trends.

The comparison of EAST and WEST is plotted in Fig. 3a. WEST displays a broader range of weathering intensities than EAST, because the western transect crosses more climatic regions, including sites of discontinuous, continuous and south of Tanggula Shan even sporadic permafrost with well-developed Cambisols. Comparable sites with intense soil formation are missing in EAST. On the other hand, EAST comprises no sites influenced by continuous permafrost without detectable current weathering processes, such as in WUD. This approximates the average weathering intensities (cf. mean and median) of EAST and WEST, but leads to a much greater variance for WEST. Moreover, the two transects are also clearly different in terms of source material with a much higher variation in WEST. To summarise, WEST displays equal scattering to TOTAL, which underlines the greater variety of soil forming and weathering conditions for WEST.

Concerning SG (Fig. 3c), homogeneity (CN-K join) cannot be interpreted, because regional variations of source materials are determining this parameter and SG are spread throughout many sites of the investigation area. Additionally, regional clustering of particular SG is biasing the values.

Environments with soils strongly affected by permafrost have generally low weathering potentials with rather homogenous conditions compared to other regions (Kimble, 2004). Under moist and cold conditions chemical weathering processes are slowed down (Brady and Weil, 2008; McLennan, 1993). Accordingly, the lowest dispersion of weathering intensities can be referred to PF (Fig. 3c). IS and CM exhibit clearly differing weathering intensities with CM having the highest and IS the lowest values of all soil groups. GL and PF indicate slightly lower weathering than CM.

Climatic trends and permafrost condition along both transects can be highlighted by the data plotted in Figures 3d and 3e. Transect EAST (Fig. 3d) shows an increasing weathering trend from E2, E1, to E3, which is coincident to the climatic gradient (increasing MAT and MAP). Moreover, especially because E2 and E1 are located close to each other, vegetative cover and permafrost characteristics become even more important:

Table 3 Product-moment correlation coefficients (Pearson) for the most important site variables. The significance is marked (** $p < 0.01$; * $p < 0.05$; others $p > 0.05$)

	MAP [mm a^{-1}]	**SM [vol. %]**	**ST [°C]**	**pH [$CaCl_2$]**	**$CaCO_3$ [%]**	**TOC [%]**	**Sand [%]**	**Silt [%]**	**Clay [%]**	**Fe t [‰]**	**Fe d [‰]**	**Fe o [‰]**	**Fe p [‰]**
MAT [°C]	0.33**	-0.41**	0.48**	-0.04	-0.19*	0.03	-0.04	-0.22*	0.47**	0.48**	0.33**	0.19*	0.03
MAP [mm a^{-1}]		0.07	0.15	-0.39**	-0.63**	0.32**	0.08	-0.15	0.11	0.25**	-0.16	0.40**	0.37**
SM [vol. %]			-0.39**	-0.16	-0.13	0.39**	-0.49**	0.62**	-0.05	-0.12	-0.33**	0.48**	0.50**
ST [°C]				0.02	-0.13	0.10	0.09	-0.21	0.18	0.04	0.10	-0.11	-0.01
pH [$CaCl_2$]					0.71**	-0.54	0.16	-0.02	-0.29**	-0.02	-0.28**	-0.22*	-0.55**
$CaCO_3$ [%]						-0.53**	0.08	0.06	-0.27**	-0.25**	-0.25**	-0.38**	-0.53**
TOC [%]							-0.23*	0.12	0.27**	-0.22*	-0.02	0.38**	0.89**
Sand [%]								-0.88**	-0.52**	-0.49**	-0.22*	-0.33**	-0.27**
Silt [%]									0.04	0.22*	0.02	0.28**	0.20*
Clay [%]										0.62**	0.43**	0.19*	0.21*
Fe t [‰]											0.47**	0.28**	-0.16
Fe d [‰]												0.02	-0.02
Fe o [‰]													0.55**

Table 3 continued

	PI	KN B	CIA	CIW	PIA	FENG	CPA	Fed/ Fet	Feo/ Fed	(Fed-Feo)/ Fet
MAT [°C]	-0.30**	-0.35**	0.47**	0.41**	0.46**	0.73**	0.51**	-0.01	0.02	-0.04
MAP [mm a^{-1}]	-0.39**	-0.61**	0.42**	0.37**	0.42**	0.39**	-0.02	-0.33**	0.41**	-0.45**
SM [vol. %]	-0.04	0.00	-0.06	-0.06	-0.07	-0.34**	-0.14	-0.29**	0.47**	-0.50**
ST [°C]	-0.17	-0.12	0.06	0.02	0.06	0.22	-0.02	0.04	-0.18	0.09
pH [$CaCl_2$]	0.78**	0.67**	-0.5**	-0.52**	-0.51**	-0.42**	-0.33**	-0.35**	0.01	-0.15
$CaCO_3$ [%]	0.85**	0.93**	-0.71**	-0.71**	-0.72**	-0.50**	-0.24**	-0.14	-0.12	0.06
TOC [%]	-0.60**	-0.37**	0.10	0.08	0.10	0.08	0.10	0.15	0.20*	-0.16
Sand [%]	0.07	0.18	-0.34**	-0.32**	-0.31**	-0.13	-0.51**	0.08	-0.21*	0.2*
Silt [%]	0.09	0.04	0.07	0.05	0.04	-0.15	0.14	-0.16	0.29**	-0.26**
Clay [%]	-0.31**	-0.44**	0.57**	0.56**	0.57**	0.54**	0.80**	0.11	-0.08	0.04
Fe t [‰]	-0.14	-0.49**	0.74**	0.71**	0.73**	0.62**	0.68**	-0.13	0.06	-0.11
Fe d [‰]	-0.41**	-0.42**	0.53**	0.54**	0.53**	0.58**	0.60**	0.79**	-0.52**	0.71**
Fe o [‰]	-0.28**	-0.34**	0.26**	0.24**	0.25**	0.13	0.13	-0.18	0.72**	-0.59**
Fe p [‰]	-0.54**	-0.39**	0.15	0.13	0.14	0.07	0.07	0.10	0.34**	-0.26**
PI		0.81**	-0.66**	-0.66**	-0.66**	-0.65**	-0.44**	-0.40**	0.04	-0.17
KN B			-0.89**	-0.88**	-0.89**	-0.70**	-0.46**	-0.17	-0.06	-0.01
CIA				0.99**	1.00**	0.82**	0.70**	0.12	0.01	0.05
CIW					1.00**	0.77**	0.70**	0.15	-0.02	0.09
PIA						0.81**	0.70**	0.13	0.00	0.06
FENG							0.76**	0.24**	-0.14	0.20*
CPA								0.26**	-0.16	0.21*
Fed/Fet									-0.63**	0.88**
Feo/Fed										-0.87**

E2 reveals instable sedimentary conditions caused by a sparse vegetation cover, leading to both strong sedimentation and erosion processes. The frequently occurring translocation processes lead to syngenetic weathering and soil formation (Dietze et al., 2012), resulting in very low in-situ weathering values.

Transect WEST is due to its length and distinct climate settings more differentiated and the composition of parent material is more diverse (cf. CN-K join for W1/W2 and W6/W7). Sites can be likewise ordered by their geographical location with the exception of W3, which features only one profile with initial soil formation as soil conditions did not change for several kilometres in this area. All horizons plot below the feldspar join, indicating no weathering processes. The other sites show a clear differentiation: WUD (W1/W2) is situated in an area with continuous permafrost and low precipitation, W4 is located south of Tanggula Pass in the transition zone from continuous to discontinuous permafrost with rising MAP and influenced by the Tropic Monsoon, and W5 is finally situated in discontinuous permafrost. W6/W7 are already strongly influenced by the Tropic Monsoon with prevailing sporadic permafrost conditions and seasonally frozen ground.

Table 4 Descriptive statistics for A-K, CN-K and A-CN joins of ternary diagrams (cf. Fig. 3)

Sample	Join	n	Range	Mean	Var.	Std. Dev.	Min	1. Q	Med.	3. Q	Max
TOTAL	A-K	125	36.33	57.22	50.22	7.09	38.08	51.84	56.17	61.91	74.42
	CN-K	125	6.77	12.93	2.20	1.48	10.07	11.73	12.89	13.86	16.84
	A-CN	125	41.58	29.85	58.71	7.66	10.04	24.50	30.46	34.97	51.62
EAST	A-K	51	19.98	56.77	38.51	6.21	47.54	50.65	58.32	61.50	67.52
	CN-K	51	4.94	12.17	1.14	1.07	10.22	11.40	12.35	12.76	15.16
	A-CN	51	23.41	31.06	51.14	7.15	18.42	25.70	29.31	38.15	41.83
WEST	A-K	74	36.33	57.53	58.69	7.66	38.08	52.50	55.35	62.04	74.42
	CN-K	74	6.77	13.45	2.28	1.51	10.07	12.43	13.57	14.31	16.84
	A-CN	74	41.58	29.02	62.97	7.94	10.04	23.52	30.55	33.68	51.62
HUA	A-K	0	15.93	60.61	12.45	3.53	51.59	58.84	60.92	62.17	67.52
	CN-K	0	4.71	12.75	0.95	0.98	10.45	12.38	12.53	13.13	15.16
	A-CN	0	19.54	26.64	19.14	4.37	18.42	24.72	26.34	29.17	37.96
WUD	A-K	28	8.45	52.59	4.27	2.07	47.76	51.53	52.50	54.02	56.21
	CN-K	28	4.19	14.14	1.02	1.01	11.71	13.50	13.97	14.73	15.90
	A-CN	28	12.40	33.27	8.73	2.96	28.13	30.98	33.41	34.78	40.53
IS	A-K	10	26.89	49.58	68.74	8.29	38.08	43.87	48.49	51.00	64.97
	CN-K	10	3.58	11.51	1.13	1.06	10.22	11.03	11.36	11.74	13.79
	A-CN	10	30.39	38.91	85.19	9.23	21.23	37.27	40.57	45.08	51.62
CM	A-K	26	26.55	59.58	70.87	8.42	47.54	53.93	59.01	67.53	74.09
	CN-K	26	6.77	12.84	4.31	2.08	10.07	10.81	12.48	14.47	16.84
	A-CN	26	28.80	27.58	82.37	9.08	13.02	19.68	28.63	31.68	41.83
GL	A-K	37	21.25	58.00	44.25	6.65	47.76	51.91	58.32	62.21	69.01
	CN-K	37	4.33	12.66	1.43	1.20	11.02	11.68	12.44	13.31	15.35
	A-CN	37	23.29	29.35	51.28	7.16	17.24	24.50	29.30	35.58	40.53
PF	A-K	52	25.40	56.96	29.20	5.40	49.02	52.48	55.66	61.10	74.42
	CN-K	52	6.19	13.44	1.32	1.15	10.45	12.72	13.33	13.99	16.64
	A-CN	52	28.35	29.60	32.16	5.67	10.04	26.04	30.96	33.74	38.38

3.1.3 Statistical differences between sampling groups

Tab. 5 lists significantly different sampling groups as a result of two-tailed t-tests with $p<0.05$ for each WI. For CIA, CIW, PIA and KN B, overall the same groups can be considered as significantly different. The only, but very crucial discrepancy of these indices to CPA is, that for CPA, EAST and WEST are calculated as significantly different and not HUA and WUD. However, the clear differences in weathering intensities of HUA and WUD were shown very clearly by the ternary diagrams (Fig. 3b). According to CIA, differences along each transect EAST and WEST are more distinct than differences between EAST and WEST, which can be supported by the ternary diagrams. This shows as well that CPA is not the appropriate WI for the investigated sites. Soil groups can be distinguished only with involvement of IS as an extreme group with lowest weathering intensities. It is important to note that KN Index B shows – although not calculated with CaO* – exactly the same differences than CIA. This underlines the principally similar characteristics of KN Index B and CIA as a measure of feldspar breakdown (cf. Fig. 2; Buggle et al., 2011; Kronberg and Nesbitt, 1981).

3.1.4 Correlations and simple regressions between WI and control variables

No significant correlations are evident between WI and SM, albeit MAP and MAT display good relationships (Tab. 3). One explanation is that long-term average data are more related to WI than short-term alternating parameters, such as SM or TOC. Moreover, since MAT and MAP do not vary within main sites compared to the other independent variables, site-specific differences related to parent material and other particular environmental conditions are indirectly traced by these findings (cf. Fig. 3). Other common features of CIA, PIA CIW, CPA and FENG are the pronounced negative relationship to soil acidity parameters and the positive correlation to clay (for PI and KN vice versa). Accordingly, increased weathering intensity can be related to higher acidity and clay content as a product of feldspar breakdown (Nesbitt and Young, 1984). No significant correlations to silt are observable, but sand is negatively correlated to CIA, PIA CIW and CPA.

The above described corresponding depth function of different WI (Fig. 2) can be confirmed by correlation analyses among them. Essentially, CIA, PIA and CIW plot almost identical ($r=0.99$) for the investigated sites. Their relationships with the carbonate-free CPA and FENG are weaker (e.g. $r=0.70$ for CPA). Interestingly, even if CaO is not corrected for KN B, the correlation of CIA and KN B is high, whereas PI only indicates a medium relationship. These findings are related to the different principles of these indices (Duzgoren-Aydin et al., 2002 and subchapter 2.4). The strong correlation of KN B with $CaCO_3$ however, leads to the conclusion, that WI using Ca without correction are biased to a large extent by calcium carbonate contents and therefore can be

not considered as useful for TOTAL, EAST and WEST sampling sets, which have no or rather different calcium carbonate contents.

Table 5 Student's t-test for most important WI, PO, and POR between sampling groups (only sig. tests shown). The level of significance is marked (*** p < 0.001; ** p < 0.01; * p < 0.05).

Parameter	Group 1	Group 2	F-test / variance	t-statistic	t-critical
CIA	HUA	WUD	unequal	10.233	2.018***
CIA	IS	CM	unequal	-3.226	2.110**
CIA	IS	PF	unequal	-2.705	2.201*
CIA	IS	GL	equal	-3.368	2.014**
CIW	HUA	WUD	unequal	7.692	2.015***
CIW	IS	CM	equal	-3.295	2.032**
CIW	IS	PF	unequal	-2.935	2.228*
CIW	IS	GL	equal	-3.438	2.014**
PIA	HUA	WUD	unequal	9.549	2.018***
PIA	IS	CM	unequal	-3.233	2.110**
PIA	IS	PF	unequal	-2.713	2.201*
PIA	IS	GL	equal	-3.305	2.014**
CPA (CIW')	East	West	unequal	-6.249	1.982***
CPA (CIW')	IS	CM	unequal	-2.850	2.042**
CPA (CIW')	IS	PF	unequal	-3.122	2.201**
CPA (CIW')	IS	GL	unequal	-3.269	2.120**
KN B	HUA	WUD	unequal	-10.233	2.018***
KN B	IS	CM	unequal	3.226	2.110**
KN B	IS	PF	unequal	2.705	2.201*
KN B	IS	GL	equal	3.368	2.014**
(Fed-Feo)/Fet	East	West	unequal	-8.189	1.989***
(Fed-Feo)/Fet	Hua	Wud	unequal	-8.784	2.037***
(Fed-Feo)/Fet	GL	PF	unequal	-5.325	1.995***
(Fed-Feo)/Fet	CM	PF	unequal	2.606	1.992*
(Fed-Feo)/Fet	IS	GL	unequal	4.303	2.101***
(Fed-Feo)/Fet	CM	GL	unequal	7.912	2.008***
Fed/Fet	East	West	unequal	-7.710	1.990***
Fed/Fet	Hua	Wud	unequal	-6.675	2.040***
Fed/Fet	GL	PF	unequal	-4.104	1.991***
Fed/Fet	IS	GL	unequal	2.475	2.101*
Fed/Fet	CM	GL	unequal	4.731	2.000***
Fep	Hua	Wud	unequal	3.833	2.045***
Fep	CM	PF	unequal	-3.942	2.000***
Fep	IS	PF	unequal	-4.328	2.000***
Fep	IS	GL	unequal	-4.858	2.014***
Fep	CM	GL	unequal	-4.467	2.013***

Based on the correlation analyses with independent variables, clay and $CaCO_3$ contents were selected for simple regression analyses to explain the variation of CIA within each sampling group (Tab. 6). For TOTAL, 32% of CIA variation can be positively explained by clay content. Comparing the two transects, WEST has a higher R^2, mainly because this transect includes more sites with well-developed Cambisols (CM) and higher weathering intensities (W6/W7). Altogether, CM expresses the highest R^2 with 65% of explained variance, referring to the soil group with the highest degree of weathering. Hydrolysis of silicates and formation of clay minerals are

major soil formation processes of Cambisols (Brady and Weil, 2008; Jenny, 1994), being responsible for clay enrichment and the strong relationship between CIA and clay content for CM (Nesbitt et al., 1996). However, type and abundance of clay minerals can bias the chemical elements ratios along the weathering profile, particularly when they originate from clay-rich parent material (Duzgoren-Aydin et al., 2002; Nesbitt and Young, 1984). Indeed, clay contents of substrates for soil formation are generally low in the investigated area on the Tibetan Plateau, with soil mostly developed in a surface layer dominated by fine sands and silts which may relativize the error. GL only exhibits 16% of explained variance, as weathering in GL is inhibited for a certain timespan at ground water influenced sites and weathering products are redistributed frequently within profiles (Fiedler and Sommer, 2004). Furthermore, constant lateral supply with fresh or diversely pre-weathered compounds is likely, as GL soils are commonly located in geomorphological depressions or valleys (Brady and Weil, 2008). To a lower extend, similar arguments can be taken for permafrost-affected soils (PF). No significant relationships are evident for IS, which is caused by predominantly fresh aeolian sediments with very low primary and secondary clay contents (Baumann et al., 2009; Yan et al., 2009).

Table 6 Simple regression analyses for CIA. The level of significance is marked (*** $p < 0.001$; ** $p < 0.01$; * $p < 0.05$; others $p > 0.05$). Direction of change is indicated by (+) for positive and (-) for negative influence.

Group	Parameter x	Parameter y	n	R^2	Std. Error Regression
TOTAL	CIA	Clay	112	0,32*** (+)	7,67
EAST	CIA	Clay	45	0,24*** (+)	8,65
WEST	CIA	Clay	66	0,40*** (+)	6,48
HUA	CIA	Clay	21	0,04 (+)	11,76
WUD	CIA	Clay	20	0,34** (+)	3,69
IS	CIA	Clay	8	0,00 (-)	6,30
CM	CIA	Clay	24	0,65*** (+)	5,83
GL	CIA	Clay	35	0,16* (+)	8,33
PF	CIA	Clay	42	0,27*** (+)	7,82
TOTAL	CIA	CaCO3	124	0,51*** (-)	4,40
EAST	CIA	CaCO3	50	0,60*** (-)	3,74
WEST	CIA	CaCO3	73	0,51*** (-)	4,54
HUA	CIA	CaCO3	26	0,03 (+)	3,11
WUD	CIA	CaCO3	27	0,03 (-)	0,81
IS	CIA	CaCO3	9	0,89*** (-)	2,36
CM	CIA	CaCO3	25	0,44*** (-)	4,76
GL	CIA	CaCO3	36	0,53*** (-)	3,38
PF	CIA	CaCO3	51	0,50*** (-)	4,77

The strong affinity of CIA and $CaCO_3$ content was clearly described in Fig 2. $CaCO_3$ as an indicator for soil acidity is one of the major parameters for soil weathering processes: the higher the $CaCO_3$ content, the lower the weathering intensity. Accordingly, the different sampling groups show high negative explained variances with higher acidity leading to enhanced weathering intensities. The highest value of 89% explained variance can be observed for IS, which is essentially due to the overall comparably high carbonate contents and insignificant clay contents (cf. Tab.

1, descriptive statistics) combined with very low weathering processes at these sites. Remarkably, carbonate dynamics within WUD and HUA are not high enough to show significant relationships.

3.2 Pedogenic oxides (PO) and pedogenic oxides ratios (POR)

3.2.1 Correlations between PO, POR, control variables, and WI

(Fed-Feo)/Fet (Arduino et al., 1984) shows the highest negative correlations with moisture parameters (Tab. 3), whereas no significant relationships are displayed for soil acidity. In contrast, Fed/Fet exhibit lower correlation coefficients for MAP and SM, but a high negative correlation with pH. Overall, the degree of activity (Feo/Fed) (Schwertmann, 1964), reacts contrarily with positive relations to moisture conditions (for a general discussion see subchapter 3.2.3).

Fep has the highest and most significant correlation with TOC contents (r=0.89). This clearly supports the idea, that pyrophosphate extracts mainly organically bound iron (Bascomb, 1968; McKeague, 1967). High organic matter contents inhibit crystallisation or even formation of iron oxides, resulting in the state of Fe fulvates (McKeague, 1967). Diverse comments questioning correlation of Fep with organic-bound Fe (e.g. Birkeland et al., 1989; Parfitt and Childs, 1988) cannot be supported by our research. Moreover, Fep correlates positively with moisture parameters and particularly with SM, whereas no significant relations to temperature variables are evident. Importantly, SM was found being the major parameter influencing TOC contents (Baumann et al., 2009) as well as soil respiration (Geng et al., 2012) positively on the Tibetan Plateau, closing the line of argument. The opposite trend can be observed for soil acidity, with both pH and $CaCO_3$ showing a comparably high correlation (see also Shi et al., 2012). Acid soil conditions correspond to inhibited turnover of organic matter and the involved formation of fulvic acids as well as humic acids (Scheffer et al., 2002). Furthermore, the latter indirectly suggests stable soil forming processes with little aeolian sediment input. The contrary situation can be frequently observed at sites with degrading permafrost (Yan et al., 2009). Fresh sediments are usually rich in carbonates inducing alkaline conditions with very low TOC contents (Baumann et al., 2009). Texture variables are only weakly correlated. Sand has a negative impact on Fep contents, which supports the above-stated relations to aeolian sedimentation.

Relationships between POR are high, while Fep reveals only low correlations to POR and none to Fed/Fet. It is crucial for the interpretation of Fep as an indicator of pedogenesis without being proportional to Fet, that Fep shows no significant correlations with Fet as the only PO-fraction (Tab. 3). Consequently, Fep results can be fully used for statistical analyses and models without taking the relation to Fet into account. Contrarily, Fed has a strong significant correlation with Fet, which renders the evaluation of POR using Fed without reference to Fet extremely vague or

impossible. Interestingly, correlation of Fep with (Fed-Feo)/Fet is negative and for Feo/Fed positive. This supports the findings, that high Fep contents are closely linked to less developed soils mainly associated with permafrost or ground water influence.

Correlations between PO and WI are low, but generally fit well to the specific characteristics of the indices. Only CPA and FENG can be significantly related to (Fed-Feo)/Fet, albeit with low correlation values. PI shows the strongest correlation with Fed/Fet, indicating similar trends in iron release. Melke (2007) found similar results in tundra soils of Spitsbergen. Otherwise, Fet-Fed correlates best with all WI except PI. This difference expresses the silicate bound iron in relation to the complete iron (Torrent and Cabedo, 1986), which of course exhibits the closest causal relation to WI. No reliable significant correlation to WI could be found for Fep, underlining its independence from general weathering processes.

3.2.2 Differences between sampling groups

Tab. 5 displays the significant different sampling groups as a result of two-tailed t-tests with $p<0.05$. Based on the correlation analyses, the two POR (Fed-Feo)/Fet and Fed/Fet as well as Fep were selected to investigate the dissimilarity between the sampling groups. With regard to POR, significant differences were found for transects and main sites. For SG, the results are similar, except CM/PF is only found different for (Fed-Feo)/Fet. Other differences were always found related to PF and GL, which are frequently influenced by redoxi-morphic processes, thus making the interpretation for POR difficult (Blume and Schwertmann, 1969; Fiedler and Sommer, 2004). The most important outcome, however, is the clear differentiation of PF and GL. This suggests considerably distinct redoxi-morphic and soil forming processes for these two SG specifically describable by PO.

As shown above, WI indicate differences between SG only by involvement of IS, whereas POR differentiate more SG clearly. WI describe the state of weathering regardless of Fe-oxides, which in turn are a very important product of soil formation processes (Kämpf et al., 2011). Consequently, POR reflect pedogenic processes much better and more in detail. To summarise, beside general limitations for the pedogenic interpretation of redoxi-morphic sites, the results are reasonable and fit well to the expected interrelations and can therefore be considered as estimations or trends.

Fep indicates a significant dissimilarity of the main sites HUA and WUD, albeit as the only PO not for EAST and WEST. Since Fep is strongly related to TOC, only SG are different, which differ greatly in TOC contents (cf. Tab. 2). GL and particularly PF account for the highest contents of TOC in the topsoil (Baumann et al., 2009) and hence are too similar.

3.2.3 Multiple linear regression model (MLR)

To account for the interrelationships as well as for the explanation capacity by combining different predictor variables, we used a multiple linear regression analysis. As independent variables we used MAT, MAP, $CaCO_3$, pH, as well as sand, silt, and clay contents. A MLR was conducted for each of the different sampling groups (TOTAL, EAST, WEST, HUA, WUD, IS, CM, GL, PF) to describe the effects on the dependent variables (POR) based on different meaningful stratification levels. Only models tested significant ($p<0.05$) were used for evaluation and interpretation (Tab. 7).

TOTAL sampling group

Based on the entire dataset (n=82) the (Fed-Feo)/Fet ratio provides the best and most reasonable result with 64% explained variance. This confirms the findings of Arduino et al. (1984) and Wagner (2005), who described this POR most useful for the estimation of the relative pedogenic age and weathering differentiation of geomorphological units. This ratio was found to be independent of varying total iron contents and general lithology, whereas Feo is low in well-weathered and high in slightly weathered samples, with Fed responding vice versa (Arduino et al., 1984). Accordingly, (Fed-Feo)/Fet parallels different weathering intensities. Moisture parameters and soil acidity are overall the most important independent parameters. Directions of the variable's effects are negative for (Fed-Feo)/Fet and Fed/Fet, however positive for Feo/Fed. Weathering intensity and iron release are lower with higher SM (cf. GL and PF sites) and pH or $CaCO_3$ contents (cf. IS sites). Very high SM values or water saturation reduce or even stop related weathering processes leading to pronounced redistribution of PO within the soil with preferential accumulation of Fed in well-aerated horizons (Blume and Schwertmann, 1969), while Fed being lowest in poorly drained soils and horizons (Fiedler and Sommer, 2004). Alkaline soil conditions inhibit feldspar weathering, iron release and thus the formation of clay minerals (Brady and Weil, 2008; Schwertmann, 1964). This is explicable by the buffer for silicate weathering and related iron release (Nesbitt et al., 1996). Respectively, soil acidity has the highest impact on Fed/Fet. Regarding texture parameters, silt and clay are mostly included into the models. Whereas higher clay contents indicate increased weathering and iron release, silt has the opposite influence in the MLR. PO commonly have a strong correlation to the clay content (McFadden and Hendricks, 1985) with high Feo and Fed values in the clay fraction, whereas Fet is texture-independent (Arduino et al., 1984). However, increased clay contents do not necessarily indicate higher in-situ weathering intensities, but can also be attributed to higher clay contents of substrates. Comparably strong chemical bond of PO and clay minerals can lead to enhanced PO contents even though overall weathering is low (McFadden and Hendricks, 1985; Schlichting and Blume, 1962; Torrent et al., 1980). Nevertheless, clayey substrates as the basis

for soil formation as well as pedogenic translocation of clay within soils are mostly uncommon on the central-eastern Tibetan Plateau. Contrarily, high silt contents, especially in topsoils, frequently indicate comparably fresh aeolian sediments (Feng et al., 2011; Schlütz and Lehmkuhl, 2009). As Feo/Fed is an expression of recent weathering activity (Schwertmann, 1964), immature and particularly redoxi-morphic soils lead to a higher Feo/Fed ratio. Consequently, moisture variables are even more dominant: higher SM leads to less developed soils and consequently to soil horizons with a high degree of recent pedogenic activity showing high contents of oxalate-extractable oxides (Schwertmann, 1964). Although being fully aware of the unreliability and instability of PO results of redoxi-morphic soils (Blume and Schwertmann, 1969; Fiedler and Sommer, 2004), the high number and diversity of samples provide a useful overall trend as well as an indication about recent pedogenetic processes. Climate parameters (MAP and MAT) are more difficult to interpret, as particularly MAT frequently indirectly reflects and describes site-specific differences (cf. discussion about correlation of WI in subchapter 3.1.4).

Albeit PO-differences are difficult to interpret without being related to Fet contents and thus only giving redundant information, they can be applied to cross-validate PO ratios and particularly to verify the directions of influence (e.g. of soil acidity). Moreover, good correspondence between Fed-Feo and (Fed-Feo)/Fet gives indirect evidence that – general parameters are to be similar – also PO-differences or POR without direct relation to Fet may provide reasonable results and can be discussed pedogenetically for the respective subsample set.

Variation of Fep can be explained with the included parameters by 63%. Soil acidity is most important, followed by SM; both closely linked to TOC (cf. correlation analyses Tab. 3). Soils with fresh aeolian sedimentation have low soil organic matter and high carbonate contents; the latter is the specific reason for the link between pH and soil organic matter in the research area. Generally, high organic matter contents hamper crystallisation of mineral surfaces of amorphous ferric hydroxides (Schwertmann, 1966) thus leading to higher Feo and Fep contents. As shown above, Fep can interpreted without relation to Fet contents, because it is mainly linked to organic matter.

EAST / WEST sampling group

EAST (n=32) has the higher p-values and greater differences between multiple R^2 and corrected R^2 for all POR, which indicates a lower explanation level than for WEST (n=50) or TOTAL. Moisture parameters and soil acidity calculate comparably to TOTAL, whereas for texture, the extreme site E2 with its high contents of partly pre-weathered and redeposited silty-sandy material is responsible for biases as well as for the vice versa influencing direction of clay (cf. subchapter 2.1). Overall, weathering intensities are lower for EAST compared to some western sites lo-

cated around Nagqu (cf. Cambisols in W6/W7), where iron release and clay formation is higher and more noticeable in regression analyses. Additionally, the climate conditions of all four sites of EAST are rather similar, whereas distinct climate differences are evident along the western transect. Therefore, climate parameters are not included into the MLR for EAST. Altogether, WEST shows the greater explained variances and highly significant results, with SM being more dominant than for EAST.

However, MAT and some acidity parameters show opposite directions than expected for WEST, which can be related to a much broader variety of geogenic background for the different sites (cf. ternary diagrams, Fig. 3a). Consequently, these results for WEST have to be interpreted with care, particularly for ratios without relation to Fet. Nevertheless, for both subsamples, the main outcomes fit well into the general context.

As described for TOTAL, Fe-differences are not interpretable without relation to Fet. This can be demonstrated by Fet-Fed (silicate-bound iron). The MLR is highly significant for WEST but not for EAST, which is caused by higher differences of silicate-bound iron between sites in WEST (cf. ternary diagrams indicate inhomogeneity, Fig. 3a).

Fep displays very low p-values and differences between multiple R^2 and corrected R^2. Soil acidity is dominant for EAST, whereas SM is the most important parameter for WEST. The higher explained variance for EAST is due to the more pronounced small-scale variability of SM and TOC as a result of discontinuous permafrost conditions.

To summarise, settings of EAST are climatically and geologically more homogenous. However, small-scale variability of SM conditions is higher in discontinuous permafrost (cf. Zhang et al., 2003). There are more extreme sites in EAST (Tab. 2); e.g. being either very moist or dry with relatively fresh sedimentary layers. Overall, the environment in discontinuous permafrost areas is more unstable than in continuous permafrost. Other parameters, such as relief position, changing vegetative cover and slope or geomorphologic activities like sedimentation by wind and water overprint the direct effects of SM (Wang et al., 2010; Zhang et al., 2003).

HUA / WUD sampling group

WUD (n=21) shows for (Fed-Feo)/Fet the highest observed explained variance with 85% ($p<0.001$) of all sampling groups and corresponding dependent variables. SM has the highest influence equally followed by clay and soil acidity. Contrarily, even though mean and variance of SM are much higher (Tab. 3), moisture parameters are not included in HUA (n=22). In contrast, soil acidity and texture having a dominant influence, leading to the assumption that moisture conditions are too similar in HUA and differences in texture / sediment composition are more

prominent within the model. The latter could be also linked to the zone of discontinuous permafrost with recently more active sedimentary processes. For Feo/Fed, the same parameters as for (Fed-Feo)/Fet are selected for both sites with exactly vice versa directions of influence in the MLR. This is confirming homogenous substrate and parent material for both main sites HUA and WUD, because Feo/Fed is calculated without reference to Fet (cf. subchapter 3.2.1). Accordingly, ratios without relation to Fet can be evaluated likewise for each of the main sites. However, the model for HUA calculates slightly insignificant (p=0.08) and also the significance for WUD is much higher for Feo/Fed (p=0.03) than for (Fed-Feo)/Fet (p=0.0008). Thus it can be said, that the degree of activity acts very indifferent and unstable for both sites. For Fed/Fet, HUA has the lower p-value and higher R^2, whereas WUD plots above the significance level. Hence, the degree of iron release varies more in HUA, which can be related to discontinuous permafrost and more complex sedimentary layers and processes.

This situation can also be observed and discussed for PO-differences. Much lower p-values than for POR and very high prediction accuracies (R^2=0.89 for WUD, R^2=0.44 for HUA) can be observed for Fed-Feo. Thus, the portion of well-crystallized iron oxides causes the main difference in the performance of (Fed-Feo)/Fet and Fed/Fet (Arduino et al., 1984). The variation of Feo and Fed is obviously lower in WUD, which can be observed for HUA vice versa (Tab. 2, variance and standard deviation). Together with the lower mean Feo and Fed contents of WUD, this provides more stable conditions for the MLR and less active weathering processes (Fig.1 and Fig. 2). For Fet-Fed, p-values are very low with high R^2, implying that silicate bound iron can be precisely described by only few parameters. Grain size parameters and in particular clay content contribute the most to the models. Higher clay content leads to a larger ΔFet/Fed with increasing Fet contents but stable Fed values. As described above, lower soil acidity also leads to a higher difference between Fet and Fed contents. Fed is appropriately linked to lower pH-values or $CaCO_3$ contents. Clay and $CaCO_3$ explain 86% of the variation for WUD. These very solid results are helpful to interpret other more inhomogeneous sampling groups correspondingly.

Fep only indicates multiple regressions with p-values around 0.05. The variation within sites is obviously not high enough, but results of MLR fit well into context (Tab. 7). Especially WUD is rather uniform concerning to TOC and SM contents (Tab. 2), thus including other variables into the model.

SG sampling groups

Since for SG soil profiles from different sites and transects are grouped together, the preconditions for soil formation and weathering are not uniform across sites. Notably, bedrock and substrates differ quite considerably (Fig. 3). This hampers the possibility of interpretation for ratios

without relation to Fet and allows only inferring rough trends and estimations. Additionally, the sample set size for MLR analyses is very low in some groups (e.g. IS and CM) making results partly not evaluable. (Fed-Feo)/Fet can only be described significantly for GL and PF; CM calculates only slightly below significance level, whereas the directions indicated by the incorporated independent variables fit well into the general concept. There is a clear difference evident between GL and PF subsamples: whereas SM is a highly significant variable for GL, PF shows general site-specific climatic parameters having the highest influence. This reflects the general preconditions required for permafrost distribution (climate-zonal soil formation). Contrarily, GL soils are linked to a greater degree to specific relief positions and can be found at all different climate conditions of the research area (azonal soil formation). The latter is also reflected by the lowest p-value for GL, indicating that direct influencing variables have a much higher impact for this sampling group. Weathering and activities related to pedogenic oxides are higher in GL because these soils also occur under warmer and moister climate conditions. Accordingly, more intense common soil forming and redoxi-morphic processes are evident, which are weakened at PF sites. Cambisol dynamics can be well demonstrated by Fed/Fet. Both the included parameters and the directions of influences are in close relation to relevant soil forming processes in Cambisols. The difference between GL and PF is also evident for this ratio. Generally, interpretation of GL is very difficult because of the complex and fast-changing processes within and between the different iron oxide fractions (see subchapter 3.2.2).

In terms of Fet-Fed, CM shows the highest significance followed by PF (both $p<0.001$), whereas GL does not reveal a significant model ($p>0.05$). Silicate-bound iron is linked to CM and PF since a higher dynamic can be found in these groups: small-scale pattern of fresh (frequently airborne) sediments and chemically weathered material.

Most importantly, only PF is significant on a very high level for Fep. Soil acidity and SM are the dominant parameters influencing the MLR in the expected directions. Lower pH means higher Fep contents (cf. strong relationship to TOC). It is an essential outcome that Fep contents very clearly differentiate GL and PF soil groups (cf. subchapter 3.2.2). This is mainly due to specific redoxi-morphic processes, soil formation processes and dynamics with corresponding organic matter under the influence of permafrost (Baumann et al., 2009; Dörfer et al., 2013). Further research is needed to gain closer insights regarding these particular relationships.

Table 7 Summary of the multiple linear regression model (MLR). The level of significance is marked (*** $p < 0.001$; ** $p < 0.01$; * $p < 0.05$; others $p > 0.05$). Directions of influence indicated by [+] for positive and [-] for negative effects of the variable on the MLR.

	POR	Variables – Ranked by significance	RSquared	RSquared adj.	Significance
TOTAL	Fed/Fet	MAP*** [-], pH*** [-], SM** [-], Silt* [-], Clay [+], MAT [-]	0.55	0.51	***
	(Fed-Feo)/Fet	MAP*** [-], SM*** [-], pH*** [-], MAT [-], Silt [-], Clay [+]	0.64	0.62	***
	Feo/Fed	SM*** [+], MAP*** [+], pH* [+], Silt [+], MAT [+], Clay [-]	0.49	0.45	***
	Fep	pH*** [-], SM*** [+], Sand* [+], Clay [+], MAP [+], MAT [+]	0.63	0.60	***
	Fet-Fed	MAP*** [+], pH*** [+], Sand*** [-], MAT [+], Clay [+], SM [-]	0.50	0.46	***
	Fed-Feo	SM*** [-], MAP*** [-], Clay* [+], pH* [-], Silt [+], MAT [+]	0.59	0.55	***
EAST	Fed/Fet	pH*** [-], SM [-], Clay [-], Sand [+]	0.41	0.32	**
	(Fed-Feo)/Fet	pH** [-], SM** [-], Clay [-], Silt [+]	0.44	0.36	**
	Feo/Fed	SM* [+], MAT [+], Silt [+], Clay [+]	0.35	0.26	*
	Fep	pH*** [-], SM [+], Clay [-], Silt [+]	0.75	0.71	***
	Fed-Feo	pH** [-], SM** [-], Clay [-], Silt [-]	0.42	0.33	**
WEST	Fed/Fet	MAT*** [-], $CaCO_3$* [-], Clay* [+], SM* [-], pH [+], Sand [+], MAP [+]	0.42	0.33	***
	(Fed-Feo)/Fet	SM*** [-], MAT*** [-], pH [+], Clay [+], Sand [-], $CaCO_3$ [-], MAP [+]	0.65	0.59	***
	Feo/Fed	SM*** [+], Sand** [+], MAT** [+], $CaCO_3$ [-], pH [-], Clay [+], MAP [+]	0.70	0.65	***
	Fep	SM*** [+], Clay* [+], pH [-], Sand [+], MAP [+], MAT [-], $CaCO_3$[-]	0.67	0.62	***
	Fet-Fed	Sand*** [-], MAT*** [+], SM*** [-], pH [+], $CaCO_3$ [-], MAP [-], Clay [-]	0.85	0.83	***
	Fed-Feo	SM*** [-], Sand*** [-], pH [+], $CaCO_3$ [-], MAT [-], Clay [+], MAP [-]	0.61	0.54	***
HUA	Fed/Fet	$CaCO_3$** [-], SM** [-], Clay [+], pH [-]	0.76	0.67	**
	(Fed-Feo)/Fet	$CaCO_3$** [-], Silt* [-], Clay [+], pH [-]	0.52	0.40	*
	Fep	SM [+], pH [-], Clay [-], $CaCO_3$ [-]	0.58	0.42	*
	Fet-Fed	Clay*** [+], Silt* [-], pH [+], $CaCO_3$ [+]	0.80	0.75	***
	Fed-Feo	$CaCO_3$** [-], Silt* [-], Clay [+], pH [+]	0.55	0.44	**
WUD	Fed/Fet	SM [-], pH [+], $CaCO_3$ [-]	0.42	0.28	
	(Fed-Feo)/Fet	SM** [-], Clay** [+], $CaCO_3$ [-]	0.90	0.85	***
	Feo/Fed	Clay* [-], SM [+], $CaCO_3$ [+]	0.72	0.59	*
	Fep	Clay* [-], $CaCO_3$ [+], SM [+]	0.64	0.48	

Table 7 continued

	POR	Variables – Ranked by significance	RSquared	RSquared adj.	Significance
WUD	Fet-Fed	Clay*** [+], $CaCO_3$ [+]	0.87	0.86	***
	Fed-Feo	Clay*** [+], SM* [-], $CaCO_3$ [-]	0.92	0.89	***
CM	Fed/Fet	pH* [-], MAP [-], Sand [+], SM [-]	0.55	0.43	*
	(Fed-Feo)/Fet	pH [-], MAP [+], Sand [+], SM [-]	0.46	0.31	
	Fet-Fed	Sand*** [-], pH [+], MAP [+], SM [-]	0.86	0.82	***
	Fed-Feo	Sand** [-], SM [-], MAP [-], pH [-]	0.69	0.61	**
GL	Fed/Fet	MAP*** [-], pH* [-], MAT [+], Sand [-], SM [-]	0.70	0.62	***
	(Fed-Feo)/Fet	MAP*** [-], SM** [-], MAT [+], pH [-], Sand [-]	0.72	0.65	***
	Feo/Fed	MAP** [+], SM* [+], Sand [-], MAT [-], pH [-]	0.60	0.50	**
	Fed-Feo	MAT [-], MAP [+], Silt [+], pH [+], SM [+], Clay [+]	0.67	0.59	***
PF	Fed/Fet	pH** [-], MAP** [-], MAT* [-], Clay [+], Sand [+], SM [+]	0.52	0.38	*
	(Fed-Feo)/Fet	MAP** [-], MAT* [-], pH [-], Clay [+], SM [-], Sand [-]	0.59	0.46	**
	Feo/Fed	MAP [+], SM [+], Sand [+], MAT [+], Clay [+], pH [+]	0.59	0.46	**
	Fep	$CaCO_3$*** [-], SM [+], Clay [+], Sand [-], MAT [+]	0.72	0.65	***
	Fet-Fed	pH*** [+], MAP*** [+], Sand [-], Clay [+], MAT [+], SM [+]	0.66	0.56	***
	Fed-Feo	MAP* [-], MAT [-], Clay [+], Sand [-], pH [-], SM [-]	0.55	0.41	**

4 Conclusions

WI, PO fractions, and POR were successfully applied to describe distinct patterns of weathering and pedogenesis for climatic gradients along and between two north-south oriented transects across the Tibetan Plateau. WI proved to mainly indicate long-term climatically induced weathering processes. Besides varying weathering duration and intensities under different climate and permafrost conditions, PO and POR additionally reflect soil formation processes on a small spatial scale depending on relief position and substrate genesis. However, at sites influenced by redox processes, Al-based WI provide more stable tools than PO for describing weathering conditions. Prevailing permafrost environments are crucial for WI and PO, showing clear differences between continuous, discontinuous, and sporadic permafrost as well as amongst degraded and non-degraded sites. This accounts particularly for the strong relationship between SM and PO ratios.

CIA proved to be the most useful and reasonable WI for assessing weathering intensities of recent soils in permafrost ecosystems, if $CaCO_3$ had been analysed in the laboratory allowing concise calculation of CaO*. According to CIA, half of all samples can be described as not or only slightly weathered. Almost 25% plot below or slightly above the feldspar join, emphasising the overall low weathering intensities. Nevertheless, the two main sites HUA and WUD can be explicitly differentiated in terms of parent material and weathering conditions by CIA. Moreover, climate trends and permafrost conditions along transects EAST and WEST can be highlighted (cf. Fig. 3).

For POR, (Fed-Feo)/Fet provides the best results with 64% explained variation by the MLR for TOTAL, showing lower weathering intensities and iron release associated with higher SM and soil acidity. Another important finding is the clear differentiability between the soil groups GL and PF, and thus among distinct redoxi-morphic and soil forming processes specifically describable by PO. Whereas SM is most important in the MLR analysis for GL, PF rather reflects general site-specific climatic parameters (zonal pedogenesis). Thus, GL is linked to a greater extend to particular relief positions and can be basically found under all climate conditions of the research area (azonal pedogenesis). It could be demonstrated that pyrophosphate extracts mainly organically bound pedogenic iron indicated by the high correlation to TOC (r=0.89). Fep correlates highly positively with SM, whereas no significant relations to temperature variables are evident. Correlation of Fep with (Fed-Feo)/Fet is negative and for Feo/Fed positive, supporting our findings that high Fep contents are closely linked to less developed and weathered soils, mainly associated with permafrost or ground water influence. Most importantly, PF is the only soil group showing a highly significant MLR for Fep. It is an essential outcome, that Fep contents clearly distinguish GL and PF soil groups, even though both typically reveal considerably high SM and TOC contents. It is crucial for a pedogenic interpretation that Fep shows no significant correla-

tions with Fet, thus Fep can be fully included into statistical analyses and models without relation to Fet.

For many profiles, notably in discontinuous permafrost, distinct lower weathering intensities can be observed for the top horizons compared to the subsoil. Beside the disconnection of turf-like topsoils from the mineral soil body, this also reflects a recent input of aeolian sediments, mainly derived from proximal source areas with related permafrost degradation processes. These processes have led to the multi-layered soil profiles predominating in the research area. Small-scale variability, particularly of SM conditions, is higher in discontinuous permafrost areas (EAST). Overall, the environment in discontinuous permafrost areas is more unstable and other parameters, such as relief position and slope or geomorphologic activities like sedimentation by wind and water are more important overprinting the direct effect of SM on weathering and pedogenesis.

To summarise, WI and POR provide promising tools to depict and evaluate both recent and past phases of instability and permafrost degradation processes, amplified by interrelated feedback mechanisms between global change and human activities over the past decades.

5 Acknowledgements

The authors would like to thank members of the Peking University expedition team and particularly Wang Liang, Yang Kuo, Mou Shanmin, Qi Shanxue, Yang Xiaoxia and Mi Zhaorong for accompanying the field work. This research was supported by the National Natural Science Foundation of China (NSFC Grant 31025005 and 31270481 to JSH) and a graduation fellowship from the state of Baden-Württemberg, Germany (Grant No. VI 4.2 – 661 7631.2/Baumann). We thank Sabine Flaiz, Christian Wolf and Katrin Drechsel for assistance with the laboratory works and Dr. Heinrich Taubald for X-ray fluorescence analyses.

6 References

Alexander, E.B., 1985. Estimating relative ages from iron-oxide/total-iron ratios of soils in the Western Po Valley, Italy - a discussion. Geoderma 35, 257–259.

Aniku, J.R., Singer, M.J., 1990. Pedogenic iron oxide trends in a marine terrace chronosequence. Soil Science Society of America Journal 54, 147–152.

An, Z., Kutzbach, J.E., Prell, W.L., Porter, S.C., 2001. Evolution of Asian monsoons and phased uplift of the Himalaya-Tibetan Plateau since Late Miocene times. Nature 411, 62–66.

Arduino, E., Barberis E., Carraro F., Forno M.G., 1984. Estimating relative ages from iron-oxide/total-iron ratios of soils in the western Po Valley, Italy. Geoderma 33, 39–52.

Bascomb, C., 1968. Distribution of pyrophosphate-extractable iron and organic carbon in soils of various groups. Eur J Soil Science 19 (2), 251–268.

Baumann, F., He, J.-S., Schmidt, K., Kühn, P., Scholten, T., 2009. Pedogenesis, permafrost, and soil moisture as controlling factors for soil nitrogen and carbon contents across the Tibetan Plateau. Global Change Biology 15 (12), 3001–3017. doi:10.1111/j.1365-2486.2009.01953.x.

Bäumler, R., 2001. Pedogenic studies in aeolian deposits in the high mountain area of eastern Nepal. Quaternary International 76/77, 93–102.

Bäumler, R., Zech, W., 2000. Quaternary paleosols, tephra deposits and landscape history in South Kamchatka, Russia. Catena 41, 199–215.

Birkeland, P.W., Burke, R.M., Benedict, J.B., 1989. Pedogenic gradients for iron and aluminium accumulation and phosphorus depletion in arctic and alpine soils as a function of time and climate. Quaternary Research 32, 193–204.

Blume, H.P., Schwertmann, U., 1969. Genetic evaluation of profile distribution of aluminium, iron, and manganese oxides. Soil Science Society of America Proceedings 33, 438–444.

Brady, N.C., Weil, R.R., 2008. The nature and properties of soils, 14th ed. Pearson Prentice Hall, Upper Saddle River, N.J, xiv, 965.

Buero, V., Schwertmann, U., 1987. Occurance and transformations of iron and manganese in a colluvial Terra Rossa toposequence of Northern Italy. Catena 14, 519–531.

Buggle, B., Glaser, B., Hambach, U., Gerasimenko, N., Marković, S., 2011. An evaluation of geo-chemical weathering indices in loess–paleosol studies. Quaternary International 240 (1-2), 12–21. doi:10.1016/j.quaint.2010.07.019.

Buggle, B., Glaser, B., Zöller, L., Hambach, U., Marković, S., Glaser, I., Gerasimenko, N., 2008. Geochemical characterization and origin of Southeastern and Eastern European loesses (Serbia, Romania, Ukraine). Quaternary Science Reviews 27 (9-10), 1058–1075. doi:10.1016/j.quascirev.2008.01.018.

Chapin III, F.S., Zavaleta, E.S., Eviner, V.T., Naylor, R.L., Vitousek, P.M., Reynolds, H.L., Hooper, D.U., Lavorel, S., Sala, O.E., Hobbie, S.E., Mack, M.C., Díaz, S., 2000. Consequences of changing biodiversity. Nature 405 (6783), 234–242. doi:10.1038/35012241.

Cheng, G., 2005. Permafrost studies in the Qinghai–Tibet Plateau for road construction. Journal of Cold Regions Engineering 19 (1), 19–29. doi:10.1061/(ASCE)0887-381X(2005)19:1(19).

Cheng, G., Wu, T., 2007. Responses of permafrost to climate change and their environmental significance, Qinghai-Tibet Plateau. J. Geophys. Res. 112 (F2). doi:10.1029/2006JF000631.

Cullers, R.L., 2000. The geochemistry of shales, siltstones and sandstones of Pennsylvanian–Permian age, Colorado, USA: implications for provenance and metamorphic studies. Lithos 51, 181–203.

Dahms, D., Favilli, F., Krebs, R., Egli, M., 2012. Soil weathering and accumulation rates of oxalate-extractable phases derived from alpine chronosequences of up to 1Ma in age. Geomorphology 151-152, 99–113. doi:10.1016/j.geomorph.2012.01.021.

Dai, F., Su, Z., Liu, S., Liu, G., 2011. Temporal variation of soil organic matter content and potential determinants in Tibet, China. Catena 85 (3), 288–294. doi:10.1016/j.catena.2011.01.015.

Diaz, M.T.J., 1989. Mineralogy of iron oxides in two soil chronosequences of central Spain. Catena 16, 291–299.

Dietze, E., Hartmann, K., Diekmann, B., IJmker, J., Lehmkuhl, F., Opitz, S., Stauch, G., Wünnemann, B., Borchers, A., 2012. An end-member algorithm for deciphering modern detrital processes from lake sediments of Lake Donggi Cona, NE Tibetan Plateau, China. Sedimentary Geology 243-244, 169–180. doi:10.1016/j.sedgeo.2011.09.014.

Domrös, M., Peng, G., 1988. The Climate of China. Springer, Berlin, Heidelberg, NewYork.

Dörfer, C., Kühn, P., Baumann, F., He, J.-S., Scholten, T., Slomp, C.P., 2013. Soil organic carbon pools and stocks in permafrost-affected soils on the Tibetan Plateau. PLoS ONE 8 (2), e57024. doi:10.1371/journal.pone.0057024.

Duzgoren-Aydin, N., Aydin, A., Malpas, J., 2002. Re-assessment of chemical weathering indices: case study on pyroclastic rocks of Hong Kong. Engineering Geology 63, 99–119.

Fang, J., Piao, S., Tang, Z., Peng, C., Ji, W., 2001. Interannual variability in net primary production and precipitation. Science 293 (5536), 1723a. doi:10.1126/science.293.5536.1723a.

FAO, 2006. Guidlines for Soil Description, 4th edn., Rome, 98 pp.

Fedo, C.M., Nesbitt, W.H., Young, G.M., 1995. Unraveling the effects of potassium metasomatism in sedimentary rocks and paleosols, with implications for paleoweathering conditions and provenance. Geol 23 (10), 921. doi:10.1130/0091-7613(1995)023<0921:UTEOPM>2.3.CO;2.

Feng, J.-L., Hu, Z.-G., Ju, J.-T., Zhu, L.-P., 2011. Variations in trace element (including rare earth element) concentrations with grain sizes in loess and their implications for tracing the provenance of eolian deposits. Quaternary International 236 (1-2), 116–126. doi:10.1016/j.quaint.2010.04.024.

Feng, J.-L., Zhu, L.-P., 2009. Origin of terra rossa on Amdo North Mountain on the Tibetan Plateau, China: Evidence from quartz. Soil Science and Plant Nutrition 55 (3), 407–420. doi:10.1111/j.1747-0765.2009.00370.x.

Feng, Z.-D., 1997. Geochemical characteristics of a loess-soil sequence in central Kansas. Soil Science Society of America Journal 61, 534–541.

Fiedler, S., Sommer, M., 2004. Water and redox conditions in wetland soils - their influence on pedogenic oxides and morphology. Soil Science Society of America Journal 68, 326–335.

Gallet, S., Jahn, B., van Vliet Lanoe, B., Dia, A., Rossello, E., 1998. Loess geochemistry and its implications for particle origin and composition of the upper continental crust. Earth and Planetary Science Letters 156, 157–172.

Gao, Q., Li, Y., Wan, Y., Lin, E., Xiong, W., Jiangcun, W., Wang, B., Li, W., 2006. Grassland degradation in Northern Tibet based on remote sensing data. J GEOGR SCI 16 (2), 165–173. doi:10.1007/s11442-006-0204-1.

Geng, Y., Wang, Y., Yang, K., Wang, S., Zeng, H., Baumann, F., Kuehn, P., Scholten, T., He, J.-S., Bond-Lamberty, B., 2012. Soil respiration in Tibetan alpine grasslands: belowground biomass and soil moisture, but not soil temperature, best explain the large-scale patterns. PLoS ONE 7 (4), e34968. doi:10.1371/journal.pone.0034968.

Harnois, L., 1988. The CIW index: a new chemical index of weathering. Sedimentary Geology 55, 319–322.

He, J.-S., Wang, X., Flynn, D.F.B., Wang, L., Schmid, B., Fang, J., 2009. Taxonomic, phylogenetic, and environmental trade-offs between leaf productivity and persistence. Ecology 90 (10), 2779–2791. doi:10.1890/08-1126.1.

He, J.-S., Wang, Z., Wang, X., Schmid, B., Zuo, W., Zhou, M., Zheng, C., Wang, M., Fang, J., 2006. A test of the generality of leaf trait relationships on the Tibetan Plateau. New Phytol 170 (4), 835–848. doi:10.1111/j.1469-8137.2006.01704.x.

Hu, H., Wang, G., Liu, G., Li, T., Ren, D., Wang, Y., Cheng, H., Wang, J., 2009. Influences of alpine ecosystem degradation on soil temperature in the freezing-thawing process on Qinghai–Tibet Plateau. Environ Geol 57 (6), 1391–1397. doi:10.1007/s00254-008-1417-7.

IUSS Working Group WRB, 2006. World reference base for soil resources. World Soil Resources Reports (103).

Jenny, H., 1994. Factors of soil formation: A system of quantitative pedology. Dover, New York, xviii, 281.

Jin, H., Li, S., Cheng, G., Shaoling, W., Li, X., 2000. Permafrost and climatic change in China. Global and Planetary Change 26, 387–404.

Kaiser, K., 2004. Pedogeomorphological transect studies in Tibet: implications for landscape history and present-day dynamics. Prace Geograficzne 200, 147–165.

Kaiser, K., Miehe, G., Barthelmes, A., Ehrmann, O., Scharf, A., Schult, M., Schlütz, F., Adamczyk, S., Frenzel, B., 2008. Turf-bearing topsoils on the central Tibetan Plateau, China: Pedology, botany, geochronology. Catena 73 (3), 300–311. doi:10.1016/j.catena.2007.12.001.

Kaiser, K., Schoch, W.H., Miehe, G., 2007. Holocene paleosols and colluvial sediments in Northeast Tibet (Qinghai Province, China): Properties, dating and paleoenvironmental implications. Catena 69 (2), 91–102. doi:10.1016/j.catena.2006.04.028.

Kämpf, N., Scheinost, A.C., Schulze, D.G., 2011. Oxide Minerals, in: Huang, P., Li Y., Sumner M.E (Eds.), Handbook of Soil Science, Properties and Processes. Part III: Soil Mineralogy. CRC Press, pp. 125–168.

Kang, S., Xu, Y., You, Q., Flügel, W.-A., Pepin, N., Yao, T., 2010. Review of climate and cryospheric change in the Tibetan Plateau. Environ. Res. Lett. 5 (1), 15101. doi:10.1088/1748-9326/5/1/015101.

Kimble, J. (Ed.), 2004. Cryosols. Permafrost-Affected Soils. Springer, Berlin.

Kronberg, B., Nesbitt, H.W., 1981. Quantification of weathering, soil geochemistry and soil fertility. Eur J Soil Science 32, 453–459.

Kühn, P., Techmer, A., Weidenfeller, M., 2013. Lower to middle Weichselian pedogenesis and palaeoclimate in Central Europe using combined micromorphology and geochemistry: the loess-paleosol sequence of Alsheim (Mainz Basin, Germany). Quaternary Science Reviews 75, 43–58. doi:10.1016/j.quascirev.2013.05.019.

Mahaney, W., Fahey, B., 1980. Morphology, composition and age of a buried paleosol, Front Range, Colorado, U.S.A. Geoderma 23, 209–218.

McFadden, L.D., Hendricks, D.M., 1985. Changes in the Content and Composition of Pedogenic Iron Oxyhydroxides in a Chronosequence of Soils in Southern California. Quaternary Research 23, 189–204.

McKeague, J.A., 1967. An evaluation of 0.1 M pyrophosohate and pyrophasphate-dithionite in comparison with oxalate as extractants of the accumulation products in podzols and some other soils. Can. J. Soil Sci. 47, 95–99.

McLennan, S.M., 1993. Weathering and Global Denudation. The Journal of Geology 101 (2), 295–303.

Mehra, O., Jackson, M., 1960. Iron oxide removal from soils and clays by a dithionite-citrate buffered with sodium bicarbonats. Clays Clay Mineral. 7, 317–327.

Melke, J., 2007. Weathering Processes in the Soils of Tundra of Western Spitsbergen. Polish Journal of Soil Science 40 (2), 217–226.

Mirabella, A., Carnicelli, S., 1992. Iron oxide mineralogy in red and brown soils developed on calcareous rocks in central Italy. Geoderma 55, 95–109.

Nesbitt, H.W., Young, G.M., 1982. Early Proterozoic climates and plate motions inferred from major element chemistry of lutites. Nature 299, 715–717.

Nesbitt, H.W., Young, G.M., 1984. Prediction of some weathering trends of plutonic and volcanic rocks based on thermodynamic and kinetic considerations. Geochimica et Cosmochimica Acta 48, 1523–1534.

Nesbitt, H.W., Young, G.M., McLennan, S., Keays, R., 1996. Effects of chemical weathering and sorting on the petrogenesis of siliciclastic sediments, with implications for provenance studies. The Journal of Geology 104, 525–542.

Niu, F., Lin, Z., Liu, H., Lu, J., 2011. Characteristics of thermokarst lakes and their influence on permafrost in Qinghai–Tibet Plateau. Geomorphology 132 (3-4), 222–233. doi:10.1016/j.geomorph.2011.05.011.

Parfitt, R., Childs, C., 1988. Estimation of forms of Fe and Al: A review, and analysis of contrasting soils by dissolution and Moessbauer methods. Australian Journal of Soil Research 26, 121–144.

Parker, A., 1970. An index of weathering for silicate rocks. Geological Magazine 107, 501–504.

Ping, C.-L., Qiu, G., Zhao, L., 2004. The periglacial environment of China, in: Kimble, J. (Ed.), Cryosols. Permafrost-Affected Soils. Springer, Berlin, pp. 275–291.

Price, J.R., Velbel, M.A., 2003. Chemical weathering indices applied to weathering profiles developed on heterogeneous felsic metamorphic parent rocks. Chemical Geology 202 (3-4), 397–416. doi:10.1016/j.chemgeo.2002.11.001.

Qiu, J., 2008. China: The third pole. Nature 454 (7203), 393–396. doi:10.1038/454393a.

Rezapour, S., Jafarzadeh, A.A., Samadi, A., Oustan, S., 2010. Distribution of iron oxides forms on a transect of calcareous soils, north-west of Iran. Archives of Agronomy and Soil Science 56 (2), 165–182. doi:10.1080/03650340902956660.

Sauer, D., Wagner, S., Brückner, H., Scarciglia, F., Mastronuzzi, G., Stahr, K., 2010. Soil development on marine terraces near Metaponto (Gulf of Taranto, southern Italy). Quaternary International 222 (1-2), 48–63. doi:10.1016/j.quaint.2009.09.030.

Scheffer, F., Schachtschabel, P., Blume, H.-P., 2002. Lehrbuch der Bodenkunde, 15th ed. Spektrum, Akad. Verl., Heidelberg [u.a.], XIV, 593 S.

Schlichting, E., Blume, H.-P., 1962. Art und Ausmaß der Veränderungen des Bestandes mobiler Oxyde in Böden aus jungpleistozänem Geschiebemergel und ihren Horizonten. J. Plant Nutr. Soil Sci. 96, 144–156.

Schlütz, F., Lehmkuhl, F., 2009. Holocene climatic change and the nomadic Anthropocene in Eastern Tibet: palynological and geomorphological results from the Nianbaoyeze Mountains. Quaternary Science Reviews 28 (15-16), 1449–1471. doi:10.1016/j.quascirev.2009.01.009.

Schwertmann, U., 1964. Differenzierung der Eisenoxide des Bodens durch Extraktion mit Ammoniumoxalat-Lösung. J. Plant Nutr. Soil Sci. 105, 194–202.

Schwertmann, U., 1966. Inhibitory Effect of Soil Organic Matter on the Crystallization of Amorphous Ferric Hydroxide. Nature 212 (5062), 645–646. doi:10.1038/212645b0.

Shi, Y., Baumann, F., Ma, Y., Song, C., Kühn, P., Scholten, T., He, J.-S., 2012. Organic and inorganic carbon in the topsoil of the Mongolian and Tibetan grasslands: pattern, control and implications. Biogeosciences 9 (6), 2287–2299. doi:10.5194/bg-9-2287-2012.

Torrent, J., Cabedo, A., 1986. Sources of iron oxides in reddish brown soil profiles from calcarenites in southern Spain. Geoderma 37, 57–66.

Torrent, J., Liu, Q., Bloemendal, J., Barrón, V., 2007. Magnetic Enhancement and Iron Oxides in the Upper Luochuan Loess–Paleosol Sequence, Chinese Loess Plateau. Soil Science Society of America Journal 71 (5), 1570. doi:10.2136/sssaj2006.0328.

Torrent, J., Schwertmann, U., Schulze, D.G., 1980. Iron oxide mineralogy of some soils of two river terrace swquences in Spain. Geoderma 23, 191–208.

Vitousek, P.M., 1997. Human Domination of Earth's Ecosystems. Science 277 (5325), 494–499. doi:10.1126/science.277.5325.494.

Wagner, M., 2005. Geomorphological and pedological investigations on the glacial history of the Kali Gandaki (Nepal Himalaya). GeoJournal 63 (1-4), 91–113. doi:10.1007/s10708-005-2397-8.

Wang, B., French, H.M., 1994. Climate controls and high-altitude permafrost, Qinghai-Xizang (Tibet) Plateau, China. Permafrost Periglac. Process. 5 (2), 87–100. doi:10.1002/ppp.3430050203.

Wang, G., Bai, W., Li, N., Hu, H., 2011. Climate changes and its impact on tundra ecosystem in Qinghai-Tibet Plateau, China. Climatic Change 106 (3), 463–482. doi:10.1007/s10584-010-9952-0.

Wang, G., Liu, L., Liu, G., Hu, H., Li, T., 2010. Impacts of grassland vegetation cover on the active-layer thermal regime, northeast Qinghai-Tibet Plateau, China. Permafrost Periglac. Process. 21 (4), 335–344. doi:10.1002/ppp.699.

Wang, S., Jin, H., Li, S., Zhao, L., 2000. Permafrost degradation on the Qinghai-Tibet Plateau and its environmental impacts. Permafrost Periglac. Process. 11, 43–53.

Xue, X., Guo, J., Han, B., Sun, Q., Liu, L., 2009. The effect of climate warming and permafrost thaw on desertification in the Qinghai–Tibetan Plateau. Geomorphology 108 (3-4), 182–190. doi:10.1016/j.geomorph.2009.01.004.

Yan, C., Song, X., Zhou, Y., Duan, H., Li, S., 2009. Assessment of aeolian desertification trends from 1975's to 2005's in the watershed of the Longyangxia Reservoir in the upper reaches of China's Yellow River. Geomorphology 112 (3-4), 205–211. doi:10.1016/j.geomorph.2009.06.003.

Yang, M., Nelson, F.E., Shiklomanov, N.I., Guo, D., Wan, G., 2010. Permafrost degradation and its environmental effects on the Tibetan Plateau: A review of recent research. Earth-Science Reviews 103 (1-2), 31–44. doi:10.1016/j.earscirev.2010.07.002.

Yang, S., Jung, H.-S., Li, C., 2004. Two unique weathering regimes in the Changjiang and Huanghe drainage basins: geochemical evidence from river sediments. Sedimentary Geology 164 (1-2), 19–34. doi:10.1016/j.sedgeo.2003.08.001.

Yang, Y., Fang, J., Smith, P., Tang, Y., Chen, A., Ji, C., Hu, H., Rao, S., Tan, K., He, J.-S., 2009. Changes in topsoil carbon stock in the Tibetan grasslands between the 1980s and 2004. Global Change Biology 15 (11), 2723–2729. doi:10.1111/j.1365-2486.2009.01924.x.

Yang, Z., Ouyang, H., Zhang, X., Xu, X., Zhou, C., Yang, W., 2011. Spatial variability of soil moisture at typical alpine meadow and steppe sites in the Qinghai-Tibetan Plateau permafrost region. Environ Earth Sci 63 (3), 477–488. doi:10.1007/s12665-010-0716-y.

Zhang, F., Wang, T., Xue, X., Han, B., Peng, F., You, Q., 2010. The response of soil CO2 efflux to desertification on alpine meadow in the Qinghai–Tibet Plateau. Environ Earth Sci 60 (2), 349–358. doi:10.1007/s12665-009-0421-x.

Zhang, Y., Ohata, T., Kadota, T., 2003. Land-surface hydrological processes in the permafrost region of the eastern Tibetan Plateau. Journal of Hydrology 283 (1-4), 41–56. doi:10.1016/S0022-1694(03)00240-3.

Scientific publications and conference contributions

Scientific papers (peer reviewed)

Baumann, F., Schmidt, K., Dörfer, C., He, J.-S., Scholten, T., Kühn, P., 2013. Pedogenesis, permafrost, substrate and topography: Plot and landscape scale interrelations of weathering processes on the central-eastern Tibetan Plateau. Geoderma (submitted).

Dörfer, C., Kühn, P., **Baumann, F.**, He, J.-S., Scholten, T., 2013. Soil Organic Carbon Pools and Stocks in Permafrost-Affected Soils on the Tibetan Plateau. Plos One 8(2): e57024.

Liu, W., Chen, S., Qin, X., **Baumann, F.**, Scholten, T., Zhou, Z., Sun, W., Zhang, T., Ren, J., Qin, D., 2012. Storage, patterns, and control of soil organic carbon and nitrogen in the northeastern margin of the Qinghai-Tibetan Plateau. Environmental Research Letters 7, 035401.

Shi, Y., **Baumann, F.**, Ma, Y., Song, C., Kühn, P., Scholten, T., He, J.-S., 2012. Organic and inorganic carbon in the topsoil of the Mongolian and Tibetan grasslands: pattern, control and implications. Biogeosciences 9, 2287-2299.

Geng, Y., Wang, Y. Yang, K., Wang, S., Zeng, H., **Baumann, F.**, Kühn, P., Scholten, T., He, J.-S., 2012. Soil Respiration in Tibetan Alpine Grasslands: Belowground Biomass and Soil Moisture, but Not Soil Temperature, Best Explain the Large-Scale Patterns. PLoS ONE 7(4): e34968.

Geng, Y., Wang, Z., Liang, C., Fang, J., **Baumann, F.**, Kühn, P., Scholten, T., He, J.-S., 2012. Effect of geographical range size on plant functional traits and the relationships between plant, soil and climate in Chinese grasslands. Global Ecology and Biogeography 21, 416-427.

Baumann, F., He, J.-S., Schmidt, K., Kühn, P., Scholten, T., 2009. Pedogenesis, permafrost, and soil moisture as controlling factors for soil nitrogen and carbon contents across the Tibetan Plateau. Global Change Biology 15, 3001–3017.

Conference contributions and other publications

Dörfer, C., **Baumann, F.**, He, J.-S., Kühn, P., Scholten, T., 2011. SOC pools and stocks in permafrost soils on the Tibetan Plateau. Jahrestagung der Deutschen Bodenkundlichen Gesellschaft (DBG) in Berlin.

Baumann, F., He, J.-S., Schmidt, K., Kühn, P., Scholten, T., 2010. Controlling factors of soil nitrogen and carbon contents across the Tibetan Plateau: soil formation, permafrost, and soil moisture. 19th World Congress of Soil Science in Brisbane, Australia.

Baumann, F., He, J.-S., Kühn, P., Scholten, T., 2009. Einfluss von Permafrostdegradation auf den C- und N- Haushalt bezüglich Pedogenese und Ökosystemfunktion. Jahrestagung der Deutschen Bodenkundlichen Gesellschaft (DBG) in Bonn.

Baumann, F., Scholten, T., Kühn, P., 2009. Pedogenesis and soil moisture, but not soil temperature best explain large-scale patterns of soil carbon and soil nitrogen contents in the permafrost ecosystems of Tibetan alpine grassland. European Geoscience Union Annual Meeting (EGU) in Wien, Österreich.

Baumann, F., He, J.-S., Kühn, P., Scholten, T., 2008. Impact of permafrost degradation on C and N stocks related to pedogenesis and ecosystem functioning. Ninth International Conference on Permafrost (NICOP) in Fairbanks, Alaska, Extended Abstracts (eds Kane DL & Hinkel KM), 19-20.

Baumann, F., He, J.-S., Kühn, P., Scholten, T., 2008. Interactions of Pedogenesis, Nitrogen and Carbon Stocks on a Transect Study Across the Qinghai-Xizang (Tibet) Plateau. Eurosoil in Wien, Österreich.

Baumann, F., Scholten, T., Kühn, P., He, J.-S., 2007. Einfluss der Pedodiversität auf den Kohlenstoff- und Stickstoffhaushalt von Steppenökosystemen entlang eines Transekts durch das Hochland von Tibet. Mitteilung Deutsche Bodenkundliche Gesellschaft, 110(1), 173-174.

Acknowledgements

First and foremost, I would like to thank my supervisor Prof. Dr. Thomas Scholten, who gave me the great opportunity to work on this interesting topic in this very special part of the world. Although this thesis did not evolve within the financial framework of a major research project, he always helped me with great enthusiasm to realise all ideas and wishes. I am very grateful for his permanent support and helpful words.

I am also very grateful to Prof. Dr. Volker Hochschild for kindly refereeing this thesis.

I particularly thank Dr. Peter Kühn for the longstanding cooperation and friendship. He gave me exceptional support not only in respect of this thesis and related laboratory works, but also regarding joint student courses and exciting field trips, which greatly broadened my horizon.

I am grateful to Dr. Karsten Schmidt, who helped me many times with his great statistical knowledge. He always had an open ear for any problems and questions doctoral students may have every now and then.

Without the help of our Chinese partners, this work would have been simply impossible. They guided me in their friendly and funny manner through all surprises daily life in China keeps ready. Therefore, I especially thank Prof. Dr. Jin-Sheng He for being such a reliable and kind partner as well as Yang Kuo, Shen Tong, Wu Yi, Ma Wenhong, Mi Zhaorong, Yang Xiaoxia and Wang Liang for supporting the field work and doing laboratory analyses. I also thank Qi Shanxue, who dug the soil pits, and substitutionary for all other drivers Mou Shanmin, who drove us sound and safe thousands of kilometres across the Tibetan permafrost-affected roads.

I also thank Corina Dörfer for participating the last field session in 2009 and for her support and friendship during this challenging trip and throughout the last years.

Moreover, I thank my former next-door neighbours Dr. Dana Pietsch and Dr. Ralf Gründling for their help and many interesting discussions.

Importantly, I am indebted to Sabine Flaiz for her uncomplicated support in laboratory analyses despite the long distance between Tübingen and Freiburg during the last years. Furthermore, I thank Jonas Daumann, Kathrin Drechsel, Christian Wolf, and Andre Velescu for help with the laboratory work.

Many thanks go to Patrick Steingrüber for providing me incredible help with the easy-going and safe transportation of the overweight luggage on all three flights to China and back.

Finally, I would like to thank my parents for their great support and understanding for all my decisions.

I am deeply grateful to my wife Anna, who was there for me at any time and supported me from every point of view with her positive and sunny nature. Finishing this thesis beside the regular work meant countless evenings, weekends and holidays spending behind the desk, and not together. Thank you a lot for your understanding and patience!